

**Synthesis of α -Oxygenated Carbonyl Compounds via Dioxygenation,
Development of Fluorescent Probes**

BY

Aditi S. Patil

B.Sc., University of Pune, India 2004

M.Sc., University of Pune, India 2006

THESIS

Submitted as partial fulfillment of the requirements
for the degree of Doctor of Philosophy in Chemistry
in the Graduate College of the
University of Illinois at Chicago, 2013

Chicago, Illinois

Defense Committee:

Laura L. Anderson, Advisor and Chair, Chemistry
Tom G. Driver, Chemistry
Duncan J. Wardrop, Chemistry
Justin T. Mohr, Chemistry
Regan J. Thomson, Northwestern University

This thesis is dedicated to my mother ~ Dr. Jyoti Patil

ACKNOWLEDGEMENTS

I would like to express my deepest gratitude to my advisor Prof. Laura L. Anderson for all her guidance and support. She has been an exceptional mentor who has motivated us, provided great advice, given us the freedom to pursue our ideas, been patient and enthusiastic and above all, helped us in all facets of life. I cannot imagine having a better advisor and mentor for my Ph.D.

I would like to thank Prof. Tom G. Driver and Prof. Duncan J. Wardrop for their encouragement and helpful ideas and discussions. I am also grateful to Prof. Justin T. Mohr and Prof. Regan J. Thomson for taking the time to serve on my defense committee.

I thank my lab mates from the Anderson Group: Dimitra Kontokosta, who has also been a great friend and confidant, Stephanie Aguilar, Dong-Liang Mo, Wiktoria Pecak, Heng-Yen Wang, Daniel Mueller, Michelle Kroc and Josiah Ballantine. I would also like to thank Kung-Pern Wang, Jingwei Li, Chunrui Sun and Ivan Volchkov from the Lee lab for all their help. I am thankful to Rhonda Staudohar, Silvia Solis and Pat Ratajczyk from the chemistry department for patiently answering all my questions. My friends Emma Mendonca, Hammad Naveed and Goutham Pattabiraman have always been there for me and have helped me prevail over setbacks.

None of this would have been possible without the love and patience of my family. My family, comprising my mother, grandparents, aunt, cousins and husband, has been a constant source of love, support and strength all these years. I would like to express my heart-felt gratitude to my family.

ASP

TABLE OF CONTENTS

<u>CHAPTER</u>	<u>PAGE</u>
Synthesis of α -Oxygenated Carbonyl Compounds via Dioxygenation	
1 Preparation of α-Oxygenated Ketones via the Dioxygenation of Alkenyl Boronic Acids	1
1.1 Abstract	1
1.2 Introduction	2
1.2.1 Boronic Acids in Organic Synthesis	2
1.3 Chan-Lam Coupling Reactions	4
1.3.1 Mechanism of the Reaction	6
1.3.2 C–N Bond Forming Reactions	7
1.3.3 C–O Bond Formation	10
1.3.4 Chan-Lam Coupling With Alkenyl Boronic Acids	11
1.4 Dioxygenation Scheme	13
1.5 α -Oxygenated Ketones	14
1.6 Arylation of <i>N</i> -Hydroxyphthalimide	17
1.7 Optimization of Conditions for Coupling of Alkenyl Boronic Acids with <i>N</i> -Hydroxyphthalimide	18
1.8 Evaluation of the Scope of the Transformation	21
1.9 Limitations of the Methodology	24
1.10 [3,3] Rearrangement to Form the Imidates	24
1.11 Trends in the [3,3] Rearrangement	26
1.12 Isolation of α - Hydroxy Ketones	27
1.13 Isolation of α -Benzoyloxy Ketones	29
1.14 Diastereoselectivity Trends in the Rearrangement	31
1.15 Single Purification Sequence	33
1.16 Exploring the Mechanism for the Reaction	35
1.16.1 Cross-Over Experiment	35
1.16.2 Radical Clock Experiment	36
1.17 Conclusion	37
1.18 Supporting Information	37
1.18.1 General Experimental Information	37
1.18.2 Experimental Procedures and Characterization Data	38
2 Diastereoselective Dioxygenation of Alkenyl Boronic Acids via Etherification and Rearrangement of <i>N</i>-hydroxyisoindolinones	115
2.1 Abstract	115
2.2 [3,3] Rearrangements in Organic Synthesis	116
2.2.1 Modes of Diastereoselective and Enantioselective Induction Through Substrate Control	118
2.2.2 Diastereoselective and Enantioselective Induction Using Chiral Reagents	126
2.3 Effect of Neighboring Stereocenter on the [3,3] Rearrangement	129
2.4 Initial Results	131

TABLE OF CONTENTS (continued)

<u>CHAPTER</u>	<u>PAGE</u>
2.4.1 Effect of a Neighboring Hydroxy Group	131
2.4.2 Effect of a 3- <i>t</i> -Butyldimethylsilyloxy Group.....	132
2.4.3 Effect of Alkyl Groups at the Stereocenter.....	133
2.5 Optimization of the Preparation and Rearrangement of 14z	135
2.6 Evaluating Different Substituents at the Stereocenter	137
2.6.1 Synthesis of 3-Alkoxy- <i>N</i> -Hydroxyisoindolinones.....	138
2.6.2 Synthesis of 3-Silyloxy- <i>N</i> -Hydroxyisoindolinones	139
2.6.3 Synthesis of 3-Allyl- <i>N</i> -Hydroxyisoindolinone	140
2.7 Determination of Relative Stereochemistry for the Imidate	141
2.8 Varying the Boronic Acids	142
2.8.1 Scope and Stereoselectivity with Disubstituted Boronic Acids.....	142
2.8.2 Scope and Stereoselectivity with Monosubstituted Boronic Acids	145
2.9 Role of Cu(OAc) ₂ in the [3,3] Rearrangement	148
2.10 Functionalization of the Imidates.....	149
2.11 Transfer of Chirality	151
2.11.1 Optimization of the Conditions for the Chiral Reduction.....	151
2.11.2 Effect of Protecting Groups on the Chiral Reduction	155
2.11.3 Testing the Effect of a Chiral <i>N</i> -hydroxyisoindolinone.....	158
2.12 Conclusion	159
2.13 Supporting Information.....	160
2.13.1 General Experimental Information	160
2.13.2 Experimental Procedures and Characterization Data	161

Development of Fluorescent Probes

3 Introduction to Lipids and Environment-Sensitive Fluorescent Probes	199
3.1 Lipids	199
3.2 Phosphatidylserine (PS).....	201
3.2.1 Functions of PS	202
3.3 Conventional Methods for Lipid Analysis.....	203
3.4 Fluorescent Probes	204
3.5 Environmentally Sensitive Fluorescent Probes	206
3.6 Conclusion	211
4 Development of New Environment Sensitive Fluorescent Probes for Lipid-Protein Interactions.....	212
4.1 Abstract	212
4.2 Introduction.....	213
4.3 Thiol Reactive Environment Sensitive Probes	214
4.3.1 Limitations of Currently Used Fluorophores.....	215
4.3.2 Desired Properties for New Probe	216

TABLE OF CONTENTS (continued)

<u>CHAPTER</u>	<u>PAGE</u>
4.4 Modification of the Protein.....	217
4.5 Design of New Environmentally Sensitive Probes.....	219
4.5.1 Fluorophore Containing Indolizine Core.....	219
4.5.2 Target Fluorophores.....	221
4.5.2 Introducing the Maleimide Side Chain.....	221
4.6 Green Fluorescent Compound.....	223
4.7 Orange Fluorescent Compound.....	226
4.7.1 Testing the Compound with Phosphatidylserine.....	228
4.7.2 Modification in the Structure of the Fluorophore.....	230
4.8 Designing new Fluorophores.....	233
4.8.1 Naphthopyranone Cores.....	233
4.8.2 Nile Red Derivatives.....	235
4.9 2-Imino-2,5-Dihydrofuran-3-Carbonitrile Containing Probe.....	239
4.9.1 Spectroscopic Properties of the Red Fluorescent Compound in Different Solvents.....	242
4.9.2 Protein Labeling and In-Vitro Lipid Binding Assay.....	243
4.10 Conclusion.....	245
4.11 Supporting Information.....	246
4.11.1 Materials and Methods.....	246
4.11.2 Experimental Procedures and Characterization Data.....	247
Cited Literature.....	266
Appendices.....	282
Vita.....	301

LIST OF TABLES

<u>TABLE</u>	<u>PAGE</u>
Table 1.1 Optimization of Reaction Conditions for the Coupling Reaction.....	19
Table 1.2 Scope of the Coupling Reaction with Mono and Disubstituted Boronic Acids	22
Table 1.3 Scope of the Coupling Reaction with Cyclic Boronic Acids	23
Table 1.4 Trends in the [3,3] Rearrangement	27
Table 1.5 α -Hydroxy Ketones Isolated following the Dioxygenation Scheme	29
Table 1.6 α -Benzoyloxy Ketones Isolated following the Dioxygenation Scheme	30
Table 1.7 Extended Optimization Table	105
Table 2.1 Optimization of the Single-Flask Dioxygenation	136
Table 2.2 Evaluating the Effect of Different Substituents on the Diastereoselectivity.....	137
Table 2.3 Using Acyclic, Disubstituted Boronic Acids	143
Table 2.4 Single-Flask Reaction with Cyclic, Disubstituted Boronic Acids	144
Table 2.5 <i>N</i> -Enoxyisoindolinones Isolated using the Etherification Reaction	146
Table 2.6 Rearrangement to form α -Oxygenated Aldehydes	147
Table 2.7 Conditions for the Chiral Reduction.....	153
Table 2.8 Optimization of Conditions for the Chiral Reduction	154
Table 2.9 Effect of Protecting Groups on the Chiral Reduction.....	158

LIST OF FIGURES

<u>FIGURE</u>	<u>PAGE</u>
Figure 2.1 Determination of Relative Stereochemistry	141
Figure 3.1 Lipid Bilayer.....	199
Figure 3.2 Structure of the Phospholipid–Phosphatidylcholine	200
Figure 3.3 Arrangement of Phospholipids in the Cell Membrane	201
Figure 3.4 Structure of Phosphatidylserine.....	202
Figure 3.5 Recognition of an Apoptotic Cell through Extracellularly Exposed PS	203
Figure 3.6 Fluorescent Probe Attached to a Protein used to Monitor the Interactions of the Protein with Lipids.....	205
Figure 3.7 Real Lifetime Images of Cells in which a Labeled Protein has Bound to the Cell Membrane.....	206
Figure 3.8 Effect of Solvent Polarity on the Emission of the Fluorophore	208
Figure 4.1 Change in the Environment of the Probe Results in an Increase in the Intensity of Emission	217
Figure 4.2 Modifications to the PKC γ Protein to Ensure Binding to both the Probe and the Lipid.....	218
Figure 4.3 Varying the Emission Properties of the Fluorescent Probe.....	220
Figure 4.4 Installing a Michael Acceptor on the Target Fluorophore	222
Figure 4.5 Expected Change in the Emission of the Fluorophore	228
Figure 4.6 No Change in the Observed Emission of the Fluorophore.....	229
Figure 4.7 Hypothesis to Explain Observed Results	229
Figure 4.8 Plot of Intensity vs Wavelength that Shows an Increase in Intensity of Emission	232
Figure 4.9 Fluorescence Emission Affected by Polarity of Solvents	243

LIST OF FIGURES (continued)

<u>FIGURE</u>	<u>PAGE</u>
Figure 4.10 Addition of PS to the Labeled Protein.....	244
Figure 4.11 Plot of Fluorescence Intensity vs PS Percentage.....	245

LIST OF SCHEMES

<u>SCHEMES</u>	<u>PAGE</u>
Scheme 1.1 Aryl Boronic Acids in the Synthesis of Aryl Amines	3
Scheme 1.2 Suzuki Reaction with Alkenyl Boronic Acids	3
Scheme 1.3 Petasis Reaction with Alkenyl Boronic Acids	4
Scheme 1.4 Buchwald-Hartwig Cross Coupling Reaction	5
Scheme 1.5 Methoxylation of Tolyboronic Ester	6
Scheme 1.6 Proposed Mechanism for the Chan-Lam Coupling Reaction.....	7
Scheme 1.7 C–N Bond Forming Reactions with <i>p</i> -Tolyboronic Acid.....	8
Scheme 1.8 Coupling of Two Heteroarenes	9
Scheme 1.9 Coupling with Oxime <i>O</i> -Carboxylates.....	9
Scheme 1.10 <i>N</i> -Amidation Reaction with <i>O</i> -Acetyl Hydroxamic Acids	10
Scheme 1.11 C(aryl sp ²)–O Bond Formation through a Cross-Coupling Reaction	10
Scheme 1.12 <i>O</i> -Arylation of <i>N</i> -Hydroxybenzotriazoles with <i>p</i> -Tolyboronic Acid.....	11
Scheme 1.13 Hartwig’s Synthesis of 3,5-Disubstituted Aryl Ethers	11
Scheme 1.14 Using Alkenyl Boronic Acids	12
Scheme 1.15 Copper Promoted Coupling of Vinyl Boronates with Aliphatic Alcohols	12
Scheme 1.16 Overall Reaction for Dioxygenation Process	13
Scheme 1.17 Dioxygenation of Alkenyl Boronic Acids.....	13
Scheme 1.18 Retrosynthetic Pathways for α -Oxygenation of Carbonyl Compounds	14
Scheme 1.19 New Retrosynthetic Pathway for α -Oxygenation	16
Scheme 1.20 Arylation of <i>N</i> -Hydroxyphthalimide	17

LIST OF SCHEMES (continued)

<u>SCHEMES</u>	<u>PAGE</u>
Scheme 1.21 Etherification of <i>N</i> -Hydroxyphthalimide with Alkenyl Boronic Acids.....	18
Scheme 1.22 Decomposition of the Boronic Acid in the Presence of O ₂	20
Scheme 1.23 Evaluating Different Alkenyl Boronic Acids.....	21
Scheme 1.24 Limitations of the Copper Mediated Coupling Reaction	24
Scheme 1.25 [3,3] Rearrangement of the <i>N</i> -Enoxyphthalimides to Afford Imidates.....	25
Scheme 1.26 Formation of α -Oxygenated Aldehydes	25
Scheme 1.27 Polymerization of the α -Oxygenated Aldehydes	25
Scheme 1.28 Isolation of α -Hydroxy Ketones.....	28
Scheme 1.29 Isolation of α -Benzoyloxy Ketones.....	29
Scheme 1.30 Effect of Hydrolysis on the Diastereoselectivity.....	32
Scheme 1.31 Hindered Rotation Leads to the Kinetic Product	33
Scheme 1.32 Rotation of C–O Bond Results in Formation of Thermodynamic Product	33
Scheme 1.33 Using an Alkenyl Boronic Acid with an Electron Donating Aryl Substituent.....	34
Scheme 1.34 Single Step Purification Sequence	34
Scheme 1.35 Single Step Purification with a Dialkyl Boronic Acid	35
Scheme 1.36 Cross-Over Experiment.....	36
Scheme 1.37 Radical Clock Experiment	36
Scheme 2.1 [3,3] Rearrangement in the Synthesis of Fronodosin B	116
Scheme 2.2 Sequential [3,3] Rearrangements in the Synthesis of A-315675	117
Scheme 2.3 Distant Chiral Centre Controlling the Stereochemical Outcome	118

LIST OF SCHEMES (continued)

<u>SCHEMES</u>	<u>PAGE</u>
Scheme 2.4 Enders' RAMP Hydrazone as a Chiral Auxiliary in the [3,3] Rearrangement	118
Scheme 2.5 Diastereoselective [3,3] Sigmatropic Aza-Claisen Rearrangement with Minimization of <i>syn</i> -Pentane Interactions	119
Scheme 2.6 Mismatched Rearrangement Destabilised by 1,3 Diaxial Interactions and <i>syn</i> -Pentane Interactions.....	120
Scheme 2.7 Diastereoselectivity Arising from Formation of Energetically Favorable Chair-like Transition State.....	121
Scheme 2.8 Diastereoselectivity Controlled by Sterics	122
Scheme 2.9 A _{1,3} -strain and Sterics Controlling Diastereoselectivity.....	122
Scheme 2.10 A _{1,3} -strain and Cieplak Effect Controlling Diastereoselectivity	123
Scheme 2.11 Diastereoselectivity Controlled by A _{1,2} -strain.....	124
Scheme 2.12 Claisen Rearrangement to Access Spirocyclic Oxindoles with Vicinal Quaternary Carbon Centers.....	125
Scheme 2.13 Claisen Rearrangement through a Boat-like Transition State.....	126
Scheme 2.14 Chiral Promoter in an Enantioselective Claisen Rearrangement	127
Scheme 2.15 Chiral Guanidinium Catalyzed Claisen Rearrangement	127
Scheme 2.16 Catalytic Diastereoselective Reductive Claisen Rearrangement	128
Scheme 2.17 Effect of a substituent at C6 on the Rearrangement Reaction.....	129
Scheme 2.18 <i>Cis</i> isomer Predominates in all other Substituted Cyclohexanones	129
Scheme 2.19 Hindered Rotation of the C–O bond because of Steric Interactions	130
Scheme 2.20 Diastereoselective [3,3] Rearrangement	131
Scheme 2.21 Effect of a Hydroxy Substituent near the Reaction Site.....	131
Scheme 2.22 Synthesis of 3- <i>t</i> -butyldimethylsilyloxy- <i>N</i> -hydroxyisoindolinone.....	132

LIST OF SCHEMES (continued)

<u>SCHEMES</u>	<u>PAGE</u>
Scheme 2.23 Etherification and Rearrangement in a Single-Flask.....	133
Scheme 2.24 Synthesis of <i>N</i> -hydroxyisoindolinone containing a Quarternary Center.....	134
Scheme 2.25 Etherification and Rearrangement of 3-ethyl-3-methyl- <i>N</i> -hydroxyisoindolinone	135
Scheme 2.26 Synthesis of 3-Alkoxy- <i>N</i> -Hydroxyisoindolinones	139
Scheme 2.27 Synthesis of 3-Silyloxy- <i>N</i> -Hydroxyisoindolinones	139
Scheme 2.28 Synthesis of 3-Allyl- <i>N</i> -hydroxyisoindolinone	140
Scheme 2.29 Evaluation of Disubstituted Boronic Acids.....	142
Scheme 2.30 Etherification Reaction with Monosubstituted Boronic Acids	146
Scheme 2.31 [3,3] Rearrangement using Monosubstituted Boronic Acids	147
Scheme 2.32 Rearrangement with the <i>N</i> -Enoxyphthalimide.....	148
Scheme 2.33 Determining the role of Cu(OAc) ₂ in the [3,3] Rearrangement.....	148
Scheme 2.34 Conversion of the Imidate to the α -Chloro Ketone.....	150
Scheme 2.35 Conversion of the Imidate to the α -Hydroxy Ketone.....	150
Scheme 2.36 Chiral Reduction with CBS Catalyst.....	152
Scheme 2.37 Reaction Scheme for Evaluating Transfer of Chirality.....	159
Scheme 3.1 Structures of Solvatochromic Probes	210
Scheme 3.2 ICT in Prodan	210
Scheme 4.1 Currently Used Environmentally Sensitive Fluorescent Probes	216
Scheme 4.2 Fluorophores Containing an Indolizine Core	219
Scheme 4.3 Target Fluorophores	221

LIST OF SCHEMES (continued)

<u>SCHEMES</u>	<u>PAGE</u>
Scheme 4.4 Synthesis of <i>p</i> -Dimethylaminocinnamaldehyde.....	223
Scheme 4.5 Formation of the α -Bromo Amide.....	224
Scheme 4.6 Formation of the Green Fluorescent Compound.....	224
Scheme 4.7 Mechanism of the Reaction to form the Indolizine Core	225
Scheme 4.8 Final steps in the synthesis of the Green Fluorescent Probe	226
Scheme 4.9 Synthesis of the Orange Fluorescent Compound	227
Scheme 4.10 Installing the Maleimide Group	227
Scheme 4.11 Modifications in the Structure of the Fluorophore.....	231
Scheme 4.12 Converting the Acetyl Group at R ₂ to the α,β -Unsaturated Ketone	231
Scheme 4.13 Conversion of the Acetyl Group to the α -Bromo Ketone	232
Scheme 4.14 ICT in Naphthopyranones	234
Scheme 4.15 Synthesis of a Probe Containing the Naphthopyranone Core	235
Scheme 4.16 General Structure of Nile Red.....	235
Scheme 4.17 Nile Red Derivatives that are Water Soluble and Red Fluorescent	236
Scheme 4.18 Synthesis of Nile Red Derivative	237
Scheme 4.19 Synthesis of Water Soluble Nile Red Derivative	238
Scheme 4.20 Proposed Modification of Nile Red	238
Scheme 4.21 2-Dicyanomethylene-3-cyano-2,5-dihydrofuran Core.....	239
Scheme 4.22 Synthesis of Red Fluorescent Compound	240
Scheme 4.23 Formation of Fluorophore with 2-Imino-2,5-dihydrofuran-3- carbonitrile Core	241
Scheme 4.24 Installing the Sulfide Acceptors	241

LIST OF ABBREVIATIONS

Ac	Acetyl ($\text{CH}_3\text{C}=\text{O}$)
bda	Benzylideneacetone
bipy (bpy)	2,2'-bipyridyl
Boc	<i>t</i> -Butyloxycarbonyl [$\text{COC}(\text{CH}_3)_3$]
BOM	Benzyloxymethyl ($\text{PhCH}_2\text{OCH}_2$ -alcohol protection)
Bz	Benzoyl (caution: sometimes used for benzyl)
Bn	Benzyl
<i>n</i> -Bu	normal Butyl
<i>t</i> -Bu	tertiary Butyl
CAN	Ceric Ammonium Nitrate
CBS	Corey-Bakshi-Shibata
Cbz	Carbobenzyloxy ($\text{BnOC}=\text{O}$)
cod	Cyclooctadiene
Cp	Cyclopentadienyl
Cp*	Pentamethylcyclopentadienyl
CSA	Camphorsulfonic Acid
Cu	Copper
CuTC	Copper(I) thiophene-2-carboxylate
Cys	Cysteine
DA	Diels-Alder Reaction
DAST	(Diethylamino)sulfur trifluoride Et_2NSF_3
DBU	1,8-Diazabicyclo[5.4.0]undec-7-ene

LIST OF ABBREVIATIONS (continued)

DCC	<i>N,N'</i> -dicyclohexyl carbodiimide
DCE	1,2-Dichloroethane
DDQ	2,3-Dichloro-5,6-dicyano-1,4-benzoquinone
de	Diastereomeric Excess
DHP	3,4-Dihydro-2 <i>H</i> -pyran
dr	Diastereomeric Ratio
DIBAL	Diisobutylaluminum Hydride
Dppe	1,2-Bis(diphenylphosphino)ethane
DMAP	4-Dimethylaminopyridine
DMF	Dimethylformamide
DMSO	Dimethyl Sulfoxide
<i>E</i>	Entgegen (opposite, trans)
ee	Enantiomeric Excess
er	Enantiomeric Ratio
LAH	Lithium Aluminum Hydride (LiAlH ₄)
LDA	Lithium Diisopropylamide
LHMDS	Lithium Hexamethyldisilazide (LiN(SiMe ₃) ₂)
<i>m</i> CPBA	<i>meta</i> -Chloroperoxybenzoic Acid
Ms	Methanesulfonyl (Mesyl, CH ₃ SO ₂)
NBS, NCS	<i>N</i> -Bromo, <i>N</i> -Chlorosuccinimide
NIS	<i>N</i> -Iodosuccinimide
PCC	Pyridinium chlorochromate

LIST OF ABBREVIATIONS (continued)

PC	Phosphatidylcholine
PPTS	Pyridinium <i>p</i> -Toluenesulfonate
Piv	Pivaloyl
<i>i</i> Pr	Isopropyl
PS	Phosphatidylserine
PTSA	<i>p</i> -Toluenesulfonic acid monohydrate
Pyr	Pyridine
RT	Room Temperature
SES	Trimethylsilylethylsulfonyl
TASF	Tris(dimethylamino)sulfonium difluorotrimethylsilicate
TBAF	Tetra- <i>n</i> -butylammonium fluoride
TBDMS	<i>t</i> -Butyldimethylsilyl
TBDPS	<i>t</i> -Butyldiphenylsilyl
TBHP	<i>t</i> -Butylhydroperoxide
TBS	<i>t</i> -Butyldimethylsilyl (also TBDMS)
TBSCl	<i>t</i> -Butyldimethylsilylchloride
TEA	Triethylamine
TES	Triethylsilyl
TIPS	Triisopropyl
Tf	Triflate (CF ₃ SO ₂)
TFA	Trifluoroacetic acid
THP	Tetrahydropyran

LIST OF ABBREVIATIONS (continued)

TIPS	Triisopropylsilyl
TIPS	Triisopropylsilylchloride
TMEDA	<i>N,N,N',N'</i> -Tetramethylethylenediamine
TMS	Tetramethylsilane, also Trimethylsilyl
TsDPEN	<i>N</i> -Tosyldiphenylethylenediamine
Tol	Toluene
Ts	Tosyl (<i>p</i> -CH ₃ C ₆ H ₄ SO ₂)
Z	Zusammen (together, cis)

SUMMARY

This thesis is divided into two parts. Part I consists of two chapters which describe a new dioxygenation reaction of alkenyl boronic acids to access α -hydroxy ketones. The methodology for a diastereoselective dioxygenation has also been reported. Part II also has two chapters which illustrate the importance of protein-lipid interactions and the development of environmentally sensitive fluorescent probes for monitoring these interactions.

In chapter 1, the Chan-Lam coupling of boronic acids and methods to synthesize α -hydroxy ketones are briefly reviewed. This is followed by a study on the optimization and the scope of the coupling reaction of alkenyl boronic acids with *N*-hydroxyphthalimide, rearrangement of the ensuing *N*-enoxyphthalimides and hydrolysis to release the α -oxygenated ketones. Chapter 2 reviews methods to control diastereoselectivity in a [3,3] rearrangement and the use of *N*-hydroxyisoindolinones to control the diastereoselectivity during the dioxygenation process.

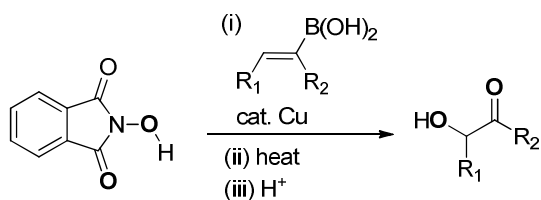
Chapter 3 describes the fundamentals of lipids, their interactions with proteins and demonstrates that the use of environmentally sensitive probes is the most desirable method for monitoring these interactions. Chapter 4 exemplifies the development of new environmentally sensitive, thiol reactive probes which can be used for the *in-situ* determination of phosphatidylserine in the *E. coli* cell.

Chapter 1 - Preparation of α -Oxygenated Ketones via the Dioxygenation of Alkenyl Boronic Acids

1.1 Abstract

Aldehydes and ketones that have oxygen substituents at the α -position are important building blocks for the synthesis of a large number of biologically active compounds. Conventional transformations which afford the α -oxygenation products of carbonyl compounds either utilize oxidants that are unstable or involve the removal of halogenated byproducts after displacement with oxygen nucleophiles. A new alternative route to α -oxygenated carbonyl compounds through the dioxygenation of vinyl boronic acids has been developed. This route avoids the use of unstable reagents and provides direct access to α -oxygenated carbonyl compounds directly from internal alkynes.

The dioxygenation of alkenyl boronic acids with *N*-hydroxyphthalimide has been achieved by a two-step process involving a copper-mediated etherification to form an *N*-enoxyphthalimide and a subsequent [3,3] rearrangement to provide α -hydroxy ketones or α -benzoyloxy ketones, after hydrolysis of the phthalimide imidate intermediate.



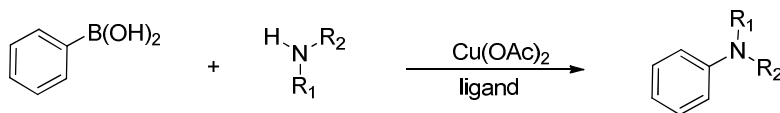
1.2 Introduction

1.2.1 Boronic Acids in Organic Synthesis

Boronic acids are amongst the most useful classes of organoboron reagents that have become popular in recent years for C–C and C–heteroatom coupling reactions.¹ Unlike many organometallic reagents and most organoboranes, boronic acids are appealing reagents to work with since they have low toxicity, are usually stable to air and moisture and react under mild conditions.² The discovery by Suzuki and Miyaura in 1979 that aryl boronic acids could be coupled with an aryl halide using a palladium catalyst sparked the chemistry of boronic acids.³ Since then, the ubiquitous use of aryl, alkenyl, and alkyl boronic acids for the formation of new C–C, C–N, and C–O bonds in cross coupling reactions is indicative of the importance of these compounds in organic synthesis.⁴

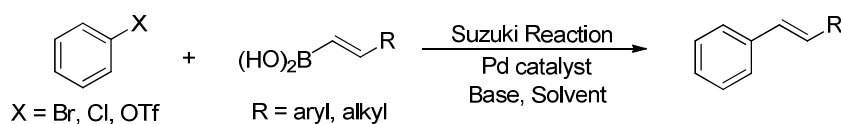
One of the earliest known reactions of aryl boronic acids is their oxidative cleavage, usually with hydrogen peroxide to give phenols, thus leading to the formation of a new C–O bond.⁵ Other oxidative reactions with NBS or NIS to give aryl halides have also been reported.⁶ Boronic acids have been used in coupling reactions with a variety of heterocyclic halides including thiophenes,⁷ thiazoles,⁷ furans,⁸ isoxazoles,⁹ pyridines,¹⁰ pyrimidines¹¹ and pyrazines¹² to form new C–C bonds, with perfect control of regiochemistry, and which cannot be formed using conventional methods of electrophilic aromatic substitution. Instead of using the more reactive halide functionality, aryl or vinyl triflates, derived from their corresponding ketones, have also been shown to undergo palladium-catalyzed couplings with boronic acids.¹³ Coupling of boronate derivatives with aryl tosylates¹⁴ and mesylates¹⁵, catalyzed by nickel and palladium complexes, have also been reported. Sulfonium salts can also be used as coupling partners with boronic acids to form new C–C bonds wherein the sulfonium salt serves as the leaving group.¹⁶ Aryl boronic acids can undergo Ullmann-type C–O and C–N bond forming reactions

with phenols,¹⁷ amines,¹⁸ amides,¹⁹ ureas,²⁰ sulfonamides,²¹ carbamates,²² and *N*-heteroaromatics²³ in the presence of copper salts to give the corresponding diaryl ethers, aryl amines (Scheme 1.1) or *N*-aryl heterocycles.



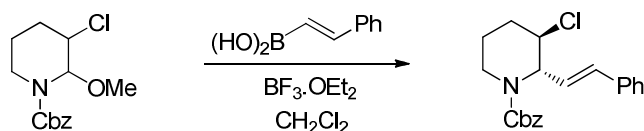
Scheme 1.1: Aryl Boronic Acids in the Synthesis of Aryl Amines

Since these *N*-aryl heterocycles are commonly found in a number of drugs,²⁴ the Ullmann-type coupling of boronic acids with cheap, commercially available reagents has been used to access large libraries of drug analogs.²⁵ Although the use of aryl boronic acids for the preparation of a variety of new bonds is well established, the reactivity of alkenyl boronic acids has not been extensively studied. Alkenyl boronic acids have been commonly used in the Suzuki reaction³ with aryl or vinyl halides or triflates using a Palladium catalyst⁴ (Scheme 1.2). This reaction is a powerful method that provides access to conjugated olefins and styrenes.



Scheme 1.2: Suzuki Reaction with Alkenyl Boronic Acids

Alkenyl boronic acids have also been utilized in the synthesis of 2,3-disubstituted piperidines as shown below in Scheme 1.3.



Scheme 1.3: Petasis Reaction with Alkenyl Boronic Acids

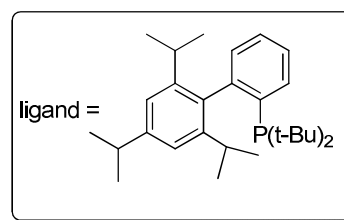
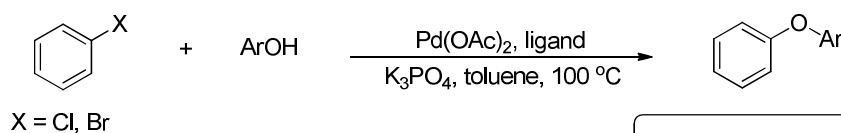
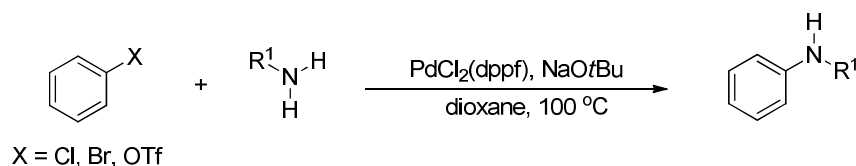
This is a Petasis-type reaction, mediated by a Lewis acid, which involves the diastereoselective introduction of aryl and vinyl moieties onto the 2-position of *N*-protected piperidinium ions.²⁶ Vinyl boronate esters are more commonly used than their corresponding boronic acid analogs in both the Suzuki reaction and the Chan Lam coupling. These boronate esters have been used in cross coupling reactions with vinyl bromides or triflates to form unsymmetrical 1,3-dienes.²⁷

1.3 Chan-Lam Coupling Reactions

The copper-mediated C–N, C–O and C–S bond formations between OH, NH, or SH containing nucleophilic substrates and aryl- or alkenyl boronic acids to form the corresponding arylated or alkenylated products are referred to as Chan–Lam coupling reactions.²⁸ The discovery of the copper-promoted Chan–Lam reaction²⁹⁻³¹ has greatly advanced carbon–heteroatom cross-coupling chemistry and is a powerful synthetic tool, because of the mild conditions required. Chan-Lam couplings provide simple and modular access to aryl ethers, anilines, and thioethers which are ubiquitous moieties in a wide range of molecules with many important applications.

The Chan-Lam C–X coupling reactions provide a synthetic alternative to the Buchwald-Hartwig cross couplings.^{32,33a} Buchwald-Hartwig reactions involve a Pd(II)

catalyzed couplings between alkyl halides (or pseudo halides) and amines to form substituted anilines or aryl halides and phenols to form diaryl ethers (Scheme 1.4).^{33b}

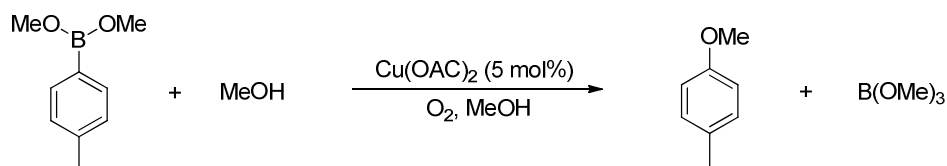


Scheme 1.4: Buchwald-Hartwig Cross Coupling Reaction

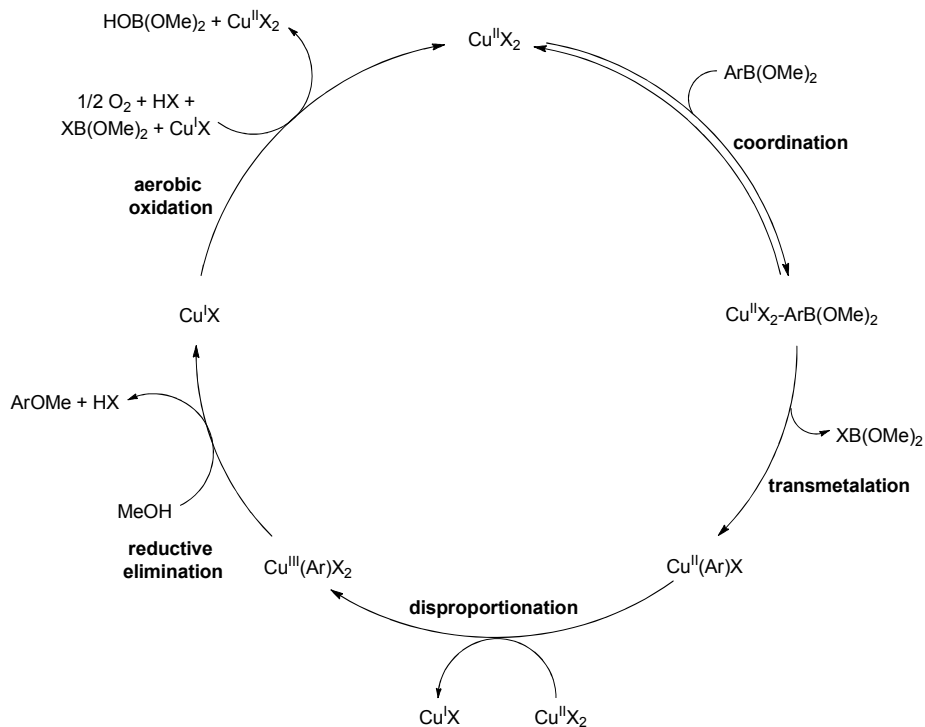
Although this palladium-catalyzed process is a very useful and well-established reaction, it has a few drawbacks. The reaction takes place only at high temperatures and requires the presence of a strong base which makes it incompatible with some functional groups. Also, the palladium catalyst which is essential for the reaction is expensive. The Chan-Lam coupling on the other hand, utilizes $\text{Cu}(\text{OAc})_2$ which is cheap and readily available. The reaction requires a mild base like pyridine and can be carried out at room temperature and under ambient conditions.

1.3.1 Mechanism of the Reaction

A mechanism for Chan–Lam *N/O*-arylations has been proposed by Stahl and co-workers based on their study of the methoxylation of tolylboronic ester (Scheme 1.5 and 1.6).³⁴ Kinetic and EPR spectroscopic studies revealed that the catalyst resting state consists of a Cu(II) species with weak anionic ligands, such as acetate or methoxide, and the turnover-limiting step is transmetalation of the aryl group from boron to the copper center. Based on the work by Ribas and co-workers,³⁵ who observed formation of a well-defined aryl–Cu(III) complex via Cu(II)-mediated C–H bond activation, Stahl and co-workers proposed that reductive elimination does not occur from Cu(II), but rather from an aryl–Cu(III) intermediate, which is formed via oxidation of a transient aryl–Cu(II) intermediate by a second equivalent of Cu(II). Therefore, in the proposed mechanism, the reaction is initiated by transmetalation of the aryl group from boron to Cu(II). The resulting aryl–Cu(II) species is oxidized by another equivalent of Cu(II) to yield an aryl–Cu(III) intermediate that can undergo facile C–O bond formation. Aerobic oxidation of Cu(I) regenerates Cu(II), the resting state of the catalyst.



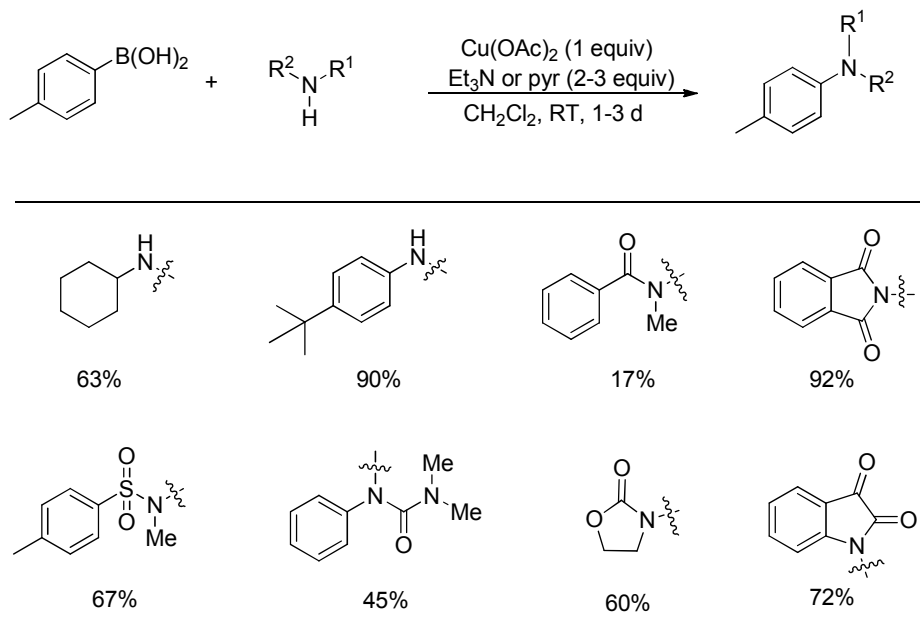
Scheme 1.5: Methoxylation of Tolylboronic Ester



Scheme 1.6: Proposed Mechanism for the Chan-Lam Coupling Reaction

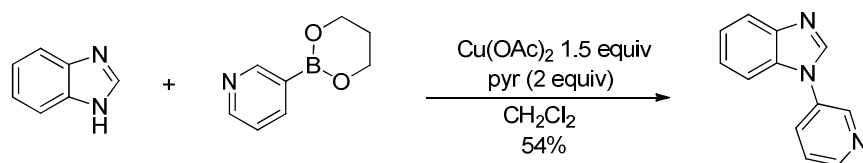
1.3.2 C–N Bond Forming Reactions

The Chan-Lam reaction has been widely used for C–N bond formation because of its high tolerance of a wide range of functional groups and because the reaction conditions are mild. In 1998, the Chan group demonstrated that a wide range of the N–H containing substrates including amines, amides, imides, ureas, carbamates and sulfonamides, underwent C–N bond formation with *p*-tolylboronic acid to afford the compounds shown below in Scheme 1.7.²⁹



Scheme 1.7: C–N Bond Forming Reactions with *p*-Tolylboronic Acid

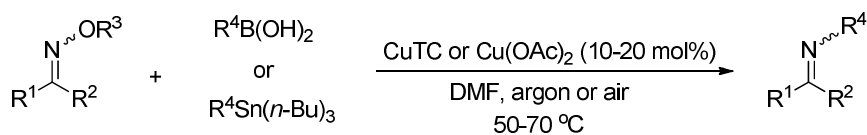
Lam and co-workers demonstrated that a variety of aromatic heterocycles, such as imidazole, pyrazole, triazoles, tetrazole, benzimidazole, and indazole undergo the Cu-mediated coupling with boronic acids to form nitrogen containing heterocycles.³¹ Pyrazoles and imidazoles were particularly amenable to the reaction conditions while electron-poor azoles such as triazoles and tetrazoles gave attenuated yields. This represents another contrasting factor with the Buchwald–Hartwig palladium-catalyzed *N*-arylation with aryl halides which works for pyrrole, indole and carbazole but not for azoles such as quinazolinediones.³⁶ Cu-mediated Chan–Lam reactions of propylene glycol boronic esters have also been extended to the coupling of two heteroarenes which provide drug-like small molecules (Scheme 1.8).³⁷



Scheme 1.8: Coupling of Two Heteroarenes

In addition, the *N*-arylation of electron deficient indoles has been achieved using diisopropylethylamine as the base. Neither triethylamine nor pyridine gave the desired product under these conditions.³⁸

This Cu-mediated C–N bond formation strategy was further extended by the Liebeskind group who used oxime *O*-carboxylates as *N*-iminating agents with either copper(I) thiophene-2-carboxylate (CuTC) or $\text{Cu}(\text{OAc})_2$ as the catalyst (Scheme 1.9) under nonbasic and nonoxidizing conditions to afford the *N*-arylated or *N*-alkenylated imines.³⁹ Other Cu(I) and Cu(II) salts such as CuCl , CuBr , CuI , CuBr_2 were also effective in catalyzing the reaction. The reaction, however, was not stereospecific and gave a mixture of *E/Z*-imine isomers.

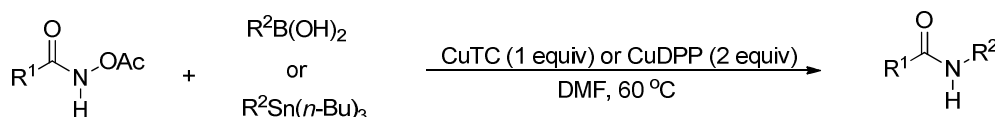


Scheme 1.9: Coupling with Oxime *O*-Carboxylates

Both electronic-rich and neutral boronic acids gave good yields, while electron-withdrawing boronic acids did not work as well under the reaction conditions. Using the more electron deficient *O*-pentafluorobenzoyl derived oximes completely suppressed the boronic acid homocoupling side reaction. The reaction with the aryl boronic acids could be carried out in

air; however, a copper(I) salt and an inert atmosphere were required when organostannanes were employed.

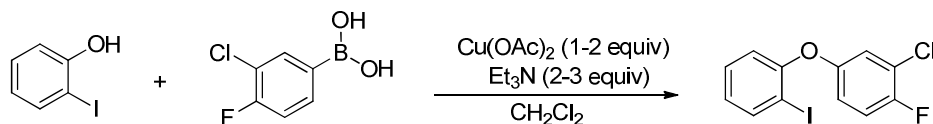
In addition, Liebeskind and co-workers also developed an *N*-amidation reaction which involved the coupling of organostannanes and boronic acids with *O*-acetyl hydroxamic acids in the presence of a Cu catalyst to afford *N*-arylated amides (Scheme 1.10).⁴⁰



Scheme 1.10: *N*-Amidation Reaction with *O*-Acetyl Hydroxamic Acids

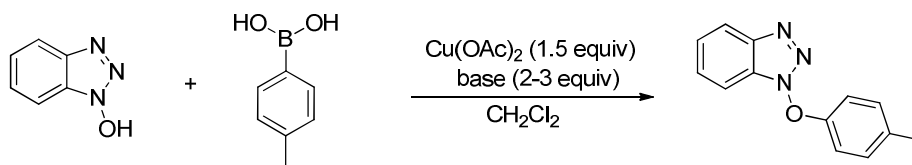
1.3.3 C–O Bond Formation

The first report for C(aryl sp^2)–O bond formation was from Chan and co-workers in 1998 (Scheme 1.11). When a phenol was treated with an arylboronic acid in the presence of stoichiometric $\text{Cu}(\text{OAc})_2$ and a base in dichloromethane at room temperature for one to two days, the corresponding diaryl ethers were obtained in good yields.²⁹



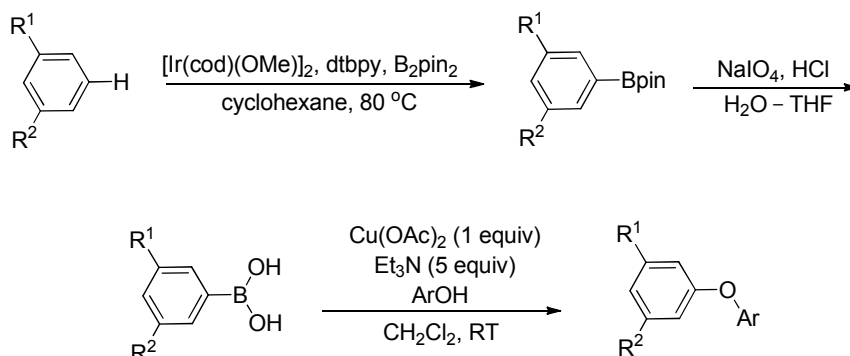
Scheme 1.11: C(aryl sp^2)–O Bond Formation through a Cross-Coupling Reaction

Lam and co-workers extended the methodology to the *O*-arylation of substrates containing an *N*-hydroxy functionality (Scheme 1.12). They reported the *O*-arylation of *N*-hydroxybenzotriazole with *p*-tolylboronic acid to provide the corresponding *O*-phenylated product.⁴¹



Scheme 1.12: *O*-Arylation of *N*-Hydroxybenzotriazoles with *p*-Tolylboronic Acid

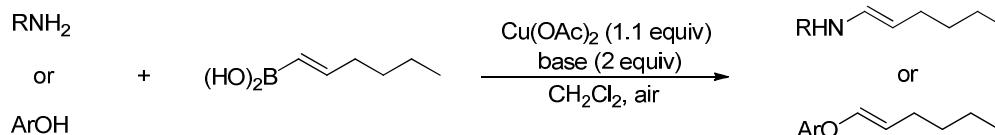
This C–O bond forming arylation methodology was also used in a progression by Hartwig and co-workers for the synthesis of 3,5-disubstituted aryl ethers by a sequential iridium-catalyzed C–H borylation followed by the hydrolysis of the boronic esters with aqueous sodium periodate to the corresponding boronic acids, and a copper-mediated coupling of the crude boronic acids with phenols (Scheme 1.13).⁴²



Scheme 1.13: Hartwig's Synthesis of 3,5-Disubstituted Aryl Ethers

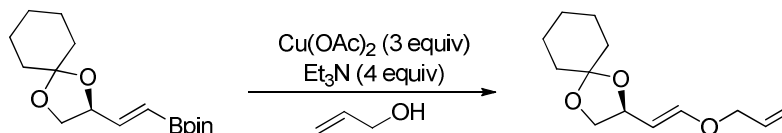
1.3.4 Chan-Lam Coupling With Alkenyl Boronic Acids

Lam and co-workers also discovered that alkenyl boronic acids undergo analogous copper-promoted alkenylation with N–H or O–H nucleophiles as that reported with aryl boronic acids (Scheme 1.14).⁴¹



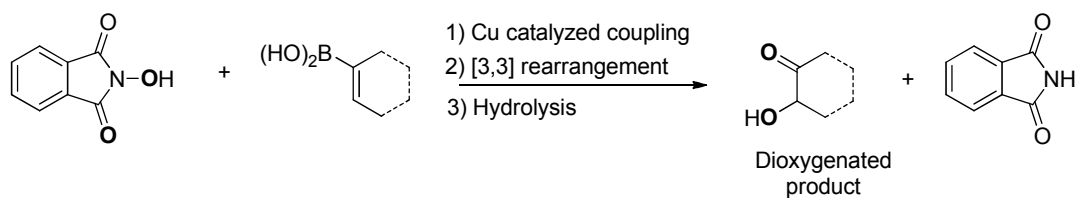
Scheme 1.14: With Alkenyl Boronic Acids

Since vinyl boronic acids are more challenging to handle than aryl boronic acids, similar Cu-mediated conditions for C–O and C–N bond forming reactions have been developed for trivinyl boroxines,⁴³ vinyl pinacolates² or the alkenyltrifluoroborate salts⁴⁴ have been used. One of the most significant advances in this area is the Merlic group's development of an allyl vinyl ether synthesis using vinyl boronates with aliphatic or allylic alcohols in the presence of anhydrous copper(II) acetate (Scheme 1.15). This reaction provides simple access to allyl vinyl ethers which are usually difficult to prepare.⁴⁵



Scheme 1.15: Copper-Promoted Coupling of Vinyl Boronates with Aliphatic Alcohols

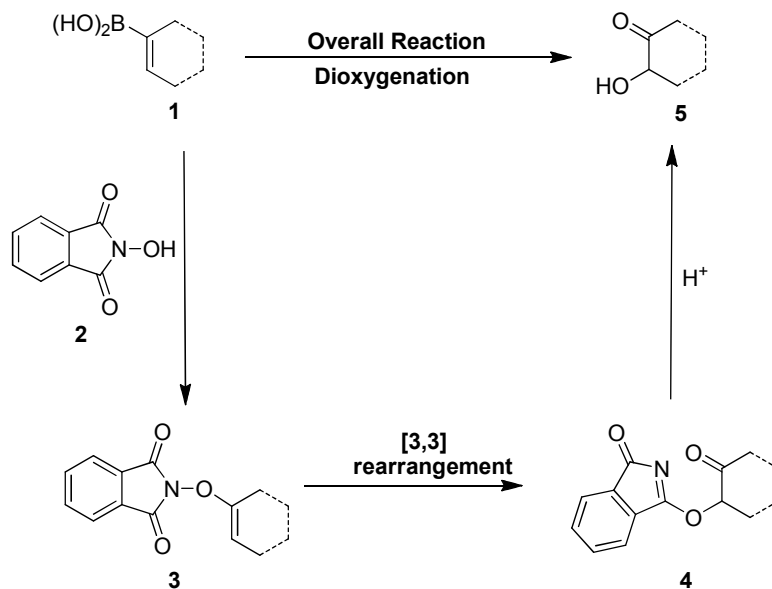
We have been successful in diversifying the reactions of alkenyl boronic acids to include dioxygenation and the synthesis of α -oxygenated ketones, by applying the Chan-Lam coupling with *N*-hydroxyphthalimide, to form a new C–O bond. The overall reaction for this process is shown below (Scheme 1.16).



Scheme 1.16: Overall Reaction for Dioxygenation Process

1.4 Dioxygenation Scheme

Towards the goal of alkenyl boronic acid dioxygenation, we have developed a novel etherification of an alkenyl boronic acid **1** with *N*-hydroxyphthalimide **2** to form an *N*-enoxyphthalimide **3**. This *N*-enoxyphthalimide, **3**, can undergo a formal [3,3] rearrangement, to give an α -oxygenated aldehyde or ketone in the form of an imidate **4** (Scheme 1.17).



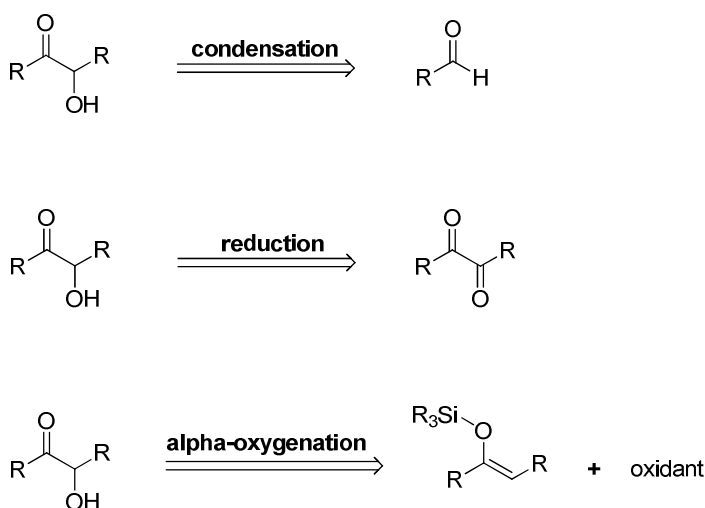
Scheme 1.17: Dioxygenation of Alkenyl Boronic Acids

Hydrolysis of the imidate **4** cleaves the C–O bond and furnishes the desired α -oxygenated carbonyl compound **5**. Thus, this new process effectively involves the

introduction of two atoms of oxygen onto the alkenyl boronic acid, converting it to an α -oxygenated aldehyde or ketone and hence has been termed as ‘dioxygenation’. Overall, this process provides α -hydroxy or α -benzoyloxy ketones in three steps from simple starting materials.

1.5 α -Oxygenated Ketones

Although α -oxygenated ketones are found in a number of natural products and drugs, the synthesis of this functional group has proved to be quite a challenge. The conventional methods for α -oxygenation of carbonyl compounds have been shown below in Scheme 1.18.



Scheme 1.18: Retrosynthetic Pathways for α -Oxygenation of Carbonyl Compounds

The first retrosynthetic pathway involves C–C bond formation through a condensation reaction such as an acyloin⁴⁶ or benzoin condensation.⁴⁷ An acyloin condensation is a reductive coupling of two esters using metallic sodium and the benzoin condensation, first reported in 1832, utilizes a cyanide nucleophile or an *N*-heterocyclic carbene to mediate the reaction between two aromatic aldehydes.⁴⁸ Aliphatic aldehydes can

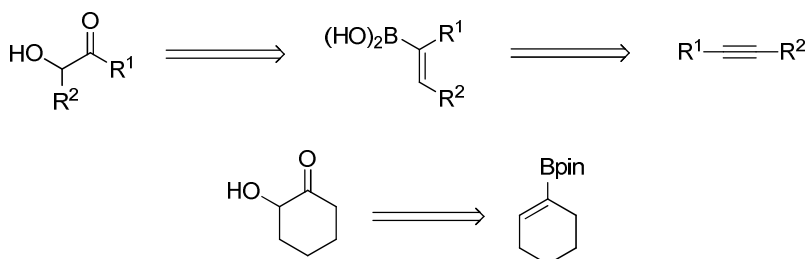
be used in the benzoin condensation when the catalyst employed is a thiazolium salt.⁴⁹ Although both the acyloin and benzoin condensation have been extensively studied and several modifications have been proposed, they are severely limited by the narrow spectrum of reagents that can be utilized. The acyloin condensation is mostly restricted to esters, while the benzoin condensation works best when one of the coupling partners is benzaldehyde.

The second retrosynthetic pathway involving the reduction of diketones to form a new C–O bond was reported by Shimizu in 2000.⁵⁰ This reaction allows access to α -hydroxy ketones and is excellent for symmetrical diketones. When asymmetric diketones are used, the reduction reaction is difficult to control and since either ketone can be reduced, a mixture of regioisomeric alcohols is obtained. This mixture of alcohols is not easily separable and hence it is hard to obtain pure α -hydroxy ketones in a good yield.

The third retrosynthetic pathway involving the formation of the C–O bond via an oxidation reaction was pioneered by Rubottom in 1974.⁵¹ The Rubottom oxidation employs *m*CPBA as an oxidant for a silyl enol ether to convert the enol ether to an α -oxygenated ketone. Other reagents which are capable of oxidizing a carbonyl compound to an α -oxygenated carbonyl compound are electrophilic oxidation reagents such as peroxides, oxone, hyperoxygenated metals, oxaziridines or hypervalent iodinated reagents.⁵² The aforementioned electrophilic oxygenation reagents provide the oxidized product in good yields, but they are unstable and potentially explosive. Hypervalent iodination reagents are more stable, but the oxidation reaction of a ketone to an α -oxygenated ketone requires the removal of iodobenzene which forms as a byproduct.^{52d} Hence, these methods for α -oxygenation are not very synthetically viable and are difficult to apply to the large scale synthesis of α -oxygenated ketones. Enamine and palladium catalysis has also allowed access

to α -oxygenated ketones, however, enamine catalysis requires the addition of an external electrophilic oxidation reagent while palladium catalysis works on substituted systems providing only tertiary alcohols.⁵³

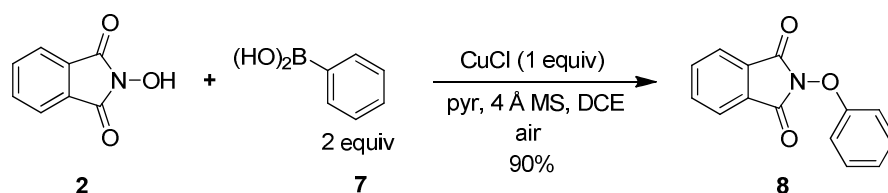
The use of the dioxygenation methodology involving the coupling of *N*-hydroxyphthalimide to alkenyl boronic acids followed by a [3,3] rearrangement and hydrolysis to form α -oxygenated aldehydes and ketones, could be used as an alternative for the synthesis of this exigent functionality. This method avoids the necessity of utilizing carbonyl compounds as precursors for oxidation to the α -oxygenated product. Internal alkynes and commercially available boronate esters have been directly converted to the desired α -oxygenated aldehydes and ketones (Scheme 1.19). Moreover, this methodology circumvents the use of electrophilic oxygenation reagents and the only byproduct from the reaction is phthalimide which is easily removed by base extraction. Also, the nature of the transition state for the [3,3]-sigmatropic reaction allows for the diastereoselective construction of the α -oxygenated stereocenter. Thus, this conversion of alkenyl boronic acids to α -oxygenated ketones provides a unique retrosynthetic disconnection for the preparation of complicated targets containing these challenging motifs.⁵⁴



Scheme 1.19: New Retrosynthetic Pathway for α -Oxygenation

1.6 Arylation of *N*-Hydroxyphthalimide

The first step towards achieving the dioxygenation of alkenyl boronic acids began with the optimization of conditions for the cross-coupling of alkenyl boronic acids and *N*-hydroxyphthalimide to form *N*-enoxyphthalimides. Since the copper-mediated arylation of *N*-hydroxyphthalimide with aryl boronic acids had been reported by Kelly and co-workers in 2001 (Scheme 1.20).⁵⁵

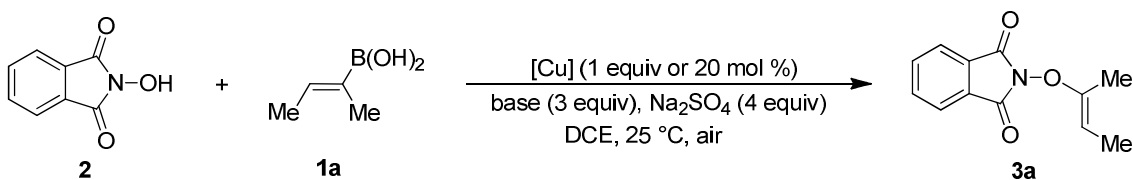


Scheme 1.20: Arylation of *N*-Hydroxyphthalimide

The cross coupling between the *N*-hydroxyphthalimide **2** and phenylboronic acid **7** was carried out by using stoichiometric $\text{Cu}(\text{OAc})_2$ or CuCl . Other Cu (I) or Cu (II) salts were ineffective in promoting the reaction. Three equivalents of the boronic acid were required and pyridine was the best base among the others tested such as Et_3N and DMAP. The yield of the *O*-arylated product **8** did not depend upon the quantity of base used; with 1 equivalent, 5 equivalents and 10 equivalents of base giving similar results. The reaction gave attenuated yields when run under an Argon atmosphere. The reaction could tolerate a wide variety of functional groups including halides, nitriles, aldehydes and esters. Both electron donating and electron deficient boronic acids could be used. After *O*-arylation of the *N*-hydroxyphthalimide, hydrazine was used to remove the phthalimide moiety, akin to Gabriel's synthesis, and release the corresponding aryloxyamine.

1.7 Optimization of Conditions for Coupling of Alkenyl Boronic Acids with *N*-hydroxyphthalimide

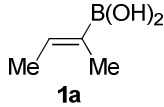
Although the copper-mediated arylation of *N*-hydroxyphthalimide had been reported, the corresponding process for vinylation had not been reported. Mixtures of copper salts, bases, desiccants as well as equivalents of reagents were tested for their efficacy in promoting the coupling reaction between *N*-hydroxyphthalimide **2** and the alkenyl boronic acid derived from 2-butyne **1a** (Scheme 1.21). The results are shown in Table 1.1.



Scheme 1.21: Etherification of *N*-Hydroxyphthalimide with Alkenyl Boronic Acids

As shown in entries 1-4 of Table 1.1, the use of 2 equivalents of boronic acid **1a** provided a higher yield of the *N*-enoxyphthalimide **3a** for both the copper-mediated and the copper-catalyzed transformations, although the difference in reaction efficiency was more striking for the catalytic process. Cu(OAc)₂ was shown to be the optimal catalyst when compared to other Cu(I) and Cu(II) salts (entries 5-9, Table 1.1) and pyridine was shown to be the optimal base when compared to other amines and inorganic bases (entries 10-13, Table 1.1). Neither the copper-mediated nor the copper-catalyzed coupling reaction showed any conversion to the desired product when run in the absence of air, and both transformations required the use of a halogenated solvent. The cross coupling process was fairly insensitive to the choice of desiccant; 4Å molecular sieves and MgSO₄ gave the desired product in only slightly attenuated yields. The optimization study concluded that treatment of a 1:2 mixture of *N*-

hydroxyphthalimide **2**: alkenyl boronic acid **1** in 1,2-dichloroethane (DCE) with Cu(OAc)₂ (1 equiv or 20 mol%), pyridine (3 equiv), and Na₂SO₄ (4 equiv) in air provided optimal conversion to the desired product **3**.

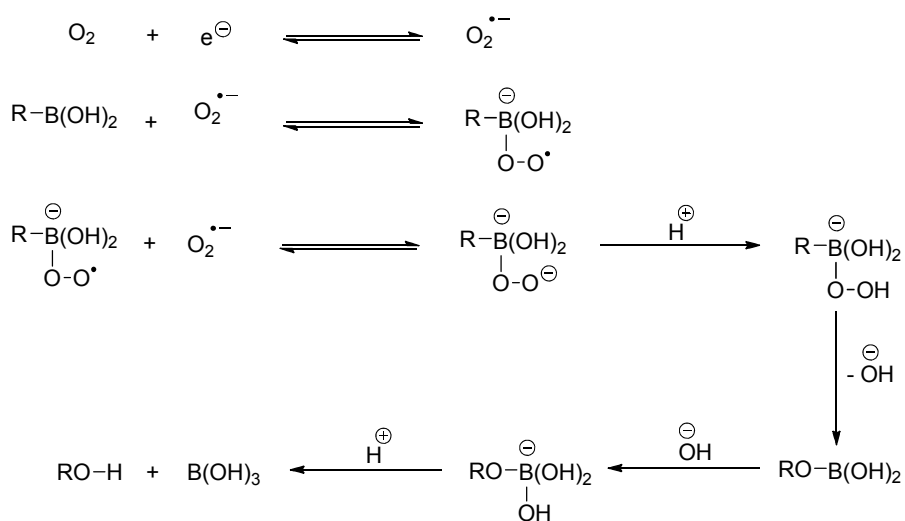
Entry	[Cu]		Base	% Yield ^a
1a				
1	Cu(OAc) ₂ (1 equiv)	1 equiv	pyr	71
2	Cu(OAc)₂ (1 equiv)	2 equiv	pyr	96
3	Cu(OAc) ₂ (20 mol %)	1 equiv	pyr	6
4	Cu(OAc)₂ (20 mol %)	2 equiv	pyr	87
5	CuCl (20 mol %)	2 equiv	pyr	7
6	CuI (20 mol %)	2 equiv	pyr	78
7	Cu(OTf) ₂ (20 mol %)	2 equiv	pyr	8
8	Cu(TFA) ₂ (20 mol %)	2 equiv	pyr	61
9	CuTC (20 mol %)	2 equiv	pyr	81
10	Cu(OAc) ₂ (20 mol %)	2 equiv	Et ₃ N	68
11	Cu(OAc) ₂ (20 mol %)	2 equiv	DABCO	NR
12	Cu(OAc) ₂ (20 mol %)	2 equiv	imidazole	NR
13	Cu(OAc) ₂ (20 mol %)	2 equiv	KOtBu	NR

^aYields determined by H¹ NMR spectroscopy with 1,3,5-trimethoxybenzene as an internal standard.

Table 1.1: Optimization of Reaction Conditions for the Coupling Reaction

A rationale for the role of O₂ in the enhancement of the reaction as well as in the decomposition of the boronic acids has been offered by Lam and co-workers¹ for the *N*-arylation of saturated heterocycles which could be applied to the above coupling reaction. The copper salt could co-ordinate to the hydroxyl group of the *N*-hydroxyphthalimide **2**.

After deprotonation by pyridine, the copper complex could undergo transmetalation with the boronic acid **1**. Molecular oxygen could then oxidize the copper complex to Cu(III), facilitating the reductive elimination of the *N*-enoxypthalimide **3**. These strong oxidizing reaction conditions could also lead to peroxide formation which would result in some decomposition of the boronic acid.⁵⁶ This happens through formation of a superoxide anion which reacts with the boronic acid (Scheme 1.22). The resulting radical species is reduced by another superoxide anion to form a peroxy anion. This peroxy anion undergoes protonation to form a boron-peroxide in which the alkyl group undergoes an irreversible migration to the peroxide. After hydrolysis of the resulting species, boronic acid and an alcohol are formed. It is because of this decomposition of the boronic acid that two equivalents are required for the reaction.



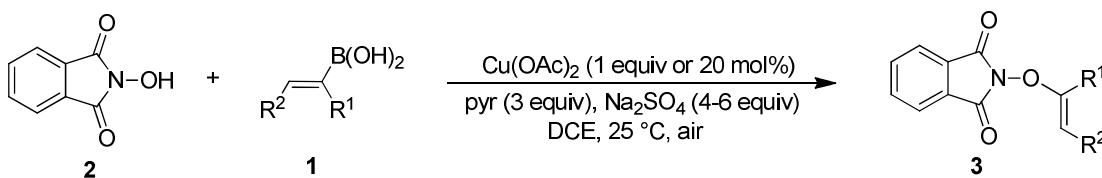
Scheme 1.22: Decomposition of the Boronic Acid in the Presence of O₂

1.8 Evaluation of the Scope of the Transformation

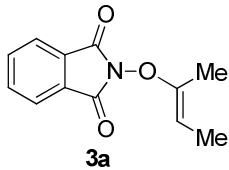
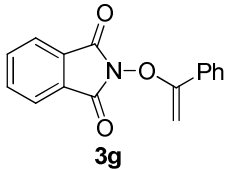
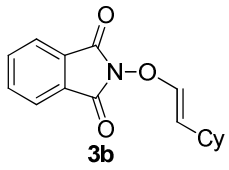
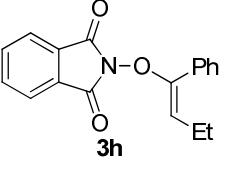
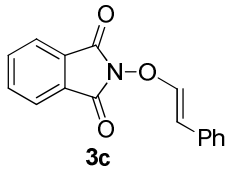
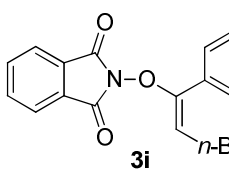
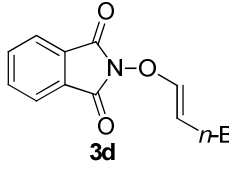
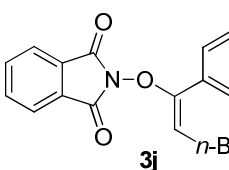
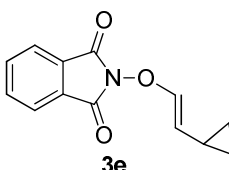
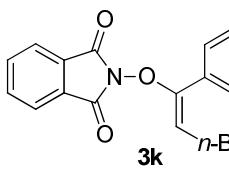
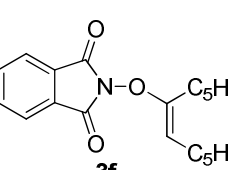
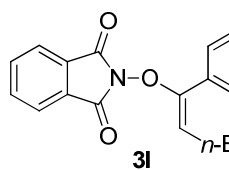
With the optimal conditions for the cross-coupling reaction in hand, the scope of the transformation was evaluated with a variety of alkenyl boronic acids to determine the tolerance for boronic acid substitution patterns.

The coupling reaction between *N*-hydroxyphthalimide **2** and a range of alkenyl boronic acids **1** was carried out using stoichiometric amounts of Cu(OAc)₂ as shown in Scheme 1.23. The reaction was also attempted with catalytic Cu(OAc)₂. Although the yields of the *N*-enoxyphthalimide **3** for the copper-mediated and the copper-catalyzed processes are similar, the reaction times for the copper-catalyzed method are much longer. The results are shown in Tables 1.2, and 1.3.

As shown below, the copper-mediated conditions converted 1- and 2-*trans*-substituted vinyl boronic acids containing both alkyl and aryl systems to the desired product with retention of alkene geometry. *Z*-Disubstituted alkenyl boronic acids which had substituents on the aryl ring also gave moderate to excellent yields. In addition, disubstituted cyclic alkenyl boronic acids were transformed to the desired *N*-enoxyphthalimides **3** under the reaction conditions. We therefore concluded that both alkyl- and aryl substituents were tolerated for the boronic acid coupling partner, as were common aryl electron-withdrawing functional groups such as nitro, fluoro, and trifluoromethyl, and common protecting groups such as ketals. Heterocyclic compounds such as the pyranyl substituted boronic acid also worked well under the reaction conditions.



Scheme 1.23: Evaluating Different Alkenyl Boronic Acids

Entry	Product	Yield ^a	Yield ^b	Entry	Product	Yield ^a	Yield ^b
1		98%	76%**	7		86%	77%
2		87%	70%	8		76%*	67%*
3		88%*	78%*	9		70%*	71%*
4		81%	70%	10		67%*	55%*
5		47%**	—	11		82%*	73%*
6		81%*	77%*	12		63%*	66%*

Yield^a refers to the yield for the Cu-mediated reactions and Yield^b refers to the yields for the Cu-catalyzed reaction.
 (* Indicates compounds made by Dr. Dong-Liang Mo and ** Indicates compounds made by Heng-Yen Wang).

Table 1.2: Scope of the Coupling Reaction with Mono and Disubstituted Boronic Acids

Entry	Product	Yield ^a	Yield ^b	Entry	Product	Yield ^a	Yield ^b
1		73%*	73%*	6		83%**	—
2		83%	76%	7		64%**	—
3		41%**	—	8		91%	89%
4		86%	80%	9		86%*	82%*
5		84%	78%	10		76%**	52%**

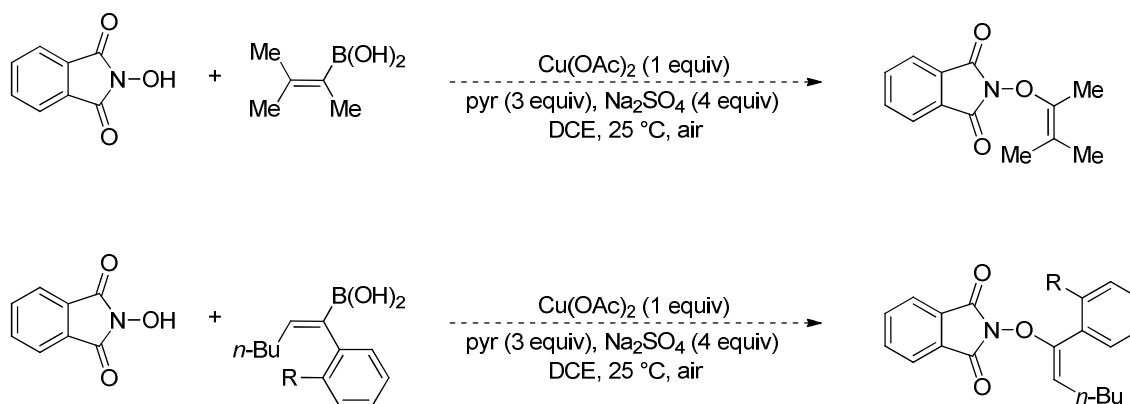
Yield^a refers to the yield for the Cu-mediated reactions and Yield^b refers to the yields for the Cu-catalyzed reaction. (* Indicates compounds made by Dr. Dong-Liang Mo and ** indicates compounds made by Heng-Yen Wang).

Table 1.3: Scope of the Coupling Reaction with Cyclic Boronic Acids

The broad scope of the copper-mediated cross-coupling of *N*-hydroxyphthalimide and alkenyl boronic acids ultimately provided an array of *N*-enoxyphthalimides to screen for the [3,3] rearrangement.

1.9 Limitations of the Methodology

Although both the copper-mediated and the copper-catalyzed transformations have a broad scope and tolerate a number of functional groups, the coupling reaction has a few limitations. Trisubstituted alkenyl boronic acids do not participate in this reaction and neither do alkenyl boronic acids containing *ortho*-substituted aryl groups as shown in Scheme 1.24. This might be because of unfavorable steric interactions between the boronic acid and the copper complex.

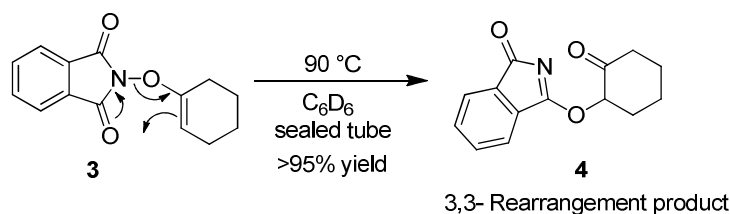


Scheme 1.24: Limitations of the Copper Mediated Coupling Reaction

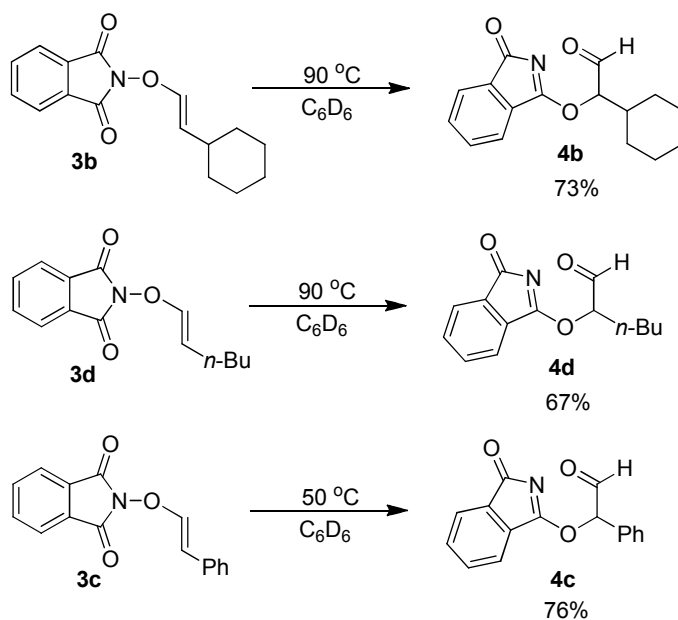
1.10 [3,3] Rearrangement to Form the Imidates

Solutions of the *N*-oxyphthalimides **3** in C₆D₆ or toluene were heated at 80-90 °C for 10-16 h to promote a [3,3] rearrangement and afford dioxygenated alkenyl boronic acids as imidates (Scheme 1.25). These rearrangements occurred in almost quantitative yields, as determined by comparison to an internal standard by H¹ NMR spectroscopy; however, the imidates were unstable when subjected to silica gel chromatography and hence could not be isolated. The α -oxygenated ketones (in the form of imidates) were immediately subjected to the hydrolysis without further purification. The α -oxygenated aldehydes (in the form of

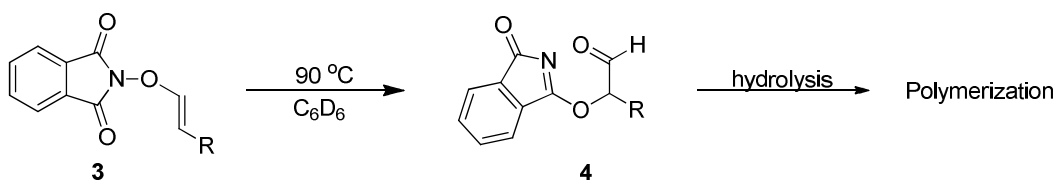
imidates) (Scheme 1.26) were not subjected to the hydrolysis conditions to avoid polymerization of the corresponding α -hydroxy aldehydes which would be the product of hydrolysis of the imidates (Scheme 1.27).



Scheme 1.25: [3,3] Rearrangement of the *N*-Enoxyphthalimides to Afford Imidates



Scheme 1.26: Formation of α -Oxygenated Aldehydes



Scheme 1.27: Polymerization of the α -Oxygenated Aldehydes

1.11 Trends in the [3,3] Rearrangement

Several aryl-substituted *N*-enoxyphthalimides exhibited thermal reactivity patterns that suggested trends in the [3,3] rearrangement activity of these compounds. *N*-Enoxyphthalimide **3c** (entry 1, Table 1.4) readily formed the α -oxygenated aldehyde when heated to only 50 °C. This transformation is in contrast to the *N*-enoxyphthalimides **3b** and **3d** (entries 2 and 3, Table 1.4), which rearranged at 90 °C, and **3g**, (entry 4), which exhibited no rearrangement reactivity even when heated to 130 °C. *N*-Enoxyphthalimides with substitution patterns such as **3h** (entry 5 in Table 1.4) with an aryl group and an alkyl group at the 2-position, underwent rearrangements to afford the corresponding imidate product at 80 °C, however, the addition of an electron-donating group to the aryl ring once again reduced the rearrangement temperature to 25-50 °C (**3w**, entry 6, Table 1.4).

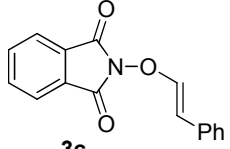
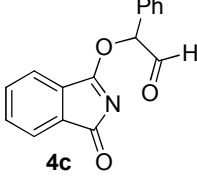
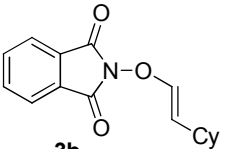
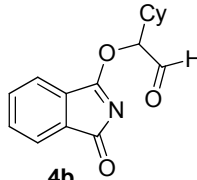
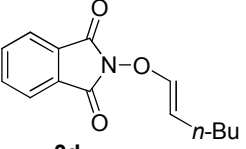
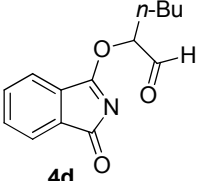
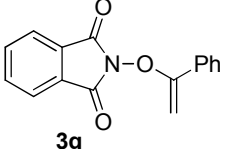
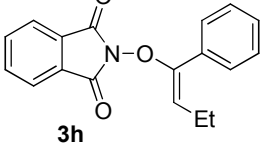
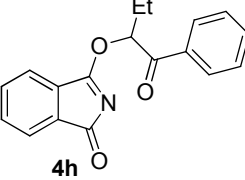
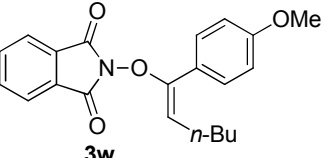
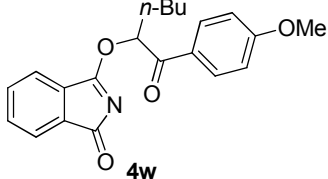
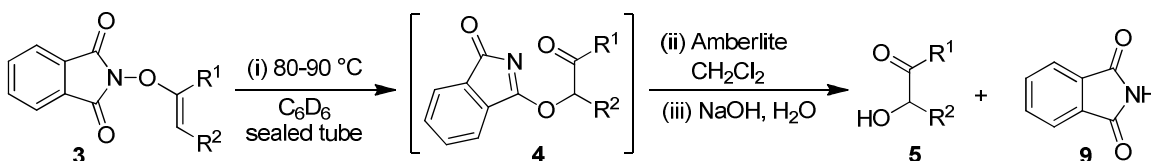
Entry	Compound	Rearrangement Product	Temperature for Rearrangement
1	 3c	 4c	50 °C
2	 3b	 4b	90 °C
3	 3d	 4d	90 °C
4	 3g	No Rearrangement	25-130 °C
5	 3h	 4h	80 °C
6	 3w	 4w	25-50 °C

Table 1.4: Trends in the [3,3] Rearrangement

1.12 Isolation of α -Hydroxy Ketones

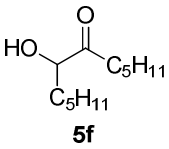
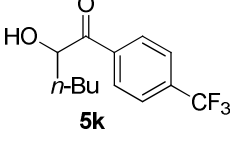
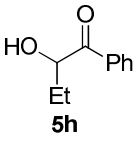
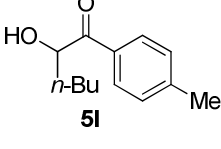
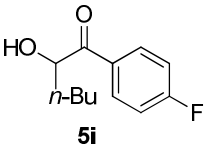
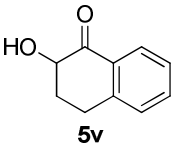
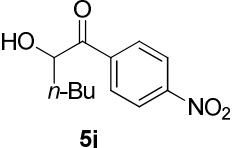
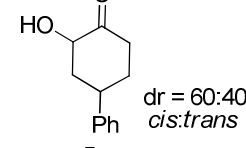
Since the imidate products **4** of the [3,3] rearrangement of the *N*-enoxyphthalimides **3** were unstable to chromatography conditions, solutions of the imidates were directly

subjected to the next step which was hydrolysis to cleave the C–O bond and liberate the α -hydroxy ketones. An ion-exchange resin, Amberlite IR 140 provided optimal yields for the cleavage of the phthalimide, but silica gel was similarly effective with longer reaction times. The phthalimide byproduct, **9**, that formed upon the hydrolysis was removed by base extraction using 1M NaOH (Scheme 1.28).



Scheme 1.28: Isolation of α -Hydroxy Ketones

The α -hydroxy ketones **5** that could be isolated immediately after hydrolysis were those that contained a bulky aryl substituent (**5h–5l**, **5v**, and **5s**) or a long chain alkyl group (**5f**) which made them non-volatile and water insoluble. The α -hydroxy ketones **5** isolated in this manner are shown below in Table 1.5. Substrates with the fluoro, trifluoromethyl, nitro and methyl substituents on the aryl ring were tolerated through both the rearrangement and hydrolysis. These compounds exhibit good yields for the α -hydroxylation sequence. For the compound **5s**, (entry 8, Table 1.5) a mixture of diastereomers was obtained. Upon conducting extensive nOe experiments on **5s**, it was confirmed that a 60:40 mixture of *cis:trans* diastereomers was obtained. The *cis* diastereomer which is the thermodynamically favored product was the major isomer.

Entry	Product	Yield	Entry	Product	Yield
1		78%	5		86%
2		90%	6		82%
3		88%	7		87%
4		75%	8		82%

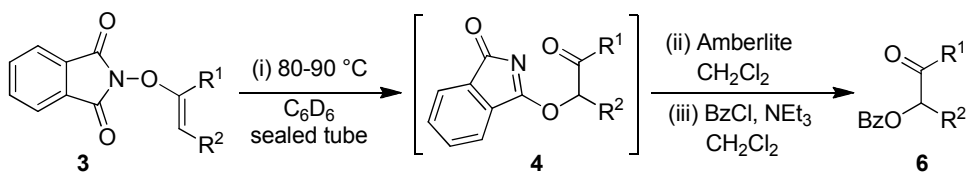
These compounds were made by Dr. Dong-Liang Mo, except compound 8 which was made by Heng-Yen Wang.

Table 1.5: α -Hydroxy Ketones Isolated following the Dioxygenation Scheme

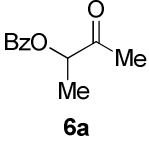
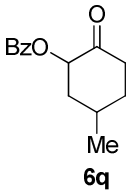
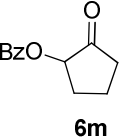
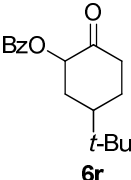
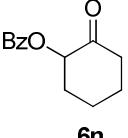
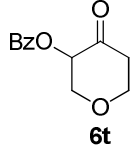
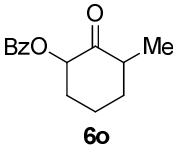
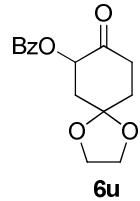
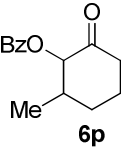
1.13 Isolation of α -Benzoyloxy Ketones

The α -hydroxy ketones **5** which were either water soluble or volatile were protected in solution immediately after the hydrolysis using benzoyl chloride and a base (Scheme 1.29).

These ketones could then be isolated as their corresponding benzoates (Table 1.6).



Scheme 1.29: Isolation of α -Benzoyloxy Ketones

Entry	Product	Yield	Entry	Product	Yield
1	 6a	86%	6	 6q	65% dr = 55:45 cis:trans
2	 6m	66%*	7	 6r	66%** dr = 75:25 cis:trans
3	 6n	67%	8	 6t	69%
4	 6o	66%** dr = 20:80 cis:trans	9	 6u	63%*
5	 6p	69% dr = 55:45 cis:trans			

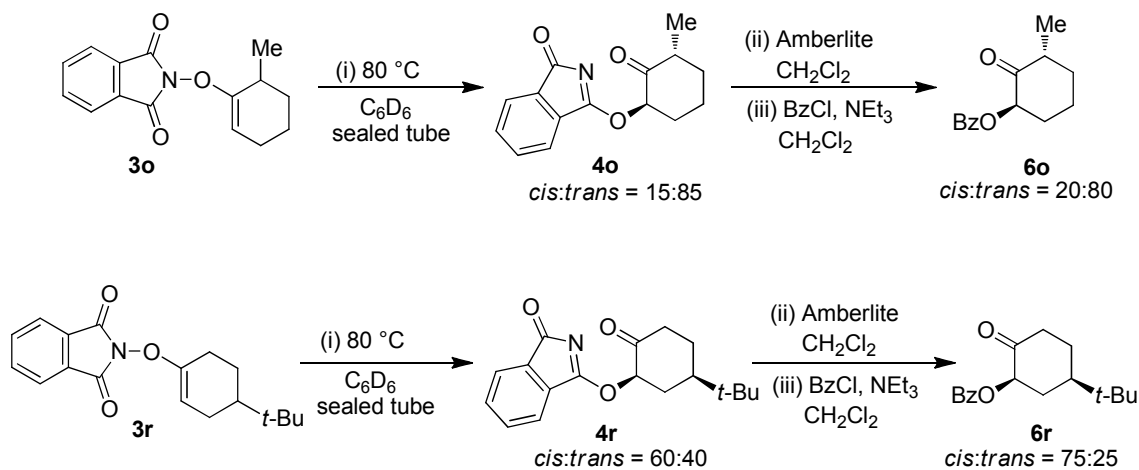
(* Indicates compounds made by Dr. Dong-Liang Mo and ** indicates compounds made by Heng-Yen Wang)

Table 1.6: α -Benzoyloxy Ketones Isolated following the Dioxygenation Scheme

1.14 Diastereoselectivity Trends in the Rearrangement

The benzoyloxy ketones **6** derived from 3- and 4- substituted cyclohexenyl boronic acids (**6p-6r**, entries 5-7 in Table 1.6) were obtained in 55:45 and 75:25, *cis/trans* diastereomeric ratios, respectively. For all these compounds, the *cis* product, which is the thermodynamically favored product, is the major although the difference is more evident for **6r** which has the bulky *t*-butyl substituent at the 4- position on the cyclohexanone ring. This is in contrast to **6o** (entry 4, Table 1.6) which has a methyl group at the 6- position on the cyclohexanone ring. For this substrate, the diastereomeric ratio obtained was 20:80 favoring the more unstable *trans* diastereomer, thus indicating that the [3,3] rearrangement to form this product was under kinetic control.

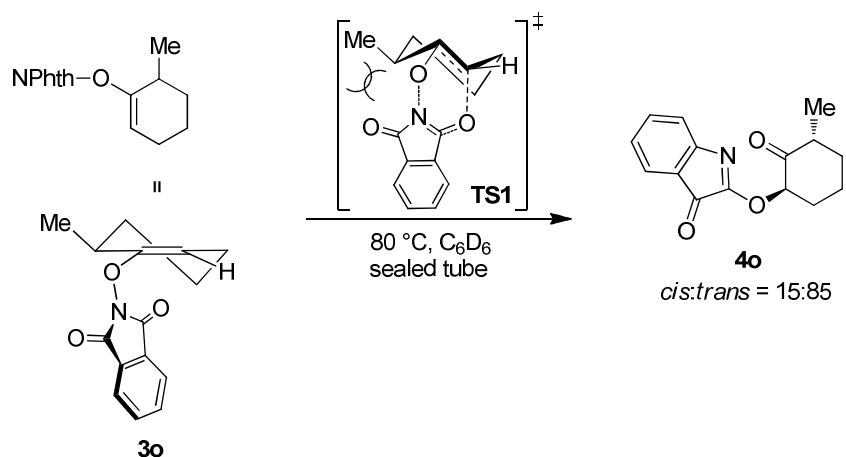
Compounds **3o**, **3p** and **3q** (entries 3-5, Table 1.4) underwent [3,3] rearrangements to give 15:85 (for **4o**), 50:50 (for **4p**, **4q**) *cis/trans* diastereomeric mixtures of the imidate products and subsequent hydrolysis formed compounds **6o**, **6p** and **6q** (entries 4-6, Table 1.6) with no significant change in the diastereomeric ratio. However, hydrolysis and protection of **3r**, containing a bulky *t*-Bu substituent (entry 6, Table 1.3) epimerized the α -benzoyl group, resulting in a change in the *cis/trans* diastereomeric ratio of 60:40 to 75:25 as shown in Scheme 1.30.



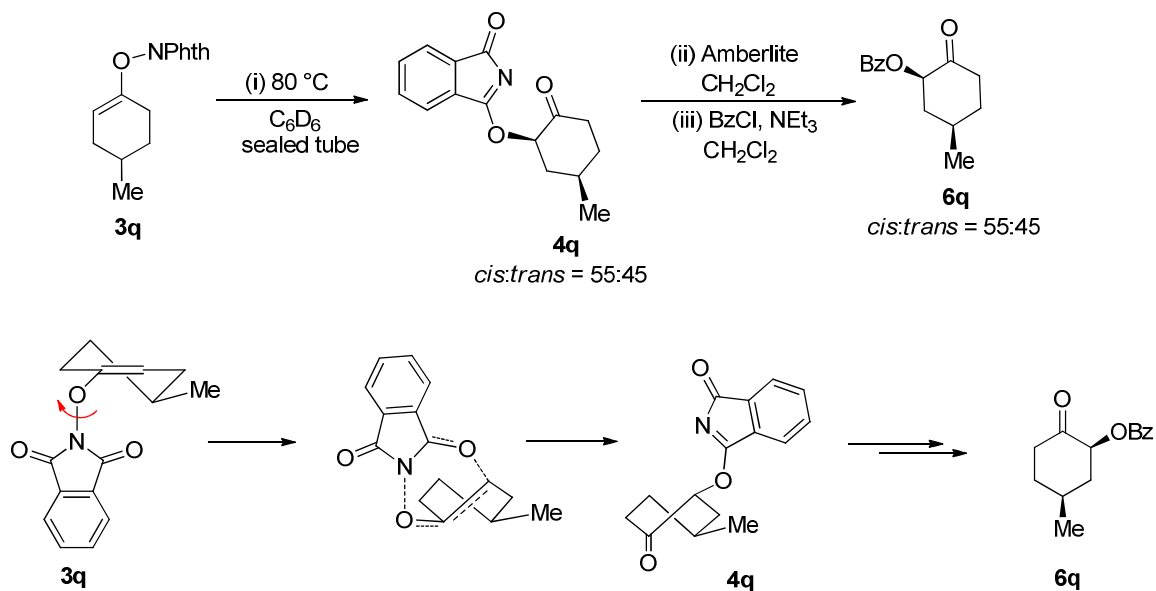
Scheme 1.30: Effect of Hydrolysis on the Diastereoselectivity

Surprisingly, the rearrangement to form **6o** (entry 4, Table 1.6) strongly favors formation of the *trans* diastereomer. It was assumed that this result is due to minimization of steric interactions as the rearrangement to form **4o** occurs via a chair transition state (TS1) in Scheme 1.31. In contrast to 4-substituted cyclohexenyl substrates such as **3q**, rotation for the approach of the carbonyl oxygen from the higher energy twist conformation to provide the *cis* diastereomer (Scheme 1.32) is inaccessible for **3o**, because of the 6-methyl substituent, which inhibits rotation of the *N*-enoxyphthalimide **3o** around the C–O bond. A moderate increase in the *cis/trans* ratio from 15:85 to 20:80 was observed upon hydrolysis and protection.

To the best of our knowledge, the diastereomeric ratio observed for **6o** represents the highest observed in favor of the *trans* isomer for 2-methylcyclohexanone α -oxygenation.⁵⁷ This implies that the dioxygenation of alkenyl boronic acids may not only provide a new retrosynthetic disconnection for the preparation of α -oxygenated carbonyl compounds, but also provides access to relative stereochemical patterns not readily available through enolate oxidation procedures.



Scheme 1.31: Hindered Rotation Leads to the Kinetic Product

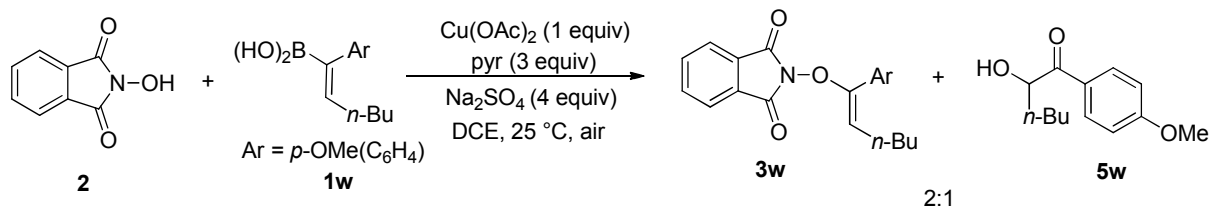


Scheme 1.32: Rotation of C–O Bond Results in Formation of Thermodynamic Product

1.15 Single Purification Sequence

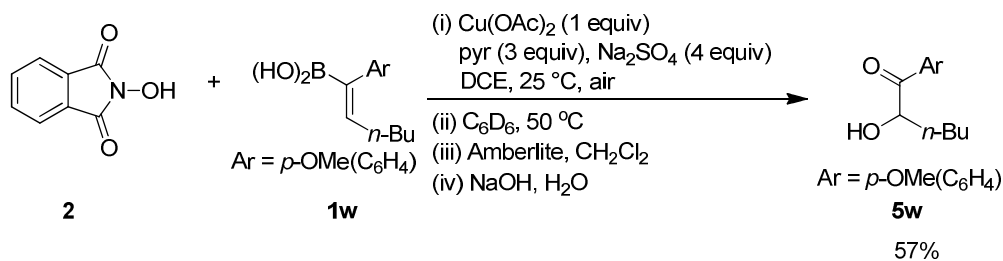
During the reaction with an alkenyl boronic acid with a methoxy substituent on the aryl group, it was noticed that the product of the coupling reaction was a 2:1 mixture of the coupling and the α -hydroxy ketone **3w:5w** (Scheme 1.33). This inspired us to determine if

the α -hydroxy ketones could be accessed with only a single purification step from the boronic acids.



Scheme 1.33: Using an Alkenyl Boronic Acid with an Electron Donating Aryl Substituent
(This work was done by Dr. Dong-Liang Mo).

To carry out this single purification sequence, the reaction mixture of the *N*-hydroxyphthalimide **2** and boronic acid **1w** was passed through silica gel to remove the Cu(OAc)₂. This was followed by heating the crude product to 50 °C for 10 h and hydrolysis, to give the α -hydroxy ketone **5w** in 57% yield over three steps (Scheme 1.34).

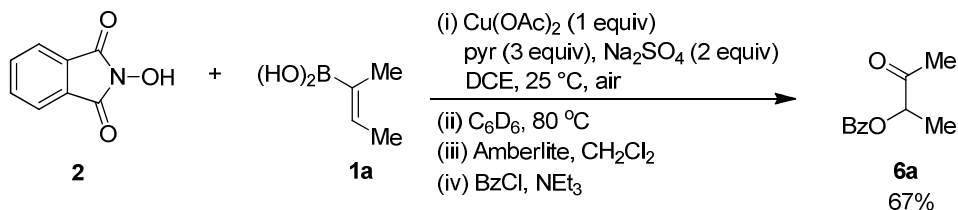


Scheme 1.34: Single Step Purification Sequence

(This work was done by Dr. Dong-Liang Mo.)

A similarly efficient process was also observed for the transformation of a *Z*-disubstituted dialkyl boronic acid **1a** to a α -benzyloxy ketone **6a** in 67% overall yield with no formal purification of intermediates, only the removal of Cu(OAc)₂ prior to rearrangement.

The final product, the α -benzoyloxy ketone **6a** was purified on silica gel, the only purification in the sequence (Scheme 1.35).



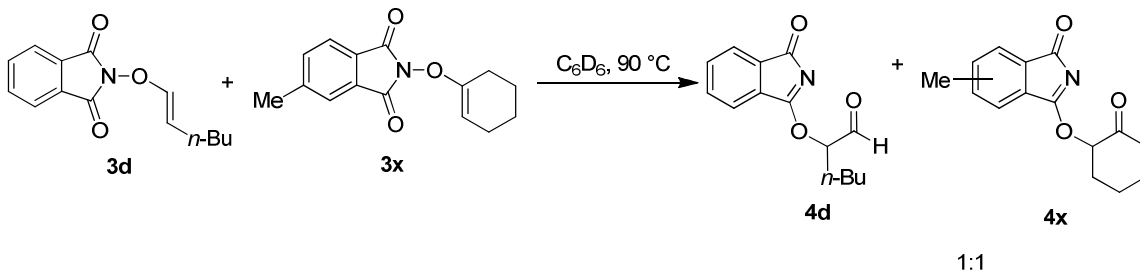
Scheme 1.35: Single Step Purification with a Dialkyl Boronic Acid

1.16 Exploring the Mechanism for the Reaction

For the future endeavors, to make the dioxygenation stereoselective, it was necessary to probe the mechanism of the reaction. It was imperative to comprehend whether the reaction was intermolecular or intramolecular and whether it followed a radical pathway. The understanding of the nature of the transition state in the pericyclic reaction would provide valuable information that could be used in controlling the stereochemistry for the rearrangement.

1.16.1 Cross-Over Experiment

The diastereoselectivity observed for the rearrangement of the substituted cyclohexenyl boronic acids suggested that the [3,3] rearrangements of *N*-enoxypthalimides **3** proceeded by a unimolecular pericyclic reaction. The intramolecular nature of the transition state was further supported by a crossover experiment using *N*-enoxypthalimides **3d** and **3x** shown below in Scheme 1.36.

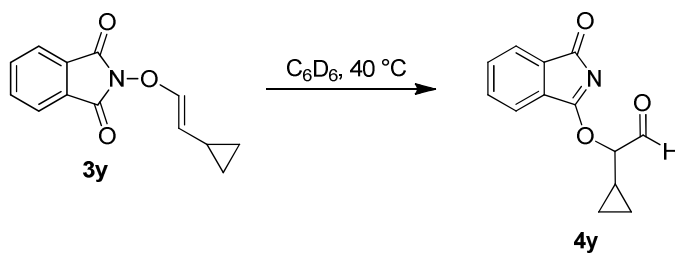


Scheme 1.36: Cross-Over Experiment

When a 1:1 mixture of these compounds, the *N*-enoxypthalimide derived from hexenyl boronic acid **3d** and the *N*-enoxypthalimide containing a methyl substituent on the benzene ring and derived from the cyclohexenyl boronic acid **3x**, was heated in C_6D_6 at $90\text{ }^\circ\text{C}$ for 18 h, the only products obtained were from the intermolecular reaction **4d** and **4x** and there was no evidence of crossover by ^1H or ^{13}C NMR spectroscopy.

1.16.2 Radical Clock Experiment

To investigate the possibility of a radical reaction pathway, a radical clock experiment was tested with *N*-enoxypthalimide bearing a vinyl cyclopropyl group **3y**. Upon heating this substrate in either the presence or the absence of Bu_3SnH (Scheme 1.37), no indication of the formation of an α,β -unsaturated aldehyde was observed, suggesting that the [3,3] rearrangement occurs through a two electron pathway and does not follow a radical pathway. This work was done by Heng-Yen Wang.



Scheme 1.37: Radical Clock Experiment

1.17 Conclusion

In summary, the dioxygenation of alkenyl boronic acids **1** with *N*-hydroxyphthalimide **2** has been achieved through a two-step process involving copper-mediated etherification to form an *N*-enoxyphthalimide **3** and a subsequent [3,3] rearrangement to provide α -hydroxy ketones **5** or α -benzoyloxy ketones **6** after hydrolysis of the phthalimide imidate **4**. This transformation provides a new retrosynthetic disconnection for the preparation of α -oxygenated carbonyl compounds directly from internal alkynes and does not require the use of a highly reactive electrophilic oxygen source or a carbonyl compound as a starting material.

1.18 Supporting Information

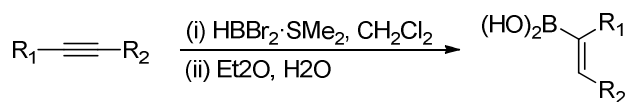
1.18.1 General Experimental Information

^1H NMR and ^{13}C NMR spectra were recorded at ambient temperature using 500 MHz spectrometers. The data are reported as follows: chemical shift in ppm from internal tetramethylsilane on the δ scale, multiplicity (br = broad, s = singlet, d = doublet, t = triplet, q = quartet, m = multiplet), coupling constants (Hz), and integration. High resolution mass spectra were acquired on an LTQ FT spectrometer, and were obtained by peak matching. Melting points are reported uncorrected. Analytical thin layer chromatography was performed on 0.25 mm extra hard silica gel plates with UV254 fluorescent indicator. Liquid chromatography was performed using forced flow (flash chromatography) of the indicated solvent system on 60Å (40 – 60 μm) mesh silica gel (SiO_2). Medium pressure liquid chromatography was performed to force flow the indicated solvent system down columns packed with 60Å (40 – 60 μm) mesh silica gel (SiO_2). Unless otherwise noted, all reagents

were obtained from commercial sources and, where appropriate, purified prior to use. THF, CH₂Cl₂, and toluene were dried by filtration through alumina according to the procedure of Grubbs.¹ TMEDA was distilled over CaH₂ and stored under N₂ prior to use. Amberlite-IR120 was washed with CH₂Cl₂ prior to use. Boronic acids 1b and 1c were commercially available from Aldrich and used as received. Boronic acids 1d and 1e were prepared according to a literature procedures. Boronic acids used for the preparation of *N*-enoxypthalimides that were not commercially available were prepared by: 1) hydroboration of the corresponding alkyne with HBBr₂·SMe₂ followed by hydrolysis, 2) hydrolysis of the corresponding boronic acid pinacol ester, or 3) formation of the corresponding vinyl anion from a hydrazone precursor followed by electrophilic trapping by B(OR)₃ and hydrolysis. The boronic acids were used as isolated from these procedures without further purification.

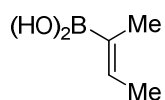
1.18.2 Experimental Procedures and Characterization Data

I. General procedure A: Preparation of boronic acids from alkynes

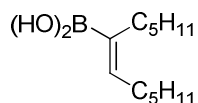


A round bottom flask was flame-dried under N₂, charged with an alkyne (1 equiv) and cooled to 0 °C with an ice-water bath. The alkyne was then diluted with a 1M solution of HBBr₂·SMe₂ in CH₂Cl₂ (1.2 equiv) and allowed to stir for 2 h. The reaction mixture was then transferred to 60 mL of a 10:1 mixture of diethyl ether and water and allowed to stir for 15 minutes. The reaction mixture was then diluted with additional diethyl ether (40 mL) and extracted with water (3 x 5 mL). The organic layer was then dried with brine (10 mL) and MgSO₄ and concentrated under reduced pressure to give a crude sample of the alkenyl

boronic acid. This crude sample was then used for the copper-coupling reaction without further purification. Any impurities carried on to the copper-coupling reaction were not observed to affect the efficiency of the process when compared to the use of a pure sample of boronic acid. The alkyne precursors for **1f** and **1h** are commercially available from Aldrich and were used without further purification. The alkyne precursors for **1i-1l** and **1w** were prepared according to literature procedures.

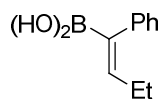
**1a**

2-Butenyl boronic acid 1a: General procedure A was followed using 2-butyne (5.00 g, 92.4 mmol) and a 1M solution of $\text{HBBr}_2 \cdot \text{SMe}_2$ in CH_2Cl_2 (81.0 mL, 81.0 mmol). Hydrolysis and workup gave **1a** as an off-white solid (6.61 g, 82 %). ^1H NMR (500 MHz; CDCl_3): δ 6.83 (q, $J = 6.5$, 1H), 1.80 (d, $J = 6.5$ Hz, 3H), 1.75 (s, 3H); ^{13}C NMR (125 MHz, CDCl_3): δ 143.6, 14.8, 12.7.

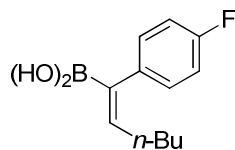
**1f**

6-Dodecen-6-yl boronic acid 1f: General procedure A was followed using 6-dodecyne (3.6 mL, 20 mmol) and a 1M solution of $\text{HBBr}_2 \cdot \text{SMe}_2$ in CH_2Cl_2 (22 mL, 22 mmol). Hydrolysis and workup gave **1f** as an oil (2.74 g, 65%). ^1H NMR (500 MHz; CDCl_3): δ 6.67 (t, $J = 7.0$ Hz, 1H), 2.20-2.19 (m, 4H), 1.43-1.25 (m, 12H), 0.90-0.89 (m, 6H), the OH of the boronic

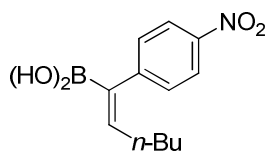
acid was too broad to be observed above the baseline; ^{13}C NMR (125 MHz, CDCl_3): δ 149.2, 32.3, 32.2, 30.1, 28.9, 28.8, 28.0, 22.7, 22.6, 14.1, 14.0, the C-B resonance was too broad to be observed; IR (thin film) 3229, 2956, 2926, 2858, 1462, 1373, 1335, 728 cm^{-1} ; HRMS (Cl^+) m/z calcd. for $\text{C}_{12}\text{H}_{26}\text{BO}_2$ ($\text{M}+\text{H}^+$) 213.2026, found 213.2028.

**1h**

1-Phenyl-1-butynyl boronic acid 1h: A modified version of general procedure A was followed using 1-phenyl-1-butyne (2.8 mL, 20 mmol) and a 1M solution of $\text{HBBr}_2 \cdot \text{SMe}_2$ in CH_2Cl_2 (22 mL, 22 mmol). The mixture of $\text{HBBr}_2 \cdot \text{SMe}_2$ and alkyne was allowed to stir for 12 h at 25 °C and then refluxed for 4h at 70 °C. The reaction mixture was then treated with 105 mL of a 2.5:1 mixture of $\text{Et}_2\text{O}:\text{H}_2\text{O}$ and allowed to stir for 1 h. Workup then gave **1h** as an oil (2.5 g, 71 %). ^1H NMR (500 MHz; CDCl_3): δ 7.62 (d, $J = 7.5$ Hz, 2H), 7.41-7.36 (m, 3H), 6.95 (t, $J = 7.5$ Hz, 1H), 2.26-2.17 (m, 2H), 0.88 (t, $J = 7.0$ Hz, 3H); ^{13}C NMR (125 MHz, CDCl_3): δ 149.1, 129.2, 128.3, 127.6, 125.8, 22.7, 14.2, the C-B resonance was too broad to be observed; IR (thin film) 3303, 2959, 2933, 2850, 1599, 1500, 1337, 1223, 830 cm^{-1} ; HRMS (EI) m/z calcd. for $\text{C}_{11}\text{H}_{15}\text{BO}_2$ ($\text{M}-\text{OH}+\text{MeOH}$) $^+$ 190.1165, found 190.1168 (in MeOH, one of the OH groups was replaced by OMe).

**1i**

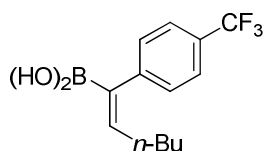
1-(*p*-F-phenyl)-1-hexynyl boronic acid **1i:** A modified version of general procedure A was followed using 1-(*p*-F-phenyl)-1-butyne (1.20 g, 7.00 mmol) and a 1M solution of $\text{HBBr}_2 \cdot \text{SMe}_2$ in CH_2Cl_2 (8.40 mL, 8.40 mmol). The mixture of $\text{HBBr}_2 \cdot \text{SMe}_2$ and alkyne was allowed to stir for 12 h at 25 °C and then refluxed for 4h at 70 °C. The reaction mixture was then treated with 105 mL of a 2.5:1 mixture of $\text{Et}_2\text{O}:\text{H}_2\text{O}$ and allowed to stir for 1 h. Workup gave **1i** as an oil (1.10 g, 74%). ^1H NMR (500 MHz; CDCl_3): δ 7.62-7.59 (m, 2H), 7.04-7.00 (m, 2H), 6.88 (t, $J = 7.0$ Hz, 1H), 2.02-1.99 (m, 1H), 1.42-1.35 (m, 2H), 1.25-1.17 (m, 3H), 0.87 (t, $J = 7.5$ Hz, 3H); ^{13}C NMR (125 MHz, CDCl_3): δ 160.3 (d, $J = 251$ Hz), 152.4, 130.6, 130.5, 114.3 (d, $J = 9.1$ Hz), 31.2, 29.9, 22.3, 13.9, the C-B resonance was too broad to be observed; IR (thin film) 3209, 2959, 2933, 2865, 1597, 1500, 1335, 1223, 830, 732 cm^{-1} ; HRMS (EI) m/z calcd. for $\text{C}_{13}\text{H}_{18}\text{BO}_2\text{F}$ (M-OH+OMe) $^+$ 236.1384, found 236.1386 (in MeOH, one of the OH groups was replaced by OMe).



1j

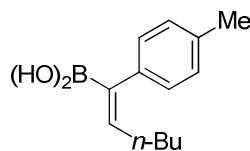
1-(*p*-NO₂-phenyl)-1-hexynyl boronic acid **1j:** A modified version of general procedure A was followed using 1-(*p*-NO₂-phenyl)-1-butyne (1.40 g, 6.90 mmol) and a 1M solution of $\text{HBBr}_2 \cdot \text{SMe}_2$ in CH_2Cl_2 (8.00 mL, 8.00 mmol). The mixture of $\text{HBBr}_2 \cdot \text{SMe}_2$ and alkyne was allowed to stir for 12 h at 25 °C and then refluxed for 4 h at 70 °C. The reaction mixture was then treated with 105 mL of a 2.5:1 mixture of $\text{Et}_2\text{O}:\text{H}_2\text{O}$ and allowed to stir for 1 h. Workup gave **1j** as an oil (1.44 g, 80 %). ^1H NMR (500 MHz; CDCl_3): δ 8.20 (d, $J = 7.5$ Hz, 2H), 7.25 (d, $J = 7.5$ Hz, 2H), 6.90 (t, $J = 7.0$ Hz, 1H), 2.03-2.00 (m, 1H), 1.40-1.31 (m, 2H), 1.24-

1.18 (m, 3H), 0.82 (t, $J = 7.5$ Hz, 3H); ^{13}C NMR (125 MHz, CDCl_3): δ 152.1, 146.6, 132.3, 131.2, 123.5, 32.4, 26.7, 22.1, 13.8, the C-B resonance was too broad to be observed; IR (thin film) 3509, 3008, 2959, 2922, 2855, 1590, 1511, 1323, 1279, 856, 748 cm^{-1} ; HRMS (ESI) m/z calcd. for $\text{C}_{12}\text{H}_{16}\text{NO}_4\text{BNa}$ ($\text{M}+\text{Na}$) $^+$ 272.1070, found 272.1076.

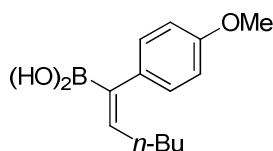


1k

1-(*p*-CF₃-phenyl)-1-hexynyl boronic acid 1k: A modified version of general procedure A was followed using 1-(*p*-CF₃-phenyl)-1-butyne (2.00 g, 8.80 mmol) and a 1M solution of $\text{HBBBr}_2 \cdot \text{SMe}_2$ in CH_2Cl_2 (9.00 mL, 9.00 mmol). The mixture of $\text{HBBBr}_2 \cdot \text{SMe}_2$ and alkyne was allowed to stir for 12 h at 25 °C and then refluxed for 4h at 70 °C. The reaction mixture was then treated with 105 mL of a 2.5:1 mixture of $\text{Et}_2\text{O}:\text{H}_2\text{O}$ and allowed to stir for 1 h. Workup gave **1k** as an oil (2.20 g, 91%). ^1H NMR (500 MHz; CDCl_3): δ 7.49 (d, $J = 8.0$ Hz, 2H), 7.13 (d, $J = 8.0$ Hz, 2H), 6.91 (t, $J = 7.5$ Hz, 1H), 2.18-2.12 (m, 1H), 1.43-1.36 (m, 2H), 1.29-1.24 (m, 3H), 0.88 (t, $J = 7.5$ Hz, 3H); ^{13}C NMR (125 MHz, CDCl_3): δ 153.6, 143.4, 129.3, 129.1, 125.3 (q, $J = 3.8$ Hz), 124.5, 31.2, 29.9, 22.3, 13.8, the C-B resonance was too broad to be observed and the sample was too insoluble to observed further $^{13}\text{C}-^{19}\text{F}$ coupling constants; IR (thin film) 3213, 2959, 2929, 2869, 1612, 1317, 1166, 1126, 1066, 837, 722 cm^{-1} ; HRMS (ESI) m/z calcd. for $\text{C}_{14}\text{H}_{18}\text{O}_2\text{BF}_3$ ($\text{M}-\text{OH}+\text{OMe}$) $^+$ 286.1352, found 286.1346 (in MeOH, one of the OH groups was replaced by OMe).

**11**

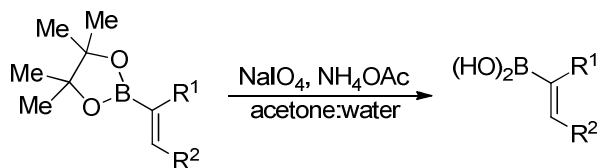
1-(*p*-Me-phenyl)-1-hexynyl boronic acid 11: A modified version of general procedure A was followed using 1-(*p*-Me-phenyl)-1-butyne (1.40 g, 8.10 mmol) and a 1M solution of $\text{HBBr}_2 \cdot \text{SMe}_2$ in CH_2Cl_2 (9.70 mL, 9.70 mmol). The mixture of $\text{HBBr}_2 \cdot \text{SMe}_2$ and alkyne was allowed to stir for 12 h at 25 °C and then refluxed for 4h at 70 °C. The reaction mixture was then treated with 105 mL of a 2.5:1 mixture of $\text{Et}_2\text{O}:\text{H}_2\text{O}$ and allowed to stir for 1 h. Workup gave **11** as an oil (1.10 g, 62%). ^1H NMR (500 MHz; CDCl_3): δ 7.82 (d, $J = 8.0$ Hz, 2H), 7.18 (d, $J = 8.0$ Hz, 2H), 6.88 (t, $J = 7.5$ Hz, 1H), 2.38 (s, 3H), 2.29-2.19 (m, 1H), 1.44-1.34 (m, 2H), 1.31-1.21 (m, 3H), 0.92 (t, $J = 7.5$ Hz, 3H); ^{13}C NMR (125 MHz, CDCl_3): δ 146.1, 135.0, 129.3, 129.0, 128.2, 31.5, 29.8, 21.3, 21.1, 13.9, the C-B resonance was too broad to be observed; IR (thin film) 3203, 2959, 2926, 2873, 1605, 1410, 1380, 1331, 808, 722 cm^{-1} ; HRMS (ESI) m/z calcd. for $\text{C}_{14}\text{H}_{21}\text{O}_2\text{B}$ (M-OH+MeOH) $^+$ 232.1634, found 232.1639 (in MeOH, one of the OH groups was replaced by OMe).

**1w**

1-(*p*-OMe-phenyl)-1-hexynyl boronic acid 1w: A modified version of general procedure A was followed using 1-(*p*-OMe-phenyl)-1-butyne (1.30 g, 7.00 mmol) and a 1M solution of $\text{HBBr}_2 \cdot \text{SMe}_2$ in CH_2Cl_2 (8.40 mL, 8.40 mmol). The mixture of $\text{HBBr}_2 \cdot \text{SMe}_2$ and alkyne was

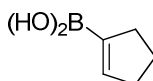
allowed to stir for 12 h at 25 °C and then refluxed for 4h at 70 °C. The reaction mixture was then treated with 105 mL of a 2.5:1 mixture of Et₂O:H₂O and allowed to stir for 1 h. Workup gave **1w** as an oil (1.45 g, 85 %). ¹H NMR (500 MHz; CDCl₃): δ 7.94 (d, *J* = 8.0 Hz, 2H), 7.09 (d, *J* = 8.0 Hz, 2H), 6.97 (t, *J* = 7.0 Hz, 1H), 3.86 (s, 3H), 2.25-2.20 (m, 1H), 1.43-1.35 (m, 2H), 1.29-1.21 (m, 3H), 0.89 (t, *J* = 7.0 Hz, 3H); ¹³C NMR (125 MHz, CDCl₃): δ 163.9, 151.5, 130.8, 130.4, 113.7, 55.3, 34.8, 29.9, 22.4, 14.0, the C-B resonance was too broad to be observed; IR (thin film) 3213, 2952, 2929, 2862, 1605, 1406, 1245, 1170, 1032, 798, 725 cm⁻¹; HRMS (ESI) *m/z* calcd. for C₁₄H₂₁O₃B (M-OH+OMe)⁺ 248.1584, found 248.1593 (in MeOH, one of the OH groups was replaced by OMe).

II. General procedure B: Preparation of boronic acids from boronic acid pinacol esters

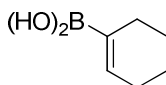


A scintillation vial was charged with alkenyl boronic acid pinacol ester (1 equiv), NaIO₄ (3 equiv), and NH₄OAc (3 equiv). These reagents were then diluted with a mixture of acetone and water in a 1:1 ratio to form a 0.04 M solution of the alkenyl boronic acid pinacol ester. The resulting slurry was allowed to stir vigorously for 2 d. The slurry was then filtered and diluted with ethyl acetate or diethyl ether and extracted with water. The organic layer was then dried with brine and MgSO₄ and concentrated under reduced pressure to give a crude sample of the alkenyl boronic acid. This crude sample was then used for the copper-coupling reaction without further purification. Any impurities carried on to the copper-coupling

reaction were not observed to affect the efficiency of the process when compared to the use of a pure sample of boronic acid. The alkenyl boronic acid pinacol ester precursors for **1n**, **1m**, **1t**, and **1u** are commercially available from Frontier Scientific and were used as received. The alkenyl boronic acid pinacol ester precursors for **1o**, **1p**, **1r**, **1s** were prepared by literature procedures.

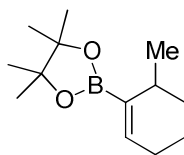
**1m**

1-Cyclopentenyl boronic acid 1m: General procedure B was used with 1-cyclopentenyl boronic acid pinacol ester (0.097 g, 0.50 mmol), NaIO₄ (0.312 g, 1.50 mmol), and NH₄OAc (0.116 g, 1.50 mmol) to give a crude sample of **1m** (0.050 g, 66%). ¹H NMR (500 MHz; CDCl₃): δ 6.83-6.81 (m, 1H), 2.43-2.20 (m, 4H), 1.85-1.79 (m, 2H), the O-H resonances were too broad to be observed; ¹³C NMR (125 MHz, CDCl₃): δ 148.3, 29.3, 28.1, 21.6, the C-B resonance was too broad to be observed; IR (thin film) 2930, 2859, 1626, 1376, 1353, 1320, 1255, 1138, 1070, 1024 cm⁻¹; HRMS (EI) m/z calcd. for C₆H₁₁BO₂ (M-OH+OMe)⁺ 126.0852, found 126.0862 (in MeOH one of the OH groups was replaced by OMe).

**1n**

1-Cyclohexenyl boronic acid 1n: General procedure B was used with 1-cyclohexenyl boronic acid pinacol ester (0.100 g, 0.480 mmol), NaIO₄ (0.308 g, 1.40 mmol), and NH₄OAc (0.111 g, 1.40 mmol) to give a crude sample of **1n** (0.037 g, 61%). ¹H NMR (500 MHz;

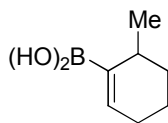
CDCl_3): δ 7.00-6.93 (m, 1H), 2.18-2.09 (m, 4H), 1.63-1.62 (m, 4H), the O-H resonances were too broad to be observed; ^{13}C NMR (125 MHz, CDCl_3): δ 145.8, 27.0, 25.4, 22.6, 22.3, the C-B resonance was too broad to be observed; IR (thin film) 2930, 2859, 1626, 1376, 1353, 1320, 1255, 1138, 1070, 1024 cm^{-1} ; HRMS (ESI) m/z calcd. for $\text{C}_{18}\text{H}_{27}\text{B}_3\text{O}_3$ (3(M-OH)) $^+$ 324.22395, found 324.22467 (mass found for the trimeric anhydride); mp 122 $^\circ\text{C}$.



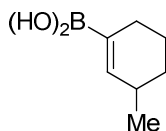
s1

Pinacol ester s1: A 100 mL round bottom flask was flame-dried under N_2 and charged with the N-tosylhydrazone of 2-methylcyclohexanone (1.48 g, 5.28 mmol), hexanes (7.4 mL), and TMEDA (15.8 mL). The resulting slurry was cooled to -78 $^\circ\text{C}$ with a dry ice-acetone bath and a 2.5 M n-BuLi solution in hexane (8.45 mL, 21.1 mmol) was added via syringe. The reaction mixture was allowed to stir at -78 $^\circ\text{C}$ for 1 h and then allowed to warm to 25 $^\circ\text{C}$. After stirring for an additional 1 h, the reaction mixture was cooled to -78 $^\circ\text{C}$ with a dry ice-acetone bath and pinacol isopropyl borate (2.15 mL, 10.6 mmol) was added via syringe. The reaction mixture was allowed to warm to 25 $^\circ\text{C}$ and stir for 3 h. The reaction was quenched with saturated $\text{NH}_4\text{Cl}_{(\text{aq})}$ solution (5 mL) and extracted with diethyl ether. The organic extracts were combined, dried with MgSO_4 , and concentrated under reduced pressure. The crude product was purified by medium pressure chromatography (1:50, ethyl acetate: hexanes) to give a light yellow oil (0.422 g, 36%). ^1H NMR (500 MHz; CDCl_3): δ 6.52-6.51 (m, 1H), 2.36 (d, $J = 5.0$ Hz, 1H), 2.02 (d, $J = 2.5$ Hz, 2H), 1.67-1.62 (m, 2H), 1.52-1.50 (m, 1H), 1.36-1.33 (m, 1H), 1.25 (s, 12H), 1.03 (d, $J = 7.0$ Hz, 3H); ^{13}C NMR (125 MHz,

CDCl₃): δ 142.3, 83.1, 30.6, 30.2, 26.9, 24.6, 21.7, 19.1, the C-B resonance was too broad to be observed above the baseline; IR (thin film) 2978, 2926, 2869, 1628, 1369, 1311, 1213, 1144, 860, 696 cm⁻¹.

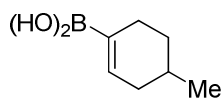
**1o**

6-Methyl-1-cyclohexenyl boronic acid 1o: General procedure B was used with 6-methyl-1-cyclohexenyl boronic acid pinacol ester s1 (0.419 g, 1.89 mmol), NaIO₄ (1.30 g, 6.08 mmol), and NH₄OAc (0.589 g, 7.64 mmol) to give a crude sample of **1o** (0.080 g, 30%) as an amorphous solid. ¹H NMR (500 MHz; CDCl₃): δ 6.93-6.92 (m, 1H), 1.68-1.66 (m, 1H), 1.58-1.56 (m, 1H), 1.47-1.45 (m, 1H), 1.35-1.33 (m, 1H), 1.22-1.18 (m, 1H), 1.10 (d, *J* = 3.5 Hz, 3H), 0.92-0.89 (m, 1H), 0.79 (t, *J* = 7.0 Hz, 1H); ¹³C NMR (125 MHz, CDCl₃): δ 145.7, 30.3, 29.2, 27.2, 21.4, 18.3, the C-B resonance was too broad to be observed above the baseline; IR (thin film) 3388, 2921, 2869, 1621, 1362, 1320, 1158, 1040, 810, 732 cm⁻¹; HRMS (ESI) *m/z* calcd. for C₇H₁₃O₂B (M)⁺ 140.1005, found 140.1009.

**1p**

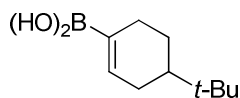
3-Methyl-1-cyclohexenyl boronic acid 1p: General procedure B was used with 3-methyl-1-cyclohexenyl boronic acid pinacol ester (0.100 g, 0.450 mmol), NaIO₄ (0.299 g, 1.40 mmol), and NH₄OAc (0.109 g, 1.40 mmol) to give a crude sample of **1p** (0.050 g, 79%) as an

amorphous solid. ^1H NMR (500 MHz; CDCl_3): δ 6.75-6.73 (m, 1H), 2.27-2.15 (m, 2H), 2.14-2.04 (m, 2H), 1.79-1.72 (m, 2H), 1.51-1.50 (m, 1H), 1.03 (d, $J = 5$ Hz, 3H), the O-H resonances were too broad to be observed; ^{13}C NMR (125 MHz, CDCl_3): δ 151.31, 31.66, 30.97, 25.52, 21.55, 21.18, the C-B resonance was too broad to be observed; IR (thin film) 2959, 2923, 2860, 1623, 1449, 1376, 1313, 1253, 740, 718 cm^{-1} ; HRMS (ESI) m/z calcd. for $\text{C}_{21}\text{H}_{33}\text{O}_3\text{B}_3$ ($3(\text{M-OH})^+$) 366.27090, found 366.27014 (mass found for the trimeric anhydride).

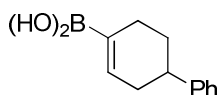


1q

4-Methyl-1-cyclohexenyl boronic acid 1q: General procedure B was used with 6-methyl-1-cyclohexenyl boronic acid pinacol ester (0.106 g, 0.472 mmol), NaIO_4 (0.303 g, 1.41 mmol), and NH_4OAc (0.109 g, 1.41 mmol) to give a crude sample of **1q** as an amorphous solid (0.380 g, 56%). ^1H NMR (500 MHz; CDCl_3): δ 6.91-6.90 (m, 1H), 2.36-2.30 (m, 2H), 2.17-2.10 (m, 1H), 1.77-1.72 (m, 3H), 1.19-1.13 (m, 1H), 0.96 (d, $J = 6.5$ Hz, 3H), the O-H resonances were too broad to be observed; ^{13}C NMR (125 MHz, CDCl_3): δ 145.4, 35.6, 31.0, 28.2, 25.6, 22.0, the C-B resonance was too broad to be observed; IR (thin film) 2952, 2914, 1626, 1379, 1324, 1258, 1229, 1093, 1009, 904.45 cm^{-1} ; HRMS (ESI) m/z calcd. for $\text{C}_{21}\text{H}_{33}\text{B}_3\text{O}_3$ ($3(\text{M-OH})^+$) 366.27090, found 366.27178 (mass found for the trimeric anhydride).

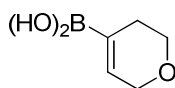
**1r**

4-*t*-Butyl-1-cyclohexenyl boronic acid 1r: General procedure B was used with 4-*t*-Butyl-1-cyclohexenyl boronic acid pinacol ester (0.128 g, 0.485 mmol), NaIO₄ (0.340 g, 1.60 mmol), and NH₄OAc (0.149 g, 1.93 mmol) to give a crude sample of **1r** (0.042 g, 48%). ¹H NMR (500 MHz; CDCl₃): δ 6.94-6.90 (m, 1H), 2.44-2.40 (m, 1H), 2.22-2.18 (m, 1H), 2.09-2.05 (m, 1H), 1.95-1.90 (m, 1H), 1.87-1.84 (m, 1H), 1.31-1.21 (m, 1H), 1.12-1.06 (m, 1H), 0.88 (s, 9H); ¹³C NMR (125 MHz, CDCl₃): δ 146.4, 44.1, 32.4, 29.0, 27.3, 24.2, 17.4, the C-B resonance was too broad to be observed above the baseline; IR (thin film) 2992, 2974, 2959, 2873, 1451, 1428, 1317, 1283, 1234, 882 cm⁻¹; HRMS (ESI) *m/z* calcd. for C₃₀H₅₁O₃B₃ (3(M-OH))⁺ 492.41175, found 492.41161 (mass found for the trimeric anhydride).

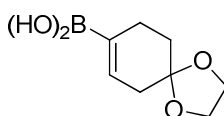
**1s**

4-Phenyl-1-cyclohexenyl boronic acid 1s: General procedure B was used with 4-phenyl-1-cyclohexenyl boronic acid pinacol ester (0.246 g, 0.897 mmol), NaIO₄ (0.603 g, 2.69 mmol), and NH₄OAc (0.353 g, 2.69 mmol) to give a crude sample of **1s** (0.155 g, 86%). ¹H NMR (500 MHz; CDCl₃): δ 7.34-7.30 (m, 2H), 7.25-7.20 (m, 3H), 7.07 (d, *J* = 2.5 Hz, 1H), 2.83-2.81 (m, 1H), 2.52-2.51 (m, 1H), 2.33-2.26 (m, 3H), 2.02-2.00 (m, 1H), 1.75-1.72 (m, 1H), the O-H resonances were too broad to be observed; ¹³C NMR (125 MHz, CDCl₃): δ 145.4, 128.4, 126.9, 126.8, 126.1, 39.9, 35.2, 29.9, 26.2, the C-B resonance was too broad to be

observed; IR (thin film) 3086, 3056, 3027, 2956, 2923, 2855, 1629, 1375, 1340, 1265 cm^{-1} ; HRMS (EI) m/z calcd. for $\text{C}_6\text{H}_9\text{O}_3\text{B}_3$ ($3(\text{M-OH})^+$) 552.31785, found 552.31834 (mass found for the trimeric anhydride).

**1o**

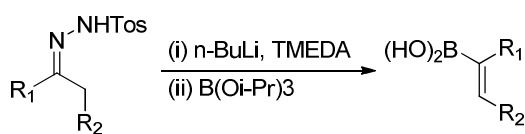
3,6-Dihydro-2H-pyran-4-boronic acid 2o: General procedure B was used with 3,6-dihydro-2H-pyran-4-boronic acid pinacol ester (0.060 g, 0.29 mmol), NaIO_4 (0.183 g, 0.856 mmol), and NH_4OAc (0.066 g, 0.86 mmol) to give a crude sample of **1o** (0.018 g, 48%). ^1H NMR (500 MHz; CDCl_3): δ 6.90-6.89 (m, 1H), 4.26-4.25 (m, 2H), 3.78-3.75 (m, 2H), 2.30-2.29 (m, 2H), the O-H resonances were too broad to be observed; ^{13}C NMR (125 MHz, CDCl_3): δ 144.4, 66.3, 64.3, 25.5, the C-B resonance was too broad to be observed; IR (thin film) 2966, 2926, 2859, 2822, 1635, 1392, 1372, 1317, 1223, 1122 cm^{-1} ; HRMS (ESI) m/z calcd. for $\text{C}_{15}\text{H}_{21}\text{B}_3\text{O}_6$ ($3(\text{M-OH})^+$) 330.16174, found 330.16138 (mass found for the trimeric anhydride); decomp. 130 $^\circ\text{C}$.

**1u**

4-Ketal-1-cyclohexenyl boronic acid 1u: General procedure B was used with 4-phenyl-1-cyclohexenyl boronic acid pinacol ester (0.066 g, 0.25 mmol), NaIO_4 (0.160 g, 0.750 mmol), and NH_4OAc (0.083 g, 0.75 mmol) to give a crude sample of **1u** (0.033 g, 70%). ^1H NMR (500 MHz; CDCl_3): δ 6.83-6.81 (m, 1H), 3.99 (s, 4H), 2.44-2.40 (m, 4H), 1.74 (m, 2H), the

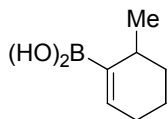
O-H resonances were too broad to be observed; ^{13}C NMR (125 MHz, CDCl_3): δ 149.4, 96.8, 64.5, 34.1, 30.6, 23.5, the C-B resonance was too broad to be observed; IR (thin film) 3416, 2926, 2895, 1631, 1365, 1343, 1114, 1058, 1028 cm^{-1} ; HRMS (ESI) m/z calcd. for $\text{C}_8\text{H}_{13}\text{BO}_4\text{Na}$ ($\text{M}+\text{Na}$) $^+$ 207.0805, found 207.0809; mp 128-130 $^\circ\text{C}$.

III. General procedure C: Preparation of boronic acids from *N*-tosyl hydrazones

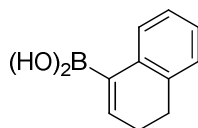


A 100 mL round bottom flask was flame-dried under N_2 and charged with *N*-tosylhydrazone (1 equiv), hexanes (3 mL/mmol hydrazone), and TMEDA (3 mL/mmol hydrazone). The resulting slurry was cooled to -78 $^\circ\text{C}$ with a dry ice-acetone bath and a 2.5 M *n*-BuLi solution in hexane (4 equiv) was added via syringe. The reaction mixture was allowed to stir at -78 $^\circ\text{C}$ for 1 h and then allowed to warm to 25 $^\circ\text{C}$. After stirring for an additional 2 h, the reaction mixture was cooled to -78 $^\circ\text{C}$ with a dry ice-acetone bath and B(Oi-Pr)_3 or B(OMe)_3 was added via syringe. After 2 h the reaction mixture was quenched with 8 M HCl, and acidified to pH 4. The aqueous layer was reserved and the organic layer was extracted with 4 M NaOH (2 x 20 mL). The aqueous phases were then combined and acidified to pH 4 with concentrated HCl, followed by extraction with diethyl ether (3 x 40 mL). The organic layers were then dried with brine and MgSO_4 and concentrated under reduced pressure to give a crude sample of the alkenyl boronic acid. This crude sample was then used for the copper-coupling reaction without further purification. Any impurities carried on to the copper-coupling reaction were not observed to affect the efficiency of the process when compared to

the use of a pure sample of boronic acid. The hydrazone precursors were prepared by literature procedures.

**1o**

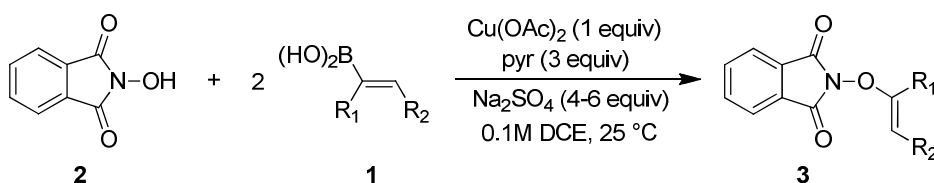
6-Methyl-1-cyclohexenyl boronic acid 1o: General procedure C was used on the *N*-tosyl hydrazone of 2-methylcyclohexanone (2.13 g, 7.61 mmol), *n*-BuLi (12.2 mL, 30.4 mmol), and B(Oi-Pr)₃ (5.26 mL, 22.8 mmol) to give crude sample **1o** (0.138 g, 13%). ¹H NMR (500 MHz; CDCl₃): δ 6.93-6.92 (m, 1H), 1.68-1.66 (m, 1H), 1.58-1.56 (m, 1H), 1.47-1.45 (m, 1H), 1.35-1.33 (m, 1H), 1.22-1.18 (m, 1H), 1.10 (d, *J* = 3.5 Hz, 3H), 0.92-0.89 (m, 1H), 0.79 (t, *J* = 7 Hz, 1H), the O–H resonances were too broad to be observed; ¹³C NMR (125 MHz, CDCl₃): δ 145.7, 30.3, 29.2, 27.2, 21.4, 18.3, the C–B resonance was too broad to be observed above the baseline; IR (thin film) 3388, 2921, 2869, 1621, 1362, 1320, 1158, 1040, 810, 732 cm⁻¹; HRMS (ESI) *m/z* calcd. for C₇H₁₃O₂B (M)⁺ 140.1005, found 140.1009.

**1v**

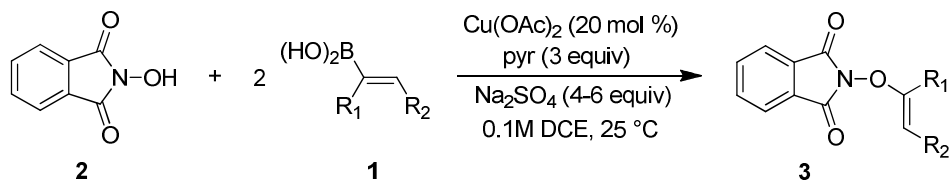
α-Tetralone boronic acid 1v: General procedure C was used with α-tetralone *N*-tosyl hydrazone¹⁹ (2.61 g, 8.30 mmol), *n*-BuLi (13.3 mL, 33.2 mmol), and B(OMe)₃ (3.70 mL, 33.2 mmol) to give crude sample **1v** (0.607 g, 42%). ¹H NMR (500 MHz; CDCl₃): δ 8.03 (d, *J* = 8.0 Hz, 1H), 7.54-7.53 (m, 1H), 7.29-7.27 (m, 1H), 7.22-7.18 (m, 2H), 2.82-2.80 (m, 2H),

2.46-2.42 (m, 2H); ^{13}C NMR (125 MHz, CDCl_3): δ 149.8, 136.0, 135.0, 127.6, 127.3, 126.8, 126.5, 27.9, 24.6, the C-B resonance was too broad to be observed above the baseline; IR (thin film) 3405, 3021, 2930, 1600, 1486, 1382, 1336, 1275, 1044, 765 cm^{-1} .

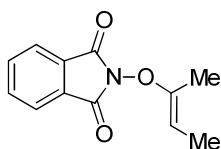
IV. Copper-Catalyzed and Copper-Promoted Etherification of *N*-Hydroxyphthalimides with Vinyl Boronic Acids (Tables 1.2, 1.3)



General procedure D: Copper-promoted etherification of *N*-hydroxyphthalimide with vinyl boronic acids. A scintillation vial was charged with *N*-hydroxyphthalimide **2** (1 equiv), vinyl boronic acid **1** (2 equiv), $\text{Cu}(\text{OAc})_2$ (1 equiv), and anhydrous Na_2SO_4 (4-6 equiv). These solids were then diluted with 1,2-dichloroethane to form a 0.1 M solution of *N*-hydroxyphthalimide. Pyridine (3 equiv) was added to the resulting slurry via syringe. The scintillation vial was then capped with a septum pierced with a ventilation needle and the reaction mixture was stirred at 25 °C for 12 h. 1,2-Dichloroethane and pyridine were removed under reduced pressure and the crude reaction mixture was purified by medium pressure chromatography (1:19 - 1:2; ethyl acetate:hexanes) to give *N*-enoxyphthalimide **3** as a white solid.



General procedure E: Copper-catalyzed etherification of *N*-hydroxyphthalimide with vinyl boronic acids. A scintillation vial was charged with *N*-hydroxyphthalimide **2** (1 equiv), vinyl boronic acid **1** (2 equiv), Cu(OAc)₂ (20 mol %), and anhydrous Na₂SO₄ (4-6 equiv). These solids were then diluted with 1,2-dichloroethane to form a 0.1 M solution of *N*-hydroxyphthalimide. Pyridine (3 equiv) was added to the resulting slurry via syringe. The scintillation vial was then capped with a septum pierced with a ventilation needle and the reaction mixture was stirred at 25 °C for 12-48 h. 1,2-Dichloroethane and pyridine were removed under reduced pressure and the crude reaction mixture was purified by medium pressure chromatography (1:19 - 1:2; ethyl acetate:hexanes) to give *N*-enoxypthalimide **3** as a white solid.



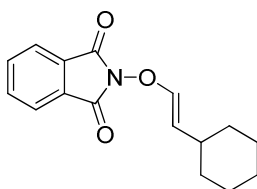
3a

***N*-Enoxypthalimide 3a:** General procedure D with *N*-hydroxyphthalimide **2** (0.050 g; 0.31 mmol), *Z*-2-buten-2-yl boronic acid **1a** (0.060 g, 0.60 mmol), Cu(OAc)₂ (0.054 g, 0.30 mmol), Na₂SO₄ (0.256 g, 1.80 mmol), and pyridine (72.6 μl, 0.900 mmol) afforded **3a** as a white solid (0.065 g, 98%) after purification using medium pressure chromatography (1:4; ethyl acetate: hexanes). ¹H NMR (500 MHz; CDCl₃): δ 7.89-7.86 (m, 2H), 7.80-7.76 (m, 2H),

4.85 (q, $J = 7.0$ Hz, 1H), 1.99 (s, 3H), 1.56 (d, $J = 7.0$ Hz, 3H); ^{13}C NMR (125 MHz, CDCl_3): δ 163.0, 152.4, 134.6, 128.9, 123.7, 96.4, 13.1, 11.2; IR (thin film) 3066, 3004, 2965, 2930, 1791, 1729, 1700, 1609, 1469, 1186 cm^{-1} ; HRMS (ESI) m/z calcd. for $\text{C}_{12}\text{H}_{11}\text{NO}_3\text{Na}$ ($\text{M}+\text{Na}$) $^+$ 240.0637, found 240.0636; mp 112-115 $^\circ\text{C}$.

General procedure E with *N*-hydroxyphthalimide **2** (0.050 g; 0.31 mmol), *Z*-2-buten-2-yl boronic acid **1a** (0.060 g, 0.60 mmol), $\text{Cu}(\text{OAc})_2$ (0.0108 g, 0.0593 mmol), Na_2SO_4 (0.256 g, 1.80 mmol), and pyridine (72.6 μl , 0.9 mmol) afforded **3a** after 48 h. *N*-Enoxy phthalimide **3a** was isolated as a white solid (0.0505 g, 76%) after purification using medium pressure chromatography (1:4; ethyl acetate: hexanes).

General procedure D with *N*-hydroxyphthalimide **2** (0.164 g; 1.01 mmol), *Z*-2-buten-2-yl boronic acid **1a** (0.201 g, 2.01 mmol), $\text{Cu}(\text{OAc})_2$ (0.183 g, 1.01 mmol), Na_2SO_4 (0.613 g, 1.80 mmol), and pyridine (240 μl , 3.015 mmol) afforded **3a** as a white solid (0.163 g, 74%).

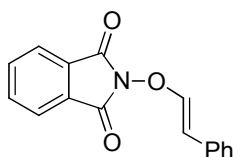


3b

***N*-Enoxyphthalimide 3b:** General procedure D with *N*-hydroxyphthalimide **2** (0.070 g; 0.43 mmol), *trans*-2-cyclohexylvinyl boronic acid **1b** (0.132 g, 0.858 mmol), $\text{Cu}(\text{OAc})_2$ (0.078 g, 0.43 mmol), Na_2SO_4 (0.260 g, 1.32 mmol), and pyridine (100 μL , 1.29 mmol) afforded **3b** as a white solid (0.101 g, 87%) after purification using medium pressure chromatography (1:4; ethyl acetate: hexanes). ^1H NMR (500 MHz; CDCl_3): δ 7.83-7.80 (m, 2H), 7.76-7.74 (m, 2H), 6.39 (d, $J = 12.5$ Hz, 1H), 5.23 (dd, $J = 12.5$ Hz, 7.5 Hz, 1H), 1.94-1.88 (m, 1H), 1.66-1.64

(m, 4H), 1.59-1.56 (m, 1H), 1.23-1.16 (m, 2H), 1.12-0.99 (m, 3H); ^{13}C NMR (125 MHz, CDCl_3): δ 162.6, 144.8, 134.7, 128.7, 123.7, 115.8, 35.9, 33.1, 25.9, 25.9; IR (thin film) 2929, 2851, 1799, 1729, 1661, 1467, 1362, 1186, 1122, 1059 cm^{-1} ; HRMS (ESI) m/z calcd. for $\text{C}_{16}\text{H}_{17}\text{NO}_3\text{Na}$ ($\text{M}+\text{Na}$) $^+$ 294.1106, found 294.1109; mp 87 $^\circ\text{C}$.

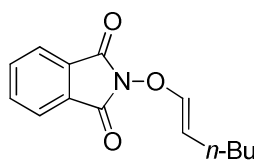
General procedure E with *N*-hydroxyphthalimide **2** (0.070 g; 0.43 mmol), *trans*-2-cyclohexylvinyl boronic acid **1b** (0.132 g, 0.860 mmol), $\text{Cu}(\text{OAc})_2$ (0.016 g, 0.086 mmol), Na_2SO_4 (0.260 g, 1.83 mmol), and pyridine (100 μL , 1.29 mmol) afforded **3c** after 48 h. *N*-Enoxy phthalimide **3b** was isolated as a white solid (0.086 g, 74%) after purification using medium pressure chromatography (1:4; ethyl acetate: hexanes).



3c

***N*-Enoxyphthalimide 3c:** General procedure D with *N*-hydroxyphthalimide **2** (0.050 g; 0.30 mmol), *trans*-2-phenylvinyl boronic acid **1c** (0.089 g, 0.60 mmol), $\text{Cu}(\text{OAc})_2$ (0.054 g, 0.30 mmol), Na_2SO_4 (0.187 g, 1.30 mmol), and pyridine (0.0724 g, 0.900 mmol) afforded **3c** as a white solid (0.069 g, 88%) after purification using medium pressure chromatography (1:9; ethyl acetate: hexanes). ^1H NMR (500 MHz; CDCl_3): δ 7.92-7.91 (m, 2H), 7.82-7.80 (m, 2H), 7.29-7.20 (m, 5H), 7.16 (d, $J = 12.5$ Hz, 1H), 6.33 (d, $J = 12.5$ Hz, 1H); ^{13}C NMR (125 MHz, CDCl_3): δ 162.5, 147.3, 134.9, 133.3, 128.8, 128.7, 127.3, 126.2, 124.0, 111.0; IR (thin film) 2922, 2835, 1730, 1600, 1497, 1366, 1179, 1108, 798 cm^{-1} ; HRMS (ESI) m/z calcd. for $\text{C}_{16}\text{H}_{12}\text{NO}_3$ ($\text{M}+\text{H}$) $^+$ 266.0817, found 266.0811; mp 110-112 $^\circ\text{C}$.

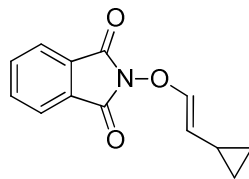
General procedure E with *N*-hydroxyphthalimide **2** (0.050 g; 0.30 mmol), *trans*-2-phenylvinyl boronic acid **1c** (0.089 g, 0.60 mmol), Cu(OAc)₂ (0.011 g, 0.060 mmol), Na₂SO₄ (0.187 g, 1.30 mmol), and pyridine (0.0724 g, 0.900 mmol) afforded **3c** after 24 h. *N*-Enoxy phthalimide **3c** was isolated as a white solid (0.062 g, 78%) after purification using medium pressure chromatography (1:9; ethyl acetate: hexanes).

**3d**

***N*-Enoxyphthalimide 3d:** General procedure D with *N*-hydroxyphthalimide **2** (0.032 g; 0.20 mmol), *trans*-1-hexenyl boronic acid **1d** (0.050 g, 0.39 mmol), Cu(OAc)₂ (0.035 g, 0.20 mmol), Na₂SO₄ (0.119 g, 0.838 mmol) and pyridine (46.8 μl, 0.581 mmol) afforded **3d** as a white solid (0.039 g, 81%) after purification using medium pressure chromatography (1:4; ethyl acetate: hexanes). ¹H NMR (500 MHz; CDCl₃): δ 7.88-7.85 (m, 2H), 7.79-7.76 (m, 2H), 6.48 (d, *J* = 12.1 Hz, 1H), 5.32 (dt, *J* = 12.1, 7.4 Hz, 1H), 1.98-1.94 (m, 2H), 1.35-1.31 (m, 4H), 0.86 (t, *J* = 7.07 Hz, 3H); ¹³C NMR (125 MHz, CDCl₃): δ 162.7 145.6, 134.7, 128.8, 123.8, 110.0, 31.6, 26.3, 22.1, 13.9; IR (thin film) 2960, 2926, 2855, 1794, 1737, 1670, 1465, 1366, 1186, 1126 cm⁻¹; HRMS (ESI) *m/z* calcd. for C₁₄H₁₆NO₃ (M+H)⁺ 246.1130, found 246.1126.; mp 41 °C.

General procedure E with *N*-hydroxyphthalimide **2** (0.020 g; 0.12 mmol), *trans*-1-hexenyl boronic acid **1d** (0.031 g, 0.24 mmol), Cu(OAc)₂ (0.004 g, 0.02 mmol), Na₂SO₄ (0.075 g, 0.053 mmol) and pyridine (0.0295 μl, 0.367 mmol) afforded **3d** after 16 h. *N*-Enoxy

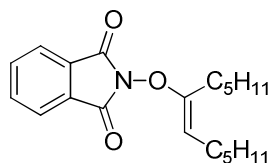
phthalimide **3d** was isolated as a white solid (0.021 g, 70%) after purification using medium pressure chromatography (1:4; ethyl acetate: hexanes).



3e

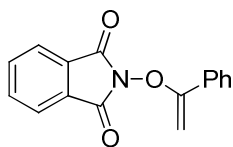
***N*-Enoxyphthalimide 3e:** General procedure D with *N*-hydroxyphthalimide **2** (0.050 g; 0.31 mmol), *trans*-2-cyclopropylvinyl boronic acid **1e** (0.0672 g, 0.601 mmol), Cu(OAc)₂ (0.054 g, 0.30 mmol), Na₂SO₄ (0.256 g, 1.80 mmol), and pyridine (72.6 μl, 0.900 mmol) afforded **3e** as a white solid (0.0333 g, 47%) after purification using medium pressure chromatography (1:4; ethyl acetate: hexanes). ¹H NMR (500 MHz; CDCl₃): δ 7.88-7.85 (m, 2H), 7.79-7.77 (m, 2H), 6.57 (d, *J* = 12.0 Hz, 1H), 5.10 (dd, *J* = 12.0 Hz, *J* = 8.5 Hz, 1H), 1.30-1.23 (m, 1H), 0.69-0.66 (m, 1H), 0.34-0.33 (m, 1H); ¹³C NMR (125 MHz, CDCl₃): δ 162.7, 145.2, 134.7, 128.8, 123.8, 114.8, 8.3, 6.1; IR (thin film) 3056, 3008, 2959, 2926, 2855, 1795, 1733, 1463, 1265, 874 cm⁻¹; HRMS (ESI) *m/z* calcd. for C₁₃H₁₂NO₃ (M+H)⁺ 230.0817, found 230.0823; mp 69-72 °C.

General procedure E with *N*-hydroxyphthalimide **2** (0.050 g; 0.31 mmol), *trans*-2-cyclopropylvinyl boronic acid **1e** (0.0672 g, 0.601 mmol), Cu(OAc)₂ (0.0108 g, 0.0593 mmol), Na₂SO₄ (0.256 g, 1.80 mmol), and pyridine (72.6 μl, 0.900 mmol) afforded **3e** after 24 h. *N*-Enoxyphthalimide **3e** was isolated as a white solid (0.0146 g, 21%) after purification using medium pressure chromatography (1:4; ethyl acetate: hexanes).

**3f**

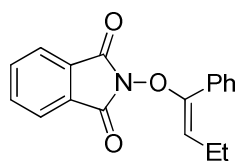
***N*-Enoxyphthalimide 3f:** General procedure D with *N*-hydroxyphthalimide **2** (0.050 g; 0.31 mmol), *Z*-6-dodecen-6-yl boronic acid **1f** (0.159 g, 0.750 mmol), Cu(OAc)₂ (0.054 g, 0.30 mmol), Na₂SO₄ (0.187 g, 1.32 mmol), and pyridine (72.4 μL, 0.901 mmol) afforded **3f** as a colorless oil (0.082 g, 81%) after purification using medium pressure chromatography (1:19; ethyl acetate: hexanes). ¹H NMR (500 MHz; CDCl₃): δ 7.88-7.85 (m, 2H), 7.77-7.76 (m, 2H), 4.67 (t, *J* = 7.5 Hz, 1H), 2.31 (m, 2H), 1.92-1.73 (m, 2H), 1.70-1.66 (m, 2H), 1.38-1.33 (m, 4H), 1.30-1.23 (m, 6H), 0.91 (t, *J* = 7.0 Hz, 3H), 0.84 (t, *J* = 6.5 Hz, 3H); ¹³C NMR (125 MHz, CDCl₃): δ 162.9, 155.7, 134.6, 129.0, 123.7, 101.3, 31.4, 31.3, 29.9, 27.9, 27.2, 26.0, 22.5, 22.4, 14.1, 14.0; IR (thin film) 2959, 2923, 2860, 1736, 1467, 1366, 1187, 1126, 878, 700cm⁻¹; HRMS (ESI) *m/z* calcd. for C₂₀H₂₇NO₃Na (M+Na)⁺ 352.1889, found 352.1875;

General procedure E with *N*-hydroxyphthalimide **2** (0.050 g; 0.31 mmol), *Z*-6-dodecen-6-yl boronic acid **1f** (0.159 g, 0.750 mmol), Cu(OAc)₂ (0.011 g, 0.060 mmol), Na₂SO₄ (0.187 g, 1.32 mmol), and pyridine (72.4 μL, 0.901 mmol) afforded **3f** after 24 h. *N*-Enoxyphthalimide **3f** was isolated as a white solid (0.078 g, 77%) after purification using medium pressure chromatography (1:19; ethyl acetate: hexanes).

**3g**

***N*-Enoxyphthalimide 3g:** General procedure D with *N*-hydroxyphthalimide **2** (0.057 g; 0.35 mmol), 1-phenylvinyl boronic acid **1g** (0.104 g, 0.703 mmol), Cu(OAc)₂ (0.064 g, 0.35 mmol), Na₂SO₄ (0.200 g, 1.41 mmol), and pyridine (84.7 μL, 1.05 mmol) afforded **3g** as a white solid (0.080 g, 86%) after purification using medium pressure chromatography (1:4; ethyl acetate: hexanes). ¹H NMR (500 MHz; CDCl₃): δ 7.92-7.89 (m, 2H), 7.80-7.77 (m, 2H), 7.75-7.74 (m, 2H), 7.41-7.39 (m, 3H), 4.88 (d, *J* = 4.0 Hz, 1H), 4.57 (d, *J* = 4.0 Hz, 1H); ¹³C NMR (125 MHz, CDCl₃): δ 162.5, 162.4, 160.2, 134.8, 134.7, 132.2, 129.7, 128.9, 128.8, 128.4, 128.3, 126.3, 126.2, 123.9, 123.8, 86.7; IR (thin film) 3064, 3030, 1794, 1730, 1648, 1493, 1468, 1373, 1262, 1189 cm⁻¹; HRMS (ESI) *m/z* calcd. for C₁₆H₁₂NO₃ (M+H)⁺ 266.0817, found 266.0817; mp 163°C.

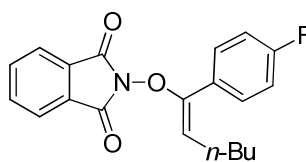
General procedure E with *N*-hydroxyphthalimide **2** (0.020g; 0.12 mmol), 1-phenylvinyl boronic acid **1g** (0.036 g, 0.24 mmol), Cu(OAc)₂ (0.004 g, 0.02 mmol), Na₂SO₄ (0.070 g, 0.49 mmol), and pyridine (29.6 μL, 0.366 mmol) afforded **3g** after 24 h. *N*-Enoxy phthalimide **3g** was isolated as a white solid (0.025 g, 77%) after purification using medium pressure chromatography (1:4; ethyl acetate: hexanes).

**3h**

***N*-Enoxyphthalimide 3h:** General procedure D with *N*-hydroxyphthalimide **2** (0.050 g; 0.31 mmol), *Z*-1-phenyl-1-buten-1-yl boronic acid **1h** (0.090 g, 0.51 mmol), Cu(OAc)₂ (0.054 g, 0.30 mmol), Na₂SO₄ (0.187 g, 1.32 mmol), and pyridine (72.4 μL, 0.901 mmol) afforded **3h**

as a white solid (0.068 g, 76%) after purification using medium pressure chromatography (1:9; ethyl acetate: hexanes). ^1H NMR (500 MHz; CDCl_3): δ 7.86-7.85 (m, 2H), 7.76-7.75 (m, 2H), 7.63 (m, 2H), 7.41-7.36 (m, 3H), 5.23 (t, $J = 7.5$ Hz, 1H), 2.09-2.05 (m, 2H), 0.94 (t, $J = 7.5$ Hz, 3H); ^{13}C NMR (125 MHz, CDCl_3): δ 163.0, 154.0, 134.6, 131.7, 129.6, 129.3, 129.0, 128.1, 123.7, 108.2, 20.3, 14.9; IR (thin film) 2963, 2934, 2857, 1733, 1366, 1187, 995, 878, 696 cm^{-1} ; HRMS (ESI) m/z calcd. for $\text{C}_{18}\text{H}_{15}\text{NO}_3\text{Na}$ ($\text{M}+\text{Na}$) $^+$ 316.0950, found 316.0941; mp 106-108 $^\circ\text{C}$.

General procedure E with *N*-hydroxyphthalimide **2** (0.050 g; 0.31 mmol), *Z*-1-phenyl-1-buten-1-yl boronic acid **1h** (0.132 g, 0.750 mmol), $\text{Cu}(\text{OAc})_2$ (0.011 g, 0.061 mmol), Na_2SO_4 (0.187 g, 1.32 mmol), and pyridine (72.4 μL , 0.901 mmol) afforded **3h** after 24 h. *N*-Enoxyphthalimide **3h** was isolated as a white solid (0.060 g, 67%) after purification using medium pressure chromatography (1:9; ethyl acetate: hexanes).

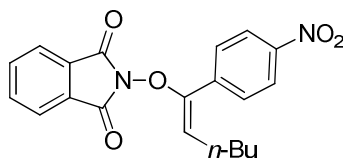


3i

***N*-Enoxyphthalimide 3i:** General procedure D with *N*-hydroxyphthalimide **2** (0.050 g; 0.31 mmol), alkenyl boronic acid **1i** (0.166 g, 0.748 mmol), $\text{Cu}(\text{OAc})_2$ (0.054 g, 0.30 mmol), Na_2SO_4 (0.187 g, 1.32 mmol), and pyridine (72.4 μL , 0.901 mmol) afforded **3i** as a white solid (0.073 g, 70%) after purification using medium pressure chromatography (1:9; ethyl acetate: hexanes). ^1H NMR (500 MHz; CDCl_3): δ 7.86-7.85 (m, 2H), 7.77-7.76 (m, 2H), 7.62-7.59 (m, 2H), 7.09-7.06 (m, 2H), 5.24 (t, $J = 7.5$ Hz, 1H), 2.05-2.01 (m, 2H), 1.34-1.28 (m, 2H), 1.26-1.21 (m, 2H), 0.78 (t, $J = 7.5$ Hz, 3H); ^{13}C NMR (125 MHz, CDCl_3): δ 163.0,

162.1 (d, $J = 248$ Hz), 153.4, 134.7, 131.7, 131.66, 128.9, 123.8, 115.2 (d, $J = 22$ Hz), 107.2, 32.2, 26.4, 22.1 13.8; IR (thin film) 2956, 2933, 2862, 1735, 1593, 1537, 1369, 1227, 845, 695 cm^{-1} ; HRMS (ESI) m/z calcd. for $\text{C}_{20}\text{H}_{19}\text{NFO}_3$ ($\text{M}+\text{H}$) $^+$ 340.1349, found 340.1350.; mp 76-78 $^{\circ}\text{C}$.

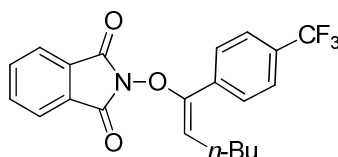
General procedure E with *N*-hydroxyphthalimide **2** (0.050 g; 0.31 mmol), alkenyl boronic acid **2i** (0.166 g, 0.748 mmol), $\text{Cu}(\text{OAc})_2$ (0.011 g, 0.060 mmol), Na_2SO_4 (0.187 g, 1.32 mmol), and pyridine (72.4 μL , 0.901 mmol) afforded **3i** after 24 h. *N*-Enoxypthalimide **3i** was isolated as a white solid (0.074 g, 71%) after purification using medium pressure chromatography (1:9; ethyl acetate: hexanes).



3j

***N*-Enoxypthalimide 3j:** General procedure D with *N*-hydroxyphthalimide **2** (0.050 g; 0.31 mmol), alkenyl boronic acid **1j** (0.186 g, 0.747 mmol), $\text{Cu}(\text{OAc})_2$ (0.054 g, 0.30 mmol), Na_2SO_4 (0.187 g, 1.32 mmol), and pyridine (72.4 μL , 0.901 mmol) afforded **3j** as a white solid (0.075 g, 67%) after purification using medium pressure chromatography (1:9; ethyl acetate: hexanes). ^1H NMR (500 MHz; CDCl_3): δ 8.26 (d, $J = 8.0$ Hz, 2H), 7.89-7.86 (m, 2H), 7.82 (d, $J = 8.0$ Hz, 2H), 7.81-7.78 (m, 2H), 5.44 (t, $J = 7.5$ Hz, 1H), 2.11-2.07 (m, 2H), 1.38-1.32 (m, 2H), 1.28-1.21 (m, 2H), 0.80 (t, $J = 7.5$ Hz, 3H); ^{13}C NMR (125 MHz, CDCl_3): δ 162.9, 152.1, 148.1, 138.3, 134.9, 130.5, 128.8, 123.9, 123.4, 110.5, 32.1, 26.5, 22.1, 13.8; IR (thin film) 2956, 2926, 2855, 1731, 1601, 1514, 1186, 856, 699 cm^{-1} ; HRMS (ESI) m/z calcd. for $\text{C}_{20}\text{H}_{19}\text{N}_2\text{O}_5$ ($\text{M}+\text{H}$) $^+$ 367.1294, found 367.1286.; mp 119-121 $^{\circ}\text{C}$.

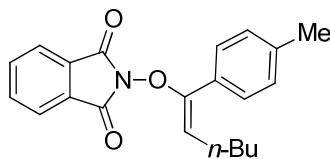
General procedure E with *N*-hydroxyphthalimide **2** (0.050 g; 0.31 mmol), alkenyl boronic acid **1j** (0.186 g, 0.747 mmol), Cu(OAc)₂ (0.011 g, 0.060 mmol), Na₂SO₄ (0.187 g, 1.32 mmol), and pyridine (72.4 μL, 0.901 mmol) afforded **3j** after 24 h. *N*-Enoxyphthalimide **3j** was isolated as a white solid (0.062 g, 55%) after purification using medium pressure chromatography (1:9; ethyl acetate: hexanes).

**3k**

***N*-Enoxyphthalimide 3k:** General procedure D with *N*-hydroxyphthalimide **2** (0.050 g; 0.31 mmol), alkenyl boronic acid **1k** (0.204 g, 0.750 mmol), Cu(OAc)₂ (0.054 g, 0.30 mmol), Na₂SO₄ (0.187 g, 1.32 mmol), and pyridine (72.4 μL, 0.901 mmol) afforded **3k** as a white solid (0.098 g, 82%) after purification using medium pressure chromatography (1:9; ethyl acetate: hexanes). ¹H NMR (500 MHz; CDCl₃): δ 7.86-7.88 (m, 2H), 7.75-7.78 (m, 4H), 7.65 (d, *J* = 8.0 Hz, 2H), 5.34 (t, *J* = 7.5 Hz, 1H), 2.05-2.09 (m, 2H), 1.30-1.36 (m, 2H), 1.21-1.27 (m, 2H), 0.79 (t, *J* = 7.5 Hz, 3H); ¹³C NMR (125 MHz, CDCl₃): δ 163.0, 152.8, 135.4, 134.8, 131.2, 130.0, 128.9, 125.1 (q, *J* = 3.7 Hz), 123.8, 122.9 (q, *J* = 270 Hz), 108.8, 32.2, 26.4, 22.1, 13.8; IR (thin film) 2963, 2929, 2855, 1739, 1327, 1170, 1118, 1070, 849, 699 cm⁻¹; HRMS (ESI) *m/z* calcd. for C₂₁H₁₉NF₃O₃ (M+H)⁺ 390.1317, found 390.1318.; mp 66-68 °C.

General procedure E with *N*-hydroxyphthalimide **2** (0.050 g; 0.31 mmol), alkenyl boronic acid **1k** (0.204 g, 0.750 mmol), Cu(OAc)₂ (0.011 g, 0.060 mmol), Na₂SO₄ (0.187 g, 1.32 mmol), and pyridine (72.4 μL, 0.901 mmol) afforded **3l** after 24 h. *N*-Enoxyphthalimide **3k**

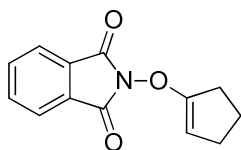
was isolated as a white solid (0.087 g, 73%) after purification using medium pressure chromatography (1:9; ethyl acetate: hexanes).



31

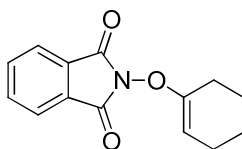
***N*-Enoxyphthalimide 31:** General procedure D with *N*-hydroxyphthalimide **2** (0.050 g; 0.31 mmol), alkenyl boronic acid **11** (0.163 g, 0.747 mmol), Cu(OAc)₂ (0.054 g, 0.30 mmol), Na₂SO₄ (0.187 g, 1.32 mmol), and pyridine (72.4 μL, 0.901 mmol) afforded **31** as a white solid (0.065 g, 63%) after purification using medium pressure chromatography (1:9; ethyl acetate: hexanes). ¹H NMR (500 MHz; CDCl₃): δ 7.86-7.84 (m, 2H), 7.76-7.74 (m, 2H), 7.49 (d, *J* = 8.0 Hz, 2H), 7.18 (d, *J* = 8.0 Hz, 2H), 5.21 (t, *J* = 7.5 Hz, 1H), 2.36 (s, 3H), 2.07-2.03 (m, 2H), 1.33-1.28 (m, 2H), 1.25-1.21 (m, 2H), 0.78 (t, *J* = 7.5 Hz, 3H); ¹³C NMR (125 MHz, CDCl₃): δ 163.1, 154.3, 139.2, 139.1, 134.5, 129.6, 129.0, 128.8, 123.7, 106.6, 32.4, 26.5, 22.1, 21.4, 13.9; IR (thin film) 2963, 2926, 2862, 1731, 1675, 1376, 1182, 882, 692 cm⁻¹; HRMS (ESI) *m/z* calcd. for C₂₁H₂₂NO₃ (M+H)⁺ 336.1600, found 336.1592.; mp 103-105 °C.

General procedure E with *N*-hydroxyphthalimide **2** (0.050 g; 0.31 mmol), alkenyl boronic acid **11** (0.163 g, 0.747 mmol), Cu(OAc)₂ (0.011 g, 0.060 mmol), Na₂SO₄ (0.187 g, 1.32 mmol), and pyridine (72.4 μL, 0.901 mmol) afforded **31** after 24 h. *N*-Enoxy phthalimide **31** was isolated as a white solid (0.068 g, 66%) after purification using medium pressure chromatography (1:9; ethyl acetate: hexanes).

**3m**

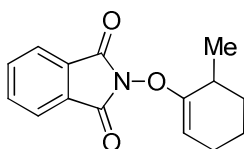
***N*-Enoxypthalimide **3m**:** General procedure D with *N*-hydroxyphthalimide **2** (0.050 g; 0.31 mmol), 1-cyclopentenyl boronic acid **1m** (0.070 g, 0.63 mmol), Cu(OAc)₂ (0.054 g, 0.30 mmol), Na₂SO₄ (0.187 g, 1.32 mmol), and pyridine (72.4 μL, 0.901 mmol) afforded **3m** as a white solid (0.051 g, 73%) after purification using medium pressure chromatography (1:19; ethyl acetate: hexanes). ¹H NMR (500 MHz; CDCl₃): δ 7.89-7.87 (m, 2H), 7.79-7.77 (m, 2H), 4.75-4.74 (m, 1H), 2.60-2.58 (m, 2H), 2.33-2.29 (m, 2H), 2.05-1.99 (m, 2H); ¹³C NMR (125 MHz, CDCl₃): δ 162.4, 159.0, 134.7, 128.8, 123.9, 99.8, 29.3, 28.1, 21.7; IR (thin film) 2938, 2858, 1736, 1464, 1186, 701 cm⁻¹; HRMS (ESI) *m/z* calcd. for C₁₃H₁₁NO₃Na (M+Na)⁺ 252.0637, found 252.0631; mp 100-102 °C.

General procedure E with *N*-hydroxyphthalimide **2** (0.050 g; 0.31 mmol), alkenyl boronic acid **1m** (0.070 g, 0.63 mmol), Cu(OAc)₂ (0.011 g, 0.060 mmol), Na₂SO₄ (0.187 g, 1.32 mmol), and pyridine (72.4 μL, 0.901 mmol) afforded **3m** after 24 h. *N*-Enoxypthalimide **3m** was isolated as a white solid (0.048 g, 68%) after purification using medium pressure chromatography (1:19; ethyl acetate: hexanes).

**3n**

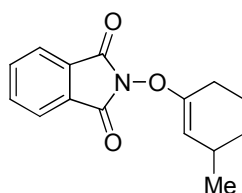
***N*-Enoxyphthalimide 3n:** General procedure D with *N*-hydroxyphthalimide **2** (0.050 g; 0.31 mmol), 1-cyclohexenyl boronic acid **1n** (0.077 g, 0.61 mmol), Cu(OAc)₂ (0.056 g, 0.31 mmol), Na₂SO₄ (0.187 g, 1.32 mmol), and pyridine (75.5 μL, 0.935 mmol) afforded **3n** as a white solid (0.062 g, 83%) after purification using medium pressure chromatography (1:4; ethyl acetate: hexanes). ¹H NMR (500 MHz; CDCl₃): δ 7.84-7.81 (m, 2H), 7.77-7.74 (m, 2H), 4.97 (t, *J* = 3.8 Hz, 1H), 2.27-2.25 (m, 2H), 2.02 (td, *J* = 6.0, 3.8 Hz, 2H), 1.74-1.64 (m, 2H), 1.54-1.50 (m, 2H); ¹³C NMR (125 MHz, CDCl₃): δ 162.8, 154.7, 134.6, 128.7, 123.6, 98.5, 24.5, 22.8, 22.4, 21.9; IR (thin film) 2928, 2852, 1790, 1730, 1688, 1465, 1445, 1366, 1186, 1120 cm⁻¹; HRMS (ESI) *m/z* calcd. for C₁₄H₁₄NO₃ (M+H)⁺ 244.0974, found 244.0976; mp 107 °C.

General procedure E with *N*-hydroxyphthalimide **2** (0.036 g; 0.220 mmol), 1-cyclohexenyl boronic acid **1n** (0.056 g, 0.44 mmol), Cu(OAc)₂ (0.008 g, 0.044 mmol), Na₂SO₄ (0.135 g, 0.951 mmol), and pyridine (57.1 μL, 0.660 mmol) afforded **3n** after 48 h. *N*-Enoxyphthalimide **3n** was isolated as a white solid (0.041 g, 76%) after purification using medium pressure chromatography (1:4; ethyl acetate: hexanes).

**3o**

***N*-Enoxyphthalimide 3o:** General procedure D with *N*-hydroxyphthalimide **2** (0.050 g; 0.31 mmol), alkenyl boronic acid **1o** (0.126 g, 0.900 mmol), Cu(OAc)₂ (0.054 g, 0.30 mmol), Na₂SO₄ (0.187 g, 1.32 mmol), and pyridine (72.4 μL, 0.90 mmol) afforded **3o** as a white solid (0.032 g, 41%) after purification using medium pressure chromatography (1:4; ethyl

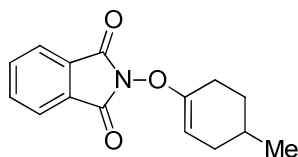
acetate: hexanes:triethylamine). ^1H NMR (500 MHz; CDCl_3): δ 7.87-7.85 (m, 2H), 7.78-7.76 (m, 2H), 4.86 (t, $J = 3.0$ Hz, 1H), 2.60-2.58 (m, 1H), 2.00-1.98 (m, 2H), 1.88-1.83 (m, 1H), 1.64-1.49 (m, 3H), 1.28 (d, $J = 7.0$ Hz, 3H); ^{13}C NMR (125 MHz, CDCl_3): δ 162.9, 158.4, 134.6, 128.9, 123.7, 97.4, 31.0, 29.9, 23.3, 19.3, 18.6; IR (thin film) 3052, 3038, 2982, 2940, 1735, 1653, 1563, 1504, 1425, 899 cm^{-1} ; HRMS (ESI) m/z calcd. for $\text{C}_{15}\text{H}_{15}\text{NO}_3\text{Na}$ ($\text{M}+\text{Na}$) $^+$ 280.0950, found 280.0944.; mp 78-80 $^\circ\text{C}$.

**3p**

***N*-Enoxyphthalimide 3p:** General procedure D with *N*-hydroxyphthalimide **2** (0.070 g; 0.43 mmol), alkenyl boronic acid **1p** (0.120 g, 0.850 mmol), $\text{Cu}(\text{OAc})_2$ (0.080 g, 0.43 mmol), Na_2SO_4 (0.260 g, 1.32 mmol), and pyridine (100 μL , 1.29 mmol) afforded **3p** as a white solid (0.090 g, 86%) after purification using medium pressure chromatography (1:4; ethyl acetate: hexanes). ^1H NMR (500 MHz; CDCl_3): δ 7.87-7.85 (m, 2H), 7.78-7.76 (m, 2H), 4.81 (d, $J = 2.8$ Hz, 1H), 2.40-2.26 (m, 3H), 1.86-1.84 (m, 1H), 1.73-1.64 (m, 2H), 1.17-1.12 (dtd, $J = 2.8, 10.3, 10.6$ Hz, 1H), 0.92 (d, $J = 10.3$ Hz, 3H); ^{13}C NMR (125 MHz, CDCl_3): δ 162.8, 154.5, 134.6, 128.8, 123.7, 104.5, 30.7, 28.8, 24.5, 22.02 21.1; IR (thin film) 2953, 2929, 2851, 1789, 1740, 1691, 1467, 1358, 1178, 1103 cm^{-1} ; HRMS (ESI) m/z calcd. for $\text{C}_{15}\text{H}_{15}\text{NO}_3\text{Na}$ ($\text{M}+\text{Na}$) $^+$ 280.0950, found 280.0944.; mp 78-80 $^\circ\text{C}$.

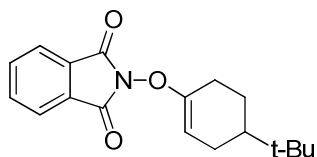
General procedure E with *N*-hydroxyphthalimide **2** (0.035 g; 0.214 mmol), alkenyl boronic acid **1p** (0.060 g, 0.428 mmol), $\text{Cu}(\text{OAc})_2$ (0.008 g, 0.043 mmol), Na_2SO_4 (0.131 g, 0.922

mmol), and pyridine (50 μ L, 0.642 mmol) afforded **3s** after 48 h. *N*-Enoxyphthalimide **3p** was isolated as a white solid (0.044 g, 80%) after purification using medium pressure chromatography (1:4; ethyl acetate: hexanes).

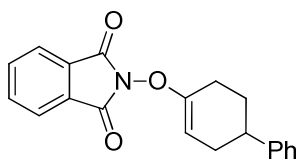
**3q**

***N*-Enoxyphthalimide 3q:** General procedure D with *N*-hydroxyphthalimide **2** (0.050 g; 0.30 mmol), alkenyl boronic acid **1q** (0.086 g, 0.61 mmol), Cu(OAc)₂ (0.055 g, 0.30 mmol), Na₂SO₄ (0.187 g, 1.32 mmol), and pyridine (72.4 μ L, 0.899 mmol) afforded **3q** as a white solid (0.066 g, 84%) after purification using medium pressure chromatography (1:4; ethyl acetate: hexanes). ¹H NMR (500 MHz; CDCl₃): δ 7.82-7.80 (m, 2H), 7.75-7.73 (m, 2H), 4.89 (t, *J* = 3.0 Hz, 1H), 2.34-2.23 (m, 2H), 2.02 (dd, *J* = 3.5 Hz, 4.0 Hz, 1H), 1.77-1.74 (m, 1H), 1.65-1.58 (m, 2H), 1.38-1.35 (m, 1H), 0.9 (d, *J* = 6.1 Hz, 3H); ¹³C NMR (125 MHz, CDCl₃): δ 162.8, 154.5, 134.6, 128.8, 123.6, 98.0, 31.1, 30.4, 28.2, 24.4, 21.0; IR (thin film) 2921, 2878, 1792, 1740, 1691, 1604, 1470, 1366, 1190, 1076 cm⁻¹; HRMS (ESI) *m/z* calcd. for C₁₅H₁₆NO₃ (M+H)⁺ 258.1130, found 258.1131; mp 109 °C.

General procedure E with *N*-hydroxyphthalimide **2** (0.030 g; 0.183 mmol), alkenyl boronic acid **1q** (0.052 g, 0.37 mmol), Cu(OAc)₂ (0.007 g, 0.037 mmol), Na₂SO₄ (0.112 g), and pyridine (0.043g, 0.549 mmol) afforded **3q** after 30 h. *N*-Enoxyphthalimide **3q** was isolated as a white solid (0.037 g, 78%) after purification using medium pressure chromatography (1:4; ethyl acetate: hexanes).

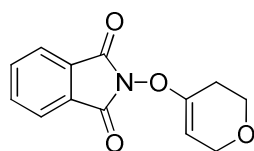
**3r**

***N*-Enoxyphthalimide 3r:** General procedure D with *N*-hydroxyphthalimide **2** (0.040 g; 0.24 mmol), alkenyl boronic acid **1r** (0.088 g, 0.48 mmol), Cu(OAc)₂ (0.044 g, 0.24 mmol), Na₂SO₄ (0.075 g, 1.1 mmol), and pyridine (60 μL, 0.72 mmol) afforded **3r** as an amorphous solid (0.060 g, 83%) after purification using medium pressure chromatography (1:4; ethyl acetate: hexanes). ¹H NMR (500 MHz; CDCl₃): δ 7.86-7.84 (m, 2H), 7.77-7.75 (m, 2H), 4.94 (d, *J* = 5.5 Hz, 1H), 2.34-2.33 (m, 2H), 2.02-1.99 (m, 1H), 1.92-1.89 (m, 1H), 1.81-1.76 (m, 1H), 1.35-1.23 (m, 2H), 0.84 (s, 9H); ¹³C NMR (125 MHz, CDCl₃): δ 162.8, 154.6, 134.6, 128.8, 123.7, 98.5, 43.7, 32.1, 27.3, 25.6, 24.1, 23.6; IR (thin film) 3056, 2990, 2978, 2933, 1735, 1421, 1186, 1369, 1168, 1092 cm⁻¹; HRMS (ESI) *m/z* calcd. for C₁₈H₂₁NO₃Na (M+Na)⁺ 322.1419, found 322.1423.

**3s**

***N*-Enoxyphthalimide 3s:** General procedure D with *N*-hydroxyphthalimide **2** (0.050 g; 0.31 mmol), alkenyl boronic acid **1s** (0.120 g, 0.594 mmol), Cu(OAc)₂ (0.054, 0.30 mmol), Na₂SO₄ (0.256 g, 1.80 mmol), and pyridine (72.7 μL, 0.901 mmol) afforded **3s** as a white solid (0.0627 g, 64%) after purification using medium pressure chromatography (4:1; ethyl acetate: hexanes). ¹H NMR (500 MHz; CDCl₃): δ 7.91-7.88 (m, 2H), 7.81-7.77 (m, 2H),

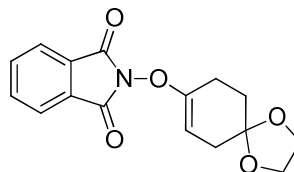
7.32-7.29 (m, 2H), 7.23-7.19 (m, 3H), 5.08 (t, $J = 2.5$ Hz, 1H), 2.84 (dddd, $J = 15.0$ Hz, $J = 8.0$ Hz, $J = 5.0$ Hz, $J = 3.0$ Hz, 1H), 2.60-2.53 (m, 1H), 2.47-2.43 (m, 1H), 2.33-2.28 (m, 1H), 2.23-2.17 (m, 1H), 2.09-2.06 (m, 1H), 2.02-1.95 (m, 1H); ^{13}C NMR (125 MHz, CDCl_3): δ 162.9, 154.6, 145.8, 134.7, 128.9, 128.5, 126.9, 126.3, 123.8, 98.2, 39.9, 31.0, 29.3, 25.1; IR (thin film) 3027, 2933, 2923, 2848, 1791, 1736, 1698, 1606, 1469, 1186 cm^{-1} ; HRMS (ESI) m/z calcd. for $\text{C}_{20}\text{H}_{18}\text{NO}_3$ ($\text{M}+\text{H}$) $^+$ 320.1287, found 320.1296.; mp 127-131 $^\circ\text{C}$.

**3t**

***N*-Enoxyphthalimide 3t:** General procedure D with *N*-hydroxyphthalimide **2** (0.022 g; 0.14 mmol), alkenyl boronic acid **1t** (0.035 g, 0.27 mmol), $\text{Cu}(\text{OAc})_2$ (0.025 g, 0.14 mmol), Na_2SO_4 (0.082 g, 0.58 mmol), and pyridine (32.7 μL , 0.408 mmol) afforded **3t** as a white solid (0.030 g, 91%) after purification using medium pressure chromatography (1:4; ethyl acetate: hexanes). ^1H NMR (500 MHz; CDCl_3): δ 7.89-7.86 (m, 2H), 7.80-7.77 (m, 2H), 4.99 (t, $J = 2.5$ Hz, 1H), 4.14 (dd, $J = 2.5$ Hz, 2.5 Hz, 2H), 3.89 (t, $J = 5.5$ Hz, 2H), 2.45 (t, $J = 5.5$ Hz, 2H); ^{13}C NMR (125 MHz, CDCl_3): δ 162.6, 152.1, 134.8, 128.8, 123.9, 97.4, 64.0, 63.9, 25.5; IR (thin film) 2931, 2849, 1790, 1733, 1698, 1609, 1465, 1360, 1230, 1186 cm^{-1} ; HRMS (ESI) m/z calcd. for $\text{C}_{13}\text{H}_{12}\text{NO}_4$ ($\text{M}+\text{H}$) $^+$ 246.0766, found 246.0766; mp 118 $^\circ\text{C}$.

General procedure E with *N*-hydroxyphthalimide **2** (0.044 g; 0.27 mmol), alkenyl boronic acid **1t** (0.070 g, 0.55 mmol), $\text{Cu}(\text{OAc})_2$ (0.008 g, 0.05 mmol), Na_2SO_4 (0.164 g, 1.16 mmol), and pyridine (65.3 μL , 0.810 mmol) afforded **3t** after 48 h. *N*-Enoxyphthalimide **3t** was

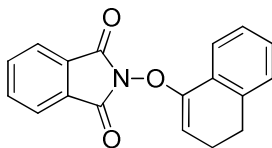
isolated as a white solid (0.059 g, 89%) after purification using medium pressure chromatography (1:4; ethyl acetate: hexanes).



3u

***N*-Enoxyphthalimide 3u:** General procedure D with *N*-hydroxyphthalimide **2** (0.050 g; 0.31 mmol), alkenyl boronic acid **1u** (0.110 g, 0.598 mmol), Cu(OAc)₂ (0.054 g, 0.30 mmol), Na₂SO₄ (0.187 g, 1.32 mmol), and pyridine (72.4 μL, 0.899 mmol) afforded **3u** as a white solid (0.079 g, 86%) after purification using medium pressure chromatography (1:3; ethyl acetate: hexanes). ¹H NMR (500 MHz; CDCl₃): δ 7.83-7.81 (m, 2H), 7.74-7.76 (m, 2H), 4.88 (s, 1H), 3.93 (s, 4H), 2.49-2.50 (m, 2H), 2.23 (s, 2H), 1.88-1.85 (m, 2H); ¹³C NMR (125 MHz, CDCl₃): δ 162.7, 153.9, 134.7, 128.8, 107.4, 96.5, 64.5, 64.4, 33.1, 30.6, 23.5; IR (thin film) 2965, 2934, 2884, 1732, 1375, 1116, 876, 733, 696 cm⁻¹; HRMS (ESI) m/z calcd. for C₁₆H₁₅NO₅Na (M+Na)⁺ 324.0848, found 324.0850; mp 135-137 °C.

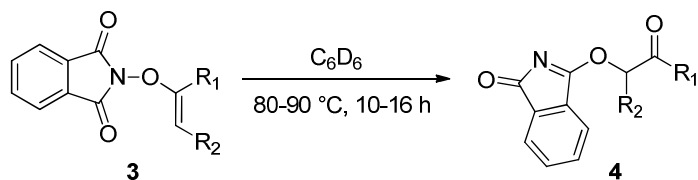
General procedure E with *N*-hydroxyphthalimide **2** (0.050 g; 0.31 mmol), alkenyl boronic acid **1u** (0.110 g, 0.598 mmol), Cu(OAc)₂ (0.011 g, 0.060 mmol), Na₂SO₄ (0.187 g, 1.32 mmol), and pyridine (72.4 μL, 0.899 mmol) afforded **3u** after 24 h. *N*-Enoxyphthalimide **3u** was isolated as a white solid (0.076 g, 82%) after purification using medium pressure chromatography (1:3; ethyl acetate: hexanes).

**3v**

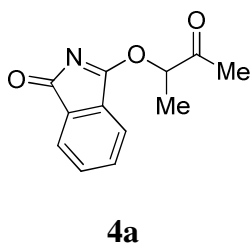
***N*-Enoxyphthalimide 3v:** General procedure D with *N*-hydroxyphthalimide **2** (0.050 g; 0.31 mmol), alkenyl boronic acid **1v** (0.106 g, 0.609 mmol), Cu(OAc)₂ (0.054 g, 0.30 mmol), Na₂SO₄ (0.256 g, 1.80 mmol), and pyridine (72.4 μL, 0.899 mmol) afforded **3v** as a light orange solid (0.068 g, 76%) after purification using medium pressure chromatography (1:2; ethyl acetate: hexanes). ¹H NMR (500 MHz; CDCl₃): δ 7.92-7.90 (m, 2H), 7.81-7.79 (m, 2H), 7.70 (d, *J* = 7.0 Hz, 1H), 7.28-7.22 (m, 2H), 7.16 (d, *J* = 7.0 Hz, 1H), 5.26 (t, *J* = 4.5 Hz, 1H), 2.81 (t, *J* = 8.0 Hz, 2H), 2.34 (td, *J* = 8.0 Hz, *J* = 4.5 Hz, 2H); ¹³C NMR (125 MHz, CDCl₃): δ 162.7, 152.2, 136.7, 134., 128.9, 128.4, 128.3, 127.3, 126.5, 123.9, 121.7, 99.4, 27.8, 21.4; IR (thin film) 3060, 2939, 2890, 2838, 1795, 1733, 1369, 1189, 1125, 874 cm⁻¹; HRMS (ESI) *m/z* calcd. for C₁₈H₁₃NO₃Na (M+Na)⁺ 314.0793, found 314.0794.; mp 110-114 °C.

General procedure E with *N*-hydroxyphthalimide **2** (0.050 g; 0.31 mmol), alkenyl boronic acid **1v** (0.106 g, 0.609 mmol), Cu(OAc)₂ (0.0108 g, 0.0593 mmol), Na₂SO₄ (0.256 g, 1.80 mmol), and pyridine (72.4 μL, 0.899 mmol) afforded **3v** after 48 h. *N*-Enoxyphthalimide **3v** was isolated as a white solid (0.0454 g, 52%) after purification using medium pressure chromatography (1:2; ethyl acetate: hexanes).

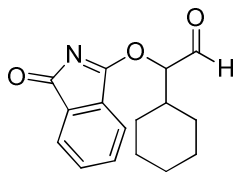
IV. Thermal Rearrangement of *N*-Enoxyphthalimides



General Procedure F: Thermal rearrangement of *N*-Enoxyphthalimides. A J-Young tube was charged with a 0.1 M solution of *N*-enoxyphthalimide **3** (1 equiv) in C₆D₆. The reaction mixture was heated to 80-90 °C for 10-16 h. Benzene-d₆ was removed from the reaction mixture under vacuum and imidate **4** was isolated as an amorphous solid or oil.

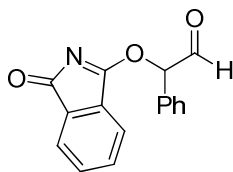


Imidate 4a: General procedure F was followed with **3a** (0.0272 g, 0.125 mmol). Heating the reaction mixture to 80 °C for 16 h afforded imidate **4a** (0.0272 g, >95% recovery) as a white solid. ¹H NMR (500 MHz; C₆D₆): δ 7.49 (d, *J* = 6.0 Hz, 1H), 7.13 (d, *J* = 6.0 Hz, 1H), 6.92-6.86 (m, 2H), 5.35 (q, *J* = 7.0 Hz, 1H), 1.79 (s, 3H), 1.20 (d, *J* = 7.0 Hz, 3H); ¹³C NMR (125 MHz, C₆D₆): δ 202.1, 184.9, 180.1, 135.9, 135.2, 132.5, 132.2, 123.6, 120.1, 80.5, 25.3, 15.6; IR (thin film) 3056, 2988, 2926, 2852, 1733, 1616, 1537, 1411, 1066, 734 cm⁻¹; HRMS (ESI) *m/z* calcd. for C₁₂H₁₂NO₃ (M+H)⁺ 218.0817, found 218.0815. ; mp 139-142 °C.

**4b**

Imidate 4b: General procedure F was followed with **3b** (0.044 g, 0.16 mmol). Heating the reaction mixture to 90 °C for 10 h afforded imidate **4b** (0.044 g, >95%) as a yellow oil. ^1H NMR (500 MHz; C_6D_6): δ 9.31 (d, $J = 6.0$ Hz, 1H), 7.52-7.50 (m, 2H), 7.14-7.12 (m, 2H), 6.96-6.91 (m, 2H), 5.30 (d, $J = 4.5$ Hz, 1H), 1.75-1.57 (m, 7H), 1.14-1.05 (m, 4H); ^{13}C NMR (125 MHz, C_6D_6): δ 195.8, 185.3, 179.9, 135.9, 135.0, 132.6, 132.2, 123.6, 120.4, 87.5, 38.6, 28.6, 27.3, 25.8; IR (thin film) 2923, 2855, 1732, 1624, 1538, 1444, 1407, 1358, 1313, 1070 cm^{-1} ; HRMS (ESI) m/z calcd. for $\text{C}_{14}\text{H}_{16}\text{NO}_3$ ($\text{M}+\text{H}$) $^+$ 246.1130, found 246.1138.

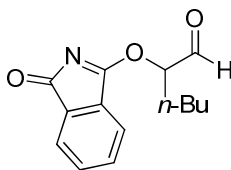
To obtain a ^1H NMR yield of this rearrangement a C_6D_6 solution of **3b** (0.042 g, 0.17 mmol) was heated to 90 °C in a J-Young tube in the presence of 1,3,5-trimethoxybenzene (0.010 g, 0.057 mmol) for 12 h. After 12 h of heating at, ^1H NMR analysis of the reaction mixture indicated that the yield of the in situ generated imidate was 73%.

**4c**

Imidate 4c: General procedure F was followed with **3c** (0.053 g, 0.20 mmol). Heating the reaction mixture to 50 °C for 10 h afforded imidate **4c** (0.053 g, >95%) as an amorphous oil. ^1H NMR (500 MHz; C_6D_6): δ 9.18 (s, 1H), 7.46 (d, $J = 7.0$ Hz, 1H), 7.28 (d, $J = 7.0$ Hz, 2H),

7.15-7.12 (m, 4H), 7.08 (d, $J = 7.0$ Hz, 1H), 6.89-6.85 (m, 1H), 6.41 (s, 1H); ^{13}C NMR (125 MHz, C_6D_6): δ 191.6, 184.8, 180.1, 135.8, 132.6, 132.3, 129.6, 129.1, 128.9, 128.5, 123.7, 123.2, 120.6, 85.4; HRMS (ESI) m/z calcd. for $\text{C}_{16}\text{H}_{12}\text{NO}_3$ ($\text{M}+\text{H}$) $^+$ submitted.

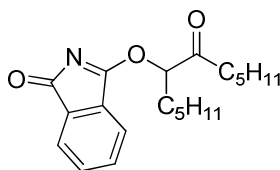
To obtain a ^1H NMR yield of this rearrangement a C_6D_6 solution of **3c** (0.051 g, 0.19 mmol) was heated to 90 °C in a J-Young tube for 12 h. After 12 h of heating, CH_2Br_2 (X 13.2 μL , 0.17 mmol) was added to the reaction mixture as a reference. ^1H NMR analysis of the reaction mixture indicated that the yield of the in situ generated imidate was 76%.



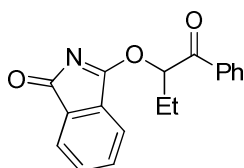
4d

Imidate 4d: General procedure F was followed with **3d** (0.025 g, 0.10 mmol). Heating the reaction mixture to 90 °C for 10 h afforded imidate **4d** (0.025 g, >95% recovery) as an amorphous solid. ^1H NMR (500 MHz; C_6D_6): δ 9.21 (s, 1H), 7.50-7.48 (m, 1H), 7.12-7.10 (m, 1H), 6.92-6.89 (m, 2H), 5.33 (dd, $J = 7.6, 5.4$ Hz, 1H), 1.62-1.57 (m, 2H), 1.28-1.23 (m, 2H), 1.23-1.14 (m, 2H), 0.83 (t, $J = 7.2$ Hz, 3H); ^{13}C NMR (125 MHz, C_6D_6): δ 195.43, 179.23, 185.11, 132.63, 132.24, 123.72, 120.38, 84.08, 28.42, 26.86, 22.32, 13.62; IR (thin film) 2959, 2930, 2868, 1733, 1617, 1536, 1467, 1405, 1358, 1315 cm^{-1} ; HRMS (ESI) m/z calcd. for $\text{C}_{16}\text{H}_{18}\text{NO}_3$ ($\text{M}+\text{H}$) $^+$ 272.1278, found 272.1284.

To obtain a ^1H NMR yield of this rearrangement a C_6D_6 solution of **3d** (0.034 g, 0.14 mmol) was heated to 90 °C in a J-Young tube in the presence of hexamethylbenzene (0.0038 g, 0.023 mmol) for 12 h. After 12 h of heating at, ^1H NMR analysis of the reaction mixture indicated that the yield of the in situ generated imidate was 67%.

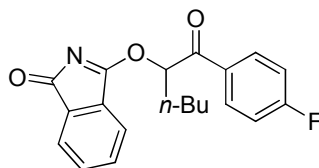
**4f**

Imidate 4f: General procedure F was followed with **3f** (0.140 g, 0.425 mmol). Heating the reaction mixture to 80 °C for 12 h afforded imidate **4f** (0.139 g, >95% recovery) as a yellow oil. ^1H NMR (500 MHz; C_6D_6): δ 7.50 (d, $J = 7.0$ Hz, 1H), 7.22 (d, $J = 6.5$ Hz, 1H), 7.00-6.94 (m, 2H), 5.57 (dd, $J = 4.5$ Hz, 8.0 Hz, 1H), 2.53-2.46 (m, 1H), 2.33-2.27 (m, 1H), 1.87-1.80 (m, 2H), 1.69-1.67 (m, 2H), 1.47-1.42 (m, 2H), 1.28-1.26 (m, 8H), 0.93-0.89 (m, 6H); ^{13}C NMR (125 MHz, C_6D_6): δ 204.2, 185.3, 180.1, 136.0, 135.2, 132.6, 132.3, 123.7, 120.5, 84.3, 38.9, 31.5, 31.3, 30.6, 25.0, 23.0, 22.6, 22.5, 13.9, 13.8; IR (thin film) 2986, 2936, 2850, 1748, 1700, 1548, 1413, 1088, 857 cm^{-1} ; HRMS (ESI) m/z calcd. for $\text{C}_{20}\text{H}_{28}\text{NO}_3$ ($\text{M}+\text{H}$) $^+$ 330.2069, found 330.2068.

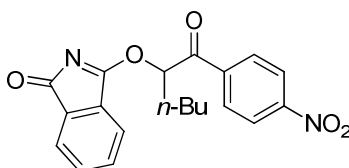
**4h**

Imidate 4h: General procedure F was followed with **3h** (0.070 g, 0.24 mmol). Heating the reaction mixture to 80 °C for 12 h afforded imidate **4h** (0.070 g, >95% recovery) as a yellow oil. ^1H NMR (500 MHz; C_6D_6): δ 7.95 (d, $J = 7.5$ Hz, 2H), 7.46-7.45 (m, 1H), 7.24-7.23 (m, 1H), 7.18-7.17 (m, 1H), 7.09 (t, $J = 7.5$ Hz, 2H), 6.92-6.91 (m, 2H), 6.46-6.43 (m, 1H), 1.93-1.90 (m, 2H), 0.94 (t, $J = 7.5$ Hz, 3H); ^{13}C NMR (125 MHz, C_6D_6): δ 194.4, 185.4, 180.2,

135.9, 135.3, 135.1, 133.4, 132.5, 132.3, 128.8, 128.5, 123.6, 120.7, 82.1, 25.1, 9.4; IR (thin film) 2985, 2930, 1744, 1700, 1533, 1413, 1071, 853, 718, 696 cm^{-1} ; HRMS (ESI) m/z calcd. for $\text{C}_{18}\text{H}_{16}\text{NO}_3$ ($\text{M}+\text{H}$)⁺ 294.1130, found 294.1139.

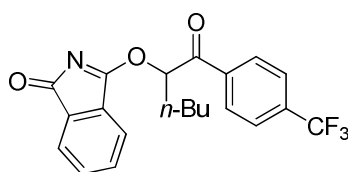
**4i**

Imidate 4i: General procedure F was followed with **3i** (0.070 g, 0.21 mmol). Heating the reaction mixture to 80 °C for 12 h afforded imidate **4i** (0.069 g, >95% recovery) as a yellow oil. ¹H NMR (500 MHz; C_6D_6): δ 7.90-7.88 (m, 2H), 7.46-7.43 (m, 1H), 7.24-7.22 (m, 1H), 6.92-6.91 (m, 2H), 6.75-6.67 (m, 2H), 6.48-6.46 (m, 1H), 1.99-1.91 (m, 2H), 1.51-1.43 (m, 2H), 1.29-1.19 (m, 2H), 0.84 (t, $J = 6.0$ Hz, 3H); ¹³C NMR (125 MHz, C_6D_6): δ 193.1, 185.3, 180.2, 164.9 (d, $J = 254$ Hz), 135.2, 132.6, 132.4, 131.3, 131.26, 128.1, 123.7, 120.7, 115.8 (d, $J = 22$ Hz), 81.0, 31.5, 27.4, 22.4, 13.7; IR (thin film) 2956, 2926, 2871, 1743, 1698, 1593, 1541, 1411, 1236, 852, 718 cm^{-1} ; HRMS (ESI) m/z calcd. for $\text{C}_{20}\text{H}_{19}\text{FNO}_3$ ($\text{M}+\text{H}$)⁺ 340.1349, found 340.1346.

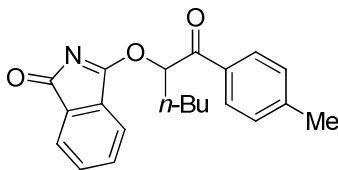
**4j**

Imidate 4j: General procedure F was followed with **3j** (0.078 g, 0.21 mmol). Heating the reaction mixture to 80 °C for 12 h afforded imidate **4j** (0.078 g, >95% recovery) as an

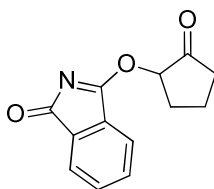
amorphous solid. ^1H NMR (500 MHz; C_6D_6): δ 7.77-7.75 (m, 3H), 7.46 (d, $J = 6.0$ Hz, 1H), 7.24-7.22 (m, 2H), 6.95-6.91 (m, 2H), 6.32 (dd, $J = 8.0$ Hz, 4.0 Hz, 1H), 1.95-1.87 (m, 2H), 1.51-1.45 (m, 2H), 1.32-1.22 (m, 2H), 0.87 (t, $J = 7.5$ Hz, 3H); ^{13}C NMR (125 MHz, C_6D_6): δ 193.9, 185.2, 180.0, 150.4, 138.9, 135.7, 134.9, 132.9, 132.5, 129.3, 123.81, 123.75, 120.7, 81.3, 31.1, 27.4, 22.4, 13.7; IR (thin film) 2959, 2933, 2868, 1746, 1703, 1532, 1411, 1346, 852, 718 cm^{-1} ; HRMS (ESI) m/z calcd. for $\text{C}_{20}\text{H}_{19}\text{N}_2\text{O}_5$ ($\text{M}+\text{H}$) $^+$ 367.1294, found 367.1292.

**4k**

Imidate 4k: General procedure F was followed with **3k** (0.080 g, 0.21 mmol). Heating the reaction mixture to 80 $^{\circ}\text{C}$ for 12 h afforded imidate **4k** (0.080 g, >95% recovery) as a yellow oil. ^1H NMR (500 MHz; C_6D_6): δ 7.90 (d, $J = 8.5$ Hz, 2H), 7.46 (d, $J = 7.0$ Hz, 1H), 7.32 (d, $J = 8.0$ Hz, 2H), 7.24-7.22 (m, 1H), 6.95-6.90 (m, 2H), 6.45 (dd, $J = 8.0$ Hz, 4.0 Hz, 1H), 1.89-1.98 (m, 2H), 1.46-1.51 (m, 2H), 1.20-1.31 (m, 2H), 0.85 (t, $J = 6.0$ Hz, 3H); ^{13}C NMR (125 MHz, C_6D_6): δ 194.0, 185.3, 180.1, 137.5, 135.8, 135.0, 132.7, 132.6 (q, $J = 35$ Hz), 132.4, 128.9, 125.8, 124.2 (q, $J = 342.5$ Hz), 123.7, 120.7, 81.4, 31.2, 27.2, 22.4, 13.7; IR (thin film) 2959, 2930, 2868, 1743, 1703, 1532, 1417, 1320, 1128, 1063, 715 cm^{-1} ; HRMS (ESI) m/z calcd. for $\text{C}_{21}\text{H}_{19}\text{F}_3\text{NO}_3$ ($\text{M}+\text{H}$) $^+$ 390.1317, found 390.1321.

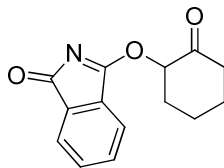
**4l**

Imidate 4l: General procedure F was followed with **3l** (0.070 g, 0.21 mmol). Heating the reaction mixture to 80 °C for 12 h afforded imidate **4l** (0.070 g, >95% recovery) as a yellow oil. ^1H NMR (500 MHz; C_6D_6): δ 8.01 (d, $J = 8.0$ Hz, 2H), 7.48-7.46 (m, 1H), 7.28-7.26 (m, 1H), 6.97-6.92 (m, 4H), 6.63-6.60 (m, 1H), 2.07-2.00 (m, 2H), 2.05 (s, 3H), 1.54-1.48 (m, 2H), 1.28-1.20 (m, 2H), 0.84 (t, $J = 7.5$ Hz, 3H); ^{13}C NMR (125 MHz, C_6D_6): δ 194.1, 185.4, 180.3, 144.3, 135.9, 135.3, 132.6, 132.5, 132.3, 129.6, 128.7, 123.6, 120.7, 81.2, 31.6, 27.5, 22.4, 21.2, 13.7; IR (thin film) 2959, 2933, 2861, 1739, 1691, 1606, 1537, 1414, 1070, 725 cm^{-1} ; HRMS (ESI) m/z calcd. for $\text{C}_{21}\text{H}_{22}\text{NO}_3$ ($\text{M}+\text{H}$) $^+$ 336.1600, found 336.1605.

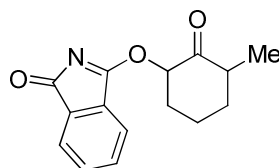
**4m**

Imidate 4m: General procedure F was followed with **3m** (0.028 g, 0.12 mmol). Heating the reaction mixture to 80 °C for 12 h afforded imidate **4m** (0.028 g, >95% recovery) as a yellow oil. ^1H NMR (500 MHz; C_6D_6): δ 7.49 (d, $J = 7.0$ Hz, 1H), 7.14 (d, $J = 6.5$ Hz, 1H), 6.94-6.85 (m, 2H), 5.46-5.43 (m, 1H), 2.22-2.17 (m, 1H), 1.86-1.73 (m, 2H), 1.64-1.56 (m, 1H), 1.44-1.36 (m, 1H), 1.18-1.15 (m, 1H); ^{13}C NMR (125 MHz, C_6D_6): δ 208.5, 185.4, 180.2, 132.5, 132.3, 128.1, 123.6, 122.9, 120.6, 81.5, 34.1, 28.0, 16.5; IR (thin film) 2958, 2923,

2850, 1748, 1700, 1413, 1388, 1088, 852 cm^{-1} ; HRMS (ESI) m/z calcd. for $\text{C}_{13}\text{H}_{12}\text{NO}_3$ ($\text{M}+\text{H}$)⁺ 230.0817, found 230.0806.

**4n**

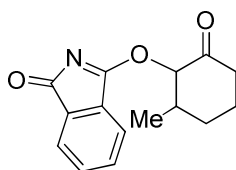
Imidate 4n: General procedure F was followed with **3n** (0.022 g, 0.090 mmol). Heating the reaction mixture to 90 °C for 10 h afforded imidate **4n** (0.022 g, >95% recovery) as a white solid. ¹H NMR (500 MHz; C_6D_6): δ 7.52-7.51 (m, 1H), 7.28-7.27 (m, 1H), 6.91-6.90 (m, 2H), 5.61 (dd, $J = 5.0, 5.0$ Hz, 1H), 2.27-2.24 (m, 1H), 2.16-2.13 (m, 1H), 1.86-1.84 (m, 1H), 1.65-1.61 (m, 1H), 1.42-1.33 (m, 2H), 1.32-1.07 (m, 2H); ¹³C NMR (125 MHz, C_6D_6): δ 201.1, 185.2, 180.5, 136.0, 135.5, 132.5, 132.2, 123.6, 120.6, 82.4, 40.3, 33.0, 26.7, 23.2; IR (thin film) 2947, 2865, 1734, 1620, 1535, 1408, 1360, 1320, 1294, 1073 cm^{-1} ; HRMS (ESI) m/z calcd. for $\text{C}_{14}\text{H}_{13}\text{NO}_3$ (M)⁺ 243.0895, found 243.0886; mp 128-130 °C.

**4o**

dr = 15:85; cis:trans

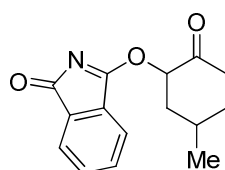
Imidate 4o: General procedure F was followed with **3o** (0.030 g, 0.12 mmol). Heating the reaction mixture to 80 °C for 12 h afforded imidate **4o** (0.029 g, >95%) as an amorphous solid. ¹H NMR *cis* diastereomer (500 MHz; C_6D_6): δ 7.50 (d, $J = 6.0$ Hz, 1H), 7.19 (d, $J =$

6.5 Hz, 1H), 6.94-6.81 (m, 2H), 5.63 (dd, $J = 13.0, 7.0$ Hz, 1H), 2.24-2.20 (m, 1H), 1.94-1.90 (m, 2H), 1.73-1.65 (m, 1H), 1.52-1.45 (m, 1H), 1.40-1.34 (m, 1H), 1.22-1.17 (m, 1H), 0.82 (d, $J = 7.0$ Hz, 3H); ^{13}C NMR *cis* diastereomer (125 MHz, C_6D_6): δ 204.8, 184.9, 180.4, 136.0, 135.4, 132.5, 132.2, 123.5, 120.6, 82.5, 43.8, 35.6, 33.4, 22.6, 13.9; ^1H NMR *trans* diastereomer (500 MHz; C_6D_6): δ 7.50 (d, $J = 6.0$ Hz, 1H), 7.19 (d, $J = 6.5$ Hz, 1H), 6.94-6.81 (m, 2H), 5.81 (dd, $J = 10.0, 5.5$ Hz, 1H), 2.69-2.63 (m, 1H), 1.94-1.90 (m, 1H), 1.88-1.83 (m, 1H), 1.52-1.45 (m, 1H), 1.40-1.34 (m, 2H), 1.22-1.17 (m, 1H), 0.96 (d, $J = 6.0$ Hz, 3H); ^{13}C NMR *trans* diastereomer (125 MHz, C_6D_6): δ 204.8, 184.9, 180.4, 136.0, 135.4, 132.5, 132.2, 123.6, 120.4, 80.7, 43.9, 33.5, 32.8, 18.9, 15.1; IR (thin film) 3057, 2977, 2938, 2868, 1733, 1613, 1536, 1409, 1267, 1151 cm^{-1} ; HRMS (ESI) m/z calcd. for $\text{C}_{15}\text{H}_{16}\text{NO}_3$ ($\text{M}+\text{H}$) $^+$ 258.1130, found 258.1130.

**4p****dr = 60:40; *cis:trans***

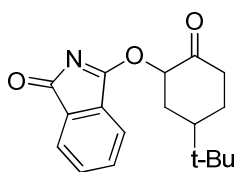
Imidate 4p: General procedure F was followed with **3p** (0.044 g, 0.16 mmol). Heating the reaction mixture to 90 °C for 14 h afforded imidate **4p** (0.044 g, >95% recovery) as an amorphous solid. ^1H NMR *cis* diastereomer (500 MHz; CDCl_3): δ 7.72-7.71 (m, 1H), 7.69-7.68 (m, 1H), 7.57-7.56 (m, 2H), 5.84 (d, $J = 5.5$ Hz, 1H), 2.91-2.86 (m, 1H), 2.55-2.53 (m, 2H), 2.11-2.02 (m, 2H), 1.86-1.85 (m, 1H), 1.71-1.66 (m, 1H), 1.10 (d, $J = 5.0$ Hz, 3H); ^1H NMR *trans* diastereomer (500 MHz; CDCl_3): δ 7.74-7.73 (m, 2H), 7.59-7.57 (m, 2H), 5.44 (d, $J = 11.5$ Hz, 1H), 2.53-2.44 (m, 2H), 2.30-2.27 (m, 1H), 2.01-1.92 (m, 2H), 1.86-1.85 (m,

1H), 1.64-1.57 (m, 1H), 1.20 (d, $J = 5.0$ Hz, 3H; ^1H NMR *cis* diastereomer (500 MHz; C_6D_6): δ 7.52-7.51 (m, 1H), 7.29-7.27 (m, 1H), 6.96-6.93 (m, 2H), 5.73 (d, $J = 5.5$ Hz, 1H), 2.50-2.47 (m, 1H), 2.29-2.22 (m, 2H), 1.50-1.39 (m, 4H), 0.93 (d, $J = 5.0$ Hz, 3H); ^{13}C NMR *cis* diastereomer (125 MHz, C_6D_6): δ 201.3, 185.8, 180.5, 136.1, 135.4, 132.4, 132.2, 123.6, 120.6, 87.7, 40.0, 39.4, 31.8, 25.2, 18.5; ^1H NMR *trans* diastereomer (500 MHz; C_6D_6): δ 7.52-7.51 (m, 1H), 7.21-7.20 (m, 1H), 6.93-6.91 (m, 2H), 5.40 (d, $J = 11.5$ Hz, 1H), 1.98-1.89 (m, 3H), 1.35-1.26 (m, 3H), 1.18-1.11 (m, 1H), 0.96 (d, $J = 5.0$ Hz, 3H); ^{13}C NMR *trans* diastereomer (125 MHz, C_6D_6): δ 200.9, 185.1, 180.5, 135.9, 135.4, 132.4, 132.2, 123.5, 120.5, 85.0, 39.9, 36.0, 29.5, 21.3, 12.3; IR (thin film) 2949, 2866, 1732, 1620, 1534, 1407, 1310, 1137, 1070, 1010 cm^{-1} ; HRMS (ESI) m/z calcd. for $\text{C}_{15}\text{H}_{16}\text{NO}_3$ ($\text{M}+\text{H}$) $^+$ 258.1130, found 258.1135.

**4q****dr = 50:50; *cis:trans***

Imidate 4q: General procedure F was followed with **3q** (0.019 g, 0.073 mmol). Heating the reaction mixture to 90 °C for 10 h afforded imidate **4q** (0.019 g, >95% recovery) as a yellow oil. ^1H NMR *cis* diastereomer (500 MHz; C_6D_6): δ 7.52-7.51 (m, 1H), 7.32-7.30 (m, 1H), 6.92-6.89 (m, 2H), 5.67 (dd, $J = 6.5, 6.5$ Hz, 1H), 2.17-2.06 (m, 2H), 1.90-1.89 (m, 1H), 1.76-1.73 (m, 1H), 1.40-1.33 (m, 2H), 0.92-0.80 (m, 1H), 0.66 (d, $J = 5.0$ Hz, 3H); ^{13}C NMR *cis* diastereomer (125 MHz, C_6D_6): 201.2, 185.1, 180.4, 136.0, 135.4, 132.2, 132.1, 120.6, 120.5, 80.0, 39.1, 36.3, 32.4, 27.2, 17.5; ^1H NMR *trans* diastereomer (500 MHz; C_6D_6): δ

7.53-7.52 (m, 1H), 7.32-7.31 (m, 1H), 6.94-6.92 (m, 2H), 5.80 (dd, $J = 6.5, 6.5$ Hz, 1H), 2.24-2.20 (m, 2H), 1.96-1.92 (m, 2H), 1.43-1.41 (m, 2H), 1.23-1.20 (m, 1H), 0.80 (d, $J = 5.0$ Hz, 3H); ^{13}C NMR *trans* diastereomer (125 MHz, C_6D_6): δ 201.8, 185.2, 180.5, 136.0, 135.4, 132.4, 132.3, 123.5, 123.4, 81.3, 40.5, 38.5, 34.4, 30.1, 20.4; IR (thin film) 2963, 2926, 2868, 1733, 1616, 1528, 1457, 1412, 1317, 1076 cm^{-1} ; HRMS (ESI) m/z calcd. for $\text{C}_{15}\text{H}_{16}\text{NO}_3$ ($\text{M}+\text{H}$) $^+$ 258.1130, found 258.1135.

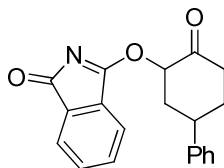


4r

dr = 60:40; *cis:trans*

Imidate 4r: General procedure F was followed with **3r** (0.0385 g, 0.1287 mmol). Heating the reaction mixture to 80 °C for 16 h afforded imidate **4r** (0.0383 g, >95% recovery) as an amorphous solid. ^1H NMR *cis* diastereomer (500 MHz; C_6D_6): δ 7.53-7.47 (m, 1H), 7.35-7.34 (m, 1H), 6.97-6.91 (m, 2H), 5.76 (dd, $J = 12.0, 6.5$ Hz, 1H), 2.38-2.24 (m, 2H), 2.02-1.95 (m, 1H), 1.64-1.59 (m, 1H), 1.56-1.51 (m, 1H), 1.42-1.35 (m, 1H), 1.05-0.96 (m, 1H), 0.73 (s, 9H); ^{13}C NMR *cis* diastereomer (125 MHz, C_6D_6): δ 201.5, 185.2, 180.5, 136.0, 135.5, 132.2, 123.6, 120.6, 82.2, 44.9, 41.0, 39.1, 34.1, 27.5, 27.2, 26.7; ^1H NMR *trans* diastereomer (500 MHz; C_6D_6): δ 7.53-7.47 (m, 1H), 7.21-7.20 (m, 1H), 6.97-6.91 (m, 2H), 5.74 (t, $J = 7.0$ Hz, 1H), 2.38-2.24 (m, 1H), 2.11-2.05 (m, 1H), 1.86-1.80 (m, 1H), 1.48-1.45 (m, 1H), 1.31-1.20 (m, 3H), 1.05-0.96 (m, 1H), 0.72 (s, 9H); ^{13}C NMR *trans* diastereomer (125 MHz, C_6D_6): δ 203.8, 184.9, 180.3, 135.8, 135.3, 133.3, 128.1, 122.8, 120.4, 81.2, 42.1,

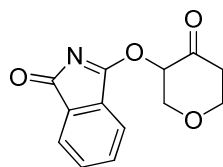
41.0, 37.6, 30.5, 26.7, 24.1; IR (thin film) 3056, 2963, 2873, 1762, 1731, 1619, 1541, 1410, 1267, 1073 cm^{-1} ; HRMS (ESI) m/z calcd. for $\text{C}_{18}\text{H}_{22}\text{NO}_3$ ($\text{M}+\text{H}$)⁺ 300.1600, found 300.1602.



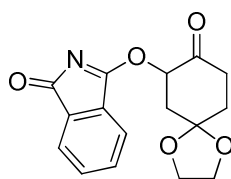
4s

dr = 55:45; *cis:trans*

Imidate 4s: General procedure F was followed with **3s** (0.0284 g, 0.0890 mmol). Heating the reaction mixture to 90 °C for 16 h afforded imidate **4s** (0.0275 g, >95% recovery) as an oil. ¹H NMR *cis* diastereomer (500 MHz; C_6D_6): δ 7.54-7.47 (m, 1H), 7.34-7.14 (m, 5H), 6.98-6.93 (m, 3H), 5.83 (dd, $J = 13.0, 6.5$ Hz, 1H), 2.73 (tdd, $J = 13.0$ Hz, $J = 6.5$ Hz, $J = 3.0$ Hz, 1H), 2.49-1.97 (m, 3H), 1.85-1.81 (m, 1H), 1.70-1.64 (m, 1H), 1.49-1.46 (m, 1H); ¹³C NMR *cis* diastereomer (125 MHz, C_6D_6): δ 200.9, 185.2, 180.5, 143.2, 136.0, 135.4, 132.5, 132.3, 128.6, 126.8, 126.7, 123.6, 120.6, 81.5, 41.4, 39.6, 37.3, 33.8; ¹H NMR *trans* diastereomer (500 MHz; C_6D_6) of the minor diastereomer: δ 7.54-7.47 (m, 1H), 7.34-7.14 (m, 5H), 6.98-6.93 (m, 3H), 5.83 (dd, $J = 9.5$ Hz, $J = 5.5$ Hz, 1H), 2.99-2.96 (m, 1H), 2.49-1.97 (m, 5H), 1.70-1.64 (m, 1H); ¹³C NMR *trans* diastereomer (125 MHz, C_6D_6): δ 202.2, 184.8, 180.2, 142.0, 135.9, 135.5, 132.3, 132.2, 128.8, 126.9, 126.7, 123.6, 120.5, 80.6, 39.4, 37.0, 36.8, 31.8; IR (thin film) 3060, 3030, 2952, 2930, 2868, 1619, 1729, 1537, 1407, 715 cm^{-1} ; HRMS (ESI) m/z calcd. for $\text{C}_{20}\text{H}_{18}\text{NO}_3$ ($\text{M}+\text{H}$)⁺ 320.1287, found 320.1292.

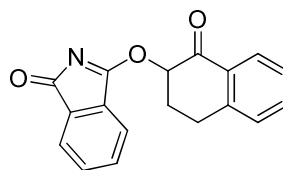
**4t**

Imidate 4t: General procedure F was followed with **3t** (0.062 g, 0.25 mmol). Heating the reaction mixture to 90 °C for 10 h afforded imidate **4t** (0.062 g, >95% recovery) as an amorphous solid. ^1H NMR (500 MHz; C_6D_6): δ 7.50-7.48 (m, 1H), 7.18-7.17 (m, 1H), 6.93-6.90 (m, 2H), 5.69 (dd, $J = 5.0, 5.0$ Hz, 1H), 4.23 (dd, $J = 10.0, 5.0$ Hz, 1H), 3.61 (dd, $J = 10.0, 5.0$ Hz, 1H), 3.37 (t, $J = 5.0$ Hz, 1H), 3.02 (dt, $J = 10.0, 5.0$ Hz, 1H), 2.21-2.14 (m, 1H), 2.04-2.01 (m, 1H); ^{13}C NMR (125 MHz, C_6D_6): δ 197.7, 184.9, 180.0, 135.9, 135.0, 132.6, 132.3, 123.7, 120.5, 78.9, 69.7, 68.0, 41.8; IR (thin film) 2966, 2926, 1727, 1613, 1538, 1467, 1408, 1382, 1206, 1073 cm^{-1} ; HRMS (ESI) m/z calcd. for $\text{C}_{13}\text{H}_{12}\text{NO}_4$ ($\text{M}+\text{H}$) $^+$ 246.0766, found 246.0758.

**4u**

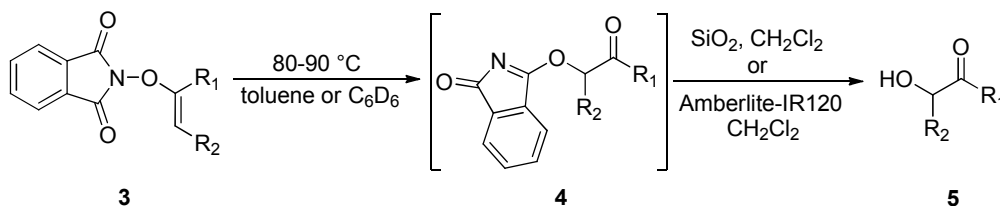
Imidate 4u: General procedure F was followed with **3u** (0.300 g, 0.996 mmol). Heating the reaction mixture to 80 °C for 12 h afforded imidate **4u** (0.290 g, >95% recovery) as an amorphous solid. ^1H NMR (500 MHz; C_6D_6): δ 7.51-7.48 (m, 1H), 7.24-7.23 (m, 1H), 6.98-6.91 (m, 2H), 6.11-6.09 (m, 1H), 3.55-3.46 (m, 4H), 2.50-2.44 (m, 2H), 2.21-2.18 (m, 2H), 1.68-1.65 (m, 2H); ^{13}C NMR (125 MHz, C_6D_6): δ 200.3, 185.1, 180.3, 136.0, 135.4, 132.5,

132.3, 123.6, 120.6, 107.0, 79.3, 64.6, 64.5, 40.3, 35.6, 34.3; IR (thin film) 2963, 2938, 2890, 1736, 1617, 1533, 1409, 1126, 1027, 718 cm^{-1} ; HRMS (ESI) m/z calcd. for $\text{C}_{16}\text{H}_{16}\text{NO}_5$ ($\text{M}+\text{H}$)⁺ 302.1004, found 302.1001.

**4v**

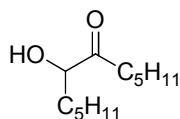
Imidate 4v: General procedure F was followed with **3v** (0.0287 g, 0.0986 mmol). Heating the reaction mixture to 80 °C for 16 h afforded imidate **4v** (0.0273 g, 95%) as an orange solid. ¹H NMR (500 MHz; C_6D_6): δ 8.16 (d, $J = 8.0$ Hz, 1H), 7.53 (d, $J = 6.0$ Hz, 1H), 7.27-7.25 (m, 2H), 7.12 (t, $J = 7.5$ Hz, 1H), 7.01-6.91 (m, 3H), 6.80 (d, $J = 7.5$ Hz, 1H), 6.03 (dd, $J = 13.5$ Hz, $J = 5.0$ Hz, 1H), 2.61-2.57 (m, 1H), 2.44-2.41 (m, 1H), 2.22 (ddd, $J = 9.0$ Hz, $J = 7.0$, $J = 4.5$ Hz, 1H), 2.06 (ddd, $J = 13.5$, 9.0, 4.5 Hz, 1H); ¹³C NMR (125 MHz, C_6D_6): δ 190.5, 185.6, 180.6, 142.9, 136.1, 135.5, 133.6, 132.5, 132.3, 131.6, 128.5, 127.9, 126.9, 123.5, 120.8, 80.9, 28.9, 27.3; IR (thin film) 3056, 2990, 2926, 2877, 2851, 1739, 1701, 1605, 1541, 1261 cm^{-1} ; HRMS (ESI) m/z calcd. for $\text{C}_{18}\text{H}_{14}\text{NO}_3$ ($\text{M}+\text{H}$)⁺ 292.0974, found 292.0976.; mp 134-138°C.

V. Synthesis of α -Hydroxy Ketones and ^1H NMR Spectroscopy Yields of Imidate Intermediates (Table 1.5)



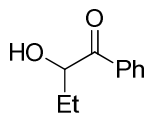
General Procedure G: Synthesis of α -Hydroxy Ketones. A J-Young tube or Teflon-sealed reaction flask was charged with N-enoxypthalimide 3 (1 equiv), hexamethylbenzene as an internal standard, and either C_6D_6 or toluene. C_6D_6 was used as the solvent if the reaction was run in a J-Young tube and toluene was used if the solvent if the reaction was run on larger scale in a Teflon-sealed reaction flask. The reaction mixture was heated to 70-90 $^\circ\text{C}$ for 10-16 h. Reaction mixtures heated in C_6D_6 were analyzed directly by ^1H NMR spectroscopy to determine the yield of imidate 4. Reaction mixtures heated in toluene were first concentrated under reduced pressure, dissolved in C_6D_6 , and analyzed by ^1H NMR spectroscopy to determine the yield of imidate 4. The crude solutions of imidate 4 were then transferred to a scintillation vial, C_6D_6 was removed under reduced pressure, and the resulting amorphous solid was dissolved in CH_2Cl_2 to form an 0.1 M solution of 4. Silica gel (0.200 g/ 0.1 mmol of 4) or Amberlite-IR120 resin (0.200 g/ 0.1 mmol of 4) was then added to the CH_2Cl_2 solution and the reaction mixture was stirred at 25 $^\circ\text{C}$ until formation of a white precipitate was observed (20 - 40 min) if Amberlite-IR120 was used or 16 h if SiO_2 was used. The silica gel or Amberlite-IR120 resin was then separated from the CH_2Cl_2 solution and washed with CH_2Cl_2 (3 x 4 mL). The filtrate was then concentrated under reduced pressure, dissolved in ethyl acetate (20 mL), and extracted with 1M $\text{NaOH}_{(\text{aq})}$ (3 x 2

mL) to remove the phthalimide byproduct. The organic layer was then concentrated under reduced pressure and purified by medium pressure chromatography (ethyl acetate:hexane) to give **5** as a white solid.

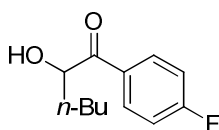


5f

α -Hydroxy Ketone 5f: General procedure G was followed by heating a C_6D_6 solution of **3f** (0.140 g, 0.425 mmol) in the presence of CH_2Br_2 (21 μ L, 0.30 mmol) in a J-Young tube for 12 h. After 12 h of heating at 80 $^{\circ}C$, 1H NMR analysis of the reaction mixture indicated that the yield of the in situ generated imidate **4f** was 90%. The imidate was then mixed with silica gel in CH_2Cl_2 and allowed to stir for 16 h. Treatment with $NaOH_{(aq)}$ and purification by chromatography gave **5f** as a clear, colorless oil (0.066 g, 78%). 1H NMR (500 MHz; $CDCl_3$): δ 4.18-4.15 (m, 1H), 3.48 (brs, 1H), 2.47-2.41 (m, 2H), 1.80-1.79 (m, 1H), 1.63-1.59 (m, 2H), 1.52-1.46 (m, 2H), 1.37-1.24 (m, 9H), 0.89-0.87 (m, 6H); ^{13}C NMR (125 MHz, $CDCl_3$): δ 212.6, 76.4, 37.8, 33.8, 31.7, 31.4, 24.5, 23.4, 22.5, 22.4, 14.0, 13.9; IR (thin film) 3472, 2959, 2922, 2855, 1709, 1466, 1376, 1130, 1058 cm^{-1} ; HRMS (ESI) m/z calcd. for $C_{12}H_{24}O_2Na$ ($M+Na$) $^+$ 223.1674, found 223.1670.

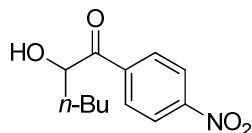
**5h**

α -Hydroxy Ketone 5h: General procedure G was followed by heating a C₆D₆ solution of **3h** (0.070 g, 0.24 mmol) in the presence of hexamethylbenzene (0.0162 g, 0.100 mmol) in a J-Young tube for 12 h. After 12 h of heating at 80 °C, ¹H NMR analysis of the reaction mixture indicated that the yield of the in situ generated imidate **4h** was >95%. The imidate was then mixed with Amberlite-IR120 in CH₂Cl₂ and allowed to stir for 3 h. Treatment with NaOH_(aq) and purification by chromatography gave **5h** as a yellow oil (0.0351 g, 90%). ¹H NMR (500 MHz; CDCl₃): δ 7.90 (d, J = 8.0 Hz, 2H), 7.63-7.60 (m, 1H), 7.48 (t, J = 8.0 Hz, 2H), 5.07-5.04 (m, 1H), 3.69 (d, J = 6.0 Hz, 1H), 1.98-1.91 (m, 1H), 1.64-1.58 (m, 1H), 0.92 (t, J = 7.5 Hz, 3H); ¹³C NMR (125 MHz, CDCl₃): δ 202.1, 133.9, 133.8, 128.9, 128.5, 74.0, 28.9, 8.9; IR (thin film) 3472, 2966, 2940, 2873, 1675, 1597, 1451, 1245, 1130, 965, 692 cm⁻¹; HRMS (ESI) m/z calcd. for C₁₀H₁₂O₂Na (M+Na)⁺ 187.0735, found 187.0736.

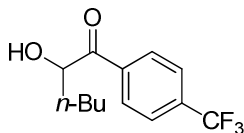
**5i**

α -Hydroxy Ketone 5k: General procedure G was followed by heating a C₆D₆ solution of **3i** (0.070 g, 0.21 mmol) in the presence of hexamethylbenzene (0.0162 g, 0.100 mmol) in a J-Young tube for 12 h. After 12 h of heating at 80 °C, ¹H NMR analysis of the reaction mixture indicated that the yield of the in situ generated imidate **4i** was 95%. The imidate was then mixed with Amberlite-IR120 in CH₂Cl₂ and allowed to stir for 3 h. Treatment with

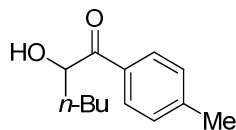
NaOH_(aq) and purification by chromatography gave **5i** as a white solid (0.038 g, 88%). ¹H NMR (500 MHz; CDCl₃): δ 7.93-7.96 (m, 2H), 7.15 (t, *J* = 8.5 Hz, 2H), 5.12-5.06 (m, 1H), 3.63 (d, *J* = 6.5 Hz, 1H), 1.84-1.82 (m, 1H), 1.53-1.47 (m, 2H), 1.34-1.24 (m, 3H), 0.85 (t, *J* = 7.5 Hz, 3H); ¹³C NMR (125 MHz, CDCl₃): δ 200.6, 166.1 (d, *J* = 255 Hz), 131.2, 130.1, 116.1 (d, *J* = 18.8 Hz), 73.0, 35.7, 27.1, 22.5, 13.9; IR (thin film) 3466, 2956, 2933, 2868, 1677, 1593, 1502, 1236, 1132, 1079, 845, 604 cm⁻¹; HRMS (ESI) *m/z* calcd. for C₁₂H₁₅FO₂Na (M+Na)⁺ 233.0954, found 233.0956; mp 45-47 °C.

**5j**

α -Hydroxy Ketone 5j: General procedure G was followed by heating a C₆D₆ solution of **3j** (0.078 g, 0.21 mmol) in the presence of hexamethylbenzene (0.0162 g, 0.100 mmol) in a J-Young tube for 12 h. After 12 h of heating at 80 °C, ¹H NMR analysis of the reaction mixture indicated that the yield of the in situ generated imidate **4j** was >95%. The imidate was then mixed with Amberlite-IR120 in CH₂Cl₂ and allowed to stir for 3 h. Treatment with NaOH_(aq) and purification by chromatography gave **5j** as a yellow oil (0.038 g, 75%). ¹H NMR (500 MHz; CDCl₃): δ 8.34 (d, *J* = 9.0 Hz, 2H), 8.06 (d, *J* = 8.5 Hz, 2H), 5.12-5.06 (m, 1H), 3.49 (d, *J* = 6.5 Hz, 1H), 1.87-1.82 (m, 1H), 1.58-1.46 (m, 2H), 1.34-1.31 (m, 3H), 0.88 (t, *J* = 7.5 Hz, 3H); ¹³C NMR (125 MHz, CDCl₃): δ 201.8, 150.7, 138.5, 129.6, 124.1, 73.7, 35.1, 27.0, 22.4, 13.8; IR (thin film) 3483, 2956, 2929, 2861, 1695, 1601, 1526, 1374, 1275, 1084, 852, 710 cm⁻¹; HRMS (ESI) *m/z* calcd. for C₁₂H₁₅NO₄Na (M+Na)⁺ 260.0899, found 260.0902.

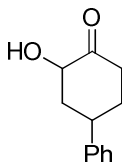
**5k**

α -Hydroxy Ketone 5k: General procedure G was followed by heating a C_6D_6 solution of **3k** (0.080 g, 0.21 mmol) in the presence of hexamethylbenzene (0.0162 g, 0.100 mmol) in a J-Young tube for 12 h. After 12 h of heating at 80 °C, 1H NMR analysis of the reaction mixture indicated that the yield of the in situ generated imidate **4k** was >95%. The imidate was then mixed with Amberlite-IR120 in CH_2Cl_2 and allowed to stir for 3 h. Treatment with $NaOH_{(aq)}$ and purification by chromatography gave **5k** as a white solid (0.046 g, 86%). 1H NMR (500 MHz; $CDCl_3$): δ 8.01 (d, $J = 8.0$ Hz, 2H), 7.76 (d, $J = 8.0$ Hz, 2H), 5.12-5.08 (m, 1H), 3.57 (d, $J = 5.0$ Hz, 1H), 1.87-1.83 (m, 1H), 1.56-1.48 (m, 2H), 1.35-1.22 (m, 3H), 0.85 (t, $J = 7.5$ Hz, 3H); ^{13}C NMR (125 MHz, $CDCl_3$): δ 201.5, 136.6, 135.0 (q, $J = 32$ Hz), 128.9, 126.0 (d, $J = 2.5$ Hz), 122.3, (d, $J = 271$ Hz), 73.5, 35.3, 27.0, 22.4, 13.9; IR (thin film) 3473, 2959, 2930, 2868, 1684, 1323, 1132, 1066, 858 cm^{-1} ; HRMS (ESI) m/z calcd. for $C_{13}H_{15}F_3O_2Na$ ($M+Na$) $^+$ 283.0922, found 283.0927; mp 40-42 °C.

**5l**

α -Hydroxy Ketone 5l: General procedure G was followed by heating a C_6D_6 solution of **3l** (0.070 g, 0.21 mmol) in the presence of hexamethylbenzene (0.0162 g, 0.100 mmol) in a J-Young tube for 12 h. After 12 h of heating at 80 °C, 1H NMR analysis of the reaction

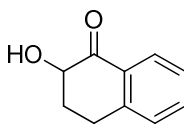
mixture indicated that the yield of the in situ generated imidate **4l** was >95%. The imidate was then mixed with silica gel in CH₂Cl₂ and allowed to stir for 12 h. Treatment with NaOH_(aq) and purification by chromatography gave **5l** as a yellow oil (0.0352 g, 82%). ¹H NMR (500 MHz; CDCl₃): δ 7.80 (d, *J* = 8.0 Hz, 2H), 7.28 (d, *J* = 8.0 Hz, 2H), 5.05-5.02 (m, 1H), 3.70 (d, *J* = 6.5 Hz, 1H), 2.43 (s, 3H), 1.88-1.83 (m, 1H), 1.54-1.45 (m, 2H), 1.37-1.33 (m, 3H), 0.92 (t, *J* = 7.5 Hz, 3H); ¹³C NMR (125 MHz, CDCl₃): δ 201.7, 144.9, 131.2, 129.6, 128.7, 73.0, 35.8, 27.1, 22.5, 21.8, 13.9; IR (thin film) 3479, 2959, 2929, 2862, 1671, 1608, 1271, 1133, 979, 826 cm⁻¹; HRMS (ESI) *m/z* calcd. for C₁₃H₁₈O₂Na (M+Na)⁺ 229.1204, found 229.1203.

**5s****dr = 60:40; cis:trans**

α -Hydroxy Ketone 5s: A C₆D₆ solution of **3s** (0.0231g, 0.0724 mmol) and trimethoxybenzene (0.0069 g, 0.041 mmol) was heated in a J-Young tube for 12 h at 90 °C. At this time, ¹H NMR analysis of the reaction mixture indicated that the yield of the in situ generated imidate **4s** was 95%.

A C₆D₆ solution of **3s** (0.124 g, 0.388 mmol) was heated in a J-Young tube at 90 °C for 16h. At this time, ¹H NMR analysis indicated that conversion to imidate **4s** was complete. The C₆D₆ solution of **4t** was then concentrated under reduced pressure and dissolved in CH₂Cl₂. The CH₂Cl₂ solution of **4s** was mixed with Amberlite-IR120 (0.2 g/ 0.1 mmol of **4s**), and allowed to stir for 30 min. Treatment with NaOH_(aq) and purification by chromatography, as

described in general procedure G, gave **5s** as an amorphous solid (0.0603 g, 82%). ^1H NMR *cis* diastereomer (500 MHz; CDCl_3): δ 7.44-7.23 (m, 5H), 4.34 (dd, $J = 12.0, 6.5$ Hz, 1H), 3.70 (brs, 1H), 3.18 (ddt, $J = 12.0, 6.0, 3.0$ Hz, 1H), 2.74-2.50 (m, 3H), 2.27-2.26 (m, 1H), 1.97-1.70 (m, 2H); ^{13}C NMR *cis* diastereomer (125 MHz, CDCl_3): δ 210.8, 143.5, 128.7, 126.7, 126.5, 74.6, 43.2, 41.3, 38.7, 34.9; ^1H NMR (500 MHz; CDCl_3) *trans* diastereomer: 7.44-7.23 (m, 5H), 4.25 (dd, $J = 10.5, 6.0$ Hz, 1H), 3.52 (bs, 1H), 3.43-3.41(m, 1H), 2.85-2.82 (m, 1H), 2.74-2.50 (m, 3H), 2.17-2.03 (m, 1H), 1.97-1.70 (m, 1H); ^{13}C NMR *trans* diastereomer (125 MHz, CDCl_3): δ 211.6, 143.5, 128.8, 126.9, 126.6, 72.3, 39.8, 36.3, 36.2, 31.1; IR (thin film) 3450, 3060, 3027, 2933, 2868, 1717, 1495, 1267, 1102, 738 cm^{-1} ; HRMS (EI) m/z calcd. for $\text{C}_{12}\text{H}_{15}\text{O}_2$ ($\text{M}+\text{H}$) $^+$ 190.09938, found 190.09968.

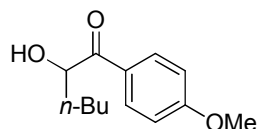
**5v**

α -Hydroxy Ketone 5v: A C_6D_6 solution of **3v** (0.0352 g, 0.121 mmol) and trimethoxybenzene (0.0050 g, 0.030 mmol) was heated to 80 $^\circ\text{C}$ in a J-Young tube for 16 h. At this time, ^1H NMR analysis of the reaction mixture indicated that the yield of the in situ generated imidate **4v** was 94%.

A C_6D_6 solution of **3v** (0.0287 g, 0.0986 mmol) was heated in a J-Young tube at 80 $^\circ\text{C}$ for 16 h. At this time, ^1H NMR analysis indicated that conversion to imidate **4v** was complete. The C_6D_6 solution of **4v** was then concentrated under reduced pressure and dissolved in CH_2Cl_2 . The CH_2Cl_2 solution of **4v** was mixed with Amberlite-IR120 (0.2 g/ 0.1mmol of 4v), and allowed to stir for 1 h. Treatment with $\text{NaOH}_{(\text{aq})}$ and purification by chromatography, as

described in general procedure G, gave **5v** as a yellow oil (0.0139 g, 87%). ^1H NMR (500 MHz; CDCl_3): δ 8.04 (d, $J = 7.5$ Hz, 1H), 7.53 (t, $J = 7.5$ Hz, 1H), 7.35 (d, $J = 7.5$ Hz, 1H), 7.27 (d, $J = 7.5$ Hz, 1H), 4.39 (dd, $J = 13.5, 5.5$ Hz, 1H), 3.91 (brs, 1H), 3.19-3.12 (m, 1H), 3.06-3.02 (m, 1H), 2.54 (dt, $J = 5.5, 4.5$ Hz, 1H), 2.04 (ddd, $J = 13.5, 8.5, 4.5$ Hz, 1H); ^{13}C NMR (125 MHz, CDCl_3): δ 199.6, 144.4, 134.2, 130.5, 128.9, 127.6, 126.9, 73.9, 31.9, 27.8; IR (thin film) 3479, 2955, 2934, 2875, 1682, 1602, 1460, 1282, 1089, 987 cm^{-1} ; HRMS (EI) m/z calcd. for $\text{C}_{10}\text{H}_{10}\text{O}_2\text{Na}(\text{M}+\text{Na})^+$ 185.0578, found 185.0580.

Conversion of **1** and **2w** to α -Hydroxy Ketone **5w**:

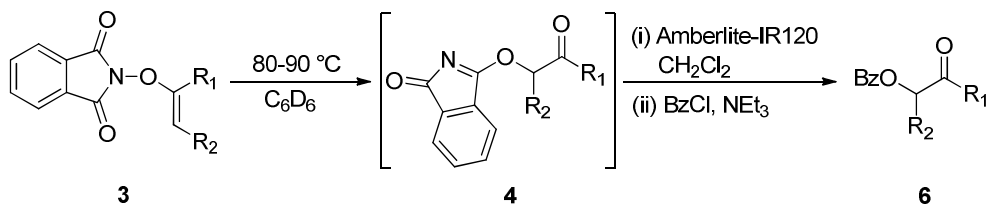


5w

General procedure C (or D) with *N*-hydroxyphthalimide **2** (0.050 g; 0.30 mmol), alkenyl boronic acid **1w** (0.210 g, 0.900 mmol), $\text{Cu}(\text{OAc})_2$ (0.054 g, 0.30 mmol), Na_2SO_4 (0.187 g, 1.30 mmol), and pyridine (72.4 μL , 0.900 mmol) afforded a mixture of **3w** and **5w** which was separated from the copper reagent using medium pressure chromatography (1:9; ethyl acetate:hexanes). The mixture of **3w** and **5w** was then subjected to general procedure G and dissolved in C_6D_6 and heated to 80 $^\circ\text{C}$ for 12 h. The crude product mixture was then mixed with Amberlite-IR120 in CH_2Cl_2 and allowed to stir for 3 h. Treatment with $\text{NaOH}_{(\text{aq})}$ and purification by chromatography gave **5w** as an amorphous solid (0.039 g, 57%). ^1H NMR (500 MHz; CDCl_3): δ 7.89 (d, $J = 8.0$ Hz, 2H), 6.96 (d, $J = 8.0$ Hz, 2H), 5.03-5.01 (m, 1H), 3.87 (s, 3H), 3.74 (d, $J = 5.0$ Hz, 1H), 1.87-1.85 (m, 1H), 1.54-1.49 (m, 2H), 1.37-1.25 (m,

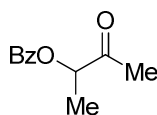
3H), 0.85 (t, $J = 7.5$ Hz, 3H); ^{13}C NMR (125 MHz, CDCl_3): δ 200.5, 164.1, 130.9, 126.5, 114.1, 72.7, 55.6, 36.0, 27.1, 22.5, 13.9; IR (thin film) 3473, 2956, 2926, 2858, 1671, 1596, 1509, 1251, 1170, 838 cm^{-1} ; HRMS (ESI) m/z calcd. for $\text{C}_{13}\text{H}_{18}\text{O}_3\text{Na}$ ($\text{M}+\text{Na}$) $^+$ 245.1154, found 245.1151.

VI. Synthesis of α -Benzoyloxy Ketones and ^1H NMR Spectroscopy Yields of Imidate Intermediates (Table 1.6)



General Procedure H: Synthesis of α -Benzoyloxy ketones. A J-Young tube or Teflon-sealed reaction flask was charged with *N*-enoxypthalimide 3 (1 equiv), hexamethylbenzene as an internal standard, and either C_6D_6 or toluene. C_6D_6 was used as the solvent if the reaction was run in a J-Young tube and toluene was used as the solvent if the reaction was run on larger scale in a Teflon-sealed reaction flask. The reaction mixture was heated to 70-90 $^\circ\text{C}$ for 10-16 h. Reaction mixtures heated in C_6D_6 were analyzed directly by ^1H NMR spectroscopy to determine the yield of imidate 4. Reaction mixtures heated in toluene were first concentrated under reduced pressure, dissolved in C_6D_6 , and analyzed by ^1H NMR spectroscopy to determine the yield of imidate 4. The crude solutions of imidate 4 were then transferred to a scintillation vial, C_6D_6 was removed under reduced pressure, and the resulting amorphous solid was dissolved in CH_2Cl_2 to form a 0.1 M solution of 4. Amberlite-IR120 resin (0.200 g per 0.1 mmol 4) was then added to the CH_2Cl_2 solution and the reaction

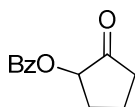
mixture was stirred at 25 °C until a white precipitate was observed (20-40 min). The Amberlite-IR120 resin was then separated from the CH₂Cl₂ solution and washed with CH₂Cl₂ (3 x 4 mL). The filtrate was then concentrated under reduced pressure to form a 0.05 M solution of **4** which was treated with NEt₃ (5-8 equiv) and benzoyl chloride (2-4 equiv), and allowed to stir for 3 h. At this time, the reaction mixture was concentrated under reduced pressure and purified by medium pressure chromatography (1:9-1:3 ethyl acetate: hexanes) to afford **6** as a white solid.

**6a**

α -Benzoyloxy Ketone 6a: A mixture of **3a** (0.0192 g, 0.0884 mmol) and hexamethylbenzene (0.028 M solution in C₆D₆) was heated in C₆D₆ (0.6 mL) in a J-Young tube for 16 h at 80 °C. At this time, ¹H NMR analysis of the reaction mixture indicated that the yield of the in situ generated imidate was 92%.

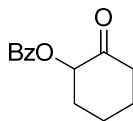
A C₆D₆ solution of **3a** (0.110 g, 0.507 mmol) was heated in a J-Young tube at 80 °C for 16 h. At this time, ¹H NMR analysis indicated that conversion to imidate **4a** was complete. The C₆D₆ solution of **4a** was then concentrated under reduced pressure and dissolved in CH₂Cl₂. Hydrolysis of imidate **4a** with Amberlite-IR120 was followed by the addition of NEt₃ (0.410 g, 4.05 mmol) and benzoyl chloride (0.285 g, 2.03 mmol) as described in general procedure H. Purification of the crude product by medium pressure chromatography (1:9 ethyl acetate: hexanes) afforded **6a** as an amorphous solid (0.0838 g, 86%). ¹H NMR (500 MHz; CDCl₃): δ 8.08 (d, J = 7.5 Hz, 2H), 7.57 (t, J = 7.5 Hz, 1H), 7.46-7.43 (m, 2H), 5.31 (q, J = 7.0 Hz, 1H),

2.23 (s, 3H), 1.52 (d, $J = 7.0$ Hz, 3H); ^{13}C NMR (125 MHz, CDCl_3): δ 205.8, 165.9, 133.4, 129.8, 129.5, 128.5, 75.5, 25.7, 16.2; IR (thin film) 3063, 2992, 2942, 2878, 1717, 1454, 1359, 1265, 1108, 738 cm^{-1} ; HRMS (ESI) m/z calcd. for $\text{C}_{11}\text{H}_{12}\text{O}_3\text{Na}$ ($\text{M}+\text{Na}$) $^+$ 215.0684, found 215.0681.

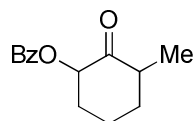


6m

α -Benzoyloxy Ketone 6m: General procedure H was followed by heating a C_6D_6 solution of **3m** (0.090 g, 0.39 mmol) in the presence of hexamethylbenzene (0.0162 g, 0.100 mmol) in a J-Young tube for 12 h. After 12 h of heating at 80 $^\circ\text{C}$, ^1H NMR analysis of the reaction mixture indicated that the yield of the in situ generated imidate was 92%. Hydrolysis of imidate **4m** with Amberlite-IR120 was followed by the addition of NEt_3 (0.446 mL, 3.34 mmol) and benzoyl chloride (0.185 mL, 1.59 mmol). Purification of the benzoyl protected α -oxygenation product by medium pressure chromatography (1:9 ethyl acetate: hexanes) afforded **6m** as a yellow oil (0.053 g, 66%). ^1H NMR (500 MHz; CDCl_3): δ 8.05 (d, $J = 8.0$ Hz, 2H), 7.55 (t, $J = 7.5$ Hz, 1H), 7.42 (t, $J = 7.5$ Hz, 2H), 5.32-5.28 (m, 1H), 2.58-2.53 (m, 1H), 2.47-2.45 (m, 1H), 2.36-2.30 (m, 1H), 2.20-2.15 (m, 1H), 2.03-1.93 (m, 2H); ^{13}C NMR (125 MHz, CDCl_3): δ 212.3, 165.8, 133.3, 129.9, 129.5, 128.4, 76.1, 35.0, 28.6, 17.3; IR (thin film) 2956, 2928, 2858, 1717, 1457, 1267, 1106, 708 cm^{-1} ; HRMS (ESI) m/z calcd. for $\text{C}_{12}\text{H}_{12}\text{O}_3\text{Na}$ ($\text{M}+\text{Na}$) $^+$ 227.0684, found 227.0691.

**6n**

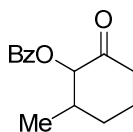
α -Benzoyloxy Ketone 6n: General procedure H was followed by heating a 0.24 M solution of **3n** (0.070 g, 0.29 mmol) in the presence of hexamethylbenzene (0.004 g, 0.02 mmol) in C_6D_6 in a J-Young tube for 10 h. After 10 h of heating at 90 °C, 1H NMR analysis of the reaction mixture indicated that the yield of the in situ generated imidate **4n** was >95%. Hydrolysis of imidate **4n** with Amberlite-IR120 was followed by the addition of NEt_3 (150 μ L, 1.43 mmol) and benzoyl chloride (70 μ L, 0.57 mmol). Purification of the crude product by medium pressure chromatography (1:6 ethyl acetate: hexanes) afforded **6n** as a white solid (0.042 g, 67%). 1H NMR (500 MHz; $CDCl_3$): δ 8.10-8.08 (m, 2H), 7.57-7.54 (m, 1H), 7.47-7.42 (m, 2H), 5.42 (dd, $J = 5.0, 5.0$ Hz, 1H), 2.58-2.57 (m, 1H), 2.49-2.40 (m, 2H), 2.10 (dtd, $J = 8.8, 5.1, 2.8$ Hz, 1H), 2.01 (ddd, $J = 8.8, 5.1, 2.8$ Hz, 1H), 1.97-1.89 (m, 1H), 1.86-1.78 (m, 1H), 1.73-1.63 (m, 1H); ^{13}C NMR (125 MHz, $CDCl_3$): δ 204.3, 165.6, 133.2, 129.9, 128.4, 77.0, 40.8, 33.3, 27.3, 23.8; IR (thin film) 2947, 2865, 1711, 1604, 1450, 1317, 1265, 1177, 1109, 1064 cm^{-1} ; HRMS (ESI) m/z calcd. for $C_{13}H_{14}O_3Na$ ($M+Na$) $^+$ 241.0841, found 241.0838; mp 86 °C.

**6o**

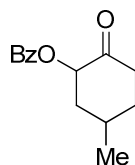
dr = 20:80; cis:trans

α -Benzoyloxy Ketone 6o: A mixture of **3o** (0.0212 g, 0.0825 mmol) and trimethoxybenzene (0.0015 g, 0.009 mmol) was heated in C₆D₆ in a J-Young tube for 16 h at 80 °C. At this time, ¹H NMR analysis of the reaction mixture indicated that the yield of the in situ generated imidate was 86%.

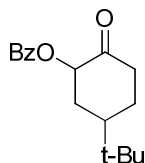
A C₆D₆ solution of **3o** (0.0468 g, 0.182 mmol) was heated in a J-Young tube at 80 °C for 16 h. At this time, ¹H NMR analysis indicated that conversion to imidate **4o** was complete. The C₆D₆ solution of **4o** was then concentrated under reduced pressure and dissolved in CH₂Cl₂. Hydrolysis of imidate **4o** with Amberlite-IR120 was followed by the addition of NEt₃ (0.1473 g, 1.456 mmol) and benzoyl chloride (0.1023 g, 0.7281 mmol) as described in general procedure H. Purification of the crude product by medium pressure chromatography (1:9 ethyl acetate: hexanes) afforded **6o** as a yellow oil (0.0279 g, 66%). ¹H NMR *cis* diastereomer (500 MHz; CDCl₃): δ 8.12-8.07 (m, 2H), 7.61-7.55 (m, 1H), 7.49-7.42 (m, 2H), 5.39-5.37 (m, 1H), 2.58 (dq, $J = 13.0, 6.0$ Hz, 1H), 2.48-2.44 (m, 1H), 2.23-2.09 (m, 2H), 2.07-1.93 (m, 2H), 1.92-1.83 (m, 1H), 1.09 (d, $J = 6.0$ Hz, 3H); ¹³C NMR *cis* diastereomer (125 MHz, CDCl₃): δ 208.7, 165.5, 133.1, 130.2, 129.8, 128.3, 77.2, 44.4, 36.1, 33.6, 23.2, 13.9; ¹H NMR *trans* diastereomer (500 MHz; CDCl₃): δ 8.12-8.07 (m, 2H), 7.61-7.55 (m, 1H), 7.49-7.42 (m, 2H), 5.38 (dd, $J = 8.0, 4.5$ Hz, 1H), 2.87 (dq, $J = 14.0, 7.0$ Hz, 1H), 2.23-2.09 (m, 2H), 2.07-1.93 (m, 2H), 1.92-1.83 (m, 1H), 1.66-1.59 (m, 1H), 1.18 (d, $J = 7.0$ Hz, 3H); ¹³C NMR *trans* diastereomer (125 MHz, CDCl₃): δ 208.7, 165.5, 133.3, 129.9, 129.8, 128.5, 76.1, 43.2, 35.2, 33.3, 19.7, 15.2; IR (thin film) 3061, 2973, 2938, 2868, 1787, 1719, 1453, 1315, 1209, 1114, 1013 cm⁻¹; HRMS (ESI) m/z calcd. for C₁₄H₁₆O₃Na (M+Na)⁺ 255.0997, found 255.1006.

**6p****dr = 55:45; *cis:trans***

α -Benzoyloxy Ketone 6p: General procedure H was followed by heating a C₆D₆ solution of **3p** (0.040 g, 0.16 mmol) in the presence of 1,3,5-trimethoxybenzene (0.002 g, 0.011 mmol) in a C₆D₆ for 12 h. After 12 h of heating at 90 °C, ¹H NMR analysis of the reaction mixture indicated that the yield of the in situ generated imidate was >95%. Hydrolysis of imidate **4p** with Amberlite-IR120 was followed by the addition of NEt₃ (100 μ L, 0.775 mmol) and benzoyl chloride (40 μ L, 0.310 mmol). Purification of the benzoyl protected α -oxygenation product by medium pressure chromatography (1:6; ethyl acetate:hexanes) afforded **6p** as a white solid (0.025 g, 69%). ¹H NMR *cis* diastereomer (500 MHz; CDCl₃): δ 8.10-8.09 (m, 2H), 7.58-7.57 (m, 1H), 7.46-7.45 (m, 2H), 5.44 (d, J = 5.5 Hz, 1H), 2.67-2.65 (m, 1H), 2.55-2.48 (m, 1H), 2.22-1.99 (m, 4H), 1.73-1.67 (m, 1H), 1.15 (d, J = 5.5 Hz, 3H); ¹³C NMR *cis* diastereomer (125 MHz, CDCl₃): δ 204.8, 165.9, 133.2, 133.1, 129.8, 128.4, 82.2, 40.4, 39.5, 32.7, 25.7, 19.0; ¹H NMR *trans* diastereomer (500 MHz; CDCl₃): δ 8.09-8.08 (m, 2H), 7.57-7.55 (m, 1H), 7.45-7.43 (m, 2H), 5.06 (d, J = 11.5 Hz, 1H), 2.50-2.41 (m, 2H), 1.97-1.92 (m, 3H), 1.86-1.78 (m, 1H), 1.66-1.57 (m, 1H), 1.08 (d, J = 5.0 Hz, 3H); ¹³C NMR *trans* diastereomer (125 MHz, CDCl₃): δ 203.8, 165.5, 133.2, 133.1, 129.8, 128.3, 79.8, 40.1, 36.7, 30.0, 22.4, 13.5; IR (thin film) 2959, 2933, 2873, 1717, 1602, 1451, 1309, 1283, 1260, 1174, 1111 cm⁻¹; HRMS (ESI) m/z calcd. for C₁₄H₁₆O₃Na (M+Na)⁺ 255.0997, found 255.0998; mp 98-100 °C.

**6q****dr = 55:45; cis:trans**

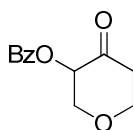
α -Benzoyloxy Ketone 6q: General procedure H was followed by heating a 0.24 M solution of **3q** (0.068 g, 0.26 mmol) in the presence of hexamethylbenzene (0.012 g, 0.072 mmol) in a C_6D_6 for 14 h. After 14 h of heating at 90 °C, 1H NMR analysis of the reaction mixture indicated that the yield of the in situ generated imidate was 96%. Hydrolysis of imidate **4q** with Amberlite-IR120 was followed by the addition of NEt_3 (0.133 g, 1.32 mmol) and benzoyl chloride (0.074 g, 0.53 mmol). Purification of the benzoyl protected α -oxygenation product by medium pressure chromatography (1:4; ethyl acetate: hexanes) afforded **6q** as a white solid (0.040 g, 65%). 1H NMR *cis* diastereomer (500 MHz; $CDCl_3$): δ 8.09-8.08 (m, 2H), 7.59-7.57 (m, 1H), 7.48-7.45 (m, 2H), 5.44 (dd, $J = 5.0, 5.0$ Hz, 1H), 2.58-2.55 (m, 2H), 2.40-2.33 (m, 2H), 2.08-1.97 (m, 2H), 1.73-1.65 (m, 1H), 1.21 (d, $J = 5.0$ Hz, 3H); ^{13}C NMR *cis* diastereomer (125 MHz, $CDCl_3$): δ 205.7, 165.5, 134.6, 133.2, 129.9, 128.4, 75.9, 40.8, 39.3, 35.1, 33.7, 21.0; 1H NMR *trans* diastereomer (500 MHz; $CDCl_3$): δ 8.08-8.07 (m, 2H), 7.56-7.55 (m, 1H), 7.45-7.42 (m, 2H), 5.41 (dd, $J = 5.0, 5.0$ Hz, 1H), 2.53-2.49 (m, 2H), 2.24-2.12 (m, 2H), 2.02-1.97 (m, 1H), 1.82-1.74 (m, 1H), 1.39-1.38 (m, 1H), 1.08 (d, $J = 5.0$ Hz, 3H); ^{13}C NMR *trans* diastereomer (125 MHz, $CDCl_3$): δ 204.4, 165.5, 134.6, 133.1, 129.8, 128.3, 74.9, 39.6, 36.9, 30.9, 27.2, 18.8; IR (thin film) 2959, 2930, 2872, 1717, 1687, 1604, 1583, 1454, 1317, 1275 cm^{-1} ; HRMS (ESI) m/z calcd. for $C_{14}H_{17}O_3$ (M+H) $^+$ 233.1178, found 233.1171; mp 95 °C.

**6r****dr = 75:25; cis:trans**

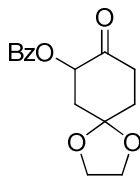
α -Benzoyloxy Ketone 6r: A mixture of **3r** (0.0482 g, 0.161 mmol) and trimethoxybenzene (0.0048 g, 0.029 mmol) was heated in C_6D_6 in a J-Young tube for 16 h at 80 °C. At this time, 1H NMR analysis of the reaction mixture indicated that the yield of the in situ generated imidate was 75%.

A C_6D_6 solution of **3u** (0.0385 g, 0.129 mmol) was heated in a J-Young tube at 80 °C for 16 h. At this time, 1H NMR analysis indicated that conversion to imidate **4r** was complete. The C_6D_6 solution of **4r** was then concentrated under reduced pressure and dissolved in CH_2Cl_2 . Hydrolysis of imidate **4r** with Amberlite-IR120 was followed by the addition of NEt_3 (0.1042 g, 1.030 mmol) and benzoyl chloride (0.0724 g, 0.5148 mmol) as described in general procedure H. Purification of the crude product by medium pressure chromatography (1:9 ethyl acetate: hexanes) afforded **6r** as an amorphous solid (0.0232 g, 66%). 1H NMR *cis* diastereomer (500 MHz; $CDCl_3$): δ 8.11-8.07 (m, 2H), 7.59-7.53 (m, 1H), 7.47-7.42 (m, 2H), 5.38 (dd, $J = 12.0, 6.0$ Hz, 1H), 2.57-2.43 (m, 3H), 2.18-2.12 (m, 1H), 1.79-1.73 (m, 2H), 1.54-1.46 (m, 1H), 0.97 (s, 9H); ^{13}C NMR *cis* diastereomer (125 MHz, $CDCl_3$): δ 206.1, 165.6, 133.2, 129.9, 129.7, 128.4, 76.6, 45.9, 39.6, 34.3, 32.3, 28.1, 27.7; 1H NMR *trans* diastereomer (500 MHz; $CDCl_3$): δ 8.11-8.07 (m, 2H), 7.59-7.53 (m, 1H), 7.47-7.42 (m, 2H), 5.28 (dd, $J = 10.5, 5.0$ Hz, 1H), 2.69-2.63 (m, 1H), 2.57-2.43 (m, 1H), 2.34-2.29 (m, 1H), 1.94-1.83 (m, 1H), 1.68-1.60 (m, 1H), 1.43-1.38 (m, 1H), 0.94 (s, 9H); ^{13}C NMR *trans*

diastereomer (125 MHz, CDCl₃): δ 206.1, 165.6, 133.4, 129.8, 129.7, 128.5, 76.2, 41.9, 38.0, 32.3, 32.3, 27.4, 26.6; IR (thin film) 3057, 2963, 2908, 2872, 1733, 1719, 1453, 1319, 1267, 1126 cm⁻¹; HRMS (ESI) m/z calcd. for C₁₇H₂₃O₃ (M+H)⁺ 275.1647, found 275.1641. Ref: OL, 2005, 7 (25), 5729 they report *cis* pdt, the major isomer.

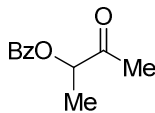
**6t**

α -Benzoyloxy Ketone 6t: General procedure H was followed by heating a 0.24 M solution of **3t** (0.060 g, 0.24 mmol) in the presence of hexamethylbenzene (0.003 g, 0.02 mmol) in a C₆D₆ for 14 h. After 14 h of heating at 90 °C, ¹H NMR analysis of the reaction mixture indicated that the yield of the in situ generated imidate was 96%. Hydrolysis of imidate **4t** with Amberlite-IR120 was followed by the addition of NEt₃ (170 μ L, 1.22 mmol) and benzoyl chloride (60 μ L, 0.49 mmol). Purification of the crude product by medium pressure chromatography (1:3 ethyl acetate: hexanes) afforded **6t** as a white solid (0.037 g, 69%). ¹H NMR (500 MHz; CDCl₃): δ 8.09-8.07 (m, 2H), 7.58-7.55 (m, 1H), 7.45-7.42 (m, 2H), 5.52 (dd, *J* = 6.5, 3.0 Hz, 1H), 4.45 (ddd, *J* = 12.5, 6.5, 3.0 Hz, 1H), 4.29 (ddd, *J* = 12.5, 6.5, 3.0 Hz, 1H), 3.73-3.68 (m, 2H), 2.86-2.79 (m, 1H), 2.79-2.56 (m, 1H); ¹³C NMR (125 MHz, CDCl₃): δ 200.5, 165.1, 133.5, 130.0, 129.9, 128.5, 74.1, 70.6, 68.5, 42.3; IR (thin film) 2975, 2923, 1720, 1606, 1454, 1320, 1274, 1206, 1122, 1099 cm⁻¹; HRMS (EI) m/z calcd. for C₁₂H₁₂O₄ (M)⁺ 220.07356, found 220.07434; mp 78 °C.

**6u**

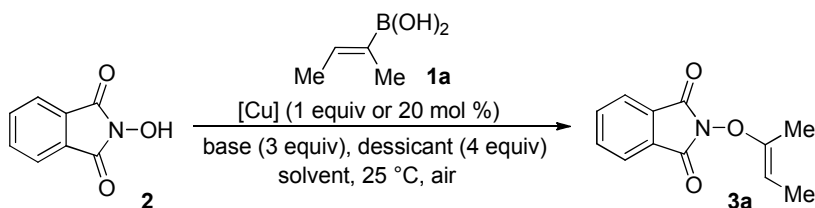
α -Benzoyloxy Ketone 6u: General procedure H was followed by heating a C_6D_6 solution of **3u** (0.100 g, 0.332 mmol) in the presence of hexamethylbenzene (0.0162 g, 0.100 mmol) in a J-Young tube for 12 h. After 12 h of heating at 80 °C, 1H NMR analysis of the reaction mixture indicated that the yield of the in situ generated imidate was 96%. Hydrolysis of imidate **4u** with Amberlite-IR120 was followed by the addition of NEt_3 (0.446 mL, 3.34 mmol) and benzoyl chloride (0.185 mL, 1.59 mmol). Purification of the crude product by medium pressure chromatography (1:2 ethyl acetate:hexanes) afforded **6u** as a white solid (0.058 g, 63%). 1H NMR (500 MHz; $CDCl_3$): δ 8.07 (d, $J = 7.5$ Hz, 2H), 7.55 (t, $J = 7.5$ Hz, 1H), 7.46-7.43 (m, 2H), 5.66 (dd, $J = 6.5, 13.0$ Hz, 1H), 4.13-4.04 (m, 4H), 2.83-2.76 (m, 1H), 2.51-2.45 (m, 2H), 2.24 (t, $J = 7.5$ Hz, 1H), 2.09-2.01 (m, 2H); ^{13}C NMR (125 MHz, $CDCl_3$): δ 203.3, 165.4, 135.3, 133.4, 129.9, 128.4, 107.4, 73.7, 65.0, 64.9, 40.3, 35.9, 34.6; IR (thin film) 2959, 2926, 2860, 1720, 1460, 1266, 1107, 1027, 706 cm^{-1} ; HRMS (ESI) m/z calcd. for $C_{15}H_{16}O_5Na$ ($M+Na$) $^+$ 299.0895, found 299.0892.; mp 75-78 °C.

Direct conversion **1a** and **2** to α -benzoyloxy ketone **6a**:

**6a**

General procedure C with *N*-hydroxyphthalimide **2** (0.164 g; 1.005 mmol), *Z*-2-buten-2-yl boronic acid **1a** (0.201 g, 2.010 mmol), Cu(OAc)₂ (0.183 g, 1.005 mmol), Na₂SO₄ (0.613 g, 1.80 mmol), and pyridine (240 μL, 3.015 mmol) afforded **3a**. The crude product mixture was separated from Cu(OAc)₂ by filtering through silica using CH₂Cl₂. The CH₂Cl₂ was then removed from crude **3a** under reduced pressure and the crude *N*-enoxypthalimide **3a** was then subjected to general procedure H. Purification of crude **6a** by medium pressure chromatography (1:3 ethyl acetate: hexanes) afforded **6a** as an amorphous solid (0.130 g, 67%).

VII. Extended Optimization Table 1.7



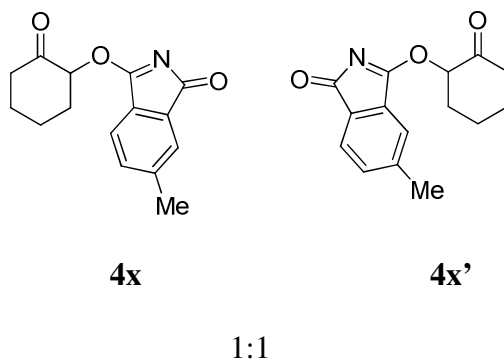
Entry	Cu	[Cu]	[1a]	base ^a	dessicant	solvent ^b	yield (%) ^c
1	Cu(OAc) ₂	1 equiv	1 equiv	pyr	Na ₂ SO ₄	DCE	71
2	Cu(OAc) ₂	1 equiv	2 equiv	pyr	Na ₂ SO ₄	DCE	96
3	Cu(OAc) ₂	1 equiv	3 equiv	pyr	Na ₂ SO ₄	DCE	92
4	Cu(OAc) ₂	20 mol %	1 equiv	pyr	Na ₂ SO ₄	DCE	6
5	Cu(OAc) ₂	20 mol %	2 equiv	pyr	Na ₂ SO ₄	DCE	87
6	Cu(OAc) ₂	20 mol %	3 equiv	pyr	Na ₂ SO ₄	DCE	99
7	CuCl	1 equiv	2 equiv	pyr	Na ₂ SO ₄	DCE	84

8	CuCl	20 mol %	2 equiv	pyr	Na ₂ SO ₄	DCE	7
9	CuI	1 equiv	2 equiv	pyr	Na ₂ SO ₄	DCE	74
10	CuI	20 mol %	2 equiv	pyr	Na ₂ SO ₄	DCE	78
11	Cu(O ₂ CCF ₃)	1 equiv	2 equiv	pyr	Na ₂ SO ₄	DCE	92
12	Cu(O ₂ CCF ₃)	20 mol %	2 equiv	pyr	Na ₂ SO ₄	DCE	61
13	Cu(OTf) ₂	1 equiv	2 equiv	pyr	Na ₂ SO ₄	DCE	60
14	Cu(OTf) ₂	20 mol %	2 equiv	pyr	Na ₂ SO ₄	DCE	8
15	CuTC	1 equiv	2 equiv	pyr	Na ₂ SO ₄	DCE	88
16	CuTC	20 mol %	2 equiv	pyr	Na ₂ SO ₄	DCE	81
17	Cu(OAc) ₂	20 mol %	2 equiv	NEt ₃	Na ₂ SO ₄	DCE	68
18	Cu(OAc) ₂	20 mol %	2 equiv	DABCO	Na ₂ SO ₄	DCE	NR
19	Cu(OAc) ₂	20 mol %	2 equiv	imidazole	Na ₂ SO ₄	DCE	NR
20	Cu(OAc) ₂	20 mol %	2 equiv	KOt-Bu	Na ₂ SO ₄	DCE	NR
21	Cu(OAc) ₂	20 mol %	2 equiv	pyr	4 Å MS	DCE	70
22	Cu(OAc) ₂	20 mol %	2 equiv	pyr	MgSO ₄	DCE	69
23	Cu(OAc) ₂	20 mol %	2 equiv	pyr	Na ₂ SO ₄	THF	12
24	Cu(OAc) ₂	20 mol %	2 equiv	pyr	Na ₂ SO ₄	toluene	NR
25	Cu(OAc) ₂	20 mol %	2 equiv	pyr	Na ₂ SO ₄	CHCl ₃	49
26	Cu(OAc) ₂	20 mol %	2 equiv	pyr	Na ₂ SO ₄	CH ₂ Cl ₂	64
27	Cu(OAc) ₂	20 mol %	2 equiv	pyr	Na ₂ SO ₄	MeCN	19

^a Changing the concentration of base did not have a significant effect on the yield of the transformation. ^bAll reaction were run at 0.1 M. ^c ¹H NMR yields based on the use of 1,3,5-trimethoxybenzene as an internal standard.

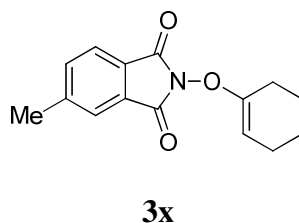
VIII. Crossover Experiment for [3,3] Rearrangement and Preparation of *N*-Enoxy Phthalimide **3x**.

Crossover Experiment: *N*-Enoxyphthalimide **3x** (0.017 g, 0.066 mmol) and *N*-Enoxy phthalimide **3d** (0.016 g, 0.066 mmol) were dissolved in C₆D₆ (0.5 mL) and transferred to a J-Young tube. An initial ¹H NMR experiment indicated a 1:1 ratio of **3x:3d**. The J-Young tube was then heated to 90 °C for 16 h. A second ¹H NMR experiment indicated a 1:1 ratio of **4x:4d**. Since the [3,3] rearrangement can occur using either carbonyl of the phthalimide moiety two regioisomers of **8** were observed in a 1:1 ratio.



Rearrangement of **3x** to give imidate **4x** as a 1:1 regioisomeric mixture. *N*-Enoxy phthalimide **3x** (0.016g, 0.060 mmol) and 1,3,5-trimethoxybenzene (0.002 g, 0.009 mmol) were dissolved in C₆D₆ (0.5 mL). The reaction mixture was heated to 90 °C for 16 h. A ¹H NMR experiment indicated a 95% yield of the desired imidate **4x** as a 1:1 mixture of regioisomers. A second batch of *N*-Enoxyphthalimide **3x** (0.028 g, 0.109 mmol) was dissolved in benzene (0.5 mL). The reaction mixture was heated to 90 °C for 16 h. The solvent was removed under reduced pressure to give a yellow oil (0.028 g, >95% conversion). ¹H NMR (500 MHz; CDCl₃) for **4x**: δ 7.48-7.47 (m, 1H), 7.35 (s, 1H), 6.76-6.74 (m, 1H), 5.67 (dd, *J* = 6.5, 6.0 Hz, 1H), 2.28-2.24 (m, 2H), 1.92 (s, 3H), 1.69-1.64 (m, 2H), 1.45-1.41

(m, 2H), 1.23-1.15 (m, 2H); ^{13}C NMR (125 MHz, CDCl_3) for 8a: δ 201.3, 185.4, 180.8, 143.6, 136.6, 134.1, 132.9, 123.5, 120.5, 82.3, 40.3, 33.1, 26.7, 23.2, 21.1; ^1H NMR (500 MHz; CDCl_3) for 4x': δ 7.24-7.23 (m, 1H), 7.11 (s, 1H), 6.74-6.72 (m, 1H), 5.64 (dd, $J = 6.5$, 6.5 Hz, 1H) 2.23-2.21 (m, 2H), 1.92 (s, 3H), 1.40-1.35 (m, 4H), 1.18-1.09 (m, 2H); ^{13}C NMR (125 MHz, CDCl_3) for 8b: 201.2, 185.1, 180.5, 143.2, 135.9, 134.2, 132.6, 124.5, 121.8, 82.2, 40.2, 33.0, 26.7, 23.2, 21.0; IR (thin film) 2950, 2865, 1727, 1613, 1532, 1431, 1389, 1356, 1294, 1086 cm^{-1} ; HRMS (ESI) m/z calcd. for $\text{C}_{15}\text{H}_{16}\text{NO}_3$ ($\text{M}+\text{H}$) $^+$ 258.1130, found 258.1129.

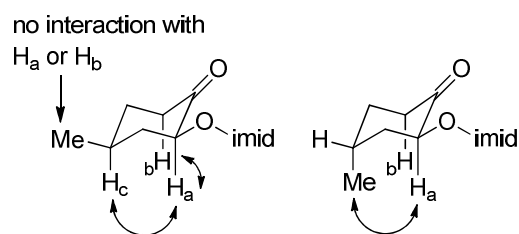


Preparation of *N*-Enoxyphthalimide 3x: A scintillation vial was charged with 3-methyl-*N*-hydroxyphthalimide (0.050g, 0.28 mmol), vinyl boronic acid **1n** (0.071 g, 0.56 mmol), $\text{Cu}(\text{OAc})_2$ (0.051 g, 0.28 mmol) and anhydrous Na_2SO_4 (0.187 g, 1.32 mmol). These solids were then diluted with DCE to form a 0.1 M solution of 3-methyl-*N*-hydroxyphthalimide. Pyridine (0.066 g, 0.84 mmol) was added to the resulting slurry via syringe. The scintillation vial was then capped with a septum pierced with a ventilation needle and the reaction mixture was stirred at 25 °C for 12 h. DCE and pyridine were removed under reduced pressure and the crude reaction mixture was purified by medium pressure chromatography (1:4; ethyl acetate:hexanes) to give *N*-Enoxyphthalimide **3x** (0.068 g, 94%) as a white solid. ^1H NMR (500 MHz; CDCl_3): δ 7.73 (d, $J = 7.7$ Hz, 1H), 7.66 (s, 1H), 7.55 (d, $J = 7.6$ Hz, 1H), 4.95 (t, $J = 3.5$ Hz, 1H), 2.51 (s, 3H), 2.30 (t, $J = 6.2$ Hz, 2H), 2.01 (dd, $J = 3.91$, 1.85 Hz, 2H), 1.75 (td, $J = 12.22$, 6.12 Hz, 2H), 1.56 (td, $J = 12.20$, 6.16 Hz, 2H); ^{13}C NMR (125

MHz, CDCl₃): δ 163.2, 163.1, 154.7, 146.1, 135.1, 129.1, 126.1, 124.3, 123.7, 98.4, 24.6, 22.9, 22.4, 22.2, 22.0; IR (thin film) 2931.27, 2846.42, 1786.72, 1732.73, 1688.37, 1613.16, 1442.49, 1363.43, 1223.60, 1097.30 cm⁻¹; HRMS (ESI) m/z calcd. for C₁₅H₁₆NO₃ (M+H)⁺ 258.1130, found 258.1126; mp 83 °C.

IX. nOe Correlation Characterization of 4q, 4o, 4p, 4s, 6q, 6o, and 6p

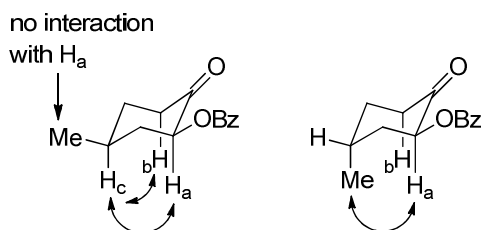
Relevant DPFGE-nOe data (mixing time 2.0 s): the peaks in the ¹H NMR spectra were assigned using ¹H NMR chemical shifts, ¹H-¹H NMR coupling constants, and ¹H-¹H NMR COSY data.



4q: *cis:trans* = 50:50

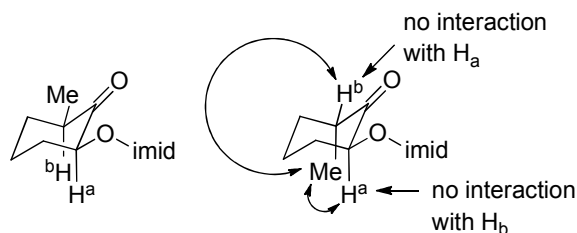
Imidate 4q: The methyl resonances at 0.80 and 0.66 ppm and the H_a methine resonances at 5.80 and 5.67 ppm are distinct for these compounds in C₆D₆. When the methyl resonance at 0.66 ppm is irradiated, no H_a methine resonance between 5-6 ppm is observed. When the H_a methine resonance at 5.67 ppm is irradiated no methyl resonance is observed. This suggests that the H_a methine at 5.67 ppm does not have a through space interaction with a methyl group. When the H_a methine at 5.67 ppm is irradiated, the H_c methine resonance at 1.39 ppm is inverted as well as the H_b α -methylene proton at 2.15 ppm. This suggests that the isomer with the methine resonance at 5.67 ppm and the methyl resonance at 0.66 ppm is the *cis* isomer. When the methyl resonance at 0.80 ppm is irradiated, the H_a methine resonance at

5.80 ppm is inverted. When the H_a methine resonance at 5.80 ppm is irradiated, the methyl resonance at 0.80 ppm is inverted. These experiments suggest that the isomer with the methine resonance at 5.80 ppm and the methyl resonance at 0.80 ppm is the *trans* isomer.



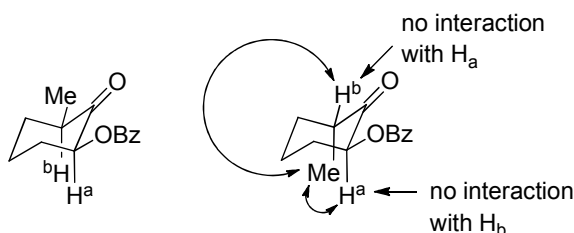
6q: *cis:trans* = 55:45

α -Benzoyloxy ketone 6q: The H_a methine resonances at 5.44 and 5.41 are overlapping for this product in $CDCl_3$. The two methyl resonances at 1.21 and 1.08 ppm are distinct in $CDCl_3$. When the methyl resonance at 1.21 ppm is irradiated, the H_a methine resonance at 5.44 ppm is not observed. When the H_a methine resonance at 5.44 ppm is irradiated the methyl resonance at 1.21 ppm is not observed. These data suggest that one of the methine resonances at 5.44 ppm does not have a through space interaction with the methyl group at 1.21 ppm. When the H_c methine at 2.00 ppm is irradiated, the H_a methine resonance at 5.44 ppm is inverted as well as the H_b α -methylene resonance at 2.35 ppm. These data suggest that the isomer with the H_b α -methylene resonance at 2.35 ppm and the methyl resonance at 1.21 ppm is the *cis* isomer. When the methyl resonance at 1.08 ppm is irradiated, the methine resonance H_a at 5.41 ppm is inverted. When the H_a methine resonance at 5.41 ppm is irradiated, only the methyl resonance at 1.08 ppm is inverted. These experiments suggest that the isomer with the methine resonance at 5.41 ppm and the methyl resonance at 1.08 ppm is the *trans* isomer.



4o: *cis:trans* = 15:85

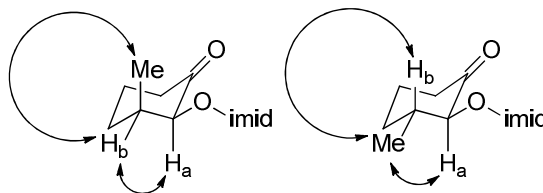
Imidate 4o: The methine resonances H_a at 5.81 and 5.63 ppm are distinct and the methyl resonances at 0.96 and 0.82 overlap for these compounds in C_6D_6 . When the H_a methine resonance at 5.81 ppm was irradiated, the methyl resonance at 0.96 was inverted but the H_b methine resonance at 2.65 ppm was not observed. When the H_b methine resonance at 2.65 ppm was irradiated, the methyl resonance at 0.96 ppm was inverted but the H_a methine resonance at 5.81 ppm was not observed. When the methyl resonance at 0.96 ppm was irradiated, the H_a methine resonance at 5.81 ppm and the H_b methine resonance at 2.65 ppm were inverted. These data suggest that the isomer with the methine resonance at 5.81 ppm and the methyl resonance at 0.96 ppm is the *trans* isomer. The ratio of the major:minor isomer was too large to collect nOe data for the minor *cis* isomer.



6o: *cis:trans* = 20:80

α -Benzoyloxy Ketone 6o: The H_a methine resonances at 5.38 ppm are coincident and the methyl resonances at 1.18 and 1.09 ppm are distinct for these compounds in $CDCl_3$. When the H_a methine resonance at 5.38 ppm was irradiated, the methyl resonance at 1.18 was

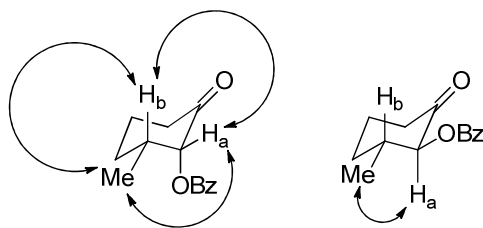
inverted but the H_b methine resonance at 2.87 ppm was not observed. When the H_b methine resonance at 2.87 ppm was irradiated the methyl resonance at 1.18 ppm was inverted but the H_a methine resonance at 5.38 ppm was not observed. When the methyl resonance at 1.18 ppm was irradiated, the H_a methine resonance at 5.38 ppm and the H_b methine resonance at 2.87 ppm were inverted. These data suggest that the isomer with the methine resonance at 5.38 ppm and the methyl resonance at 1.18 ppm is the *trans* isomer. The ratio of the major:minor isomer was too large to collect nOe data for the minor *cis* isomer.



4p: *cis:trans* = 55:45

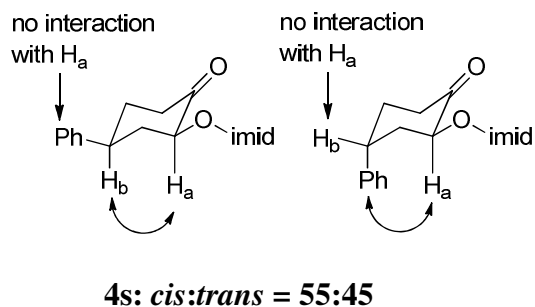
Imidate 4p: The methyl resonances at 1.20 and 1.10 ppm and the H_a methine resonances at 5.84 and 5.44 ppm are distinct for these compounds in CDCl₃. When the methyl resonance at 1.10 ppm is irradiated, the H_b methine resonance at 2.90 ppm is inverted but the H_a methine resonance at 5.84 ppm is not observed. When the H_b methine resonance at 2.90 ppm is irradiated the methyl resonance at 1.10 ppm and the H_a methine resonance at 5.84 ppm are inverted. When the H_a methine resonance at 5.84 ppm is irradiated the H_b methine resonance at 2.90 ppm is inverted but the methyl resonance at 1.10 ppm is not observed. These data suggest that the isomer with the methine resonances at 5.84 and 2.90 ppm and the methyl resonance at 1.10 ppm is the *cis* isomer. When the methyl resonance at 1.20 ppm is irradiated, the H_a methine resonance at 5.44 ppm is inverted. When the H_a methine resonance at 5.44 ppm is irradiated, the methyl resonance at 1.20 ppm is inverted. When the H_b methine

resonance at 2.29 ppm is irradiated, only the methyl resonance at 1.20 ppm is inverted and the H_a methine resonance at 5.44 ppm is not observed. These data suggest that the isomer with the methine resonance at 5.44 ppm and the methyl resonance at 1.20 ppm is the *trans* isomer.



6p: *cis:trans* = 55:45

α -Benzoyloxy Ketone 6p: The methyl resonances at 1.15 and 1.08 ppm and the H_a methine resonances at 5.44 and 5.06 ppm are distinct for these compounds in $CDCl_3$. When the methine resonance H_a at 5.44 ppm was irradiated, the H_b methine resonance at 2.66 ppm and the methyl resonance at 1.08 ppm were inverted. When the H_b methine resonance at 2.66 ppm was irradiated, the H_a methine at 5.44 ppm was inverted and the methyl resonance at 1.08 ppm was inverted. When both methyl groups were irradiated together, both the 5.44 ppm and 5.06 ppm methines were inverted. These data suggest that the isomer with the methine resonance at 5.44 ppm and the methyl resonance at 1.08 ppm is the *cis* isomer. When the H_a methine resonance at 5.06 ppm was irradiated, the methyl group at 1.15 ppm was inverted but the methine resonance at 1.86 ppm was not observed. When both methyl groups were irradiated together, both the 5.44 ppm and the 5.06 ppm methines were inverted. These data suggest that the isomer with the methine resonance at 5.06 ppm and the methyl resonance at 1.15 ppm is the *trans* isomer.

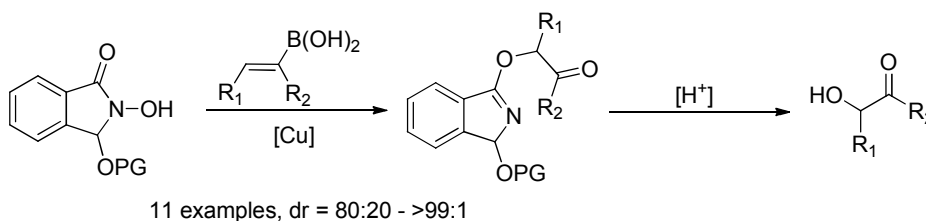


Imidate 4s: The methine resonances H_a at 5.98 and 5.83 ppm and the methine resonances H_b at 3.3 and 2.8 ppm are distinct for these compounds in $CDCl_3$. When the H_a methine resonance at 5.98 was irradiated, the H_b methine resonance at 3.31 ppm was inverted but the phenyl resonances were not observed. When the H_b methine resonance at 3.31 ppm was irradiated, the H_a methine resonance at 5.98 ppm and the phenyl resonance at 7.38 ppm were inverted. These data suggest that the isomer with the methine resonance at 5.98 ppm is the *cis* isomer. When the H_a methine resonance at 5.83 ppm was irradiated the phenyl resonance at 7.56 ppm was inverted but the H_b methine resonance at 2.83 ppm was not observed. These data suggest that the isomer with the methine resonance at 5.83 ppm is the *trans* isomer.

Chapter 2 - Diastereoselective Dioxygenation of Alkenyl Boronic Acids via Etherification and Rearrangement of *N*-Hydroxyisoindolinones

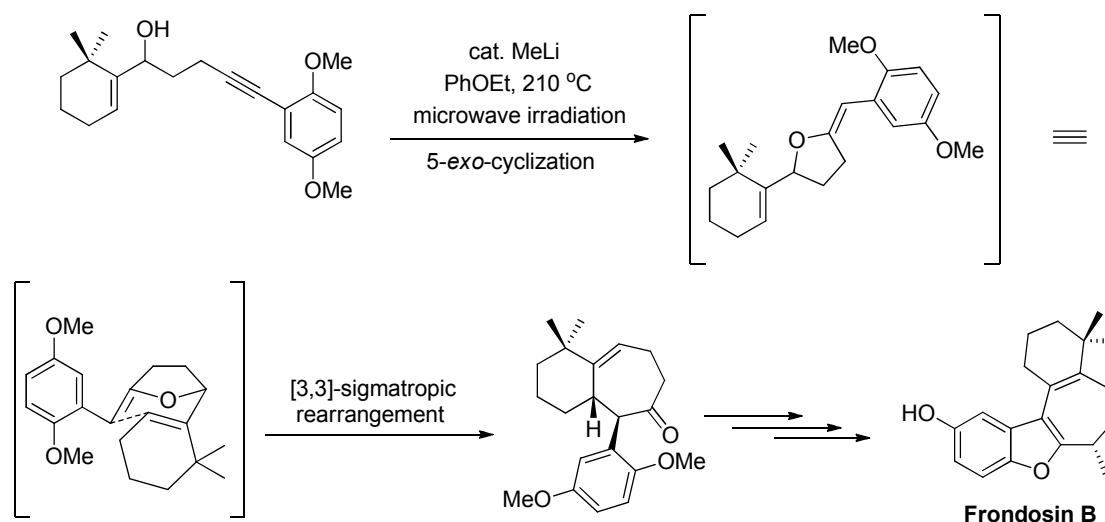
2.1 Abstract

We have developed a new alternative route to α -oxygenated ketones through the dioxygenation of vinyl boronic acids. The overall process consists of a copper-catalyzed etherification of *N*-hydroxyphthalimide with an alkenyl boronic acid, followed by a subsequent [3,3] rearrangement of the resulting *N*-enoxyphthalimide, and hydrolysis of the ensuing imidate. Our initial discovery has been further modified to afford the diastereoselective dioxygenation of vinyl boronic acids with 3-hydroxyisoindolinones. The scope of the method and the dependence of the diastereoselectivity on the identity of the protecting group and the boronic acid have been evaluated. Relative stereochemistry of the α -oxygenated ketones, mechanistic implications and the assessment of a chiral nonracemic 3-hydroxyisoindolinone as an oxygenation reagent have also been investigated.



2.2 [3,3] Rearrangements in Organic Synthesis

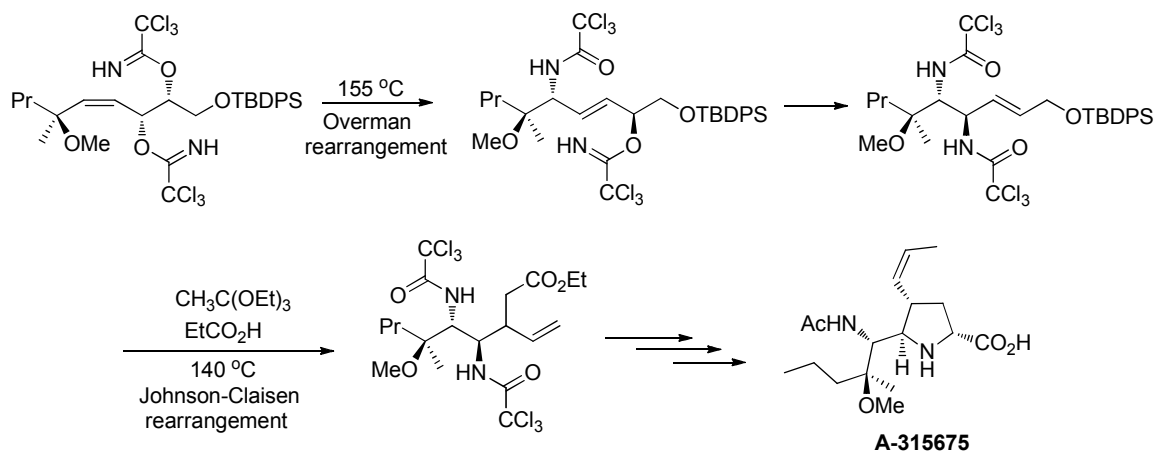
The [3,3] sigmatropic reaction, since its discovery in 1912,⁵⁸ occupies a unique position as a powerful, reliable, and well-defined method for the stereoselective construction of carbon–carbon and carbon–heteroatom bonds.⁵⁹ While many other reactions can unite two subunits and create a new bond, a sigmatropic rearrangement is unique in its ability to enable structural reorganization and hence is widely utilized in the construction of molecules of high complexity. A recent application that illustrates the [3,3]-sigmatropic rearrangement as a key step in the synthesis of the natural product, Frondosin B,⁶⁰ is shown below in Scheme 2.1. Frondosins are bioactive sesquiterpene hydroquinones which are being evaluated as new anticancer and antiviral agents.



Scheme 2.1: [3,3] Rearrangement in the Synthesis of Frondosin B

An extensive use of sigmatropic rearrangements, including the trichloroacetimidate rearrangement (the Overman rearrangement) was utilized in the synthesis of the anti-influenza agent A-315675 developed at Abbott Laboratories

(Scheme 2.2). In this synthesis, the bis-trichloroacetimidate undergoes a double [3,3]-sigmatropic rearrangement through chair-like transition states.⁶¹

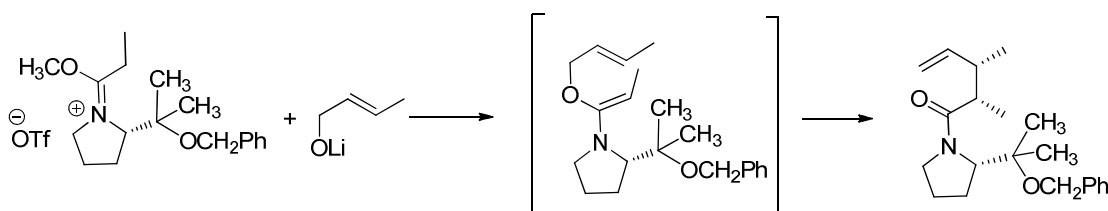


Scheme 2.2: Sequential [3,3] Rearrangements in the Synthesis of A-315675

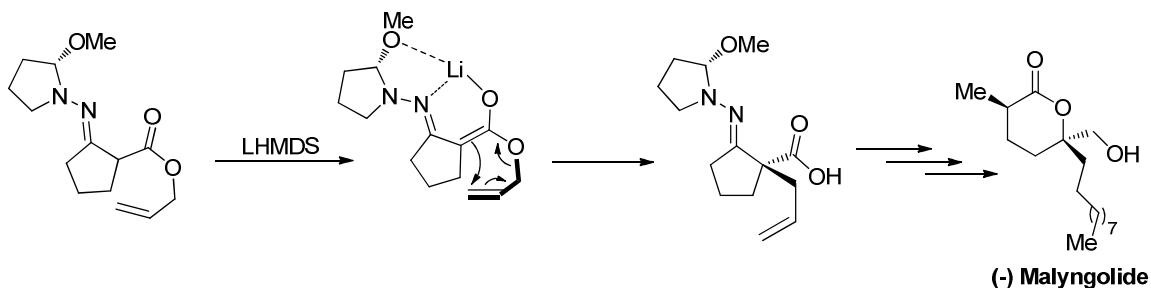
Since [3,3] rearrangement reactions involve bond breaking and bond formation events that occur through a cyclic array of interacting orbitals, diastereoselectivity is generally high for these processes.⁶² The potential of [3,3]-sigmatropic rearrangements to simultaneously create two adjacent stereocentres with high levels of diastereoselectivity has been exploited extensively in organic synthesis, notably by the application of the Cope and Claisen rearrangements in total synthesis.⁶³ For addressing vicinal quaternary carbons, these transformations have only been applied in a diastereoselective manner using substrates containing pre-existing stereogenic centers, either as part of cleavable auxiliaries or structural features of the target molecule.⁶⁴

2.2.1 Modes of Diastereoselective and Enantioselective Induction Through Substrate Control

The common method to induce diastereoselectivity and enantioselectivity in a [3,3] sigmatropic reaction is by substrate control. Asymmetric Claisen rearrangements have been studied where intramolecular chirality transfer from a chiral center at any position near the rearrangement system is used to control the stereoselectivity and create enantiomerically enriched products.⁶⁵ This approach was developed by Welch, who employed the amidacetal modification of the Claisen rearrangement reaction, incorporating an optically active amine component into one of the reagents. Addition of an allylic alkoxide to the iminium salt yields a product, which immediately rearranges giving the amide as the major product (Scheme 2.3).⁶⁶

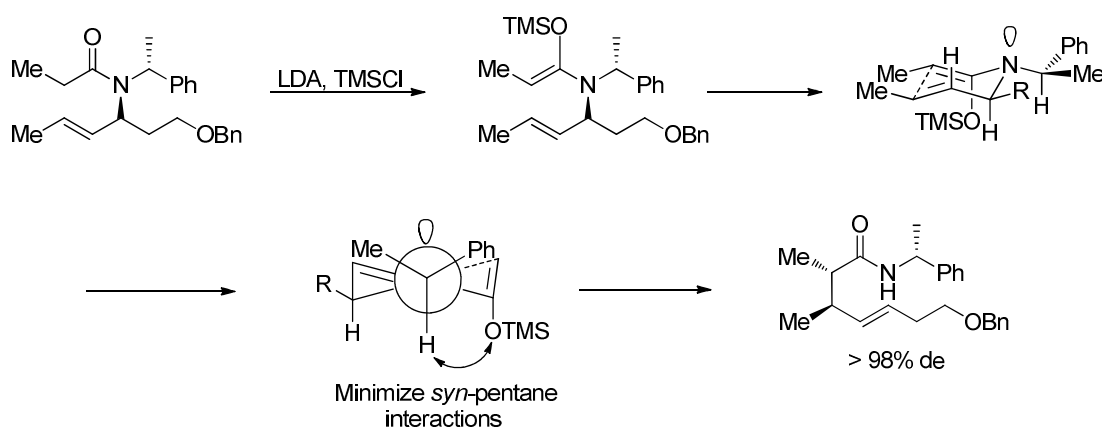


Scheme 2.3: Distant Chiral Centre Controlling the Stereochemical Outcome



Scheme 2.4: Enders' RAMP Hydrazone as a Chiral Auxiliary in the [3,3] Rearrangement

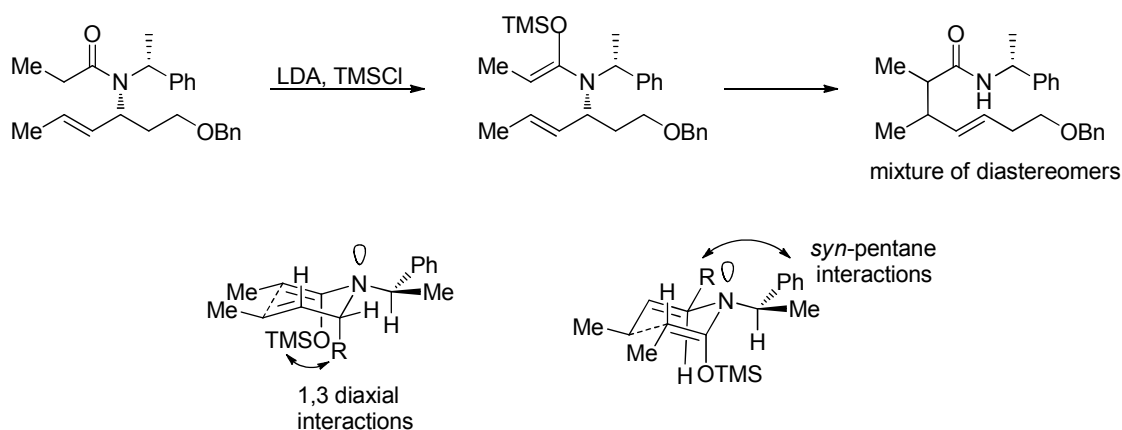
A similar strategy utilizing Enders' RAMP⁶⁷ [(*R*)-1-amino-2-methoxymethylpyrrolidine] hydrazone as a chiral auxiliary to set up the quaternary centre via a [3,3] rearrangement was devised by Enders et al. in the total synthesis of (-) Malyngolide.⁶⁸ In this reaction (Scheme 2.4), co-ordination of the Li ion with the methoxy group blocks the lower face of the ring system, and hence the rearrangement can occur only from the upper face leading to the observed stereochemistry in the product.



Scheme 2.5: Diastereoselective [3,3] Sigmatropic Aza-Claisen Rearrangement with Minimization of *syn*-Pentane Interactions

Davies and co-workers reported their results regarding investigations on the double diastereoselective [3,3] sigmatropic aza-Claisen rearrangement of diastereomeric benzyl ethers shown in Schemes 2.5 and 2.6 containing both an *N*- α -methylbenzyl group and an adjacent stereogenic centre.⁶⁹ The high levels of diastereoselectivity observed upon rearrangement of the chiral amide may be elucidated by the reaction proceeding via the *Z*-*N,O*-silyl ketene aminal through a chair like transition state in which all the bulky alkyl substituents occupy pseudo-equatorial positions (Scheme 2.5). The double diastereoselectivity observed in the rearrangement may be rationalised by the

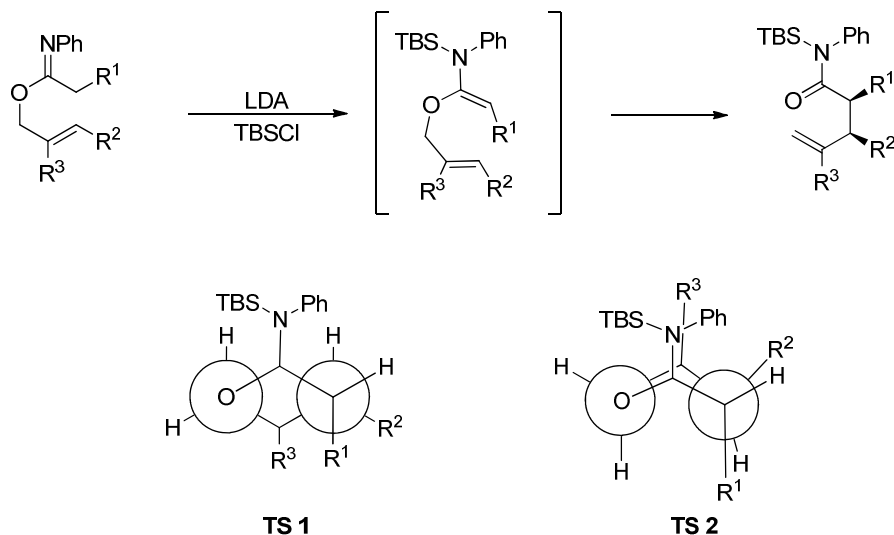
minimization of both *syn*-pentane⁷⁰ and 1,3-diaxial interactions in the chair transition state. The nitrogen lone pair is assumed to occupy a position between the C(α)Ph and C(α)Me substituents, anti to C(α)H, minimising the dominant *syn*-pentane interaction with the trimethylsilyloxy group of the ketene aminal. This conformation enables the largest C(α)Ph substituent to occupy a position anti to the *N*-allyl fragment, with the C(α)Me group eclipsing the C(3)R substituent.⁷¹



Scheme 2.6: Mismatched Rearrangement Destabilised by 1,3 Diaxial Interactions and *syn*-Pentane Interactions

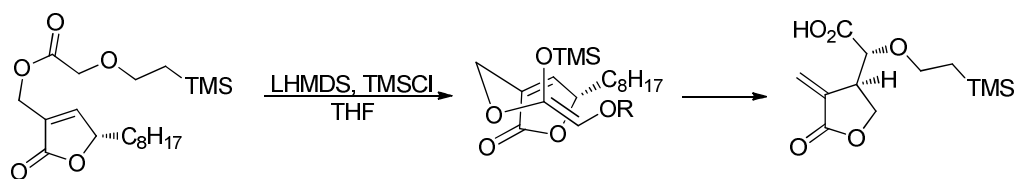
To determine whether this highly diastereoselective rearrangement represented the matched or mismatched reaction manifold, the diastereomeric benzyl ether was subjected to rearrangement under identical conditions (Scheme 2.6). In this case, an inseparable mixture of three diastereomeric products was obtained in a 50:30:20 ratio. Application of this transition state model to the mismatched rearrangement indicates that the expected chair transition states would be destabilised by 1,3 diaxial interactions between the C(3)R group and the trimethylsilyloxy group in or by *syn*-pentane interactions with the C(α)Ph substituent. The difference in energy between these

transition states for the rearrangement is therefore diminished, resulting in the observed low levels of diastereoselectivity.



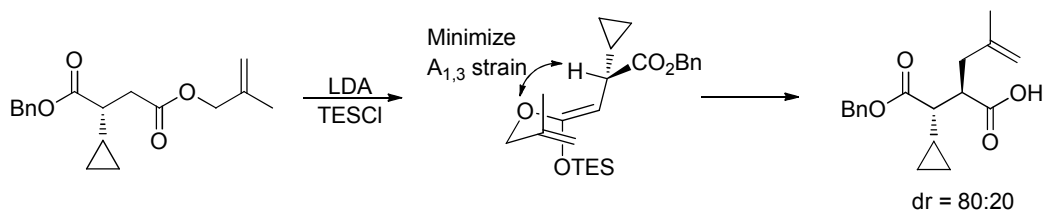
Scheme 2.7: Diastereoselectivity Arising from Formation of Energetically Favorable Chair-like Transition State

N-silyl ketene acetals generated from prochiral allyl *N*-phenylimidates underwent a diastereoselective Claisen rearrangement as shown in Scheme 2.7. The *N*-phenylimidates when treated with LDA and TBSCl formed the *N*-silyl ketene *N,O*-acetals^{72,73} which were more than 99% *Z*-configured to minimize $A_{1,3}$ -strain.⁷⁴ The competition between the chair transition state **TS 1** and the boat transition state **TS 2** is responsible for the relative configuration of the products. Since the boat transition state **TS 2** involves eclipsing interactions between the bulky amine and R^3 , it is energetically disfavored. The reaction therefore proceeds through the chair transition state **TS 1**, leading to the observed *cis*-diastereoselectivity in the product.



Scheme 2.8: Diastereoselectivity Controlled by Sterics

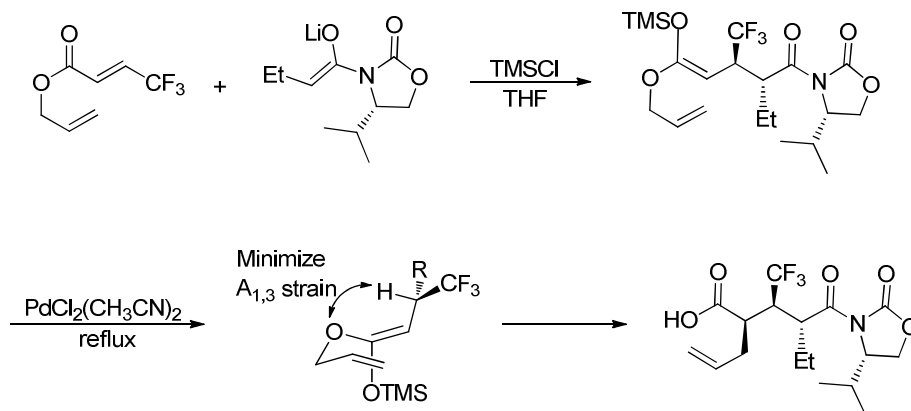
Burke et al. have reported the formation of butyrolactones through a [3,3] rearrangement where the rearrangement diastereoselectivity is controlled by the sterics of the substrate⁷⁵ (Scheme 2.8). These butyrolactones could then be transformed into Isoavenaciolide⁷⁶ and other related targets. In this case, the selective enolization of a glycolate in the presence of a butenolide afforded the *Z*-silyl ketene acetal. The [3,3] rearrangement then occurred from the face opposite to the bulky octenyl chain via a chair transition state to afford the *exo* methylene butyrolactone.



Scheme 2.9: $A_{1,3}$ -strain and Sterics Controlling Diastereoselectivity

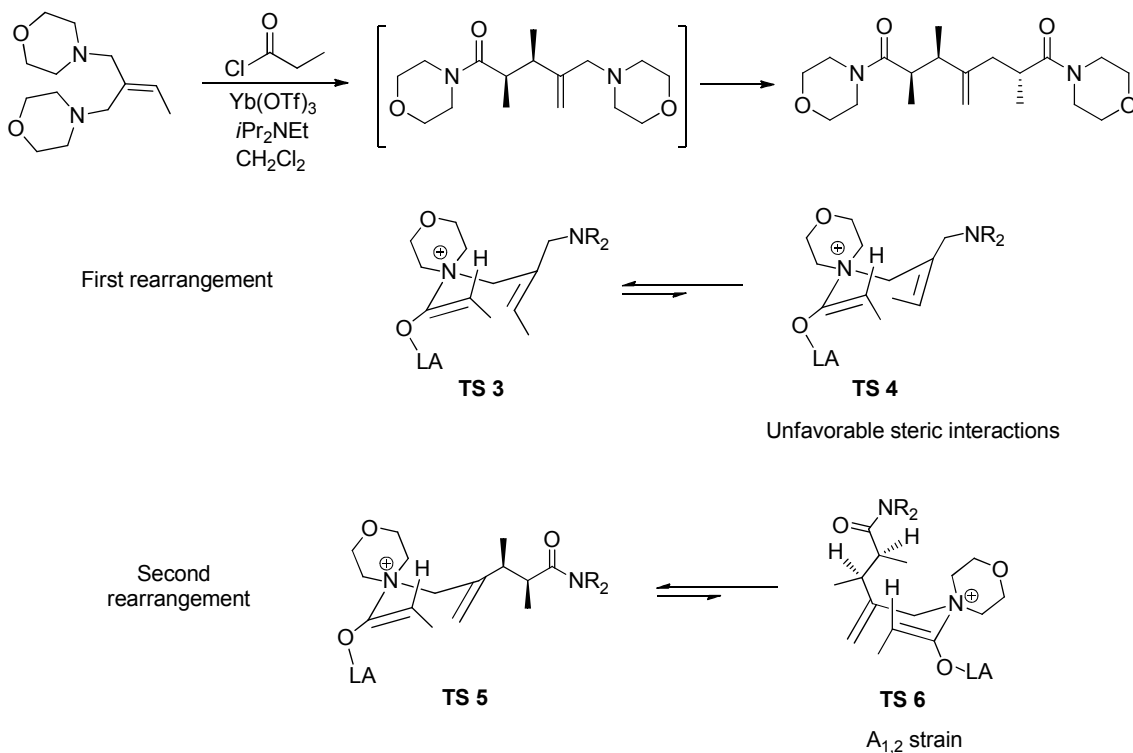
Selective enolization of an allyl ester followed by a diastereoselective [3,3] rearrangement was reported by Pratt et. al.⁷⁷ The facial selectivity for the rearrangement was directed by allylic strain (Scheme 2.9). The preferred lower energy conformation for the silyl ketene acetal was the one in which the ether oxygen was eclipsed with the allylic proton thus leading to a minimization of $A_{1,3}$ -strain.⁷⁸ The alkene would then approach the

silyl ketene acetal from the face *syn* to the smaller carboxybenzyl substituent. The product was obtained in a 80:20 diastereoselective ratio.



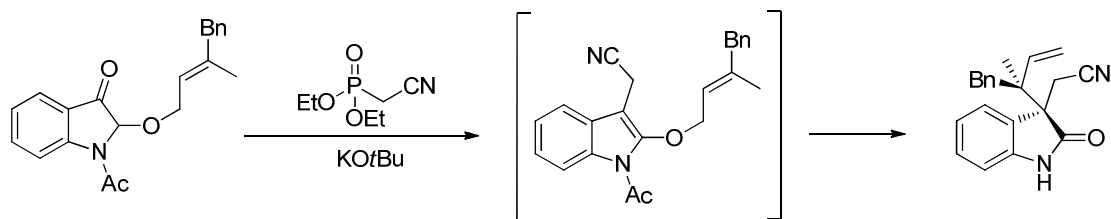
Scheme 2.10: $A_{1,3}$ -strain and Cieplak Effect Responsible for Diastereoselectivity

The Evans oxazolidinone⁷⁹ was employed by Yamazaki and coworkers (Scheme 2.10) for the diastereoselective Michael addition of the lithiated enolate to the β - CF_3 acrylates to afford the allyl silyl ketene acetals as intermediates.⁸⁰ The rearrangement occurred via the *Z*-silyl ketene acetal where the lowest energy conformation adopted by the molecule would be the one that would minimize the $A_{1,3}$ -strain. Preferential attack by the allyl group *syn* to the CF_3 group would give the product with the observed stereochemistry. This facial selectivity was rationalized by the authors by suggesting that due to the Cieplak effect, the new bond was formed *anti* to the more electron rich C–C σ^* bond.⁸¹



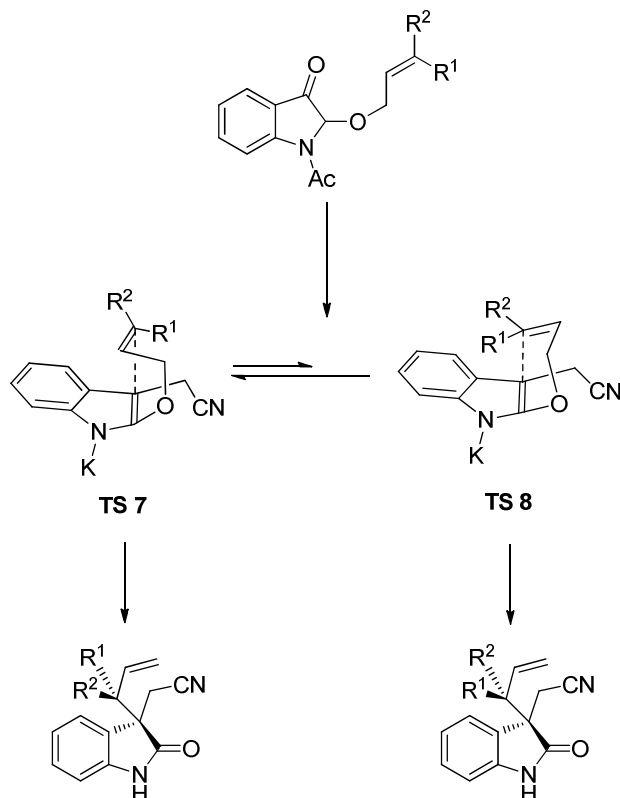
Scheme 2.11: Diastereoselectivity Controlled by $A_{1,2}$ -Strain

An iterative Claisen rearrangement as shown in Scheme 2.11 was developed by MacMillan and Dong using allylic bis-amines and Yb(OTf)_3 as the catalyst.⁸² This process involved a double rearrangement which yielded the product in a high yield and excellent diastereoselectivity. The first rearrangement occurred via the less hindered chair transition state **TS 3** to form the *syn* pentenamide followed by the second rearrangement which was dictated by minimization of $A_{1,2}$ -strain.⁷⁸ This propensity for reducing the allylic strain, led to a preference for **TS 5**. This hypothesis matches the stereochemistry of the observed product.



Scheme 2.12: Claisen Rearrangement to Access Spirocyclic Oxindoles with Vicinal Quaternary Carbon Centers

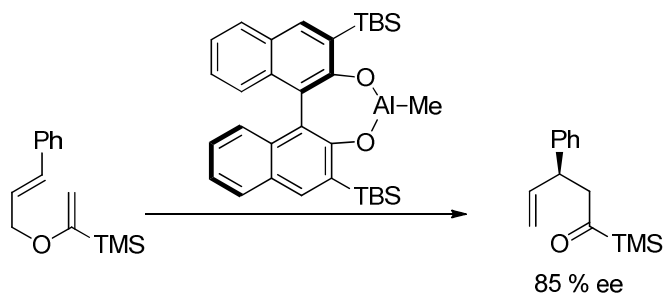
An efficient approach to spirocyclic oxindoles⁸³ with vicinal quaternary carbon centers was reported in 2011 (Scheme 2.12).⁸⁴ The reaction involves the Horner-Wadsworth-Emmons olefination of 2-allyloxyindolin-3-ones⁸⁵ with cyanomethylphosphonate followed by successive isomerization, deacylation, and an anion-accelerated Claisen rearrangement to give the 3,3-disubstituted oxindoles in high yield and diastereoselectivity. The stereochemistry of the products indicates that the Claisen rearrangement progresses predominantly via a boat-like transition state **TS 8** over the chair-like **TS 7**. The chair-like transition state **TS 8** is disfavored because of steric repulsion of the two substituents (R^1 , R^2) with the indole ring (Scheme 2.13).



Scheme 2.13: Claisen Rearrangement through a Boat-like Transition State

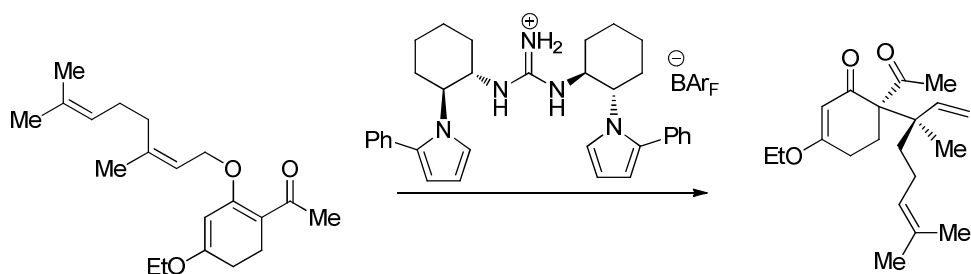
2.2.2 Diastereoselective and Enantioselective Induction Using Chiral Reagents

Asymmetric induction in a [3,3] rearrangement could be brought about by using a chiral reagent or catalyst. Yamamoto et al.⁸⁶ reported a modified binaphthol–aluminum catalyst which served as a chiral promoter for the Claisen rearrangement of an aliphatic allyl vinyl ether (Scheme 2.14). In this case a stoichiometric amount of the promoter was required.

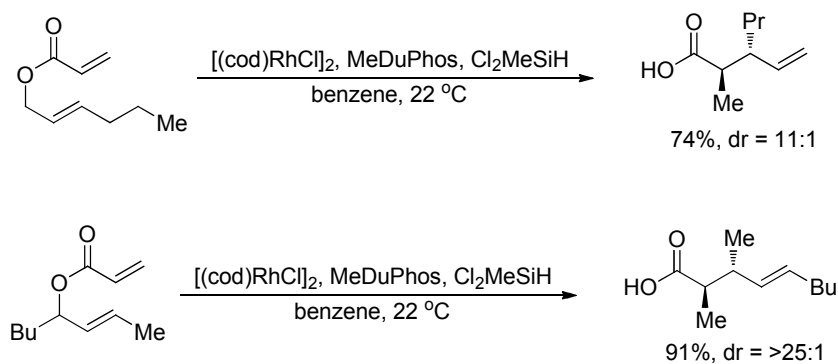


Scheme 2.14: Chiral Promoter in an Enantioselective Claisen Rearrangement

Chiral guanidinium catalyzed Claisen rearrangements of cyclic *O*-allyl β -ketoesters have been reported by Jacobsen and co-workers.⁸⁷ The guanidinium functions as a hydrogen bond donor catalyst which controls the stereochemistry during the rearrangement (Scheme 2.15). Chiral azolium salts have been used for the enantioselective annulation reaction between enols and ynals to form enantiomerically enriched dihydropyranones via an *N*-heterocyclic carbene catalyzed variant of the Claisen rearrangement.⁸⁸



Scheme 2.15: Chiral Guanidinium Catalyzed Claisen Rearrangement



Scheme 2.16: Catalytic Diastereoselective Reductive Claisen Rearrangement

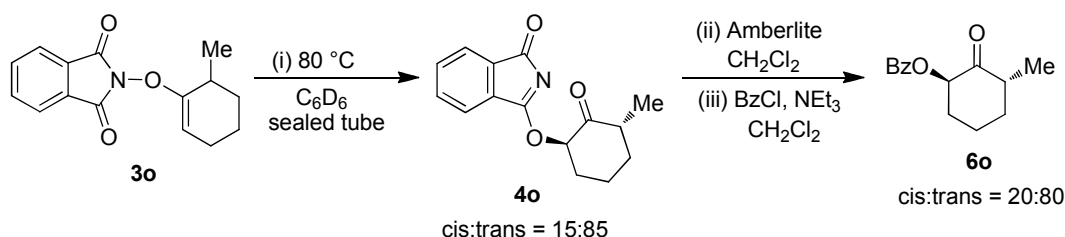
A catalytic diastereoselective reductive Claisen rearrangement was developed by the Morken group in 2002 which is shown in Scheme 2.16. The catalyst prepared from $[(cod)RhCl]_2$ and Me-DuPhos, was utilized for the chemoselective and stereoselective reduction of allyl acrylates to *E*-silyl ketene acetals. These intermediates then participated in a Claisen rearrangement via a chair-like transition state, providing γ, δ -unsaturated carboxylic acids with a high level of diastereoselectivity. This method provides an alternative for the ester enolate Claisen rearrangement which requires the use of a strong base for enolate generation.⁸⁹

Since our methodology for the dioxygenation of alkenyl boronic acids to access α -oxygenated ketones involved a [3,3] rearrangement, we hypothesized that including a stereocenter on the substrate would have some effect in controlling the facial selectivity for the rearrangement and this would enable us to achieve a diastereoselective or an enantioselective rearrangement. To accomplish this chiral induction through substrate control via a distant stereocenter on the molecule, we conjectured the use of 3-substituted-*N*-hydroxyisoindolinones instead of *N*-hydroxyphthalimide as precursors for the etherification and rearrangement. This would allow us to examine the

diastereoselectivity for the rearrangement and observe the relative stereochemistry of the product.

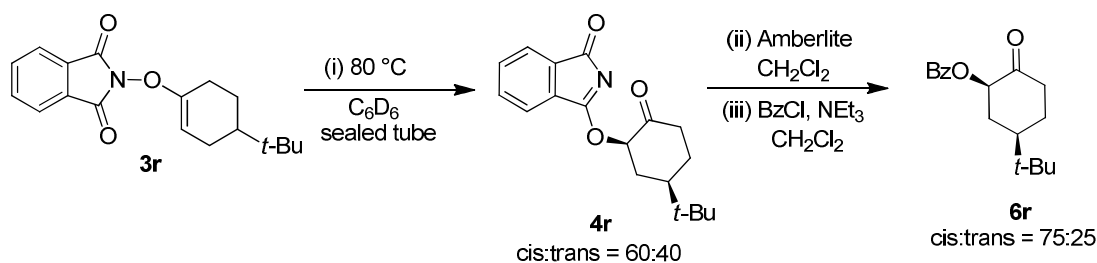
2.3 Effect of Neighboring Stereocenter on the [3,3] Rearrangement

While examining the [3,3] rearrangement for the dioxygenation of boronic acids as reported in Chapter 1, we were intrigued by the discovery that having a substituent at the 6-position could alter the stereo-chemical outcome of the reaction as shown in Scheme 2.17.



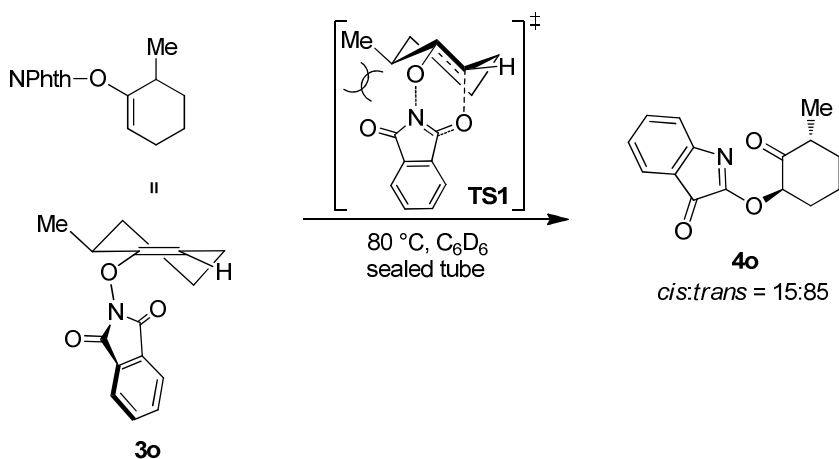
Scheme 2.17: Effect of a substituent at C6 on the Rearrangement Reaction

This result, where the *trans*-isomer was the major product, was in contrast to all other substituted cyclohexyl systems which gave the *cis*-isomer as the major product. An example is shown in Scheme 2.18.



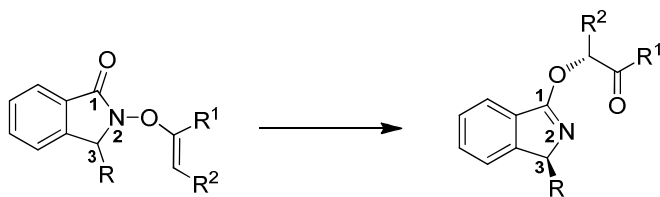
Scheme 2.18: *Cis*-isomer Predominates in all other Substituted Cyclohexanones

We attributed this result to hindered rotation for the C–O bond because of steric interactions with the 6-methyl substituent. This leads to the higher energy twist boat conformation which results in the *trans*-isomer (Scheme 2.19).⁹⁰



Scheme 2.19: Hindered Rotation of the C–O bond because of Steric Interactions

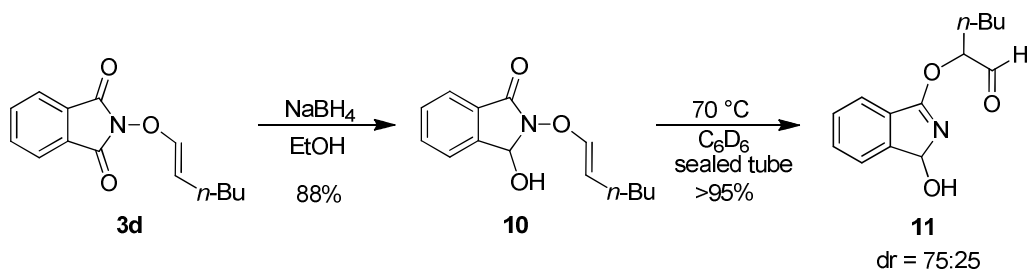
This stereochemical outcome of the reaction, led us to believe that there was an effect that the existing stereocenter had on the [3,3] rearrangement, especially if the existing stereocenter was close to the reaction site. We therefore wanted to investigate the outcome of introducing a stereocenter on the phthalimide portion of the molecule and examining the diastereoselectivity of the rearrangement. We have determined that the intramolecular chirality transfer from a stereocenter on the *N*-hydroxyisolidinone does occur to make the reaction diastereoselective, and that the nature of the substituent at on the isoindolinone has an impact on controlling the stereochemistry at the newly formed stereocenter (Scheme 2.20).



Scheme 2.20: Diastereoselective [3,3] Rearrangement

2.4 Initial Results

2.4.1 Effect of a Neighboring Hydroxy Group

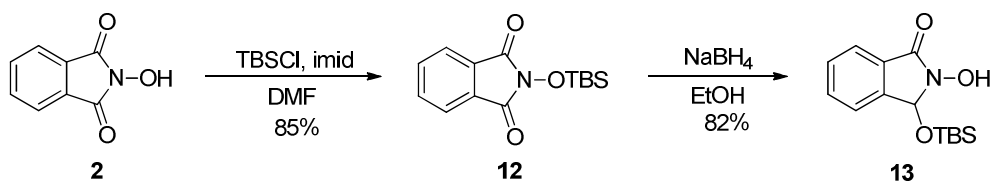


Scheme 2.21: Effect of a Hydroxy Substituent near the Reaction Site

N-enoxypthalimide **3d**, was treated with NaBH_4 in EtOH, which reduced one of the carbonyls to the alcohol to form the 3-hydroxy-*N*-enoxisoindolinone **10** (Scheme 2.21). When a 0.1 M solution of **10** was heated at 70 °C in C_6D_6 , a 75:25 ratio of diastereomers for imidate **11** were observed. This proved that the hydroxyl group did have an effect on the [3,3] rearrangement and that the stereochemistry of the substituent at the adjacent stereocenter plays an important role in determining the facial selectivity of the rearrangement.

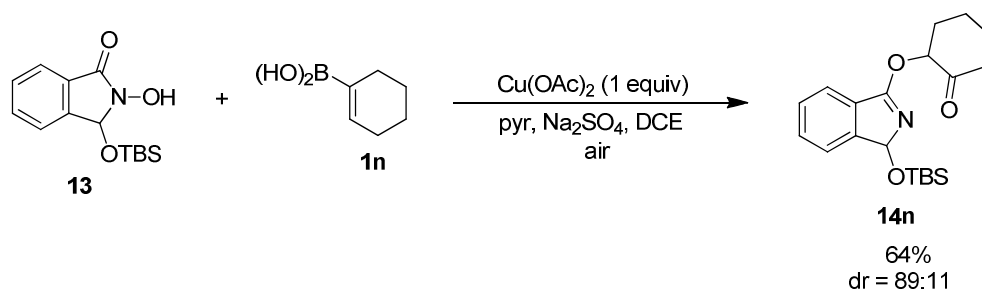
2.4.2 Effect of a 3-*t*-butyldimethylsilyloxy Group

Since the compound **11** with a hydroxyl group gave a 75:25 mixture of diastereomers in the [3,3] rearrangement, we envisioned that increasing the bulk of the substituent at the sp^3 center would result in a more diastereoselective reaction. To achieve higher diastereoselectivity, we replaced the hydroxyl group with a *t*-butyldimethylsilyloxy functionality. Protection of the hydroxyl group in **10** with TBSCl was unsuccessful; hence we devised a synthesis for the 3-*t*-butyldimethylsilyloxy-*N*-hydroxyisoindolinone as shown below (Scheme 2.22). This route was based on the synthesis of 1,2-oxazaheterocycles containing an isoindolone moiety developed by Bartovic in 2000.⁹¹ Protection of the hydroxyl group of *N*-hydroxyphthalimide gave the *O*-silylated product. Reduction of one of the carbonyls with sodium borohydride was followed by the *in situ* migration of the silyl group, to yield the 3-*t*-butyldimethylsilyloxy-*N*-hydroxyisoindolinone **13**.



Scheme 2.22: Synthesis of 3-*t*-butyldimethylsilyloxy-*N*-hydroxyisoindolinone

When the *N*-hydroxyisoindolinone **13** was treated with cyclohexenyl boronic acid **1n**, under the Cu-mediated etherification conditions, we were surprised to discover that instead of isolating the *N*-enoxyisoindolinone, a spontaneous rearrangement occurred under the etherification conditions, to give the imidate product directly (Scheme 2.23). Thus, the etherification and rearrangement could be achieved in a single flask.

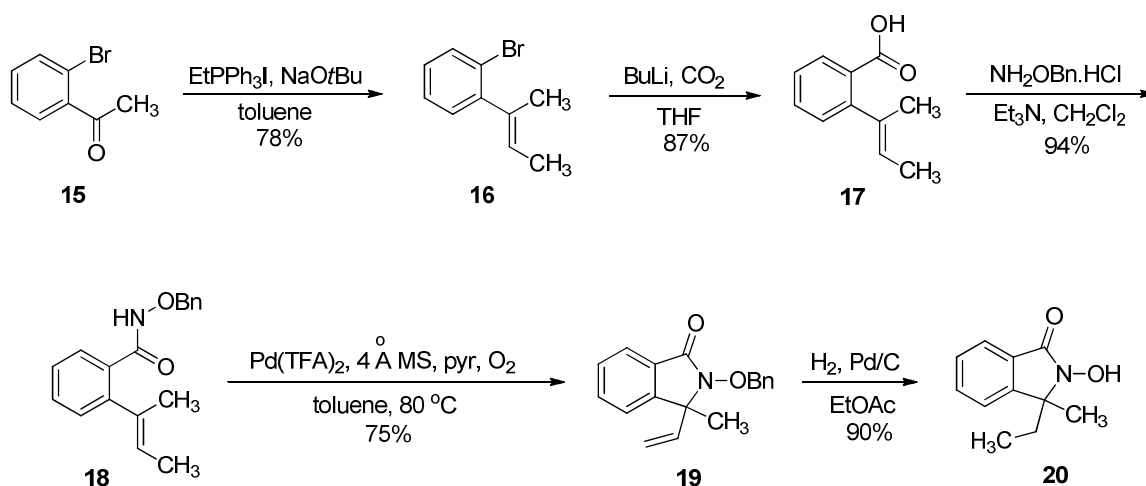


Scheme 2.23: Etherification and Rearrangement in a Single-Flask

The diastereomeric ratio obtained was 89:11, which suggested that increasing the steric volume of the substituent had an impact on controlling which face the rearrangement occurred, thus making the reaction more diastereoselective.

2.4.3 Effect of Alkyl Groups at the Stereocenter

After having established that a substituent on the sp^3 hybridized carbon of the *N*-enoxyisoindolinone has an effect on determining the stereochemistry at the newly formed α -oxygenated stereocenter, we then synthesized compound **20** which had an all carbon quaternary center at C_3 . This compound was synthesized according to the procedure developed by Stoltz and co-workers⁹² (Scheme 2.24). 2'-bromoacetophenone **15** was subjected to a Wittig reaction with ethyltriphenylphosphonium iodide in the presence of sodium *t*-butoxide to yield 1-bromo-2-(but-2-en-2-yl)benzene **16** as a 2:1 mixture of *Z*:*E* isomers. Conversion of the bromide to the carboxylic acid was followed by treatment with *O*-benzylhydroxylamine to give amide **18**. A Pd-catalyzed oxidative Wacker cyclization resulted in the desired 3-methyl-3-vinyl-*N*-benzyloxyisoindolinone **19**. Hydrogenolysis with hydrogen gas and Pd/C deprotected the benzyl group and also reduced the vinyl functionality to give the 3-ethyl-3-methyl-*N*-hydroxyisoindolinone **20**.

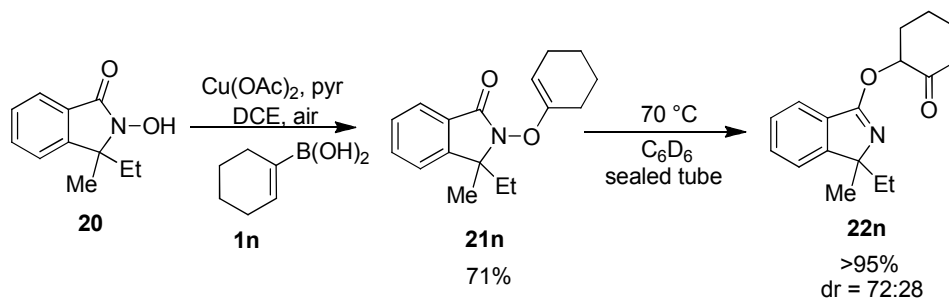


Scheme 2.24: Synthesis of *N*-hydroxyisoindolinone containing a Quarternary Center

There was a two-fold objective behind the synthesis and evaluation of compound **20**. First, we wanted to assess whether the Cu-mediated etherification with an alkenyl boronic acid and the ensuing [3,3] rearrangement would occur in the presence of a sterically congested center near the reaction site and secondly to determine whether the presence of an oxygen atom at the stereocenter was critical in making the [3,3] rearrangement diastereoselective.

When compound **20** was subjected to the etherification reaction with cyclohexenyl boronic acid **1n** in the presence of Cu(OAc)_2 , it gave the *N*-enoxyisoindolinone **21n** in a 71% yield. This proved that the etherification reaction with the *N*-hydroxyisoindolinone was not sensitive to steric effects and could occur even when a quarternary center was adjacent to the reactive site. Upon heating compound **21n** in benzene, the imidate product **22n** was formed in a diastereomeric ratio of 72:28 (Scheme 2.25). This suggests that the [3,3] rearrangement is affected by the steric interactions of

the cyclic TS and that the reaction probably proceeds from the less sterically hindered approach of the carbonyl and the enol ether.



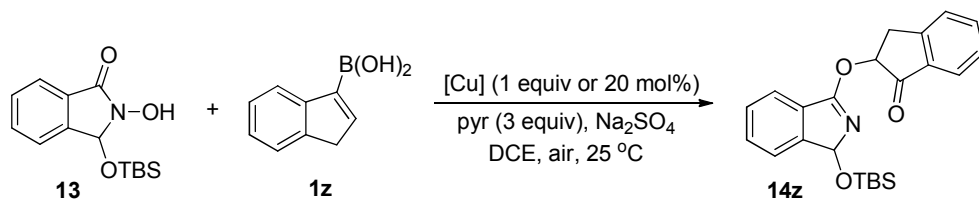
Scheme 2.25: Etherification and Rearrangement of 3-ethyl-3-methyl-*N*-hydroxyisoindolinone

We chose to pursue the OTBS isoindolinone for further studies of the diastereoselective method.

2.5 Optimization of the Preparation and Rearrangement of 14z

After discovering the single flask etherification and [3,3] rearrangement, we wanted to optimize the reaction conditions (Table 2.1). With $\text{Cu}(\text{OAc})_2$, we realized that the optimum time for the reaction was 12h, which gave us an NMR yield of 100% (entry 4, Table 2.1). The isolated yield in this case was 71%. This suggests that even though the imidate products are stable enough to be isolated, they decompose to some extent on florisil[®] during purification. At times less than 12h, the yields for the reaction were significantly lower (entries 1-3, Table 2.1). When 20 mol % of $\text{Cu}(\text{OAc})_2$ was used, the reaction required 3d to go to completion during which the imidate product started to decompose. Hence the reaction with 20 mol % of $\text{Cu}(\text{OAc})_2$ gave a lower yield of 73%

(entry 5, Table 2.1). Other Cu salts like CuTC, CuCl and CuBr (entries 6-8, Table 2.1) gave lower yields of the imidate product. Our optimization study concluded that using one equivalent of Cu(OAc)₂, two equivalents of boronic acid and three equivalents of pyridine with Na₂SO₄ as the desiccant in DCE (0.1 M) in the presence of air for 12h led to complete conversion of the isoindolinone to the imidate.



Entry	[Cu]	Time	Yield ^a
1	Cu(OAc) ₂ (1 equiv)	2 h	6%
2	Cu(OAc) ₂ (1 equiv)	3 h	24%
3	Cu(OAc) ₂ (1 equiv)	8 h	60%
4	Cu(OAc) ₂ (1 equiv)	12 h	100% (71%) ^b
5	Cu(OAc) ₂ (20 mol%)	3 d	73%
6	CuTC (1 equiv)	12 h	74%
7	CuCl (1 equiv)	12 h	57%
8	CuBr (1 equiv)	12 h	76%

Yield^a refers to NMR yields with 1,3,5-trimethoxybenzene as the internal standard. b refers to the isolated yield which was 71 %

Table 2.1: Optimization of the Single-Flask Dioxygenation

2.6 Evaluating Different Substituents at the Stereocenter

Since the 3-*t*-butyldimethylsilyloxy-*N*-hydroxyisoindolinone substrate reacted with cyclohexenyl boronic acid to yield the imidate product directly, and with good diastereoselectivity, we wanted to evaluate different functional groups (instead of OTBS), and examine whether we could still achieve the etherification and rearrangement in a single flask reaction while also studying the impact of varying the substituents on the diastereoselectivity of the [3,3] rearrangement. We synthesized *N*-hydroxyisoindolinones with varying substituents at the stereocenter and used them in the Cu-mediated etherification reaction with indenyl boronic acid **1z** (Table 2.2).

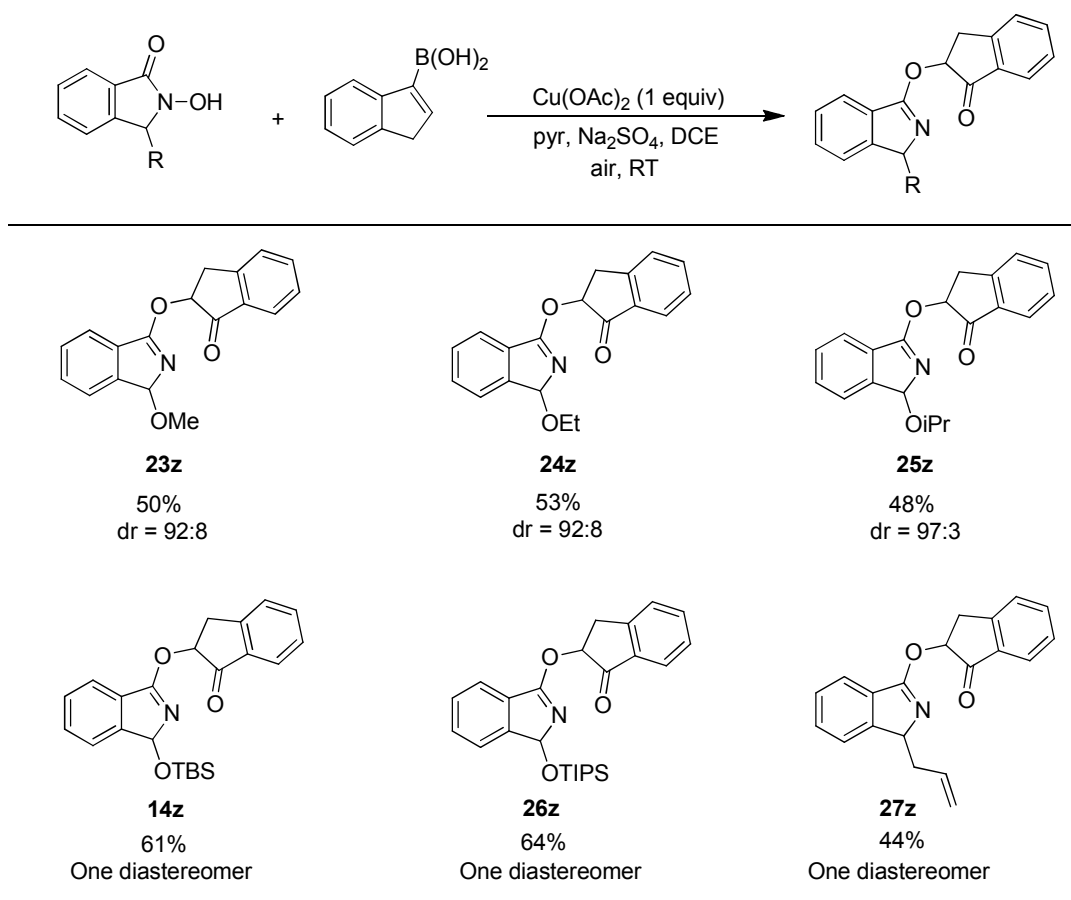


Table 2.2: Evaluating the Effect of Different Substituents on the Diastereoselectivity

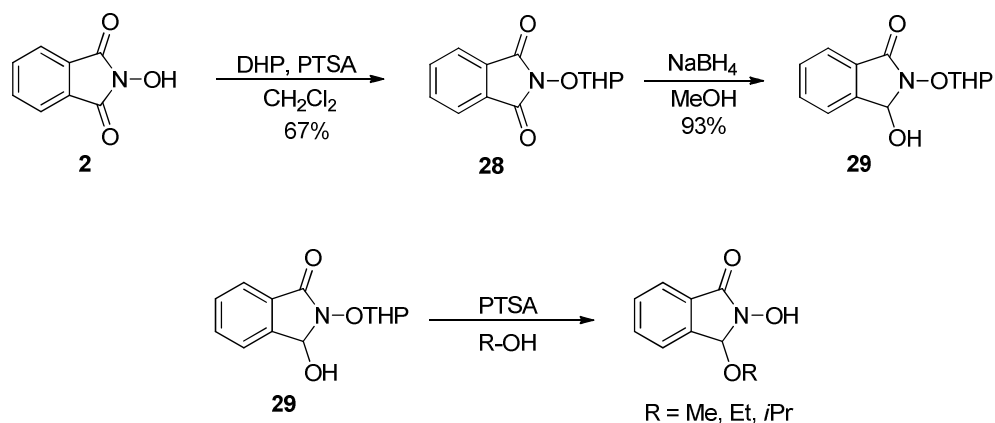
(dr determined by using ^1H NMR spectroscopy)

As seen from Table 2.2 above, for all the substituted *N*-hydroxyisoindolinones, both the etherification and rearrangement reactions occurred sequentially and the crude ^1H NMR spectrum of the reaction mixture showed only the imidate product with no traces of the etherification product. The imidates were unstable when subjected to silica gel, but could be isolated using flash chromatography on florisil[®]. Regarding the effect on the diastereoselectivity; the compounds **23z** and **24z** having a methoxy or an ethoxy functional group gave a 92:8 mixture of diastereomers, while increasing the bulk to an isopropoxy group in **25z**, resulted in a slightly higher diastereomeric ratio of 97:3. With a bulky silyloxy group such as OTBS or OTIPS, (**14z** and **26z**) only one diastereomer was observed by both ^1H NMR and ^{13}C NMR spectroscopy. Replacing the oxygen-based substituent with an allyl group in compound **27z** also gave the product as a single diastereomer.

Although the [3,3] rearrangement with the *N*-hydroxyisoindolinones proceeded with high diastereoselectivity with most of the substituents at the stereocenter, we decided to test the tolerance for the substitution on the boronic acids on the etherification and rearrangement with **13** since it could be easily synthesized in a high yield. The syntheses for all the 3-substituted-*N*-hydroxyisoindolinones are shown below.

2.6.1 Synthesis of 3-Alkoxy-*N*-Hydroxyisoindolinones

The 3-Alkoxy-*N*-Hydroxyisoindolinones were synthesized as shown below in Scheme 2.26.

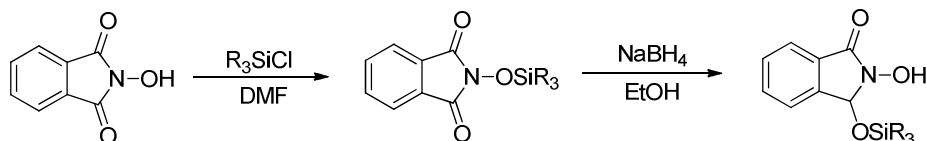


Scheme 2.26: Synthesis of 3-Alkoxy-*N*-Hydroxyisoindolinones

THP protection of *N*-hydroxyphthalimide was followed by reduction of one of the carbonyls with sodium borohydride to yield compound **29**. When this compound was treated with 4-toluenesulfonic acid in MeOH, the deprotection of the OTHP group was accompanied by the displacement of the hydroxyl group by MeOH in the presence of the acid to yield the 3-methoxy-*N*-hydroxyisoindolinone as the product. Upon changing the alcohol solvent from MeOH to EtOH and *i*PrOH, the corresponding 3-alkoxy-*N*-hydroxyisoindolinones were obtained.

2.6.2 Synthesis of 3-Silyloxy-*N*-Hydroxyisoindolinones

The 3-silyloxy-*N*-hydroxyisoindolinones were synthesized according to Scheme 2.27.

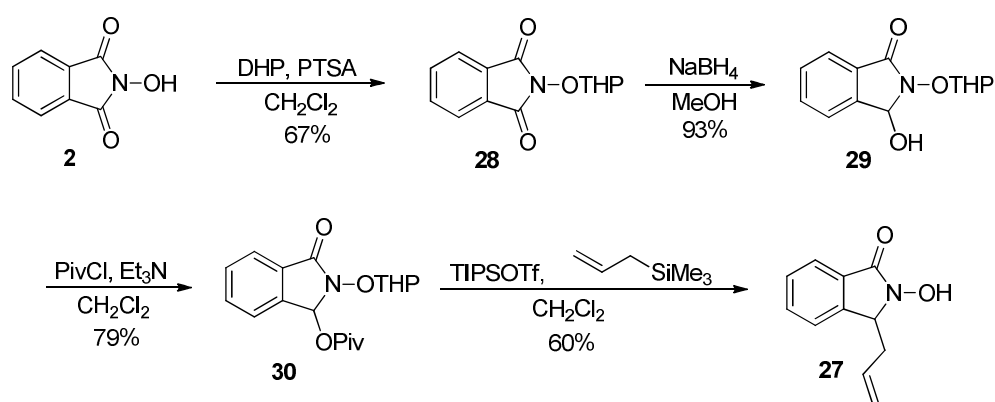


Scheme 2.27: Synthesis of 3-Silyloxy-*N*-Hydroxyisoindolinones

Protection of the hydroxyl group of *N*-hydroxyphthalimide with either TBSCl or TIPSCl gave the *O*-silylated product. Reduction of one of the carbonyls with sodium borohydride was followed by the *in situ* migration of the silyl group, to yield the 3-silyloxy-*N*-hydroxyisoindolinones, which were isolated as white solids.

2.6.3 Synthesis of 3-Allyl-*N*-Hydroxyisoindolinone

The 3-allyl-*N*-hydroxyisoindolinone was synthesized as per the procedure shown below in Scheme 2.28. Compound **29** was synthesized as before, after protection of *N*-hydroxyphthalimide with THP and reduction with sodium borohydride. The resulting alcohol was protected using pivaloyl chloride to form compound **30**. This compound was then subjected to allyltrimethylsilane in the presence of TIPSOTf to give the desired product **27**. This reaction was based on the methodology developed by Othman and co-workers⁹³ where nucleophilic substitution by allyltrimethylsilane occurs onto the *N*-acyliminium ion formed from **30** in the presence of TIPSOTf.



Scheme 2.28: Synthesis of 3-Allyl-*N*-hydroxyisoindolinone

After having prepared a variety of hydroxyisoindolinones, we wanted to evaluate the reactivity of **13** with substituted boronic acids and determine the relative stereochemistry of the product.

2.7 Determination of Relative Stereochemistry for the Imidate

The relative stereochemistry for compound **14z** was determined by X-ray analysis. The results indicate that the substituent on the hydroxyisoindolinone (Figure 1) and the newly formed stereocenter at the α -oxygenated ketone are on opposite faces. This supports the hypothesis that the [3,3] rearrangement occurs from the sterically less hindered face i.e. opposite to the group at the stereocenter on the hydroxyisoindolinone. The X-ray analysis was done by Prof. Donald Wink at UIC.

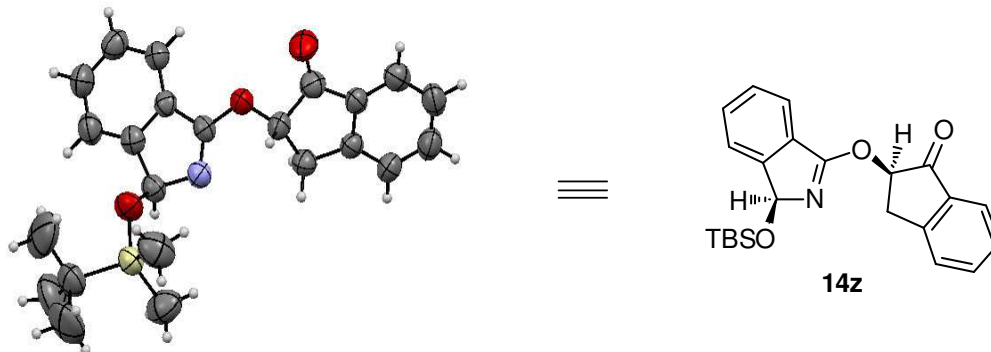
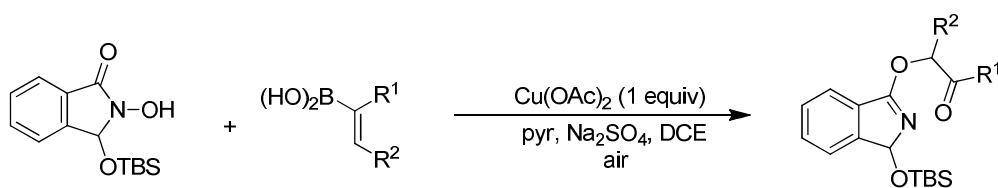


Figure 2.1: Determination of Relative Stereochemistry

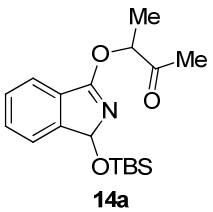
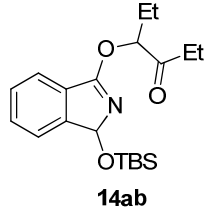
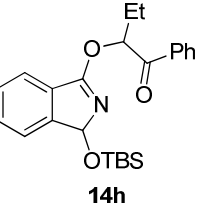
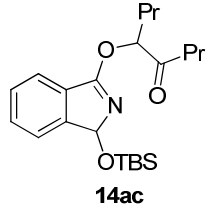
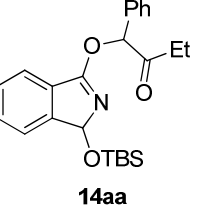
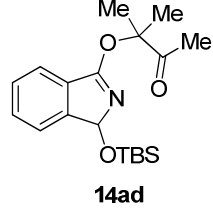
2.8 Varying the Boronic Acids

2.8.1 Scope and Stereoselectivity with Disubstituted Boronic Acids

After having established the conditions for the single flask reaction and determining the relative stereochemistry of the product, we wanted to examine the tolerance for the substitution on the boronic acids. The substrate that we chose was the 3-*t*-butyldimethylsilyloxy-*N*-hydroxyisoindolinone **13** and the boronic acids evaluated were disubstituted (Scheme 2.29).



Scheme 2.29: Evaluation of Disubstituted Boronic Acids

Entry	Product	Yield ^a	dr	Entry	Product	Yield ^a	dr
1	 14a	65%	One diastereomer	4	 14ab	61%	dr = 80:20
2	 14h	59%	One diastereomer	5	 14ac	72%	dr = 80:20
3	 14aa	61%	One diastereomer	6	 14ad	63%	–

Yield^a refers to isolated yields

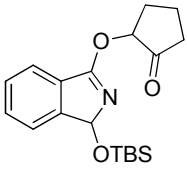
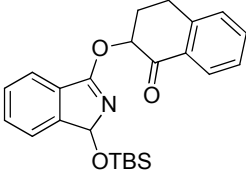
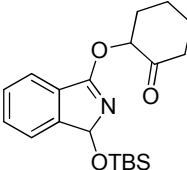
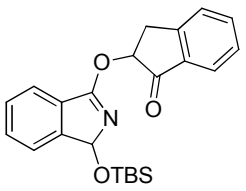
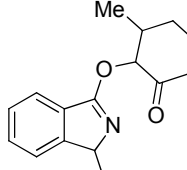
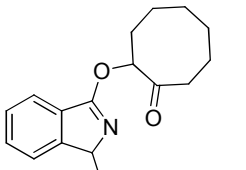
Table 2.3: Using Acyclic, Disubstituted Boronic Acids

The single-flask reaction tolerates acyclic boronic acids with alkyl and aryl substituents at either position of the boronic acid. The reaction with 3-methyl-2-buten-2-yl boronic acid forms compound **14ad** (entry 6, Table 2.3) which contains an α -oxygenated quaternary center. This proves that our dioxygenation methodology could be used for the construction of the otherwise difficult to synthesize quaternary stereocenters. The 3-methyl-2-buten-2-yl boronic acid has previously been used in the Suzuki-Miyaura reaction for coupling with aromatic iodides in the presence of $\text{Pd}(\text{PPh}_3)_2\text{Cl}_2$.⁹⁴ It has also been utilized in the Liebeskind-Srogl cross-coupling⁹⁵ with borondipyrromethene (BODIPY) dyes⁹⁶ in the presence of a Pd catalyst and tris(2-furyl)phosphine as a

ligand.⁹⁷ Our reaction which involves the coupling of the 3-methyl-2-buten-2-yl boronic acid with **13** represents the first example for the use of a trisubstituted alkenyl boronic acid in a Chan-Lam coupling reaction.

Regarding the stereoselectivity for the reaction, as seen from Table 2.3, the imidate **14a** (entry 1, Table 2.3) was isolated as a single diastereomer. One diastereomer was also observed for the compounds **14h** and **14aa**, (entries 2 and 3, Table 2.3) which had a phenyl substituent on the boronic acid. The imidates **14ab** and **14ac** (entries 4 and 5, Table 2.3) were obtained as an 80:20 mixture of diastereomers.

The results for the reaction of **13** with cyclic disubstituted boronic acids are illustrated below in Table 2.4.

Entry	Product	Yield ^a	dr	Entry	Product	Yield ^a	dr
1	 14m	64%	dr = 80:20	4	 14v	66%	One diastereomer
2	 14n	71%	dr = 89:11	5	 14z	61%	One diastereomer
3	 14p	64%	dr = 69:31	6	 14ae	57%	One diastereomer

Yield^a refers to isolated yields

Table 2.4: Single-Flask Reaction with Cyclic, Disubstituted Boronic Acids.

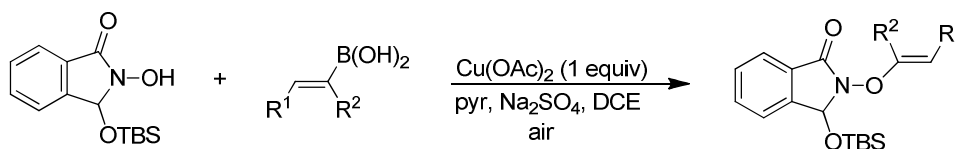
The Cu-mediated one pot etherification and rearrangement reaction works well with cyclic disubstituted boronic acids (Table 2.4). Large rings as well as fused ring systems give the desired product in moderate yields. With the cyclopentenyl boronic acid **1m**, the imidate **14m** (entry 1, Table 2.4) was obtained as an 80:20 mixture of diastereomers. Increasing the steric volume of the boronic acid, from the five membered cyclopentenyl boronic acid to the six membered cyclohexenyl boronic acid **1n**, led to an increase in the dr of the imidate **14n** (entry 2, Table 2.4) to 89:11. Although the imidate **14p** (entry 3, Table 2.4) has three stereocenters, only two diastereomers were observed by ^1H NMR and ^{13}C NMR spectroscopy in the reaction of **13** with **1p**. The imidates derived from the larger ring containing cyclooctenyl boronic acid **14ae** (entry 6, Table 2.4) and from the fused ring systems **14v** and **14z**, (entries 4 and 5, Table 2.4) were isolated as single diastereomers.

The results with the disubstituted boronic acids indicate that the reaction is controlled by steric effects, and a higher diastereomeric ratio is obtained when a bulky boronic acid is used due to increased interactions in the transition state.

2.8.2 Scope and Stereoselectivity with Monosubstituted Boronic Acids

When monosubstituted boronic acids were treated with **13**, the only product isolated was the etherification product (Scheme 2.30), though there were traces of the rearrangement product for the compound **31d** at when it was kept at room temperature. In this case, the *in situ* [3,3] rearrangement to form the imidate did not occur, especially for

substrates **31af** and **31g**. This might be attributed to the fact that the formation of the α -oxygenated aldehydes has a higher energy barrier since they are less stable than the corresponding α -oxygenated ketones.



Scheme 2.30: Etherification Reaction with Monosubstituted Boronic Acids

The *N*-enoxyisoindolinones isolated in this manner are shown below in Table 2.5.

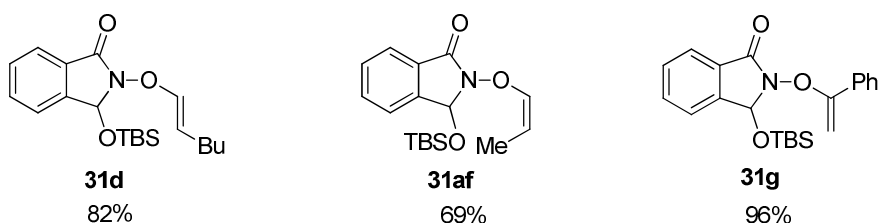
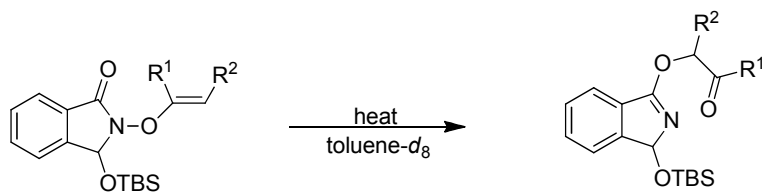


Table 2.5: *N*-enoxyisoindolinones Isolated using the Etherification Reaction

As seen above in Table 2.5, the 1-hexenyl boronic acid **1d** gives the etherification product **31d** in a 82% yield. The reaction also worked with the *Z*-1-propen-1-yl boronic acid **1af**, to form the imidate **31af** in a moderate yield of 69%. This could be because of increased steric interactions between the methyl group on the boronic acid and the *N*-hydroxyisoindolinone. The 1-phenylvinyl boronic acid **1g** also underwent the reaction to form the *N*-enoxyisoindolinone **31g**.

Heating a solution of the *N*-enoxyisoindolinones in toluene-*d*₈ (Scheme 2.31), gave the imidates as shown below in Table 2.6.



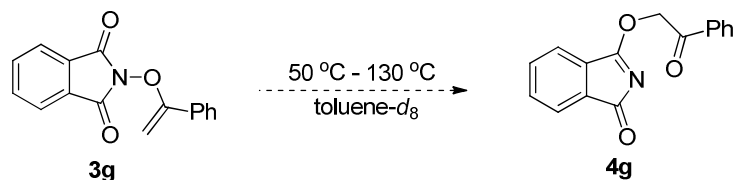
Scheme 2.31: [3,3] Rearrangement using Monosubstituted Boronic Acids

Entry	Product	Temperature for Rearrangement	Yield	dr
1	 14d	50 °C	100%	One diastereomer
2	 14af	65 °C	100%	dr = 75:25
3	 14g	80 °C	96%	–

Table 2.6: Rearrangement to form α -Oxygenated Aldehydes. Yields refer to isolated yields.

It is evident from Table 2.6 that the *N*-enoxisoindolinone **31d** has the lowest energy barrier, and can form the imidate **14d** at 50 °C. The compound **31af** requires a higher temperature of 65 °C and forms the α -oxygenated aldehyde **14af** as a 75:25 mixture of diastereomers. The *N*-enoxisoindolinone **31g** obtained using 1-phenylvinyl

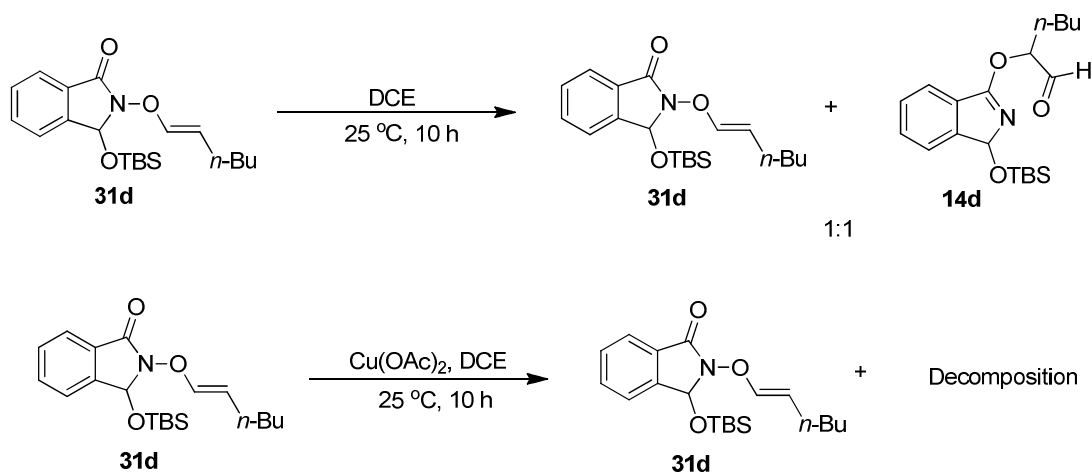
boronic acid **1g**, also formed the imidate **14g** at 80 °C. During our previous studies on *N*-enoxyphthalimide **3g**, there was no rearrangement even when it was heated to 130 °C (Scheme 2.32), hence the isoindoline system seems to be more activated than the phthalimide and more susceptible to forming the imidate through the [3,3] rearrangement.



Scheme 2.32: Rearrangement with the *N*-Enoxyphthalimide

2.9 Role of Cu(OAc)₂ in the [3,3] Rearrangement

In order to determine whether the *in situ* rearrangement that followed the etherification was catalyzed by the Cu(OAc)₂ present in the reaction mixture, we used the *N*-enoxyisoindoline **31d** and tested it for the [3,3] rearrangement both in the presence and absence of Cu(OAc)₂. The results are shown below in Scheme 2.33.



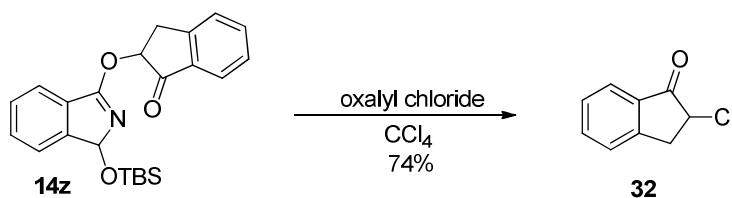
Scheme 2.33: Determining the role of Cu(OAc)₂ in the [3,3] Rearrangement

In the absence of Cu(OAc)₂, the *N*-enoxyisoindolinone **31d** was stirred in DCE at room temperature overnight. Spectroscopic analysis revealed that after 10h, a 1:1 mixture of the starting material and product was obtained. When the same compound was treated with one equivalent of Cu(OAc)₂ in DCE and stirred at room temperature for 10h, there was starting material and some decomposition. These results indicate that the [3,3] rearrangement appears to be thermally driven and does not depend on any catalysis by the Cu(OAc)₂. The Cu(OAc)₂ may actually be responsible for the decomposition of the α -oxygenated aldehyde that forms in the reaction.

2.10 Functionalization of the Imidates

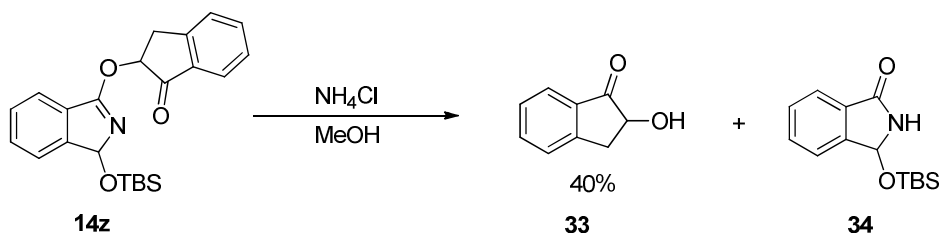
Our one pot etherification and rearrangement had a broad substrate scope and good to excellent diastereoselectivity for the substrates; hence, we wanted to expand the methodology further by demonstrating the synthetic utility of the imidates. We began by screening a variety of conditions for the functionalization of the imidates such as using nucleophiles like NaN₃, NaSPh, Lewis acids like ZnCl₂, bases like Ag₂O and oxidation with DDQ. Conversion of the ketone to an olefin with Tebbe reagent,⁹⁸ and treatment with electrophiles such as *m*CPBA and methyl iodide were also attempted but only led to decomposition. We finally discovered that treating the imidate **14z** with oxalyl chloride effectively converted it to the α -chloro ketone **32** as shown in Scheme 2.34. Since the starting material is racemic, the α -chloro ketone isolated is also racemic. An imidate with a fixed configuration at the stereocenter on the hydroxyisoindolinone will have to be utilized to determine the absolute stereochemistry at the α -chloro center. Since the

rearrangement is diastereoselective, the configuration at the α -oxygenated center of the imidate will be determined by the stereochemistry of the center on the isoindolinone, and this in turn would be reflected in the stereochemistry at the α -chloro center. This transfer of stereochemistry would be observed provided that there was no epimerization during the reaction with oxalyl chloride.



Scheme 2.34: Conversion of the Imidate to the α -Chloro Ketone

We also discovered that treating the imidate **14z** with ammonium chloride in aqueous MeOH, hydrolyzed the imidate to form the α -hydroxy ketone **33** as demonstrated in Scheme 2.35. In this case, the 3-*t*-butyldimethylsilyloxyisoindolinone **34** was also isolated along with the desired α -hydroxy ketone, which supports our methodology where the *N*-hydroxyisoindolinone could be used as an auxiliary to control the diastereoselectivity of the rearrangement and then be easily cleaved.



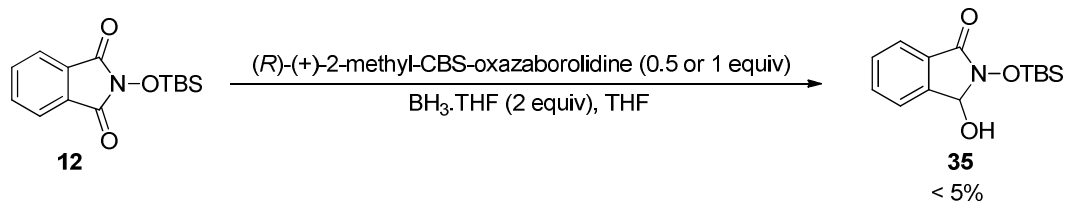
Scheme 2.35: Conversion of the Imidate to the α -Hydroxy Ketone

2.11 Transfer of Chirality

Since our [3,3] rearrangement proceeded with high diastereoselectivity, we wanted to evaluate if the stereochemistry and enantiomeric excess (% ee) of a chiral *N*-hydroxyisoindolinone could be carried through the etherification and rearrangement reactions and whether the imidate or the final α -hydroxy ketone would have the same enantiomeric excess value as the starting chiral *N*-hydroxyisoindolinone. We therefore wanted to determine if the stereochemistry of a chiral *N*-hydroxyisoindolinone would transfer to the imidate and the α -hydroxy ketone through a diastereoselective rearrangement,

2.11.1 Optimization of the Conditions for the Chiral Reduction

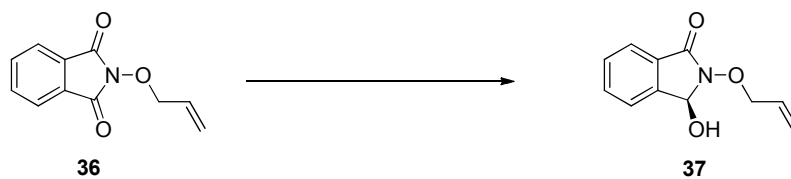
We hypothesized that a chiral *N*-hydroxyisoindolinone could be obtained via a stereospecific reduction of one of the carbonyls of the *N*-hydroxyphthalimide **2**. The chiral reduction was first attempted with the CBS catalyst.⁹⁹ The reaction was tried with **12** and the (*S*)-(-)-*o*-tolyl-CBS-oxazaborolidine¹⁰⁰ or (*R*)-(+)-2-methyl-CBS-oxazaborolidine with various boranes such as BH₃.THF, BH₃.pyr, and catechol borane in a variety of solvents. No reaction occurred when (*S*)-(-)-*o*-tolyl-CBS-oxazaborolidine was employed as the catalyst, irrespective of the borane or the solvent used. With the (*R*)-(+)-2-methyl-CBS-oxazaborolidine and BH₃.THF in THF, the reaction did give the reduced product **35** but the yield was low (< 5 %) and there was no migration of the TBS group as illustrated in Scheme 2.36.



Scheme 2.36: Chiral Reduction with CBS Catalyst

With such a low yield, and difficulty in separation from byproducts, we could not effectively determine the enantiomeric ratio (er) of the resulting alcohol. Also, all attempts to force the TBS group to migrate were unsuccessful.

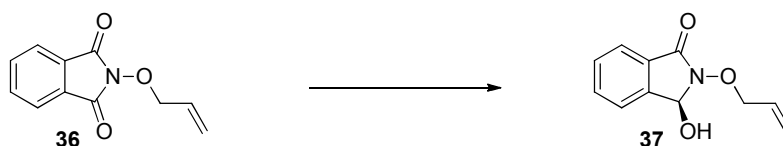
The chiral reduction of the *N*-allyloxyisindoline-1,3-dione **36** was therefore endeavored with different reagents and conditions. We chose the *N*-allyloxyisindoline-1,3-dione **36** since the OTBS group in the *N*-*t*-butyldimethylsilyloxyisindoline-1,3-dione **12** was sensitive to both acidic and basic conditions. Some of the optimization study is shown in Table 2.7. As seen from Table 2.7, none of the CBS based reagents were successful in reducing the carbonyl group.



Entry	Reaction Conditions	Result
1	(<i>R</i>)-(+)-2-methyl-CBS-oxazaborrolidine, BH ₃ .THF, Toluene	No reaction
2	(<i>R</i>)-(+)-2-methyl-CBS-oxazaborrolidine, BH ₃ .THF, THF	No reaction
3	(<i>R</i>)-(+)-2-methyl-CBS-oxazaborrolidine, BH ₃ .diethylaniline, Toluene	Decomposition
4	(<i>R</i>)-(+)-2-methyl-CBS-oxazaborrolidine, BH ₃ .diethylaniline, THF	Decomposition
5	(1 <i>R</i> ,2 <i>S</i>)-(+)-cis-1-Amino-2-indanol, BH ₃ .THF, Toluene	No reaction
6	CuF ₂ , (<i>R</i>)-BINAP, Et ₃ SiH	No reaction

Table 2.7: Conditions for the Chiral Reduction

The conditions for catalytic asymmetric reductions are shown in Table 2.8. Metals like Ir and Rh had no impact on the reaction and the starting material was isolated with little or no conversion to the product. Using Ru as the metal catalyst, and formic acid as the reducing agent in dichloromethane, namely the Noyori reduction conditions,¹⁰¹ finally gave some conversion to the product. The reaction optimization is illustrated below.



Entry	Catalyst	Solvent	Temp	Source of 'H'	Result
1	RuCl(<i>R</i> -BINAP)	THF	RT	H ₂	No reaction
2	RuCl(<i>R</i> -BINAP)	Toluene	RT	H ₂	No reaction
3	RuCl(<i>p</i> -cymene)TsDPEN	THF	RT	H ₂	No reaction
4	RuCl(<i>p</i> -cymene)TsDPEN	Toluene	RT	H ₂	SM + decomposition
5	RuCl(<i>p</i> -cymene)TsDPEN	THF + 1 equiv EtOH	RT	H ₂	No reaction
6	RuCl(<i>p</i> -cymene)TsDPEN	Toluene + 1 equiv EtOH	RT	H ₂	No reaction
7	RuCl(<i>p</i> -cymene)TsDPEN	Neopentyl alcohol	RT	H ₂	No reaction
8	RuCl(<i>p</i> -cymene)TsDPEN	<i>t</i> -butyl alcohol	RT	H ₂	No reaction
9	RuCl(<i>p</i> -cymene)TsDPEN	EtOH	RT	H ₂	SM + Some product
10	RuCl(<i>p</i> -cymene)TsDPEN	Allyl alcohol	RT	H ₂	No reaction
11	RuCl(<i>p</i> -cymene)TsDPEN	<i>i</i> PrOH	RT	H ₂	No reaction
12	RuCl(<i>p</i> -cymene)TsDPEN	1,4-Dioxane	RT	H ₂	No reaction
13	RuCl(<i>p</i> -cymene)TsDPEN	DME	RT	H ₂	No reaction
14	RuCl(<i>p</i> -cymene)TsDPEN (0.01 equiv)	CH ₂ Cl ₂ , 6 h	RT	HCO ₂ H + Et ₃ N	SM:Prod = 2.5:1
15	RuCl(<i>p</i>-cymene)TsDPEN (0.01 equiv)	CH₂Cl₂, 19 h	RT	HCO₂H + Et₃N	50% isolated yield
16	RuCl(<i>p</i>-cymene)TsDPEN (0.01 equiv)	CH₂Cl₂, 12 h	40 °C	HCO₂H + Et₃N	50% isolated yield
17	RuCl(<i>p</i> -cymene)TsDPEN (0.1 equiv)	CH ₂ Cl ₂ , 6 h	RT	HCO ₂ H + Et ₃ N	< 10%

Table 2.8: Optimization of Conditions for the Chiral Reduction. The Ru catalyst refers to Ru(*p*-cymene)[(*R,R*)TsDPEN]. RT refers to 25 °C

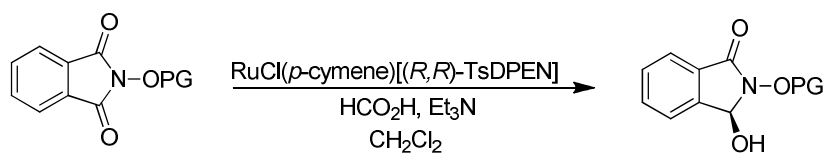
The optimization study concluded that using 0.01 equivalents of Ru(*p*-cymene)[(*R,R*)TsDPEN] with formic acid and triethylamine in dichloromethane either at room temperature or 40 °C gave the alcohol product **37** in a 50% yield. However, a higher er of 2.1:1 was obtained when the reaction was carried out at room temperature as compared to an er of 1.7:1 when the reaction was carried out at 40 °C. With a higher catalyst loading, a significant decrease in the yield was observed. Using hydrogen as the reducing agent was ineffective even when a highly polar solvent was used. With these optimized conditions in hand, we wanted to explore the effect of other protecting groups on the er.

2.11.2 Effect of Protecting Groups on the Chiral Reduction

To investigate the effect that the protecting groups on the *N*-hydroxyphthalimide, had on the chiral reduction, we synthesized substrates with a variety of protecting groups. The sterics and electronics of the protecting groups were varied in an effort to determine some trend in the chiral reduction which we could use to better the er of the alcohol product. As determined above, the allyl protected *N*-hydroxyphthalimide **36** gave a 50% yield of the alcohol product which had an er of 2.1:1 (entry 1, Table 2.9). Increasing the size of the protecting group to a *t*-butyl moiety led to decomposition under the reduction conditions (entry 2, Table 2.9). Substituting the allyl group for a benzyl functionality in compound **39**, gave the desired product with an er of 2.3:1. Placing a naphthyl group (**40**), which is bulkier and more electron withdrawing than the benzyl group led to an increase

in the yield but with a slight decrease in the er. Using the extremely bulk mesityl group, **41**, gave the same er as that observed with the benzyl (entries 3, 4 and 5, Table 2.9). Probing the effect of electronics on the reduction with electron donating and electron withdrawing substituents on the benzyl group, showed that electron-donating groups were tolerated but only decomposition was observed with the *p*-CF₃ benzyl group (entries 6 and 7, Table 2.9). All silyl containing protecting groups also led to decomposition.

Thus the enantiomeric ratio of the alcohol product was approximately 2:1, irrespective of the size or the electronics of the protecting group used.



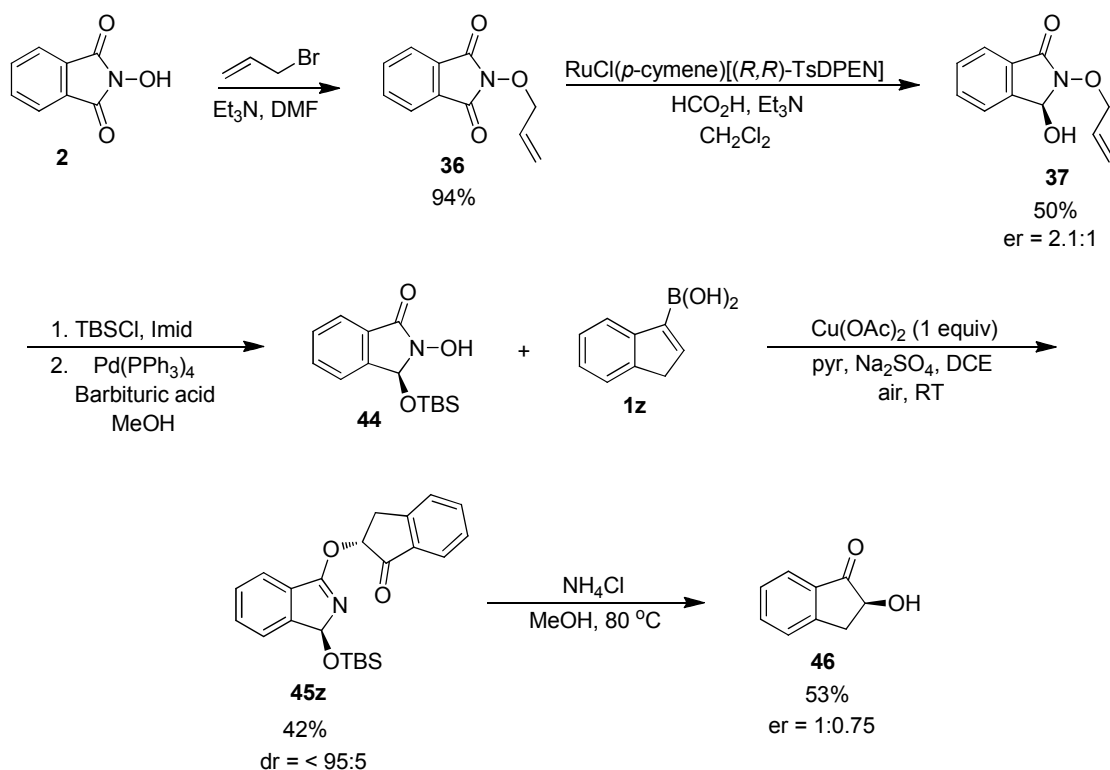
Entry	Product	Yield	er
1	 37	50%	2.1:1
2	 38	Decomposition	–
3	 39	50%	2.3:1
4	 40	65%	2.1:1
5	 41	48%	2.3:1
6	 42	Decomposition	–
7	 43	44%	2.1:1

Table 2.9: Effect of Protecting Groups on the Chiral Reduction. Determination of er was done by Mosher ester analysis with (*R*)-(+)- α -Methoxy- α -trifluoromethylphenylacetic acid.¹⁰²

2.11.3 Testing the Effect of a Chiral *N*-hydroxyisoindolinone

Having optimized the conditions for the chiral reduction and determined that the best er we could obtain was 2:1, we wanted to test our hypothesis for the chirality transfer through the diastereoselective rearrangement.

Protection of the chiral alcohol **37** with TBSCl, followed by deprotection of the allyl group gave the chiral 3-*t*-butyldimethyl-*N*-hydroxyisoindolinone which was immediately reacted with the indenyl boronic acid **1z**. The etherification was directly followed by the rearrangement to give the imidate **45z** which had a dr of <95:5. Hydrolysis of the imidate with ammonium chloride gave the α -hydroxy ketone **46** which had an enantiomeric ratio of 1:0.75. Thus starting with an er of 2.1:1 for the chiral 3-hydroxy-*N*-allyloxyisoindolinone, we observed some erosion of chirality since the final product had an er of 1:0.75. This suggests that the rearrangement is highly diastereoselective and probably decides the stereochemistry at the α -oxygenated center on the imidate, but there might be some epimerization either in the presence of Cu(OAc)₂ or during the hydrolysis with ammonium chloride. This route therefore needs further analysis of the imidates with either a chiral GC or chiral SFC to determine the er at the imidate stage.



Scheme 2.37: Reaction Scheme for Evaluating Transfer of Chirality. Determination of er was done by Mosher Analysis with (*R*)-(+)- α -Methoxy- α -trifluoromethylphenylacetic acid.¹⁰² The absolute stereochemistry at the indolinone and the α -oxygenated stereocenter (above and henceforth) has not been determined. The use of dashes and wedges is just to indicate a chiral center and does not specify the actual configuration at that stereocenter.

2.12 Conclusion

We have developed a new diastereoselective dioxygenation reaction that proceeds with good to excellent diastereoselectivity to form α -oxygenated ketones as imidates. The reaction of 3-substituted-*N*-hydroxyisoindolinones with alkenyl boronic acids forms the *N*-enoxyisoindolinones which undergo an *in situ* [3,3] rearrangement to form the imidates. The rearrangement reaction is found to proceed with high diastereoselectivity and the size

of the substituent on the isoindolinone plays an important role in controlling the facial selectivity. The imidate products can be derivatized to α -hydroxy ketones and α -chloro ketones. We have also tried to investigate the transfer of chirality from an enantiomerically enriched *N*-hydroxyisoindolinone to the imidates and the α -hydroxy ketones.

2.13 Supporting Information

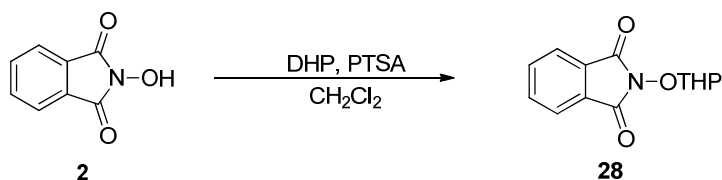
2.13.1 General Experimental Information:

^1H NMR and ^{13}C NMR spectra were recorded at ambient temperature using 500 MHz spectrometers. The data are reported as follows: chemical shift in ppm from internal tetramethylsilane on the δ scale, multiplicity (br = broad, s = singlet, d = doublet, t = triplet, q = quartet, m = multiplet), coupling constants (Hz), and integration. High resolution mass spectra were acquired on an LTQ FT spectrometer, and were obtained by peak matching. Melting points are reported uncorrected. Analytical thin layer chromatography was performed on 0.25 mm extra hard silica gel plates with UV254 fluorescent indicator. Liquid chromatography was performed using forced flow (flash chromatography) of the indicated solvent system on 60Å (40 – 60 μm) mesh silica gel (SiO_2). Medium pressure liquid chromatography was performed to force flow the indicated solvent system down columns packed with 60Å (40 – 60 μm) mesh silica gel (SiO_2). Unless otherwise noted, all reagents were obtained from commercial sources and, where appropriate, purified prior to use. THF, CH_2Cl_2 , and toluene were dried by filtration through alumina according to the procedure of Grubbs.¹ TMEDA was distilled

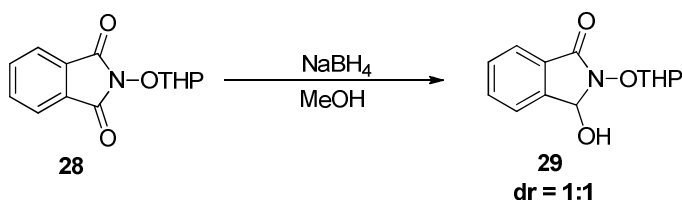
over CaH_2 and stored under N_2 prior to use. Amberlite-IR120 was washed with CH_2Cl_2 prior to use.

2.13.2 Experimental Procedures and Characterization Data

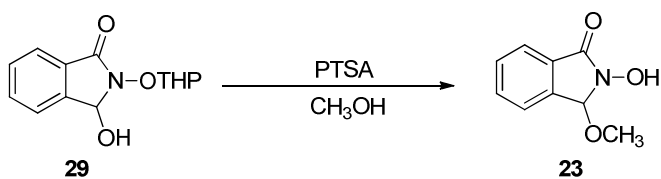
II. Preparation of 3-substituted-*N*-hydroxyisoindolinones



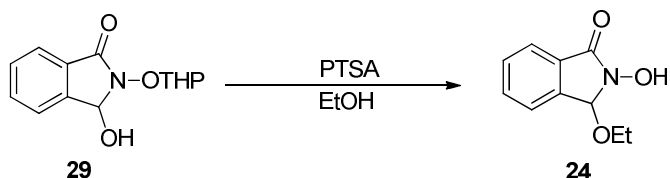
2-((tetrahydro-2H-pyran-2-yl)oxy)isoindoline-1,3-dione 28: To a solution of the *N*-hydroxyphthalimide **2** (5.0 g, 30.65 mmol) in CH_2Cl_2 (30 ml) at 0 °C, was added the 3,4-dihydro-2*H*-pyran (1.2 equiv, 3.4 ml, 36.78 mmol) followed by PTSA (0.1 equiv, 0.583 g, 3.07 mmol). The reaction was stirred at 0 °C for 30 mins and then at room temperature for 2 h. The reaction was quenched by the addition of water, and extracted with CH_2Cl_2 (3 x 15 ml). The organic layer was washed with brine and dried with MgSO_4 . The solvent was removed under reduced pressure and the crude reaction mixture purified by medium pressure chromatography on silica gel with 1:4 ethyl acetate:hexanes to give **28** as a white solid (5.1 g, 67 %). ^1H NMR (500 MHz; CDCl_3): δ 7.83-7.80 (m, 2H), 7.73-7.72 (m, 2H), 5.42-5.40 (m, 1H), 4.53-4.48 (m, 1H), 3.67-3.63 (m, 1H), 2.12-2.08 (m, 1H), 1.96-1.65 (m, 5H); ^{13}C NMR (125 MHz, CDCl_3): δ 163.8, 134.2, 129.1, 123.4, 103.1, 62.3, 27.7, 24.8, 17.6; IR (thin film) 2963, 2940, 2899, 2858, 1783, 1726, 1613, 1460, 1375, 1280, 1186 cm^{-1} ; HRMS (ESI) m/z calcd. for $\text{C}_{13}\text{H}_{13}\text{NO}_4\text{Na}$ ($\text{M}+\text{Na}$) $^+$ 270.0742, found 270.0740; mp 115 °C.



3-hydroxy-2-((tetrahydro-2H-pyran-2-yl)oxy)isoindolin-1-one 29: A solution of 2-((tetrahydro-2H-pyran-2-yl)oxy)isoindoline-1,3-dione **28** (7.5 g, 30.65 mmol) in MeOH (40 ml) was cooled to 0 °C and NaBH₄ (1.5 equiv, 1.7 g, 45.97 mmol) was added slowly to the reaction mixture. After the evolution of H₂ was complete, the reaction was warmed to room temperature and stirred for 2 h when TLC indicated complete consumption of **28**. The MeOH was removed *in vacuo* and the residue dissolved in EtOAc. Saturated NH₄Cl was added followed by extraction with EtOAc (3 x 20 ml). The organic layer was washed with water and brine, dried with MgSO₄ and concentrated under reduced pressure to give **29** as a white solid (7.1 g, 93 %) which was used without further purification. ¹H NMR first diastereomer (500 MHz; CDCl₃): δ 7.82-7.78 (m, 1H), 7.65-7.57 (m, 3H), 5.94 (s, 1H), 5.33-5.28 (m, 1H), 4.38-4.35 (m, 1H), 3.71-3.65 (m, 2H), 1.92-1.85 (m, 6H); ¹³C NMR first diastereomer (125 MHz, CDCl₃): δ 165.9, 141.3, 133.4, 129.9, 129.1, 123.8, 123.6, 104.5, 83.5, 64.6, 28.3, 24.9, 19.8; ¹H NMR second diastereomer (500 MHz; CDCl₃): δ 7.78-7.75 (m, 1H), 7.66-7.49 (m, 3H), 5.93 (s, 1H), 5.03-5.02 (m, 1H), 4.17-4.16 (m, 1H), 3.91-3.86 (m, 1H), 3.51-3.50 (m, 1H), 1.86-1.53 (m, 6H); ¹³C NMR second diastereomer (125 MHz, CDCl₃): δ 165.3, 141.1, 133.1, 129.8, 128.7, 123.8, 123.3, 103.4, 82.6, 63.9, 30.6, 25.4, 19.7; IR (thin film) 3291, 2946, 2889, 1724, 1675, 1616, 1467, 1388, 1284, 1141 cm⁻¹; HRMS (ESI) m/z calcd. for C₁₃H₁₆NO₄ (M+H)⁺ 250.1079, found 250.1072; mp 129 °C.

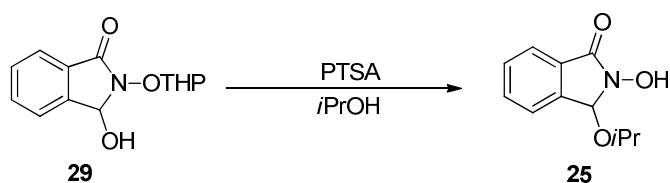


3-methoxy-*N*-hydroxyisoindolinone 23: The above compound 3-hydroxy-2-((tetrahydro-2*H*-pyran-2-yl)oxy)isoindolin-1-one **29** (1 g, 4.01 mmol) was dissolved in MeOH (15 ml) and PTSA (0.1 equiv, 0.076 g, 0.40 mmol) was added to the reaction mixture. The reaction was stirred at room temperature for 12 h. The MeOH was removed under reduced pressure and the crude reaction mixture purified by medium pressure chromatography on silica gel with 2:1 ethyl acetate:hexanes to give **23** as a white solid (0.503 g, 70 %). ¹H NMR (500 MHz; CDCl₃): δ 9.98 (bs, 1H), 7.75-7.74 (m, 1H), 7.61-7.59 (m, 1H), 7.52-7.49 (m, 2H), 5.89 (s, 1H), 3.36 (s, 3H); ¹³C NMR (125 MHz, CDCl₃): δ 166.2, 138.4, 132.8, 130.1, 129.9, 123.5, 123.4, 88.3, 53.0; IR (thin film) 3082, 2928, 2830, 1695, 1663, 1613, 1502, 1460, 1353, 1223, 1141 cm⁻¹; HRMS (ESI) *m/z* calcd. for C₉H₁₀NO₃ (M+H)⁺ 180.0661, found 180.0668; mp 115 °C.

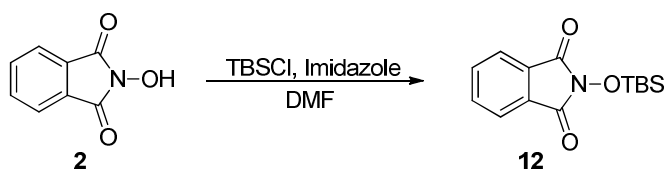


3-ethoxy-*N*-hydroxyisoindolinone 24: The 3-hydroxy-2-((tetrahydro-2*H*-pyran-2-yl)oxy) isoindolin-1-one **29** (1 g, 4.01 mmol) was dissolved in EtOH (15 ml) and PTSA (0.1 equiv, 0.076 g, 0.40 mmol) was added to the reaction mixture. The reaction was stirred at room temperature for 12 h. The EtOH was removed under reduced pressure and

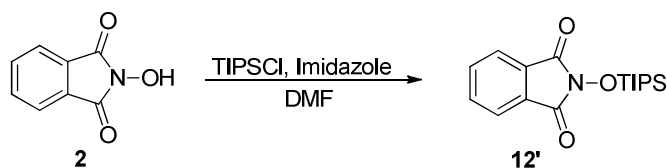
the crude reaction mixture purified by medium pressure chromatography on silica gel with 2:1 ethyl acetate:hexanes to give **24** as a white solid (0.519 g, 67 %). ^1H NMR (500 MHz; CDCl_3): δ 7.74-7.71 (m, 1H), 7.60-7.57 (m, 1H), 7.53-7.48 (m, 2H), 5.89 (s, 1H), 3.72-3.62 (m, 2H), 1.29 (dd, $J = 11.5, 6.9$ Hz, 3H); ^{13}C NMR (125 MHz, CDCl_3): δ 166.2, 139.0, 132.8, 132.7, 129.9, 123.5, 123.4, 87.9, 62.2, 15.3; IR (thin film) 3070, 2975, 2824, 1710, 1666, 1616, 1517, 1467, 1369, 1237, 1160 cm^{-1} ; HRMS (ESI) m/z calcd. for $\text{C}_{10}\text{H}_{12}\text{NO}_3$ ($\text{M}+\text{H}$) $^+$ 194.0817, found 194.0820; mp 121 $^\circ\text{C}$.



3-isopropoxy-N-hydroxyisoindolinone 25: The 3-hydroxy-2-((tetrahydro-2H-pyran-2-yl)oxy) isoindolin-1-one **29** (1 g, 4.01 mmol) was dissolved in *i*PrOH (15 ml) and PTSA (0.1 equiv, 0.076 g, 0.40 mmol) was added to the reaction mixture. The reaction was stirred at room temperature for 12 h. The *i*PrOH was removed under reduced pressure and the crude reaction mixture purified by medium pressure chromatography on silica gel with 2:1 ethyl acetate:hexanes to give **25** as an amorphous white solid (0.515 g, 62 %). ^1H NMR (500 MHz; CDCl_3): δ 9.92 (bs, 1H), 7.70-7.69 (m, 1H), 7.59-7.56 (m, 1H), 7.49-7.45 (m, 2H), 5.85 (s, 1H), 4.28-4.23 (m, 1H), 1.37 (d, $J = 6.0$ Hz, 3H), 1.31 (d, $J = 6.1$ Hz, 3H); ^{13}C NMR (125 MHz, CDCl_3): δ 166.0, 139.6, 132.6, 129.8, 129.5, 123.5, 123.2, 87.1, 71.8, 23.4, 22.7; IR (thin film) 3146, 2950, 1780, 1704, 1609, 1464, 1373, 1350, 1180, 1065 cm^{-1} ; HRMS (ESI) m/z calcd. for $\text{C}_{11}\text{H}_{14}\text{NO}_3$ ($\text{M}+\text{H}$) $^+$ 208.0974, found 208.0982.

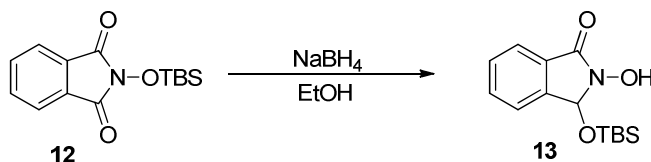


2-((*t*-butyldimethylsilyl)oxy)isoindoline-1,3-dione **12:** To the *N*-hydroxyphthalimide **2** (5.0 g, 31 mmol) in DMF (15 ml) at 0 °C was added imidazole (1.5 equiv, 3.2 g, 46.5 mmol) followed by TBSCl (1 equiv, 4.6 g, 31 mmol). The reaction was allowed to warm up to room temperature and stirred at that temperature for 10 h. The reaction was quenched with NH₄Cl and extracted with EtOAc (3 x 20 ml). The organic layer was washed with water and dried with MgSO₄. The crude reaction mixture was purified by medium pressure chromatography on silica gel with 1:3 ethyl acetate:hexanes to give **12** as a white solid (6.87 g, 80 %). ¹H NMR (500 MHz; CDCl₃): δ 7.81-7.78 (m, 2H), 7.72-7.70 (m, 2H), 1.07 (s, 9H), 0.28 (s, 6H); ¹³C NMR (125 MHz, CDCl₃): δ 163.9, 134.1, 129.1, 123.2, 25.6, 18.3, -4.9; IR (thin film) 2934, 2899, 2861, 1793, 1729, 1470, 1378, 1259, 1188, 1132, 1078 cm⁻¹; HRMS (ESI) *m/z* calcd. for C₁₄H₂₀NO₃Si (M+H)⁺ 278.1212, found 278.1207; mp 58 °C.



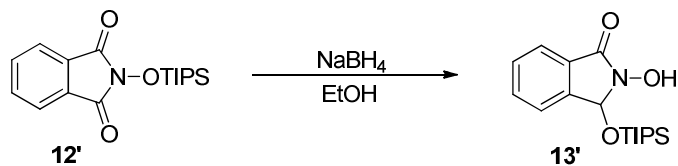
2-((triisopropylsilyl)oxy)isoindoline-1,3-dione **12':** To the *N*-hydroxyphthalimide **2** (5.0 g, 31 mmol) in DMF (15 ml) at 0 °C was added imidazole (1.5 equiv, 3.2 g, 46.5 mmol) followed by TIPSCl (1 equiv, 6.63 ml, 31 mmol). The reaction was allowed to warm up to room temperature and stirred at that temperature for 10 h. The reaction was quenched

with NH_4Cl and extracted with EtOAc (3 x 20 ml). The organic layer was washed with water and dried with MgSO_4 . The crude reaction mixture was purified by medium pressure chromatography on silica gel (1:3 ethyl acetate:hexanes) to give **12'** as a white solid (8.41 g, 85 %). ^1H NMR (500 MHz; CDCl_3): δ 7.80-7.79 (m, 2H), 7.72-7.70 (m, 2H), 1.38-1.33 (m, 3H), 1.18-1.16 (m, 18H); ^{13}C NMR (125 MHz, CDCl_3): δ 164.1, 134.1, 129.1, 123.2, 17.6, 12.5; IR (thin film) 2943, 2868, 1789, 1732, 1460, 1378, 1245, 1188, 1132, 1078 cm^{-1} ; HRMS (ESI) m/z calcd. for $\text{C}_{17}\text{H}_{26}\text{NO}_3\text{Si}$ ($\text{M}+\text{H}$) $^+$ 320.1682, found 320.1680; mp 78 $^\circ\text{C}$.

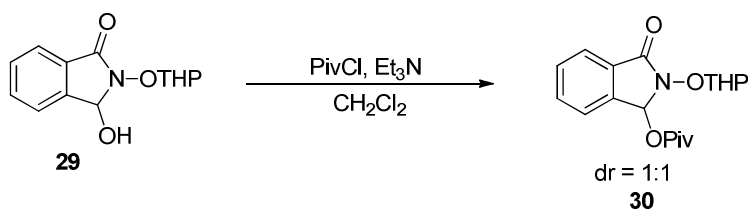


3-*t*-butyldimethylsilyloxy-*N*-hydroxyisoindolinone 13: To the 2-((*t*-butyldimethylsilyloxy)isoindoline-1,3-dione **12** (4.0 g, 14.42 mmol) in MeOH (30 ml) at 0 $^\circ\text{C}$ was added NaBH_4 (1.5 equiv, 0.818 g, 21.63 mmol). After the evolution of H_2 was complete, the reaction was warmed to room temperature and stirred for 4 h. The MeOH was removed *in vacuo* and the residue dissolved in EtOAc. Saturated NH_4Cl was added followed by extraction with EtOAc (3 x 20 ml). The organic layer was washed with water and brine, dried with MgSO_4 and concentrated under reduced pressure. The crude reaction mixture was purified by medium pressure chromatography on silica gel (1:1 ethyl acetate:hexanes) to give **13** as a white solid (3.30 g, 82 %). ^1H NMR (500 MHz; CDCl_3): δ 10.08 (bs, 1H), 7.68-7.67 (m, 1H), 7.58-7.54 (m, 1H), 7.46-7.43 (m, 2H), 5.97 (s, 1H), 1.00 (s, 9H), 0.34 (s, 3H), 0.30 (s, 3H); ^{13}C NMR (125 MHz, CDCl_3): δ 165.5, 141.9, 132.5, 129.5, 129.3, 123.2, 122.9, 83.2, 25.7, 18.2, -4.1, -4.8; IR (thin film) 3114, 2928,

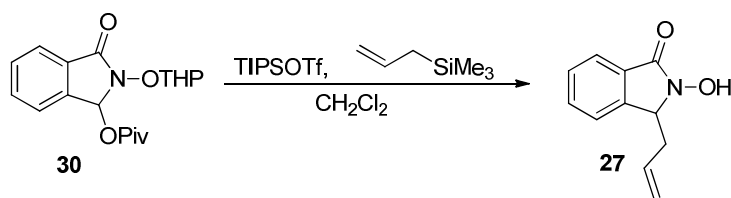
2886, 2858, 1701, 1616, 1505, 1467, 1398, 1356, 1255, 1158 cm^{-1} ; HRMS (ESI) m/z calcd. for $\text{C}_{14}\text{H}_{22}\text{NO}_3\text{Si}$ ($\text{M}+\text{H}$) $^+$ 280.1369, found 280.1371; mp 147 $^{\circ}\text{C}$.



3-triisopropylsilyloxy-N-hydroxyisoindolinone 13': To the 2-((triisopropylsilyloxy)isoindolinone-1,3-dione **12'** (4.0 g, 12.52 mmol) in MeOH (30 ml) at 0 $^{\circ}\text{C}$ was added NaBH_4 (1.5 equiv, 0.710 g, 18.78 mmol). After the evolution of H_2 was complete, the reaction was warmed to room temperature and stirred for 4 h. The MeOH was removed *in vacuo* and the residue dissolved in EtOAc. Saturated NH_4Cl was added followed by extraction with EtOAc (3 x 20 ml). The organic layer was washed with water and brine, dried with MgSO_4 and concentrated under reduced pressure. The crude reaction mixture was purified by medium pressure chromatography on silica gel (1:1 ethyl acetate:hexanes) to give **13'** as a white solid (3.05 g, 76 %). ^1H NMR (500 MHz; CDCl_3): δ 9.82 (bs, 1H), 7.69-7.67 (m, 1H), 7.57-7.55 (m, 1H), 7.51-7.50 (m, 1H), 7.47-7.44 (m, 1H), 6.26 (s, 1H), 1.37-1.33 (m, 3H), 1.20-1.18 (m, 18H); ^{13}C NMR (125 MHz, CDCl_3): δ 165.7, 142.2, 132.5, 129.4, 129.3, 123.2, 123.1, 83.4, 18.1, 18.0, 12.6; IR (thin film) 3089, 2934, 2864, 1685, 1660, 1499, 1460, 1341, 1233, 1163, 1126 cm^{-1} ; HRMS (ESI) m/z calcd. for $\text{C}_{17}\text{H}_{28}\text{NO}_3\text{Si}$ ($\text{M}+\text{H}$) $^+$ 322.1838, found 322.1841; mp 151 $^{\circ}\text{C}$.

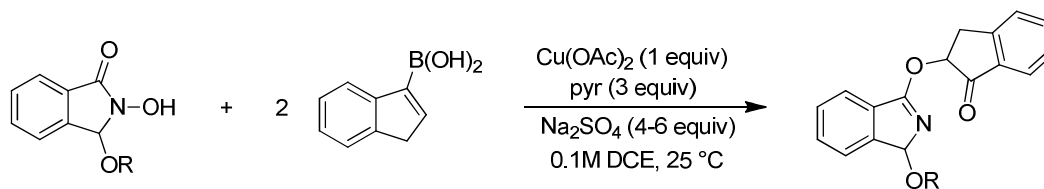


3-oxo-2-((tetrahydro-2H-pyran-2-yl)oxy)isoindolin-1-yl pivalate 30: The 3-hydroxy-2-((tetrahydro-2H-pyran-2-yl)oxy)isoindolin-1-one **29** (2.0 g, 8.02 mmol) was suspended in CH₂Cl₂ (20 ml) at 0 °C and Et₃N (2 equiv, 2.2 ml, 16.04 mmol) was added to the reaction mixture. This was followed by the dropwise addition of PivCl (1.3 equiv, 1.3 ml, 10.43 mmol). The reaction was then stirred at room temperature for 8 h. Saturated NH₄Cl was added to the reaction followed by extraction with CH₂Cl₂ (3 x 10 ml). The organic layer was washed with brine and dried with MgSO₄. The solvent was removed under reduced pressure and the residue purified by medium pressure chromatography on silica gel (1:4 ethyl acetate:hexanes) to give **30** as a white solid (1.89 g, 71 %) which is a 1:1 mixture of diastereomers. ¹H NMR first diastereomer (500 MHz; CDCl₃): δ 7.84-7.82 (m, 1H), 7.61-7.59 (m, 2H), 7.46-7.44 (m, 1H), 7.15 (s, 1H), 5.32-5.30 (m, 1H), 4.32-4.25 (m, 1H), 3.72-3.69 (m, 1H), 1.91-1.78 (m, 6H), 1.25 (s, 9H); ¹³C NMR first diastereomer (125 MHz, CDCl₃): δ 178.5, 166.2, 139.2, 133.2, 130.4, 129.7, 123.9, 123.7, 103.3, 82.2, 62.5, 39.1, 28.3, 26.9, 25.0, 18.3; ¹H NMR second diastereomer (500 MHz; CDCl₃): δ 7.84-7.82 (m, 1H), 7.57-7.53 (m, 2H), 7.41-7.40 (m, 1H), 7.15 (s, 1H), 5.25-5.23 (m, 1H), 4.32-4.25 (m, 1H), 3.63-3.60 (m, 1H), 1.64-1.54 (m, 6H), 1.24 (s, 9H); ¹³C NMR second diastereomer (125 MHz, CDCl₃): δ 178.5, 165.3, 139.2, 133.1, 130.3, 129.6, 123.8, 123.5, 102.4, 79.3, 62.1, 39.1, 28.1, 26.9, 25.0, 18.1; IR (thin film) 2965, 2868, 1720, 1482, 1391, 1366, 1277, 1201, 1123, 1081 cm⁻¹; HRMS (ESI) m/z calcd. for C₁₈H₂₄NO₅ (M+H)⁺ 334.1654, found 334.1646; mp 83 °C.

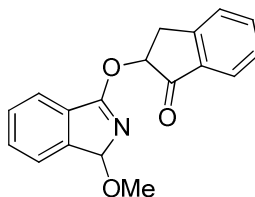


3-allyl-*N*-hydroxyisoindolinone 27: To the compound **30** (0.400 g, 1.19 mmol) in CH₂Cl₂ (7 ml) was added trimethylallylsilane (2 equiv, 0.38 ml, 2.39 mmol) followed by TIPSOTf (10 mol %, 0.03 ml, 0.119 mmol) and the reaction stirred at room temperature for 10 h. The solvent was removed under reduced pressure and the residue purified by medium pressure chromatography on silica gel (2:1 ethyl acetate:hexanes) to yield **27** as a pale pink oil (0.115 g, 51 %). The compound is unstable and used immediately for the next step. ¹H NMR (500 MHz; CDCl₃): δ 7.72-7.70 (m, 1H), 7.52-7.49 (m, 1H), 7.42-7.39 (m, 2H), 5.64-5.57 (m, 1H), 5.13 (d, *J* = 17.0 Hz, 1H), 5.00-4.97 (m, 1H), 4.77 (dd, *J* = 6.2, 3.7 Hz, 1H), 2.94-2.89 (m, 1H), 2.79-2.75 (m, 1H); ¹³C NMR (125 MHz, CDCl₃): δ 165.0, 145.7, 141.7, 131.5, 130.1, 128.4, 123.0, 122.5, 119.5, 61.9, 34.5; IR (thin film) 3076, 2911, 1717, 1616, 1568, 1464, 1373, 1312, 1227, 1180, 1148 cm⁻¹; HRMS (ESI) *m/z* calcd. for C₁₁H₁₂NO₂ (M+H)⁺ 190.0868, found 190.0861.

V. Copper-Promoted Etherification and Rearrangement of 3-substituted-*N*-hydroxyisoindolinones with Vinyl Boronic Acids (Table 2.2).

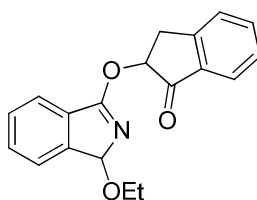


General procedure J: Copper-promoted etherification and rearrangement of 3-substituted-*N*-hydroxyisoindolinones with vinyl boronic acids. A scintillation vial was charged with the 3-substituted-*N*-hydroxyisoindolinones (1 equiv), vinyl boronic acid **1z** (2 equiv), Cu(OAc)₂ (1 equiv), and anhydrous Na₂SO₄ (4-6 equiv). These solids were then diluted with 1,2-dichloroethane to form a 0.1 M solution of *N*-hydroxyisoindolinone. Pyridine (3 equiv) was added to the resulting slurry via syringe. The scintillation vial was then capped with a septum pierced with a ventilation needle and the reaction mixture was stirred at 25 °C for 12 h. The reaction mixture was filtered through a plug of florisil[®] with EtOAc to remove the Cu(OAc)₂. The solvents were removed under reduced pressure and the crude reaction mixture was purified by flash chromatography on florisil[®] (1:4 - 1:2; ethyl acetate:hexanes) to give the α -oxygenated ketones.

**23z****dr = 92:8**

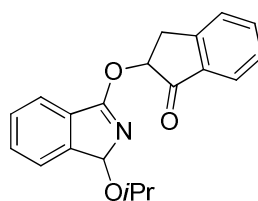
α -oxygenated ketone 23z: General procedure **J** with 3-methoxy-*N*-hydroxyisoindolinone **23** (0.060 g; 0.334 mmol), alkenyl boronic acid **1z** (0.107 g, 0.668 mmol), Cu(OAc)₂ (0.061 g, 0.334 mmol), Na₂SO₄ (0.224 g, 1.57 mmol), and pyridine (81 μ L, 1.00 mmol) afforded **23z** as a white solid (0.049 g, 50%) and a dr of 92:8 after purification using flash chromatography on florisil[®] (1:4; ethyl acetate: hexanes). ¹H NMR major diastereomer

(500 MHz; CDCl₃): δ 7.85-7.83 (m, 1H), 7.65-7.64 (m, 1H), 7.57-7.55 (m, 2H), 7.48-7.40 (m, 4H), 5.86 (s, 1H), 5.81 (dd, *J* = 7.2, 5.24 Hz, 1H), 3.87 (dd, *J* = 16.98, 7.23 Hz, 1H), 3.32-3.25 (m, 4H); ¹³C NMR major diastereomer (125 MHz, CDCl₃): δ 200.4, 169.4, 150.6, 149.0, 135.8, 134.8, 132.4, 130.2, 129.1, 128.1, 126.7, 124.5, 123.2, 121.0, 95.8, 77.6, 53.7, 33.6; ¹H NMR minor diastereomer (500 MHz; CDCl₃): δ 7.89-7.88 (m, 1H), 7.76-7.73 (m, 1H), 7.57-7.55 (m, 2H), 7.48-7.40 (m, 4H), 5.97 (s, 1H), 5.80 (m, 1H), 3.56 (dd, *J* = 16.2, 7.9 Hz, 1H), 3.14 (s, 3H), 3.00 (dd, *J* = 16.2, 4.6 Hz, 1H); ¹³C NMR minor diastereomer (125 MHz, CDCl₃): δ 200.4, 164.8, 163.1, 149.0, 135.8, 134.8, 132.4, 130.2, 129.1, 128.1, 126.7, 124.5, 123.2, 121.0, 95.8, 77.6, 53.7, 26.7; IR (thin film) 2965, 2930, 1736, 1625, 1603, 1570, 1459, 1395, 1333, 1274, 1189 cm⁻¹; HRMS (ESI) *m/z* calcd. for C₁₈H₁₆NO₃ (M+H)⁺ 294.1130, found 294.1127; decomposed at 101 °C.

**24z****dr = 92:8**

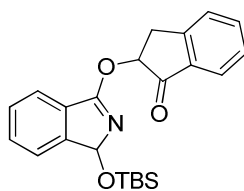
α -oxygenated ketone 24z: General procedure **J** with 3-ethoxy-*N*-hydroxyisoindolinone **24** (0.080 g; 0.410 mmol), alkenyl boronic acid **1z** (0.132 g, 0.820 mmol), Cu(OAc)₂ (0.074 g, 0.410 mmol), Na₂SO₄ (0.298 g, 2.09 mmol), and pyridine (100 μ L, 1.23 mmol) afforded **24z** as a white solid (0.067 g, 53%) and a dr of 92:8 after purification using flash chromatography on florisil[®] (1:4; ethyl acetate: hexanes). ¹H NMR major diastereomer (500 MHz; CDCl₃): δ 7.85-7.84 (m, 1H), 7.87-7.84 (m, 1H), 7.58-7.55 (m, 2H), 7.48-7.41

(m, 4H), 5.90 (s, 1H), 5.79 (dd, $J = 6.9, 5.3$ Hz, 1H), 3.87 (dd, $J = 17.0, 6.9$ Hz, 1H), 3.61 (m, 1H), 3.52 (m, 1H), 3.26 (dd, $J = 17.0, 5.3$ Hz, 1H), 1.21 (t, $J = 6.9$, 3H); ^{13}C NMR major diastereomer (125 MHz, CDCl_3): δ 200.5, 169.2, 150.6, 149.6, 135.8, 134.8, 132.3, 130.1, 129.0, 128.1, 126.7, 124.5, 123.2, 120.9, 95.1, 77.5, 62.0, 33.7, 15.4; ^1H NMR minor diastereomer (500 MHz; CDCl_3): δ 7.93-7.92 (m, 1H), 7.75-7.74 (m, 1H), 7.58-7.55 (m, 2H), 7.48-7.41 (m, 4H), 5.87 (s, 1H), 5.51-5.50 (m, 1H), 3.79-3.71 (m, 1H), 3.61-3.60 (m, 1H), 3.52-3.50 (m, 1H), 3.31-3.29 (m, 1H), 1.29 (t, $J = 6.9$ Hz, 3H); ^{13}C NMR minor diastereomer (125 MHz, CDCl_3): δ 200.5, 169.2, 150.6, 149.6, 134.3, 134.8, 132.3, 130.1, 129.0, 128.1, 126.7, 124.0, 123.5, 120.9, 95.1, 77.5, 62.0, 33.7, 15.4; IR (thin film) 2972, 2906, 2871, 1726, 1622, 1571, 1470, 1388, 1328, 1261, 1183 cm^{-1} ; HRMS (ESI) m/z calcd. for $\text{C}_{19}\text{H}_{18}\text{NO}_3\text{Si}$ ($\text{M}+\text{H}$) $^+$ 308.1287, found 308.1279; decomposed at 110 $^\circ\text{C}$.

**25z****dr = 97:3**

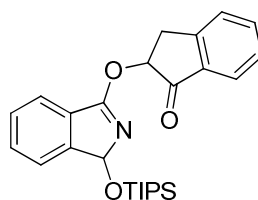
α -oxygenated ketone 25z: General procedure **J** with 3-isopropoxy-*N*-hydroxyisoindolinone **25** (0.080 g; 0.386 mmol), alkenyl boronic acid **1z** (0.123 g, 0.772 mmol), $\text{Cu}(\text{OAc})_2$ (0.070 g, 0.386 mmol), Na_2SO_4 (0.298 g, 2.09 mmol), and pyridine (93 μL , 1.158 mmol) afforded **25z** as a white solid (0.060 g, 48%) and a dr of 97:3 after purification using flash chromatography on florisil[®] (1:4; ethyl acetate: hexanes) as a

97:3 mixture of diastereomers. ^1H NMR major diastereomer (500 MHz; CDCl_3): δ 7.86-7.84 (m, 1H), 7.66-7.63 (m, 1H), 7.55-7.54 (m, 2H), 7.47-7.40 (m, 4H), 5.83 (s, 1H), 5.69 (dd, $J = 7.6, 4.7$ Hz, 1H), 3.91-3.90 (m, 1H), 3.83 (dd, $J = 16.4, 7.6$ Hz, 1H), 3.32 (dd, $J = 16.4, 4.7$ Hz, 1H), 1.26 (d, $J = 5.9$ Hz, 3H), 1.09 (d, $J = 6.0$ Hz, 3H); ^{13}C NMR major diastereomer (125 MHz, CDCl_3): δ 200.5, 168.7, 150.5, 135.6, 134.8, 132.2, 130.0, 128.8, 127.9, 126.6, 124.4, 124.0, 123.1, 120.8, 94.2, 77.6, 70.3, 33.5, 23.4, 22.7; ^1H NMR minor diastereomer (500 MHz; CDCl_3): δ 7.94-7.92 (m, 2H), 7.60-7.59 (m, 2H), 7.35-7.29 (m, 4H), 5.87 (s, 1H), 5.44-5.41 (m, 1H), 3.83 (dd, $J = 16.4, 7.6$ Hz, 1H), 3.70-3.63 (m, 1H), 3.05 (dd, $J = 16.4, 3.9$ Hz, 1H), 1.35 (d, $J = 5.0$ Hz, 3H), 1.09 (d, $J = 6.0$ Hz, 3H); ^{13}C NMR minor diastereomer (125 MHz, CDCl_3): δ 200.5, 168.7, 150.3, 135.0, 134.8, 132.2, 130.1, 128.8, 127.9, 126.6, 124.2, 124.0, 123.1, 120.8, 94.2, 77.6, 70.3, 33.9, 23.4, 22.7; IR (thin film) 2968, 2930, 2855, 1726, 1629, 1577, 1463, 1404, 1372, 1274, 1151 cm^{-1} ; HRMS (ESI) m/z calcd. for $\text{C}_{20}\text{H}_{20}\text{NO}_3$ ($\text{M}+\text{H}$) $^+$ 322.1443, found 322.1436; decomposed at 120 $^\circ\text{C}$.

**14z****dr = >95:5**

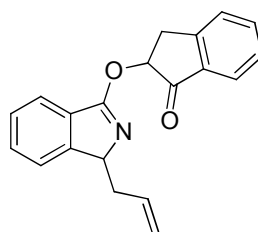
α -oxygenated ketone 14z: General procedure **J** with 3-*t*-butyldimethylsilyloxy-*N*-hydroxyisoindolinone **13** (0.100 g; 0.357 mmol), alkenyl boronic acid **1z** (0.114 g, 0.714 mmol), $\text{Cu}(\text{OAc})_2$ (0.065 g, 0.357 mmol), Na_2SO_4 (0.373 g, 2.62 mmol), and pyridine

(86.6 μL , 1.071 mmol) afforded **14z** as a white solid (0.086 g, 61%) and a single diastereomer after purification using flash chromatography (1:4; ethyl acetate: hexanes) on fluorisil. ^1H NMR (500 MHz; CDCl_3): δ 7.84-7.83 (m, 1H), 7.65-7.62 (m, 1H), 7.53-7.37 (m, 6H), 5.95 (s, 1H), 5.54-5.52 (m, 1H), 3.76 (dd, $J = 16.7, 7.8$ Hz, 1H), 3.43 (dd, $J = 16.7, 4.5$ Hz, 1H), 0.87 (s, 9H), 0.08 (s, 3H), -0.07 (s, 3H); ^{13}C NMR (125 MHz, CDCl_3): δ 200.5, 167.7, 152.6, 150.3, 135.6, 135.1, 131.6, 130.0, 128.5, 127.9, 126.7, 124.3, 122.7, 120.8, 90.7, 77.9, 33.1, 25.8, 18.1, -4.1, -4.6; IR (thin film) 2927, 2854, 1727, 1629, 1609, 1579, 1469, 1396, 1329, 1272, 1186 cm^{-1} ; HRMS (ESI) m/z calcd. for $\text{C}_{23}\text{H}_{28}\text{NO}_3\text{Si}$ ($\text{M}+\text{H}$) $^+$ 394.1838, found 394.1846; decomposed at 84-85 $^\circ\text{C}$.

**26z****dr = >95:5**

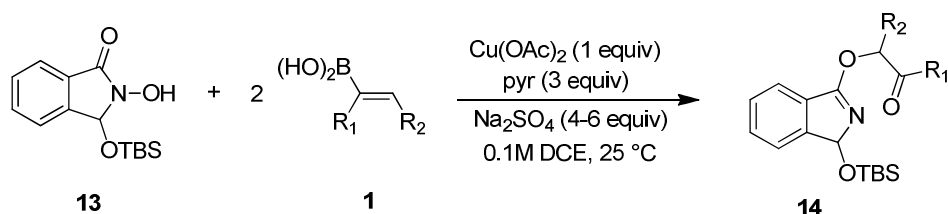
α -oxygenated ketone 26z: General procedure **J** with 3-isopropoxy-*N*-hydroxyisoindolinone **13'** (0.080 g; 0.248 mmol), alkenyl boronic acid **1z** (0.080 g, 0.497 mmol), $\text{Cu}(\text{OAc})_2$ (0.045 g, 0.248 mmol), Na_2SO_4 (0.299 g, 2.11 mmol), and pyridine (60 μL , 0.744 mmol) afforded **26z** as a white solid (0.069 g, 64%) as a single diastereomer after purification using flash chromatography on florisil[®] (1:3; ethyl acetate: hexanes). ^1H NMR (500 MHz; CDCl_3): δ 7.84-7.83 (m, 1H), 7.65-7.64 (m, 1H), 7.55-7.52 (m, 2H), 7.48-7.38 (m, 4H), 5.98 (s, 1H), 5.37 (dd, $J = 5.0, 5.0$ Hz, 1H), 3.70 (dd, $J = 10.0, 5.0$ Hz, 1H), 3.53 (dd, $J = 10.0, 5.0$ Hz, 1H) 1.05-0.97 (m, 21H); ^{13}C NMR (125 MHz, CDCl_3): δ

200.4, 167.0, 152.7, 150.2, 135.4, 135.2, 131.6, 129.8, 128.4, 127.7, 126.6, 124.3, 122.6, 120.6, 90.3, 78.1, 32.6, 17.8, 17.7, 12.1; IR (thin film) 2942, 2864, 1727, 1628, 1606, 1576, 1465, 1396, 1272, 1191 cm^{-1} ; HRMS (ESI) m/z calcd. for $\text{C}_{26}\text{H}_{34}\text{NO}_3$ ($\text{M}+\text{H}$)⁺ 436.2308, found 436.2306; decomposed at 114-115 $^{\circ}\text{C}$.

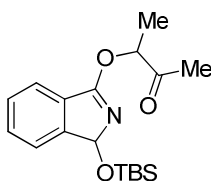
**27z****dr = >95:5**

α -oxygenated ketone 27z: General procedure **J** with 3-allyl-*N*-hydroxyisoindolinone **27** (0.055 g; 0.290 mmol), alkenyl boronic acid **1z** (0.093 g, 0.580 mmol), $\text{Cu}(\text{OAc})_2$ (0.053 g, 0.290 mmol), Na_2SO_4 (0.205 g, 1.44 mmol), and pyridine (70 μL , 0.870 mmol) afforded **27z** as an amorphous white solid (0.058 g, 66%) after purification using flash chromatography on florisil[®] (1:3; ethyl acetate: hexanes). ^1H NMR (500 MHz; CDCl_3): δ 7.86-7.84 (m, 1H), 7.67-7.64 (m, 1H), 7.60-7.59 (m, 1H), 7.50-7.35 (m, 5H), 5.81-5.72 (m, 2H), 5.07-5.01 (m, 2H), 4.75 (t, $J = 6.4$ Hz, 1H), 3.86 (dd, $J = 17.0, 7.7$ Hz, 1H), 3.23 (dd, $J = 17.0, 4.6$ Hz, 1H), 2.60-2.57 (m, 2H); ^{13}C NMR (125 MHz, CDCl_3): δ 201.0, 168.0, 153.7, 150.8, 135.7, 134.9, 134.4, 132.3, 129.1, 128.0, 127.3, 126.7, 124.5, 122.3, 120.9, 117.4, 68.3, 77.2, 37.6, 33.9; IR (thin film) 2953, 2934, 2855, 1774, 1714, 1600, 1571, 1467, 1381, 1290, 1188 cm^{-1} ; HRMS (ESI) m/z calcd. for $\text{C}_{20}\text{H}_{18}\text{NO}_2$ ($\text{M}+\text{H}$)⁺ 304.1338, found 304.1343.

IV. Copper-Promoted Etherification and Rearrangement of 3-*t*-butyldimethylsilyloxy-*N*-hydroxyisindolinones with Vinyl Boronic Acids (Tables 2.3 and 2.4).

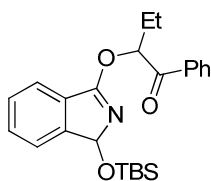


General procedure K: Copper-promoted etherification and rearrangement of 3-*t*-butyldimethylsilyloxy-*N*-hydroxyisindolinones with vinyl boronic acids. A scintillation vial was charged with 3-*t*-butyldimethylsilyloxy-*N*-hydroxyisindolinone **13** (1 equiv), vinyl boronic acid **1** (2 equiv), $\text{Cu}(\text{OAc})_2$ (1 equiv), and anhydrous Na_2SO_4 (4-6 equiv). These solids were then diluted with 1,2-dichloroethane to form a 0.1 M solution of *N*-hydroxyisindolinone. Pyridine (3 equiv) was added to the resulting slurry via syringe. The scintillation vial was then capped with a septum pierced with a ventilation needle and the reaction mixture was stirred at 25 °C for 8 h. The reaction mixture was filtered through a plug of florisil[®] with EtOAc to remove the $\text{Cu}(\text{OAc})_2$. The solvents were removed under reduced pressure and the crude reaction mixture was purified by flash chromatography on florisil[®] (1:4 - 1:2; ethyl acetate:hexanes) to give α -oxygenated ketones **14**.



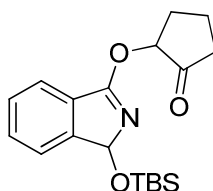
14a**dr = >95:5**

α -oxygenated ketone 14a: General procedure **K** with 3-*t*-butyldimethylsilyloxy-*N*-hydroxyisoindolinone **13** (0.140 g; 0.50 mmol), *Z*-2-buten-2-yl boronic acid **1a** (0.100 g, 1.00 mmol), Cu(OAc)₂ (0.091 g, 0.50 mmol), Na₂SO₄ (0.470 g, 3.30 mmol), and pyridine (120 μ l, 1.50 mmol) afforded **14a** as a colorless liquid (0.108 g, 65%) as a single diastereomer after purification using flash chromatography on florisil[®] (1:4; ethyl acetate: hexanes). ¹H NMR (500 MHz; CDCl₃): δ 7.54-7.44 (m, 2H), 7.43-7.39 (m, 2H), 5.96 (s, 1H), 5.35 (q, *J* = 5.0 Hz, 1H), 2.24 (s, 3H), 1.54 (d, *J* = 5.0 Hz, 3H), 0.93 (s, 9H), 0.18 (s, 3H), 0.02 (s, 3H); ¹³C NMR (125 MHz, CDCl₃): δ 207.2, 168.3, 152.6, 131.6, 130.1, 128.6, 122.8, 120.5, 90.9, 78.5, 25.7, 25.4, 18.1, 16.6, -4.0, -4.6; IR (thin film) 2956, 2928, 2858, 1729, 1625, 1581, 1470, 1401, 1255, 1192, 1116 cm⁻¹; HRMS (ESI) *m/z* calcd. for C₁₈H₂₈NO₃Si (M+H)⁺ 334.1838, found 334.1844.

**14h****dr = >95:5**

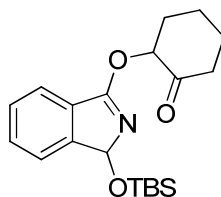
α -oxygenated ketone 14h: General procedure **K** with 3-*t*-butyldimethylsilyloxy-*N*-hydroxyisoindolinone **13** (0.087 g; 0.312 mmol), *Z*-1-phenyl-1-buten-1-yl boronic acid **1h** (0.110 g, 0.624 mmol), Cu(OAc)₂ (0.057 g, 0.312 mmol), Na₂SO₄ (0.320 g, 2.25 mmol), and pyridine (90 μ L, 0.936 mmol) afforded **14h** as a white solid (0.075 g, 59%)

as a single diastereomer after purification using flash chromatography (1:4; ethyl acetate: hexanes) on florisil[®]. ¹H NMR (500 MHz; CDCl₃): δ 8.07-8.05 (m, 2H), 7.60-7.57 (m, 2H), 7.49-7.40 (m, 5H), 6.17 (t, *J* = 5.0 Hz, 1H), 5.94 (s, 1H), 2.09-2.04 (m, 2H), 1.14 (t, *J* = 5.0 Hz, 3H), 0.80 (s, 9H), -0.06 (s, 3H), -0.26 (s, 3H); ¹³C NMR (125 MHz, CDCl₃): δ 196.9, 168.5, 152.6, 135.4, 133.2, 131.7, 129.9, 128.6, 128.5, 128.4, 122.7, 120.7, 91.1, 79.5, 25.7, 25.4, 18.0, 10.1, -4.3, -4.7; IR (thin film) 2928, 2855, 1699, 1627, 1598, 1576, 1471, 1403, 1218, 1117, 1027 cm⁻¹; HRMS (ESI) *m/z* calcd. for C₂₄H₃₂NO₃Si (M+H)⁺ 410.2151, found 410.2157; decomposed at 68 °C.

**14m****dr = 80:20**

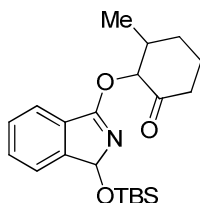
α -oxygenated Ketone 14m: General procedure **K** with 3-*t*-butyldimethylsilyloxy-*N*-hydroxyisoindolinone **13** (0.175 g; 0.625 mmol), 1-cyclopentenyl boronic acid **1m** (0.140 g, 1.25 mmol), Cu(OAc)₂ (0.114 g, 0.625 mmol), Na₂SO₄ (0.650 g, 4.57 mmol), and pyridine (150 μ L, 1.87 mmol) afforded **14m** as a colorless liquid (0.138 g, 64%) in an 80:20 ratio of diastereomers after purification using flash chromatography on florisil[®] (1:3; ethyl acetate: hexanes). ¹H NMR major diastereomer (500 MHz; CDCl₃): δ 7.51-7.48 (m, 2H), 7.41-7.35 (m, 2H), 6.00 (s, 1H), 5.32 (t, *J* = 5.0 Hz, 1H), 2.65-2.60 (m, 1H), 2.41-2.38 (m, 2H), 2.18-2.13 (m, 2H), 1.93-1.88 (m, 1H), 0.94 (s, 9H), 0.19 (s, 3H), 0.01 (s, 3H); ¹³C NMR major diastereomer (125 MHz, CDCl₃): δ 212.3, 168.0, 152.4, 131.7,

129.9, 128.5, 122.7, 120.7, 90.8, 79.2, 35.2, 28.2, 25.8, 18.1, 17.1, -3.8, -4.2; ^1H NMR minor diastereomer (500 MHz; CDCl_3): δ 7.43-7.35 (m, 4H), 6.00 (s, 1H), 5.32 (t, $J = 5.0$ Hz, 1H), 2.65-2.60 (m, 1H), 2.41-2.38 (m, 2H), 2.18-2.13 (m, 2H), 1.93-1.88 (m, 1H), 0.91 (s, 9H), 0.19 (s, 3H), 0.09 (s, 3H); ^{13}C NMR minor diastereomer (125 MHz, CDCl_3): δ 212.3, 168.0, 152.4, 131.7, 129.9, 128.5, 122.7, 120.7, 90.8, 79.2, 35.2, 28.2, 25.7, 18.1, 17.1, -3.8, -4.2; IR (thin film) 2929, 2856, 1706, 1576, 1470, 1401, 1361, 1255, 1099, 1072 cm^{-1} ; HRMS (ESI) m/z calcd. for $\text{C}_{19}\text{H}_{28}\text{NO}_3\text{Si}$ ($\text{M}+\text{H}$) $^+$ 346.1828, found 346.1842.

**14n****dr = 89:11**

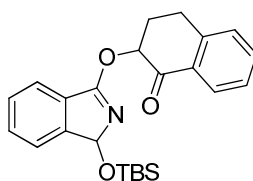
α -oxygenated ketone 14n: General procedure **K** with 3-*t*-butyldimethylsilyloxy-*N*-hydroxyisoindolinone **13** (0.133 g; 0.476 mmol), 1-cyclohexenyl boronic acid **1n** (0.120 g, 0.950 mmol), $\text{Cu}(\text{OAc})_2$ (0.086 g, 0.476 mmol), Na_2SO_4 (0.500 g, 3.52 mmol), and pyridine (110 μL , 1.428 mmol) afforded **14n** as a white solid (0.121 g, 71%) in an 89:11 ratio of diastereomers after purification using flash chromatography on florisil[®] (1:3; ethyl acetate: hexanes). ^1H NMR major diastereomer (500 MHz; CDCl_3): δ 7.56-7.50 (m, 2H), 7.41-7.37 (m, 2H), 5.97 (s, 1H), 5.58 (dd, $J = 11.7, 5.9$ Hz, 1H), 2.56-2.44 (m, 2H), 2.12-1.94 (m, 4H), 1.87-1.65 (m, 2H), 0.90 (s, 9H), 0.09 (s, 3H), -0.01 (s, 3H); ^{13}C NMR major diastereomer (125 MHz, CDCl_3): δ 204.7, 168.2, 152.6, 131.8, 129.9, 128.4, 122.7, 120.8, 91.1, 79.9, 40.7, 33.7, 27.5, 25.8, 23.8, 18.1, -3.9, -4.1; ^1H NMR minor

diastereomer (500 MHz; CDCl₃): δ 7.66-7.48 (m, 4H), 6.10 (s, 1H), 5.58 (dd, J = 11.7, 5.9 Hz, 1H), 2.45-2.41 (m, 2H), 2.03-1.82 (m, 4H), 1.68-1.51 (m, 2H), 0.91 (s, 9H), 0.15 (s, 3H), 0.02 (s, 3H); ¹³C NMR minor diastereomer (125 MHz, CDCl₃): δ 204.7, 169.5, 152.6, 132.5, 129.9, 128.4, 123.5, 120.8, 91.1, 79.2, 40.7, 33.7, 27.5, 25.8, 23.8, 18.1, -3.9, -4.1; IR (thin film) 2929, 2857, 1731, 1626, 1575, 1471, 1361, 1328, 1288, 1120, 1025 cm⁻¹; HRMS (ESI) m/z calcd. for C₂₀H₃₀NO₃Si (M+H)⁺ 360.1995, found 360.1988; decomposed at 91 °C.

**14p****dr = 69:31**

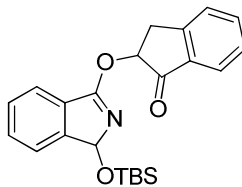
α -oxygenated ketone 14p: General procedure **K** with 3-*t*-butyldimethylsilyloxy-*N*-hydroxyisoindolinone **13** (0.100 g; 0.357 mmol), alkenyl boronic acid **1p** (0.100 g, 0.714 mmol), Cu(OAc)₂ (0.065 g, 0.714 mmol), Na₂SO₄ (0.373 g, 2.62 mmol), and pyridine (90 μ L, 1.07 mmol) afforded **14p** as a semi-solid (0.085 g, 64%) as a 69:31 mixture of diastereomers after purification using flash chromatography (1:4; ethyl acetate: hexanes) on florisil[®]. ¹H NMR major diastereomer (500 MHz; CDCl₃): δ 7.54-7.51 (m, 2H), 7.43-7.41 (m, 2H), 5.98 (s, 1H), 5.27 (d, J = 10.0 Hz, 1H), 2.54-2.47 (m, 3H), 2.09-1.95 (m, 4H), 1.18 (d, J = 5.0 Hz, 3H), 0.89 (s, 9H), 0.05 (s, 3H), -0.16 (s, 3H); ¹³C NMR major diastereomer (125 MHz, CDCl₃): δ 204.2, 168.6, 152.7, 133.0, 129.9, 128.4, 122.8, 120.7, 91.2, 85.0, 40.4, 40.0, 32.8, 26.0, 25.8, 25.6, 18.8, -3.9, -4.0; ¹H NMR minor

diastereomer (500 MHz; CDCl₃): δ 7.58-7.57 (m, 2H), 7.41-7.38 (m, 2H), 6.01 (s, 1H), 5.54 (d, J = 10.0 Hz, 1H), 2.20-2.07 (m, 4H), 1.72-1.62 (m, 3H), 1.10 (d, J = 5.0 Hz, 3H), 0.90 (s, 9H), 0.10 (s, 3H), -0.11 (s, 3H); ¹³C NMR minor diastereomer (125 MHz, CDCl₃): δ 205.6, 168.2, 152.7, 133.0, 129.9, 129.7, 123.8, 123.1, 82.9, 82.2, 37.4, 31.1, 29.8, 25.8, 23.2, 18.0, 13.6, -3.9, -4.0; IR (thin film) 2928, 2855, 1733, 1626, 1471, 1319, 1249, 1194, 1121, 1046 cm⁻¹; HRMS (ESI) m/z calcd. for C₂₁H₃₂NO₃Si (M+H)⁺ 374.2151, found 374.2153.

**14v****dr = >95:5**

α -oxygenated ketone 14v: General procedure **K** with 3-*t*-butyldimethylsilyloxy-*N*-hydroxyisoindolinone **13** (0.080 g; 0.287 mmol), alkenyl boronic acid **1v** (0.100 g, 0.574 mmol), Cu(OAc)₂ (0.052 g, 0.287 mmol), Na₂SO₄ (0.300 g, 2.11 mmol), and pyridine (70.0 μ L, 0.861 mmol) afforded **14v** as a white solid (0.077 g, 66%) and a single diastereomer after purification using flash chromatography (1:4; ethyl acetate: hexanes) on fluorisil. ¹H NMR (500 MHz; CDCl₃): δ 8.08-8.06 (m, 1H), 7.61-7.60 (m, 1H), 7.55-7.51 (m, 2H), 7.46-7.39 (m, 2H), 7.37-7.34 (m, 1H), 7.30-7.29 (m, 1H), 6.07 (s, 1H), 5.94 (dd, J = 13.1, 4.7 Hz, 1H), 3.32-3.26 (m, 1H), 3.16-3.13 (m, 1H), 2.68-2.64 (m, 1H), 2.50-2.42 (m, 1H), 0.92 (s, 9H), 0.14(s, 3H), -0.05 (s, 3H); ¹³C NMR (125 MHz, CDCl₃): δ 192.9, 168.4, 152.7, 143.1, 133.7, 132.1, 131.9, 129.9, 128.6, 128.5, 127.8, 126.9, 122.7, 120.9, 91.1, 78.1, 29.4, 28.0, 25.9, 18.1, -3.8, -4.1; IR (thin film) 2952, 2928, 2854, 1704,

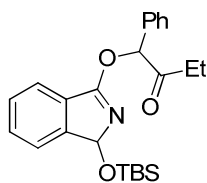
1626, 1603, 1575, 1471, 1460, 1327, 1249 cm^{-1} ; HRMS (ESI) m/z calcd. for $\text{C}_{24}\text{H}_{30}\text{NO}_3\text{Si}$ ($\text{M}+\text{H}$)⁺ 408.1995, found 408.1985; decomposed at 128 °C.



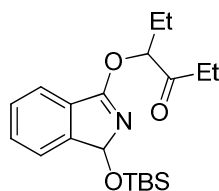
14z

dr = >95:5

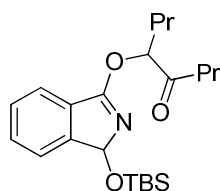
α -oxygenated ketone 14z: General procedure **K** with 3-*t*-butyldimethylsilyloxy-*N*-hydroxyisoindolinone **13** (0.150 g; 0.536 mmol), alkenyl boronic acid **1z** (0.172 g, 1.07 mmol), $\text{Cu}(\text{OAc})_2$ (0.097 g, 0.536 mmol), Na_2SO_4 (0.500 g, 3.52 mmol), and pyridine (130 μL , 1.61 mmol) afforded **14z** as a white solid (0.128 g, 61%) and a single diastereomer after purification using flash chromatography (1:4; ethyl acetate: hexanes) on fluorisil. ^1H NMR (500 MHz; CDCl_3): δ 7.84-7.83 (m, 1H), 7.65-7.62 (m, 1H), 7.53-7.37 (m, 6H), 5.95 (s, 1H), 5.54-5.52 (m, 1H), 3.76 (dd, $J = 16.7, 7.8$ Hz, 1H), 3.43 (dd, $J = 16.7, 4.5$ Hz, 1H), 0.87 (s, 9H), 0.08 (s, 3H), -0.07 (s, 3H); ^{13}C NMR (125 MHz, CDCl_3): δ 200.5, 167.7, 152.6, 150.3, 135.6, 135.1, 131.6, 130.0, 128.5, 127.9, 126.7, 124.3, 122.7, 120.8, 90.7, 77.9, 33.1, 25.8, 18.1, -4.1, -4.6; IR (thin film) 2927, 2854, 1727, 1629, 1609, 1579, 1469, 1396, 1329, 1272, 1186 cm^{-1} ; HRMS (ESI) m/z calcd. for $\text{C}_{23}\text{H}_{28}\text{NO}_3\text{Si}$ ($\text{M}+\text{H}$)⁺ 394.1838, found 394.1846; decomposed at 84-85 °C.

**14aa****dr = >95:5**

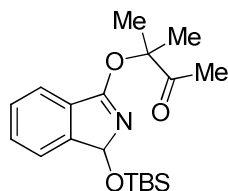
α -oxygenated ketone 14aa: General procedure **K** with 3-*t*-butyldimethylsilyloxy-*N*-hydroxyisoindolinone **13** (0.060 g; 0.214 mmol), alkenyl boronic acid **1aa** (0.076 g, 0.429 mmol), Cu(OAc)₂ (0.039 g, 0.214 mmol), Na₂SO₄ (0.224 g, 1.57 mmol), and pyridine (50 μ L, 0.642 mmol) afforded **14aa** as a white solid (0.053 g, 61%) and a single diastereomer after purification using flash chromatography (1:4; ethyl acetate: hexanes) on fluorisil. ¹H NMR (500 MHz; CDCl₃): δ 7.60-7.51 (m, 4H), 7.44-7.39 (m, 5H), 6.30 (s, 1H), 5.98 (s, 1H), 2.70-2.62 (m, 1H), 2.63-2.53 (m, 1H), 1.00 (t, $J = 7.2$ Hz, 3H), 0.95 (s, 9H), 0.19 (s, 3H), 0.02 (s, 3H); ¹³C NMR (125 MHz, CDCl₃): δ 205.6, 168.3, 152.6, 134.4, 131.5, 130.1, 128.9, 128.8, 128.5, 127.7, 122.8, 120.7, 91.1, 83.5, 31.5, 25.9, 18.1, 7.1, -4.0, -4.5; IR (thin film) 2930, 2858, 1729, 1625, 1570, 1469, 1388, 1326, 1258, 1193, 1125 cm⁻¹; HRMS (ESI) m/z calcd. for C₂₄H₃₂NO₃Si (M+H)⁺ 410.2151, found 410.2144; decomposed at 80 °C.

**14ab****dr = 80:20**

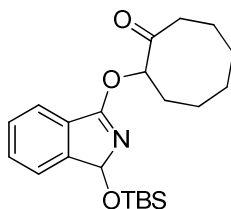
α -oxygenated ketone 14ab: General procedure **K** with 3-*t*-butyldimethylsilyloxy-*N*-hydroxyisoindolinone **13** (0.105 g; 0.375 mmol), alkenyl boronic acid **1ab** (0.096 g, 0.750 mmol), Cu(OAc)₂ (0.068 g, 0.375 mmol), Na₂SO₄ (0.333 g, 2.34 mmol), and pyridine (90 μ L, 1.125 mmol) afforded **14ab** as a colorless liquid (0.083 g, 61%) and an 80:20 ratio of diastereomers after purification using flash chromatography (1:4; ethyl acetate: hexanes) on fluorisil. ¹H NMR major diastereomer (500 MHz; CDCl₃): δ 7.52-7.47 (m, 2H), 7.39-7.34 (m, 2H), 5.93 (s, 1H), 5.23 (dd, $J = 13.9, 8.1$ Hz, 1H), 2.68-2.59 (m, 1H), 2.57-2.45 (m, 1H), 1.92-1.88 (m, 2H), 1.06-1.01 (m, 6H), 0.91 (s, 9H), 0.16 (s, 3H), -0.01 (s, 3H); ¹³C NMR major diastereomer (125 MHz, CDCl₃): δ 209.0, 168.7, 152.5, 131.7, 130.0, 128.5, 122.7, 120.4, 90.9, 83.1, 31.5, 25.8, 24.8, 18.1, 9.7, 6.9, -4.0, -4.6; ¹H NMR minor diastereomer (500 MHz; CDCl₃): δ 7.52-7.47 (m, 2H), 7.39-7.34 (m, 2H), 5.92 (s, 1H), 5.38 (q, $J = 6.9$ Hz, 1H), 2.68-2.59 (m, 1H), 2.57-2.45 (m, 1H), 1.64-1.57 (m, 1H), 1.53-1.50 (m, 1H), 1.21 (t, $J = 7.1$ Hz, 3H), 1.06-1.03 (m, 3H), 0.93 (s, 9H), 0.19 (s, 3H), 0.07 (s, 3H); ¹³C NMR minor diastereomer (125 MHz, CDCl₃): δ 209.0, 168.7, 152.5, 131.7, 130.0, 128.5, 122.7, 120.4, 90.8, 82.9, 32.1, 25.9, 24.6, 18.2, 9.7, 7.2, -3.9, -4.5; IR (thin film) 2934, 2858, 1726, 1625, 1571, 1464, 1391, 1319, 1249, 1192, 1072 cm⁻¹; HRMS (ESI) m/z calcd. for C₂₀H₃₂NO₃Si (M+H)⁺ 362.2151, found 362.2138.

**14ac****dr = 80:20**

α -oxygenated ketone 14ac: General procedure **K** with 3-*t*-butyldimethylsilyloxy-*N*-hydroxyisoindolinone **13** (0.100 g; 0.357 mmol), alkenyl boronic acid **1ac** (0.111 g, 0.714 mmol), Cu(OAc)₂ (0.065 g, 0.357 mmol), Na₂SO₄ (0.373 g, 2.62 mmol), and pyridine (86.6 μ L, 1.071 mmol) afforded **14ac** as a clear oil (0.100 g, 72%) in a 80:20 ratio of diastereomers after purification using flash chromatography (1:4; ethyl acetate: hexanes) on fluorisil. ¹H NMR major diastereomer (500 MHz; CDCl₃): δ 7.56-7.51 (m, 2H), 7.44-7.40 (m, 2H), 5.96 (s, 1H), 5.28 (dd, $J = 8.5, 4.3$ Hz, 1H), 2.65-2.58 (m, 1H), 2.53-2.46 (m, 1H), 1.95-1.80 (m, 2H), 1.67-1.50 (m, 4H), 1.00 (t, $J = 7.5$ Hz, 3H), 0.93 (s, 9H), 0.89 (t, $J = 7.5$ Hz, 3H), 0.18 (s, 3H), 0.01 (s, 3H); ¹³C NMR major diastereomer (125 MHz, CDCl₃): δ 208.8, 168.6, 152.5, 131.8, 130.0, 128.5, 122.8, 120.5, 90.9, 82.0, 40.2, 33.3, 25.8, 18.8, 18.7, 16.3, 13.8, 13.7, -4.0, -4.6; ¹H NMR minor diastereomer (500 MHz; CDCl₃): δ 7.56-7.51 (m, 2H), 7.44-7.40 (m, 2H), 5.94 (s, 1H), 5.23 (dd, $J = 7.2, 5.2$ Hz, 1H), 2.65-2.58 (m, 1H), 2.53-2.46 (m, 1H), 1.97-1.89 (m, 2H), 1.54-1.48 (m, 2H), 1.33-1.36 (m, 2H), 1.07 (t, $J = 7.6$ Hz, 3H), 0.96 (t, $J = 7.6$ Hz, 3H), 0.93 (s, 9H), 0.21 (s, 3H), 0.09 (s, 3H); ¹³C NMR minor diastereomer (125 MHz, CDCl₃): δ 208.8, 168.6, 152.5, 131.8, 129.9, 128.5, 122.7, 120.5, 90.6, 81.7, 40.6, 38.1, 25.9, 18.3, 18.1, 16.6, 13.9, 13.7, -3.8, -4.5; IR (thin film) 2960, 2934, 2855, 1736, 1628, 1574, 1398, 1375, 1242, 1198, 1123 cm⁻¹; HRMS (ESI) m/z calcd. for C₂₂H₃₆NO₃Si (M+H)⁺ 390.2464, found 390.2465.

**14ad**

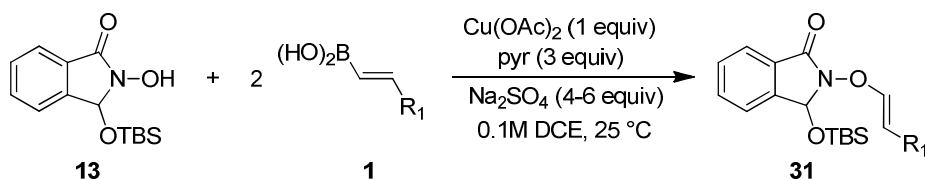
α -oxygenated ketone 14ad: General procedure **K** with 3-*t*-butyldimethylsilyloxy-*N*-hydroxyisoindolinone **13** (0.049 g; 0.175 mmol), alkenyl boronic acid **1ad** (0.040 g, 0.350 mmol), Cu(OAc)₂ (0.032 g, 0.175 mmol), Na₂SO₄ (0.183 g, 1.29 mmol), and pyridine (40 μ L, 0.525 mmol) afforded **14ad** as a colorless liquid (0.038 g, 68 %) after purification using flash chromatography on florisil[®] (1:3; ethyl acetate: hexanes). ¹H NMR (500 MHz; CDCl₃): δ 7.51-7.39 (m, 4H), 5.94 (s, 1H), 2.18 (s, 3H), 1.68 (s, 3H), 1.67 (s, 3H), 0.94 (s, 9H), 0.22 (s, 3H), 0.10 (s, 3H); ¹³C NMR (125 MHz, CDCl₃): δ 207.7, 166.7, 152.2, 132.4, 129.9, 128.5, 122.6, 120.5, 90.8, 85.9, 25.9, 24.1, 23.6, 23.4, 18.2, -4.1, -5.0; IR (thin film) 2953, 2926, 2884, 2854, 1719, 1626, 1605, 1578, 1470, 1390, 1255, 1194 cm⁻¹; HRMS (ESI) *m/z* calcd. for C₁₉H₃₀NO₃Si (M+H)⁺ 348.1995, found 348.1994.

**14ae****dr = >95:5**

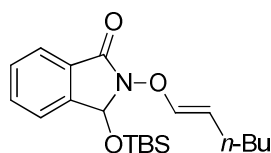
α -oxygenated ketone 14ae: General procedure **K** with 3-*t*-butyldimethylsilyloxy-*N*-hydroxyisoindolinone **13** (0.127 g; 0.454 mmol), alkenyl boronic acid **1ae** (0.140 g, 0.909 mmol), Cu(OAc)₂ (0.082 g, 0.454 mmol), Na₂SO₄ (0.470 g, 3.30 mmol), and pyridine (110 μ L, 1.362 mmol) afforded **14ae** as a colorless liquid (0.101 g, 57%) and a single diastereomer after purification using flash chromatography (1:4; ethyl acetate: hexanes) on florisil[®]. ¹H NMR (500 MHz; CDCl₃): δ 7.56-7.54 (m, 1H), 7.50-7.48 (m, 1H), 7.43-

7.37 (m, 2H), 5.95 (s, 1H), 5.48 (dd, $J = 8.5, 3.8$ Hz, 1H), 2.74-2.69 (m, 1H), 2.52-2.39 (m, 1H), 2.25-2.19 (m, 1H), 2.15-2.08 (m, 1H), 2.02-2.01 (m, 2H), 1.87-1.83 (m, 1H), 1.61-1.53 (m, 4H), 1.45-1.37 (m, 1H), 0.92 (s, 9H), 0.14 (s, 3H), -0.05 (s, 3H); ^{13}C NMR (125 MHz, CDCl_3): δ 212.7, 168.3, 152.5, 131.7, 129.9, 128.5, 122.7, 120.7, 91.0, 80.3, 41.2, 33.3, 28.1, 25.9, 25.8, 24.9, 23.2, 21.4, -4.0, -4.4; IR (thin film) 2933, 2852, 1724, 1622, 1573, 1466, 1395, 1326, 1241, 1186, 1125 cm^{-1} ; HRMS (ESI) m/z calcd. for $\text{C}_{22}\text{H}_{34}\text{NO}_3\text{Si}$ ($\text{M}+\text{H}$) $^+$ 388.2308, found 388.2300.

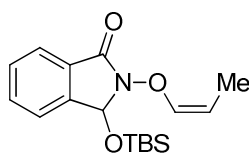
II. Copper-Promoted Etherification of 3-*t*-butyldimethylsilyloxy-*N*-hydroxyisoindolinones with Monosubstituted Vinyl Boronic Acids (Table 2.5).



General procedure L: A scintillation vial was charged with 3-*t*-butyldimethylsilyloxy-*N*-hydroxyisoindolinone **13** (1 equiv), vinyl boronic acid **1** (2 equiv), $\text{Cu}(\text{OAc})_2$ (1 equiv), and anhydrous Na_2SO_4 (4-6 equiv). These solids were then diluted with 1,2-dichloroethane to form a 0.1 M solution of 3-*t*-butyldimethylsilyloxy-*N*-hydroxyisoindolinone. Pyridine (3 equiv) was added to the resulting slurry via syringe. The scintillation vial was then capped with a septum pierced with a ventilation needle and the reaction mixture was stirred at 25 °C for 12 h. 1,2-Dichloroethane and pyridine were removed under reduced pressure and the crude reaction mixture was purified by medium pressure chromatography (1:19 - 1:2; ethyl acetate:hexanes) to give *N*-enoxyisoindolinones **31**.

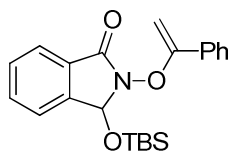
**31d**

***N*-enoxyisoindolinone 31d:** General procedure **L** with 3-*t*-butyldimethylsilyloxy-*N*-hydroxyisoindolinone **13** (0.164 g; 0.586 mmol), *E*-1-hexen-1-yl boronic acid **1d** (0.150 g, 1.17 mmol), Cu(OAc)₂ (0.106 g, 0.586 mmol), Na₂SO₄ (0.507 g, 3.56 mmol), and pyridine (143 μl, 1.76 mmol) afforded **31d** as a colorless liquid (0.174 g, 82%) after purification using flash chromatography on silica gel (1:4; ethyl acetate: hexanes). ¹H NMR (500 MHz; CDCl₃): δ 7.79 (d, *J* = 7.4 Hz, 1H), 7.61 (dd, *J* = 7.6, 7.4 Hz, 1H), 7.49 (t, *J* = 7.4 Hz, 1H), 7.44 (d, *J* = 7.6 Hz, 1H), 6.45 (d, *J* = 12.3 Hz, 1H), 5.98 (s, 1H), 5.26 (td, *J* = 12.3, 7.4 Hz, 1H), 1.96-1.92 (m, 2H), 1.33-1.29 (m, 4H), 0.95 (s, 9H), 0.86 (t, *J* = 6.9 Hz, 3H), 0.27 (s, 3H), 0.20 (s, 3H); ¹³C NMR (125 MHz, CDCl₃): δ 165.1, 147.1, 142.1, 133.2, 129.8, 128.7, 123.8, 123.1, 107.4, 82.5, 32.0, 26.5, 25.6, 22.1, 18.0, 13.8, -4.3, -4.5; IR (thin film) 2955, 2928, 2857, 1740, 1667, 1466, 1361, 1252, 1203, 1117 cm⁻¹; HRMS (ESI) *m/z* calcd. for C₂₀H₃₂NO₃Si (M+H)⁺ 362.2151, found 362.2142.

**31af**

***N*-enoxyisoindolinone 31af:** General procedure **L** with 3-*t*-butyldimethylsilyloxy-*N*-hydroxyisoindolinone **13** (0.078 g; 0.277 mmol), *Z*-1-propen-1-yl boronic acid **1af**

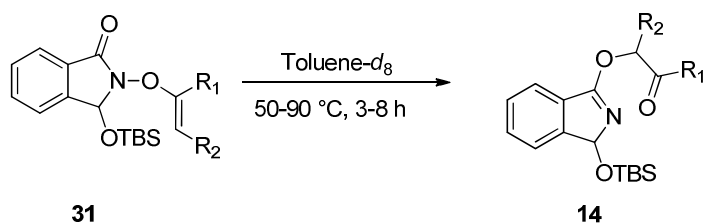
(0.048 g, 0.555 mmol), Cu(OAc)₂ (0.050 g, 0.277 mmol), Na₂SO₄ (0.290 g, 2.04 mmol), and pyridine (70 μ l, 0.831 mmol) afforded **31af** as a white solid (0.061 g, 69%) after purification using flash chromatography on silica gel (1:4; ethyl acetate: hexanes). ¹H NMR (500 MHz; CDCl₃): δ 7.81 (d, J = 7.5 Hz, 1H), 7.63 (t, J = 7.5 Hz, 1H), 7.52 (t, J = 7.5 Hz, 1H), 7.46 (d, J = 7.5 Hz, 1H), 6.39 (dd, J = 6.9, 1.4 Hz, 1H), 6.01 (s, 1H), 4.60 (p, J = 6.9 Hz, 1H), 1.71 (dd, J = 6.9, 1.4 Hz, 3H), 0.97 (s, 9H), 0.29 (s, 3H), 0.22 (s, 3H); ¹³C NMR (125 MHz, CDCl₃): δ 165.3, 148.7, 142.0, 133.3, 129.8, 128.7, 123.8, 123.1, 101.9, 82.8, 25.6, 18.1, 9.3, -4.5, -4.5; IR (thin film) 2928, 2857, 1738, 1669, 1617, 1470, 1353, 1252, 1116, 1071 cm⁻¹; HRMS (ESI) m/z calcd. for C₁₇H₂₆NO₃Si (M+H)⁺ 320.1682, found 320.1683; mp 50 °C.

**31g**

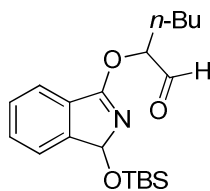
***N*-enoxisoindolinone 31g:** General procedure **L** with 3-*t*-butyldimethylsilyloxy-*N*-hydroxyisoindolinone **13** (0.060 g; 0.214 mmol), 1-phenylvinyl boronic acid **1g** (0.064 g, 0.429 mmol), Cu(OAc)₂ (0.039 g, 0.214 mmol), Na₂SO₄ (0.224 g, 1.58 mmol), and pyridine (50 μ l, 0.642 mmol) afforded **31g** as a colorless liquid (0.078 g, 96%) after purification using flash chromatography on silica gel (1:4; ethyl acetate: hexanes). ¹H NMR (500 MHz; CDCl₃): δ 7.97-7.95 (m, 1H), 7.87-7.86 (m, 1H), 7.72-7.65 (m, 3H), 7.57-7.37 (m, 4H), 6.17 (s, 1H), 4.88-4.86 (m, 2H), 0.95 (s, 9H), 0.25 (s, 3H), 0.12 (s, 3H); ¹³C NMR (125 MHz, CDCl₃): δ 165.0, 159.8, 142.5, 133.3, 133.2, 129.9, 129.0, 128.8, 128.6, 128.2, 125.9, 123.9, 123.3, 82.8, 25.6, 18.0, -4.4, -4.5; IR (thin film) 2955,

2928, 2857, 1739, 1667, 1467, 1360, 1315, 1202, 1117 cm^{-1} ; HRMS (ESI) m/z calcd. for $\text{C}_{22}\text{H}_{28}\text{NO}_3\text{Si}$ ($\text{M}+\text{H}$)⁺ 382.1838, found 382.1849.

III. Thermal Rearrangement of *N*-Enoxyisoindolinones (Table 2.6).



General Procedure M: A J-Young tube was charged with a 0.1 M solution of *N*-enoxisoindolinone **31** (1 equiv) in Toluene- d_8 . The reaction mixture was heated to 50–90 °C for 3–8 h. Toluene- d_8 was removed from the reaction mixture under vacuum and imidate **14** was isolated as an oil.

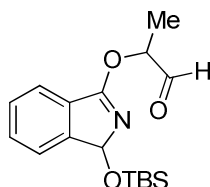


14d

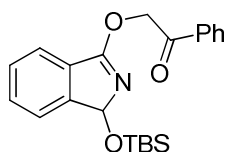
dr = >95:5

α -oxygenated aldehyde 14d: General procedure **M** was followed with **31d** (0.040 g, 0.130 mmol). Heating the reaction mixture to 50 °C for 3 h afforded imidate **14d** (0.040 g, >95% recovery) as a yellow oil and a single diastereomer. ^1H NMR (500 MHz; C_6D_6): δ 9.51 (s, 1H), 7.28–7.37 (m, 1H), 7.38–6.99 (m, 3H), 5.92 (s, 1H), 5.11–5.08 (m, 1H), 1.68–1.66 (m, 2H), 1.24–1.21 (m, 4H), 1.03 (s, 9H), 0.83 (t, J = 5.0 Hz, 3H), 0.29 (s, 3H),

0.16 (s, 3H); ^{13}C NMR (125 MHz, CDCl_3): δ 198.6, 168.6, 152.3, 131.5, 129.8, 128.7, 122.7, 120.2, 91.1, 81.7, 29.2, 27.1, 25.7, 22.4, 18.1, 13.6, -4.0, -4.9; IR (thin film) 2955, 2929, 2858, 1738, 1576, 1400, 1379, 1254, 1122, 1075 cm^{-1} ; HRMS (ESI) m/z calcd. for $\text{C}_{20}\text{H}_{32}\text{NO}_3\text{Si}$ ($\text{M}+\text{H}$) $^+$ 362.2151, found 362.2139.

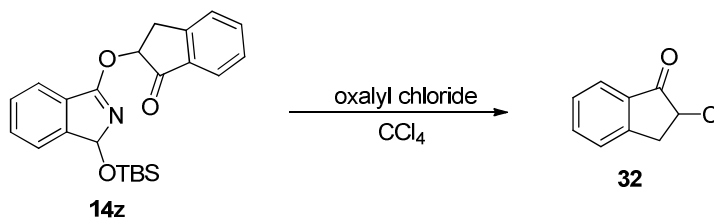
**14af****dr = 75:25**

α -oxygenated aldehyde 14af: General procedure **M** was followed with **31af** (0.030 g, 0.093 mmol). Heating the reaction mixture to 65 $^\circ\text{C}$ for 3 h afforded imidate **14af** (0.030 g, >95% recovery) as a yellow oil and a 75:25 mixture of diastereomers. ^1H NMR major diastereomer (500 MHz; C_6D_6): δ 9.40 (s, 1H), 7.36-7.33 (m, 2H), 7.07-6.99 (m, 2H), 5.87 (s, 1H), 5.12 (q, $J = 7.0$ Hz, 1H), 1.21 (d, $J = 7.0$ Hz, 3H), 1.03 (s, 9H), 0.28 (s, 3H), 0.17 (s, 3H); ^{13}C NMR major diastereomer (125 MHz, CDCl_3): δ 197.9, 168.3, 152.9, 131.5, 129.7, 128.2, 122.7, 120.3, 90.8, 77.9, 25.7, 19.5, 14.2, -3.9, -4.8; ^1H NMR minor diastereomer (500 MHz; C_6D_6): δ 9.45 (s, 1H), 7.36-7.33 (m, 2H), 7.11-7.08 (m, 2H), 5.90 (s, 1H), 5.07 (q, $J = 8.1$ Hz, 1H), 0.81 (d, $J = 8.1$ Hz, 3H), 1.02 (s, 9H), 0.15 (s, 3H), 0.02 (s, 3H); ^{13}C NMR minor diastereomer (125 MHz, CDCl_3): δ 198.4, 168.3, 149.2, 132.4, 129.3, 127.8, 123.4, 120.3, 91.0, 82.6, 25.5, 18.1, 14.2, -3.9, -4.7; IR (thin film) 2929, 2885, 2856, 1708, 1626, 1574, 1470, 1399, 1253, 1195, 1118 cm^{-1} ; HRMS (ESI) m/z calcd. for $\text{C}_{17}\text{H}_{26}\text{NO}_3\text{Si}$ ($\text{M}+\text{H}$) $^+$ 320.1682, found 320.1689.

**14g**

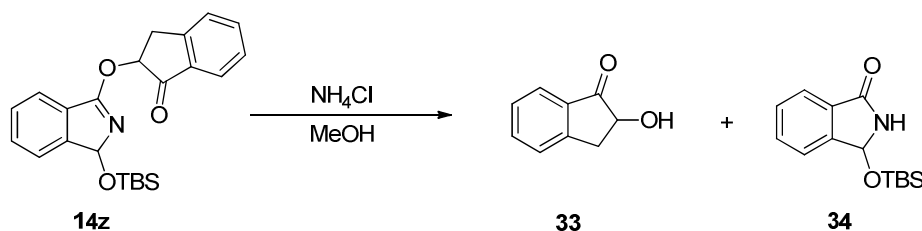
α -oxygenated aldehyde 14g: General procedure **M** was followed with **31g** (0.070 g, 0.183 mmol). Heating the reaction mixture to 80 °C for 6 h afforded imidate **14g** (0.066 g, 94% recovery) as a yellow oil. ^1H NMR (500 MHz; C_6D_6): δ 7.72-7.72 (m, 3H), 7.50-7.49 (m, 1H), 7.37-7.36 (m, 1H), 7.13-7.07 (m, 4H), 5.92 (s, 1H), 5.32 (d, $J = 7.1$ Hz, 2H), 0.99 (s, 9H), 0.20 (s, 3H), 0.09 (s, 3H); ^{13}C NMR (125 MHz, CDCl_3): δ 191.2, 168.6, 153.1, 135.0, 132.7, 129.5, 128.2, 128.1, 127.6, 124.5, 122.5, 120.5, 90.9, 69.1, 25.7, 18.0, -3.9, -4.6; IR (thin film) 2927, 2855, 1707, 1685, 1628, 1598, 1471, 1390, 1249, 1189 cm^{-1} ; HRMS (ESI) m/z calcd. for $\text{C}_{22}\text{H}_{28}\text{NO}_3\text{Si}$ ($\text{M}+\text{H}$) $^+$ 382.1838, found 382.1841.

V. Functionalization of Imidates

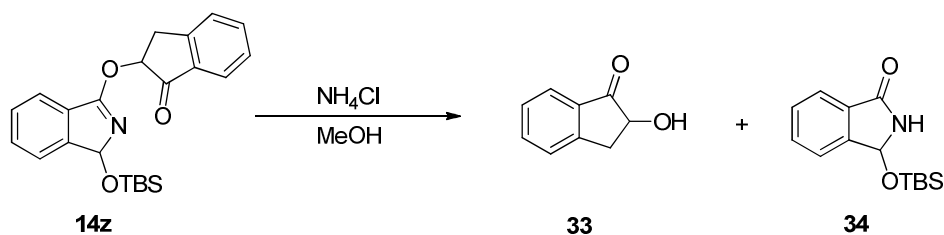


2-chloro-2,3-dihydro-1H-inden-1-one 32: To the imidate **14z** (0.040 g, 0.101 mmol) in CCl_4 (2 ml) was added the oxalyl chloride (8 μl , 0.101 mmol) and the reaction stirred at room temperature for 12 h. The volatiles were removed in vacuo and the crude reaction mixture was purified by medium pressure chromatography on silica gel with 1:4 ethyl acetate:hexanes to give **32** as an amorphous white solid (0.012 g, 74 %). ^1H NMR (500

MHz; CDCl₃): δ 7.84-7.83 (m, 1H), 7.68-7.66 (m, 1H), 7.47-7.43 (m, 2H), 4.56 (dd, J = 7.3, 3.8 Hz, 1H), 3.78 (dd, J = 17.4, 7.3 Hz, 1H), 3.30 (dd, J = 17.4, 3.8 Hz, 1H); ¹³C NMR (125 MHz, CDCl₃): δ 199.2, 150.7, 136.1, 133.8, 128.3, 126.4, 125.1, 55.7, 37.5; ; IR (thin film) 2956, 2954, 1767, 1726, 1609, 1578, 1470, 1429, 1324, 1277, 1158 cm⁻¹; HRMS (ESI) m/z calcd. for C₉H₈OCl (M+H)⁺ 167.0264, found 167.0273.

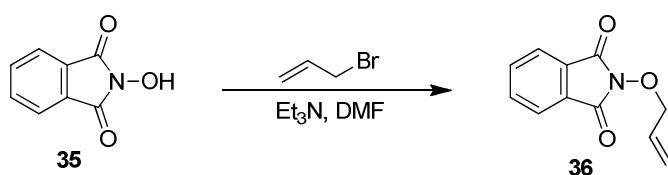


2-hydroxy-2,3-dihydro-1H-inden-1-one 33: To a solution of the imidate **14z** (0.030 g, 0.076 mmol) in MeOH:H₂O (2 ml, 1:1) was added NH₄Cl (0.007 g, 0.125 mmol) and the reaction heated to 90 °C for 2 h. MeOH was removed under reduced pressure and the residue was extracted with EtOAc (3 x 7 ml). The organic layer was dried with MgSO₄ and concentrated *in vacuo*. The crude reaction mixture was purified by medium pressure chromatography on silica gel with 1:2 ethyl acetate:hexanes to give **33** as an amorphous white solid (0.006 g, 53 %). ¹H NMR (500 MHz; CDCl₃): δ 7.78-7.76 (m, 1H), 7.66-7.64 (m, 1H), 7.47-7.46 (m, 1H), 7.42-7.39 (m, 1H), 4.54 (dd, J = 7.8, 5.1 Hz, 1H), 3.58 (dd, J = 16.5, 7.8 Hz, 1H), 3.02 (dd, J = 16.5, 5.1 Hz, 1H), 2.92 (s, 1H); ¹³C NMR (125 MHz, CDCl₃): δ 206.3, 150.8, 135.8, 134.0, 128.1, 126.8, 124.4, 74.3, 35.1; IR (thin film) 3469, 2982, 1732, 1609, 1470, 1366, 1299, 1252, 1154, 1047 cm⁻¹; HRMS (ESI) m/z calcd. for C₉H₈O₂ (M)⁺ 148.0524, found 148.0531.

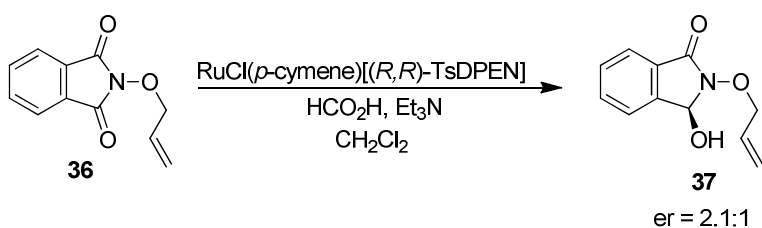


3-((*t*-butyldimethylsilyl)oxy)isoindolinone 34: To a solution of the imidate **14z** (0.030 g, 0.076 mmol) in MeOH:H₂O (2 ml, 1:1) was added NH₄Cl (0.007 g, 0.125 mmol) and the reaction heated to 90 °C for 2 h. MeOH was removed under reduced pressure and the residue was extracted with EtOAc (3 x 7 ml). The organic layer was dried with MgSO₄ and concentrated *in vacuo*. The crude reaction mixture was purified by medium pressure chromatography on silica gel with 1:1 ethyl acetate:hexanes to give **34** as an amorphous white solid (0.006 g, 53 %) ¹H NMR (500 MHz; CDCl₃): δ 7.81-7.79 (m, 1H), 7.60-7.58 (m, 1H), 7.52-7.49 (m, 2H), 6.49 (bs, 1H), 6.12 (s, 1H), 0.93 (s, 9H), 0.16 (s, 3H), 0.03 (s, 3H); ¹³C NMR (125 MHz, CDCl₃): δ 169.5, 146.2, 134.2, 132.5, 129.5, 123.6, 123.4, 79.2, 25.6, 17.9, -4.0, -4.1; IR (thin film) 3209, 3099, 2931, 2855, 1685, 1609, 1473, 1435, 1350, 1255, 1104 cm⁻¹; HRMS (ESI) *m/z* calcd. for C₁₄H₂₂NO₂Si (M)⁺ 264.1420, found 264.1419.

VI. Transfer of Chirality



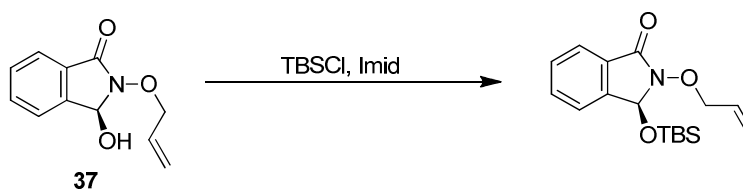
***N*-(allyloxy)isoindoline-1,3-dione **36**:** To the *N*-hydroxyphthalimide **2** (1 g, 6.13 mmol) in DMF (6 ml) at 0 °C was added DBU (1.5 equiv, 1.4 ml, 9.19 mmol) followed by allyl bromide (1.5 equiv, 0.80 ml, 9.19 mmol). The reaction was then stirred at room temperature for 2 h. Water was added to the reaction mixture and it was extracted with CH₂Cl₂ (3 x 20 ml). The organic layer was dried with MgSO₄ and the solvent removed under reduced pressure to give **36** as a white solid (1.2 g, 94 %) which did not require further purification. ¹H NMR (500 MHz; CDCl₃): δ 7.83-7.81 (m, 2H), 7.75-7.73 (m, 2H), 6.14-6.08 (m, 1H), 5.36 (dd, *J* = 23.0, 5.8 Hz, 2H), 4.69 (d, *J* = 6.7 Hz, 2H); ¹³C NMR (125 MHz, CDCl₃): δ 163.7, 134.4, 131.2, 128.8, 123.5, 122.5, 78.8; IR (thin film) 2943, 1789, 1720, 1606, 1464, 1420, 1375, 1350, 1186, 1113 cm⁻¹; HRMS (ESI) *m/z* calcd. for C₁₁H₁₀NO₃ (M+H)⁺ 204.0661, found 204.0664; mp 57 °C.



3-hydroxy-*N*-allyloxyisoindolinone **37:** To an oven dried 25 ml round bottom flask was added the RuCl(*p*-cymene)[(*R,R*)-TsDPEN] (0.01 equiv, 15 mg) under a N₂ atmosphere followed by CH₂Cl₂ (7 ml). The *N*-(allyloxy)isoindoline-1,3-dione **36** (0.500 g, 2.46 mmol) was then added followed by Et₃N (4.8 equiv, 1.5 ml, 11.8 mmol) and a dropwise addition of HCO₂H (5 equiv, 0.5 ml, 12.3 mmol) all under a N₂ atmosphere. The reaction was then stirred at room temperature for 19 h. The volatiles were removed under reduced pressure and the residue purified by medium pressure chromatography on silica gel (1:1 ethyl acetate:hexanes) to give **37** as a white solid (0.400 g, 40 %). ¹H NMR (500 MHz;

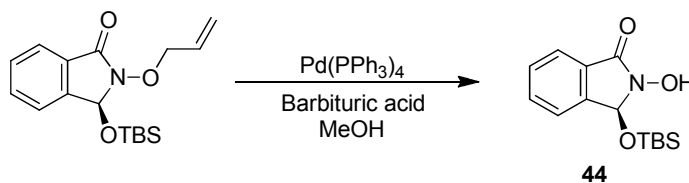
CDCl₃): δ 7.60-7.59 (m, 1H), 7.58-7.44 (m, 2H), 7.46-7.40 (m, 1H), 6.06-6.01 (m, 1H), 5.88 (s, 1H), 5.61 (bs, 1H), 5.31-5.19 (m, 2H), 4.61 (d, $J = 3.8$ Hz, 2H); ¹³C NMR (125 MHz, CDCl₃): δ 165.2, 141.2, 132.9, 132.4, 129.7, 128.9, 123.4, 123.2, 120.4, 82.5, 78.2; IR (thin film) 3275, 2938, 1679, 1638, 1609, 1460, 1381, 1312, 1214, 1148, 1065 cm⁻¹; HRMS (ESI) m/z calcd. for C₁₁H₁₂NO₃ (M+H)⁺ 206.0817, found 206.0822; mp 110 °C.

Determination of er: The 3-hydroxy-*N*-allyloxyisoindolinone **37** (0.010 g, 0.052 mmol) was dissolved in CH₂Cl₂ (0.5 ml). DCC (1.3 equiv, 0.014 g, 0.068 mmol) was added followed by (*R*)-(+)- α -methoxy- α -trifluoromethylphenylacetic acid (1.3 equiv, 0.016 g, 0.068 mmol) and a few crystals of DMAP. The reaction was stirred at room temperature for 14 h. The solvent was removed under reduced pressure and the residue purified by medium pressure chromatography on silica gel (1:2 ethyl acetate:hexanes) to give the product as a white solid. ¹HNMR analysis revealed that the product was a 2.1:1 mixture of enantiomers.



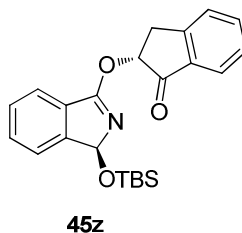
3-*t*-butyldimethylsilyloxy-*N*-allyloxyisoindolinone: To a solution of the 3-hydroxy-*N*-allyloxyisoindolinone **37** (0.200 g, 1.05 mmol) in CH₂Cl₂ (4 ml) at 0 °C was added imidazole (1.1 equiv, 0.077 g, 1.15 mmol) followed by TBSCl (1.1 equiv, 0.173 g, 1.15 mmol). The reaction was allowed to warm up to room temperature and stirred at that temperature for 10 h. The reaction was quenched with NH₄Cl and extracted with EtOAc (3 x 20 ml). The organic layer was washed with water and dried with MgSO₄. The crude

reaction mixture was purified by medium pressure chromatography on silica gel with 1:3 ethyl acetate:hexanes to give the 3-*t*-butyldimethylsilyloxy-*N*-allyloxyisoindolinone as an amorphous white solid (0.302 g, 90 %). ^1H NMR (500 MHz; CDCl_3): δ 7.79-7.78 (m, 1H), 7.59-7.57 (m, 1H), 7.51-7.48 (m, 1H), 7.43-7.42 (m, 1H), 6.13-6.09 (m, 1H), 5.97 (s, 1H), 5.39 (dd, $J = 17.2, 1.2$ Hz, 1H), 5.31 (dd, $J = 11.1, 1.2$ Hz, 1H), 4.75 (dd, $J = 11.1, 7.1$ Hz, 1H), 4.64 (dd, $J = 11.1, 6.0$ Hz, 1H), 0.97 (s, 9H), 0.30 (s, 3H), 0.24 (s, 3H); ^{13}C NMR (125 MHz, CDCl_3): δ 165.1, 141.8, 132.8, 132.1, 129.7, 129.5, 123.5, 122.9, 120.2, 82.4, 77.8, 25.6, 18.0, -4.2, -4.3; IR (thin film) 2953, 2931, 2858, 1726, 1467, 1359, 1255, 1198, 1119, 1069 cm^{-1} ; HRMS (ESI) m/z calcd. for $\text{C}_{17}\text{H}_{26}\text{NO}_3\text{Si}$ ($\text{M}+\text{H}$) $^+$ 320.1682, found 320.1681.

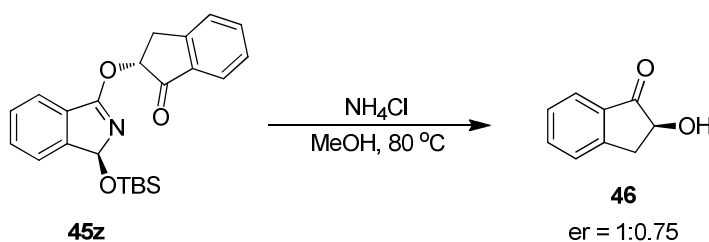


3-*t*-butyldimethylsilyloxy-*N*-hydroxyisoindolinone 44: The barbituric acid (2 equiv, 0.024 g, 0.187 mmol) was mixed with 3-*t*-butyldimethylsilyloxy-*N*-allyloxyisoindolinone (0.030 g, 0.093 mmol) in a 25 ml round bottom flask, Pd(PPh₃)₄ (5 mol %, 0.005 g, 4.6 μmol) was added to the flask under an atmosphere of N_2 . MeOH (0.8 ml) was added last and the reaction stirred under N_2 atmosphere for 1.5 h after which the MeOH was removed under reduced pressure. EtOAc was added to the reaction and it was extracted with saturated Na_2CO_3 (8 x 10 ml) to remove all the excess barbituric acid. The organic layer was dried with MgSO_4 and concentrated *in vacuo*. The crude reaction mixture was

purified by medium pressure chromatography on silica gel with 2:1 ethyl acetate:hexanes to give **44** as a white solid (0.020 g, 77 %). The spectral data matches **13**.



Imidate 45z: Same procedure as that for **14z**. The spectral data matches **14z**.

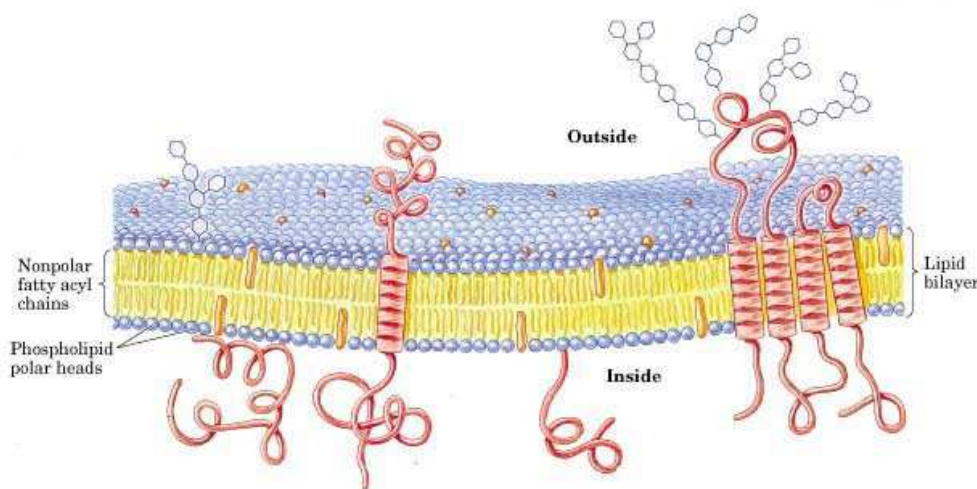


2-hydroxy-2,3-dihydro-1H-inden-1-one 46: The spectral data matches **33** above.

Determination of er: The 2-hydroxy-2,3-dihydro-1H-inden-1-one **46** (0.008 g, 0.053 mmol) was dissolved in CH_2Cl_2 (0.4 ml). DCC (1.3 equiv, 0.014 g, 0.069 mmol) was added followed by (*R*)-(+)- α -methoxy- α -trifluoromethylphenylacetic acid (1.3 equiv, 0.017 g, 0.069 mmol) and a few crystals of DMAP. The reaction was stirred at room temperature for 14 h. The solvent was removed under reduced pressure and the residue purified by medium pressure chromatography on silica gel (1:3 ethyl acetate:hexanes) to give the product as a white solid. ^1H NMR analysis revealed that the product was a 1:0.75 mixture of enantiomers.

Chapter 3- Introduction to Lipids and Environment-Sensitive Fluorescent Probes**3.1 Lipids**

A lipid bilayer forms the outer stratum in a eukaryotic cell and divides the cell into different structural and functional identities.¹⁰³ Lipids, which are an integral part of the cell membrane; control a myriad of cellular processes. Lipid constituents regulate processes such as signal transduction,¹⁰⁴ endomembrane transport,¹⁰⁵ cell proliferation,¹⁰⁶ apoptosis¹⁰⁷ and metabolism.¹⁰⁸ Many lipids serve as site specific membrane signals that regulate the activity of membrane and soluble proteins.¹⁰⁹ Lipids also confer unique dielectric and permeability properties to the cell membrane.¹¹⁰

**Figure 3.1:** Lipid Bilayer

Taken from www.uoguelph.ca/~fsharom/research/research.html¹¹¹

Lipids are generally made up of non-polar fatty acid chains with a phosphate polar head group.¹¹² They are therefore referred to as phospholipids. Phospholipids make up about 70% of the total lipid content of a mammalian cell. The remaining 30% consists of cholesterol, sphingomyelin and glycopospholipids.¹⁰³

Figure 3.2 depicts the structure of the phospholipid; Phosphatidylcholine. As shown in the figure, the long chain fatty acid has a glycerol backbone which is bound to a phosphate moiety through the free primary alcohol of the glycerol unit. This structure comprising the long chain fatty acid, the glycerol backbone and the phosphate is present in all phospholipids. The phospholipids vary at the group connected to one of the oxygen atoms of the phosphate moiety. When a choline group is bound to the phosphate, the phospholipid is known as Phosphatidylcholine. Instead of a choline, if a serine group is bound to the phosphate, the lipid is known as Phosphatidylserine.¹¹³

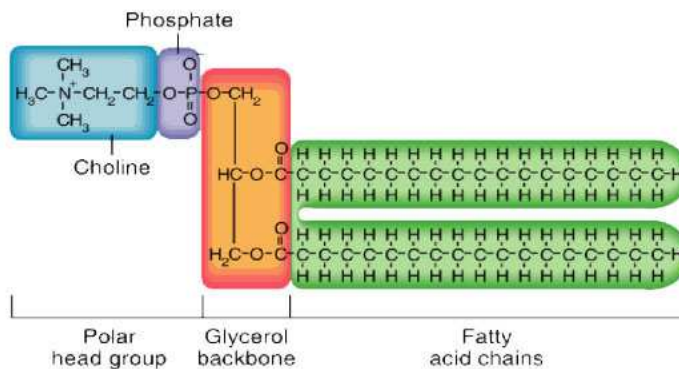


Figure 3.2: Structure of the phospholipid – Phosphatidylcholine

Taken from <http://hrsbstaff.ednet.ns.ca/>¹¹⁴

Among the phospholipids found in the cell membrane, choline containing lipids such as phosphatidylcholine (PC) and sphingomyelin are found in the exoplasmic region of the cell membrane and the aminophospholipids including phosphatidylserine (PS) and phosphatidylethanolamine occur in the cytosolic part of the cell membrane (Figure 3.3).¹¹⁵

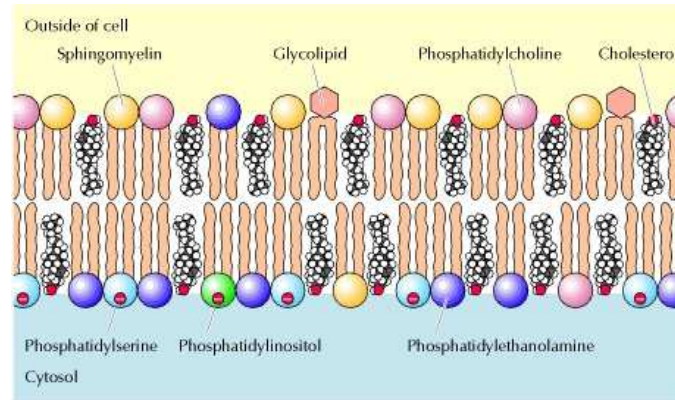


Figure 3.3: Arrangement of Phospholipids in the Cell Membrane

Taken from <http://asweexplore.blogspot.com>¹¹⁶

In the phospholipids, PC is the most prevalent and accounts for 40-50% of the total lipid content.¹¹⁷ Phosphatidylethanolamine (PE) is about 20-45% depending on the type of tissue. Phosphatidylinositol, Phosphatidylserine (PS) and Phosphatidic acid are present in lesser amounts.¹¹⁸ Although PS is a relatively minor constituent of the cell membrane, its low abundance is outweighed by its physiological properties.

3.2 Phosphatidylserine (PS)

Phosphatidylserine was first isolated by Folch and co-workers in 1942.¹¹⁹ Phosphatidylserine is a phospholipid that is comprised of a long chain fatty acid, a glycerol backbone and the polar head group which consists of phosphate functionality bound to a serine moiety as shown in Figure 3.4. The fatty acid chains in PS vary among different cell types and organelles.¹⁰³

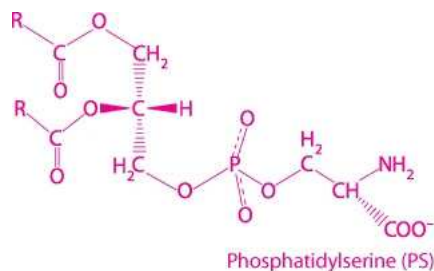


Figure 3.4: Structure of Phosphatidylserine

Taken from <http://www.xenabioherbals.net/phosphatidylserine-555188.html>¹²⁰

PS is an anionic phospholipid with three ionizable groups; the phosphate functional group, the amino moiety and the carboxylate. PS usually chelates to a Ca ion through the oxygen atoms of the phosphate and the carboxylate. This results in a change in the conformation of the polar head group from linear to cyclic. The chelation is important for some of the biological functions of PS, especially bone formation.¹²¹

3.2.1 Functions of PS

Since PS is the predominant anionic species on the surface of the lipid,¹²² it confers a negative charge on the inner leaflet of the plasma membrane which helps in the binding of polycations and proteins with cationic clusters.¹²³ This is a mode of protein recruitment for several regulatory and structural proteins such as protein kinase C,¹²⁴ annexin,¹²⁵ and spectrin.¹²⁶ One of the most important functions of PS is in the regulation of apoptosis. When cells undergo programmed cell death, PS moves to the exoplasmic region where it acts as a trigger for macrophage recognition which facilitates the removal of the apoptotic cells¹²⁷⁻¹³⁰ (Figure 3.5).

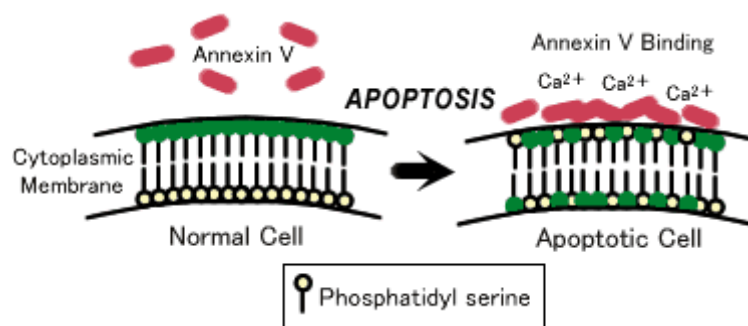


Figure 3.5: Recognition of an Apoptotic Cell through Extracellularly Exposed PS

Taken from <http://www.biocat.com>¹³¹

Thus, PS facilitates removal of apoptotic cells and their potentially toxic components in a non-inflammatory manner. This function of PS is especially important for the development of the lungs and the brain and in processes where apoptosis plays an important role.¹³²

PS is responsible for the key signal that starts the coagulation cascade eventually leading to the clotting of blood.¹³³ When activated, platelets present in blood expose PS on their outer surface. This exposure of PS triggers the attachment of clotting factors and prothrombin to the platelets. These prothrombinase complexes promote coagulation.¹³⁴ A dysfunction in these PS associated processes can lead to cancer, chronic autoimmunity and infections.¹³⁵ It is therefore imperative to develop a method that allows for the detection, monitoring and quantification of PS and other lipids to understand these complex membrane-mediated biological processes.

3.3 Conventional Methods for Lipid Analysis

Conventional methods for the characterization and analysis of lipids involve a physical separation of lipids from cells using a liquid-liquid extraction¹³⁶ or

saponification of the lipid.¹³⁷ Thin-layer chromatography is used to separate the lipids into phospholipid classes¹³⁸ which can then be derivatized, acetylated using radioactive acetic anhydride, oxidized or measured by colorimetric analysis.^{139,140} These approaches lack the sensitivity required for the analysis of subcellular membranes and are time consuming.¹⁴¹ More recently, chromatography followed by mass spectroscopy such as GC-MS,¹⁴² LC-MS¹⁴³ and nano ESI-FTMS¹⁴⁴ has been used for lipid fingerprinting and classification. These methods, however, involve the isolation of the lipid from the cell and hence do not provide a spatiotemporal *in situ* quantification of lipid molecules. Also, lipid lability may lead to low reproducibility in sample preparation.

3.4 Fluorescent Probes

The *in situ* detection of PS in intact cells could potentially be the most effective method for the understanding of lipid mediated processes. Florescent probes have been utilized for this purpose.¹⁴⁵ The unique features of fluorescence techniques in comparison with other methods that are capable of monitoring lipid-protein interactions (NMR, FTIR, etc.) are their ultimate sensitivity up to a single-molecule level and their ability to operate in biological systems of varying complexity. Fluorescent probes provide information on the properties of their molecular environment directly by changing their fluorescence characteristics (wavelength maximum, fluorescence intensity, and/or fluorescence lifetime).¹⁰³

The change in the fluorescence signal from light to dark (or the reverse), at a single wavelength, is usually recorded as the change in fluorescence intensity. Because the change in fluorescence intensity can be easily observed, high spectral resolution in

these measurements is not needed.¹⁴⁶ Fluorescence quenching/enhancement is commonly used in different sensing and imaging technologies.¹⁴⁷ Small fluorescent probes or nanoparticles are either covalently conjugated to molecules of interest (such as lipids, proteins and RNA) or used as stains to detect the target compounds (lipids, DNA).¹⁴⁸ In cellular research, these probes can penetrate spontaneously into the cell and label genetically prepared protein binding sites. The labeled proteins can thus be detected as they move through the cytoplasm of the cell (Figure 3.6). This is useful in monitoring the interactions of the proteins with various other sub-cellular components and studying the downstream events of such interactions.¹⁴⁹

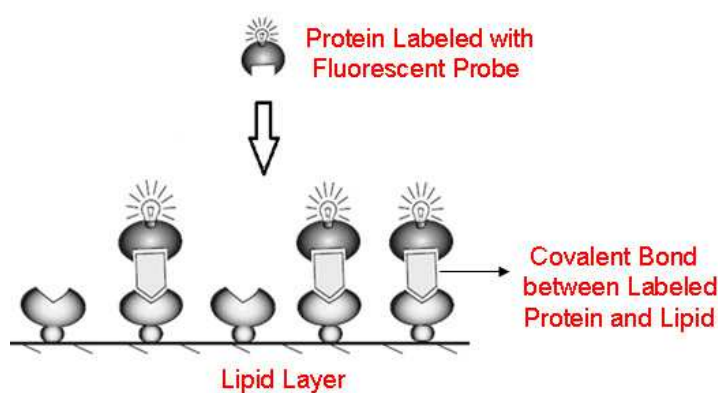


Figure 3.6: Fluorescent Probe Attached to a Protein can be used to monitor the Interactions of the Protein with Lipids. Taken from: <http://books.google.com/books> "Introduction to Fluorescence Sensing" by Alexander P. Demchenko¹⁴⁹

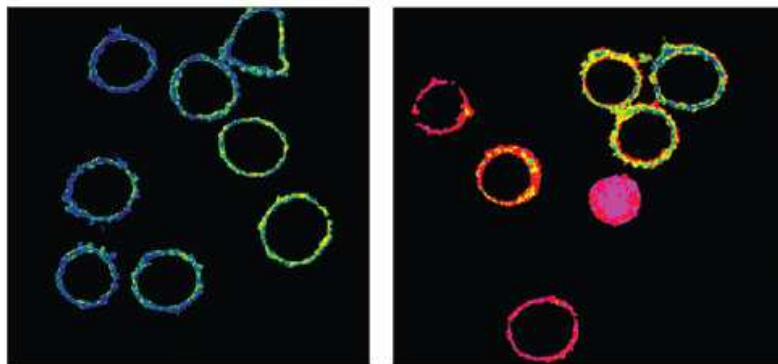


Figure 3.7: Real Lifetime Images of Cells in which a Labeled Protein has bound to the Cell Membrane. Taken from: <http://books.google.com/books> “Introduction to Fluorescence Sensing” by Alexander P. Demchenko¹⁴⁹

Cell Imaging can be carried out by using a fluorescent probe which is used to bind to a protein. When this labeled protein binds to the cell membrane, the membrane begins to fluoresce, and thus this method can be used for imaging to cells under a microscope (Figure 3.7).¹⁵⁰

3.5 Environmentally Sensitive Fluorescent Probes

Environment sensitive fluorophores are being used for cell imaging and detection of cellular components. These probes provide information on the properties of their molecular environment directly by changing their fluorescence characteristics (wavelength maximum, fluorescence intensity, and/or fluorescence lifetime).¹⁰³ Since we were using the environmentally sensitive fluorescent probes to detect lipid-protein interactions, it was important to understand the membrane properties and how they are reflected in the spectroscopic response of the fluorescent probes.

Microviscosity of lipid membranes (the reciprocal to fluidity) is the measure of frictional resistance to the rotational and translational motion of molecules.¹⁵¹ Membrane microviscosity can be estimated by fluorescence anisotropy of rod shaped probes (typically diphenylhexatriene (DPH)), which is a consequence of their rotational motion in the membrane.¹⁵² Microviscosity could also be measured by the fluorescence intensity of molecular rotors. Molecular rotors are fluorophores that exhibit strong variations in their fluorescence quantum yield depending on their intramolecular rotation, which is in turn dependent on the viscosity of the environment of the rotor. In more viscous media the rotations of the molecular rotor are slowed down, which increases the fluorescence intensity of the fluorophore. After they are incorporated into lipid membranes, these fluorophores monitor the microviscosity of their surroundings at their sites of location.¹⁵³

The polarity of lipid membranes is a property addressed with the use of fluorescent probes.^{154,155} Initially, the absorption and emission spectra of a probe are measured as a function of polarity by using a solution of the probe in organic solvents of varying polarities. Since the probes are environmentally sensitive, there should be a shift in the emission spectrum of the fluorophore as the polarity of the organic solvents changes from polar to non-polar and this shift can be expressed in empirically established units.¹⁵⁶ The shift in fluorescence emission is because of the difference in the energies of the fluorophore ground and excited states, which can vary based on the dipole-dipole interactions of the probe with its environment. The effect of the solvent polarity on fluorescence emission is shown below.

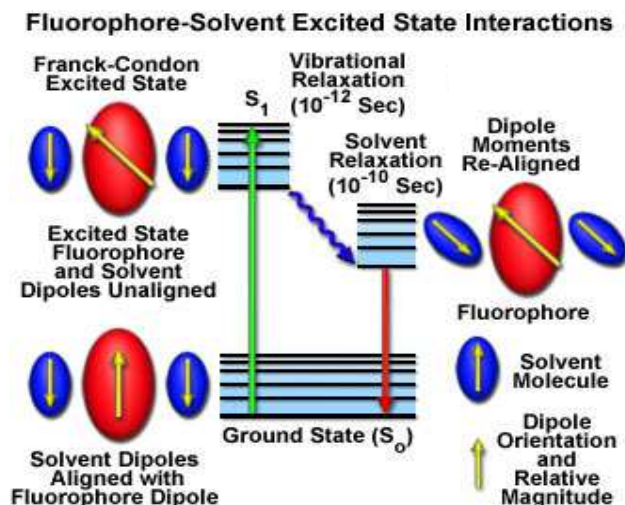


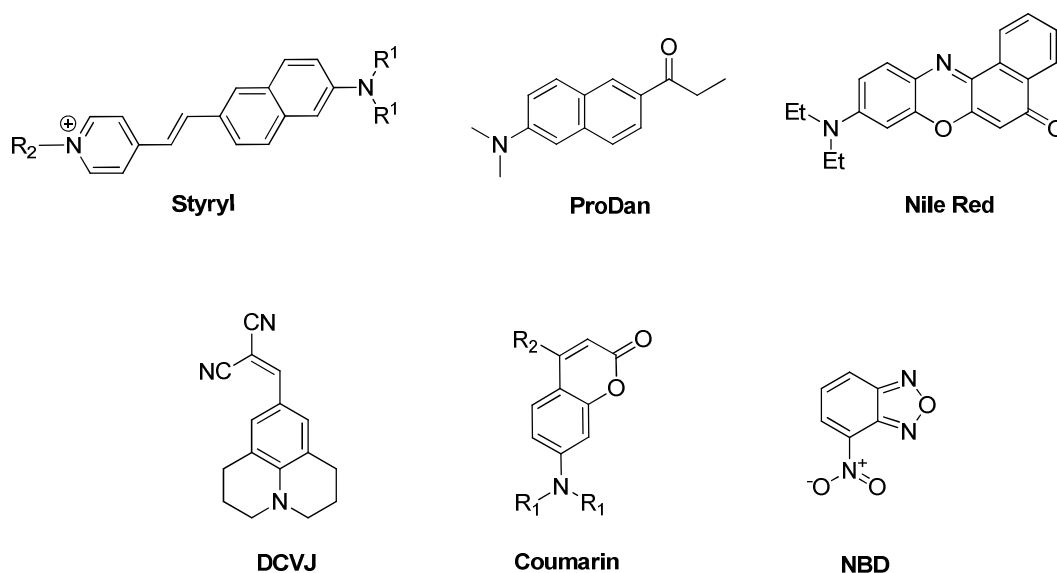
Figure 3.8: Effect of Solvent Polarity on the Emission of the Fluorophore

Taken from <http://micro.magnet.fsu.edu/primer/java/jablonski/solventeffects/>¹⁵⁶

After the fluorophore has been excited to higher vibrational levels of the first excited singlet state ($S(1)$), excess vibrational energy is rapidly lost to surrounding solvent molecules. This results in the relaxation of the fluorophore to the lowest vibrational energy level (occurring in the picosecond time scale). Solvent molecules then reorient their dipole around the excited fluorophore, thus assisting in stabilizing and further lowering the energy level of the excited state of the fluorophore. This process is known as Solvent Relaxation (Figure 3.8). The solvent relaxation is a slower process that requires between 10 and 100 picoseconds and has the effect of reducing the energy separation between the ground and excited states of the fluorophore, which in turn results in a red shift (to longer wavelengths) of the fluorescence emission. Increasing the solvent polarity produces a correspondingly larger reduction in the energy level of the excited state, while decreasing the solvent polarity reduces the solvent effect on the excited state

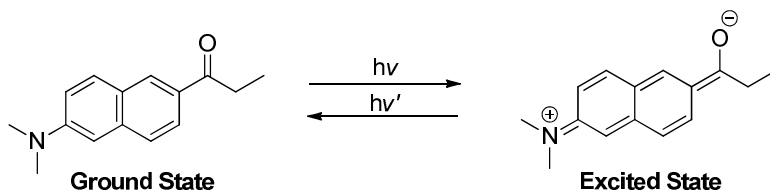
energy level. The polarity of the fluorophore also determines the sensitivity of the excited state to solvent effects.^{156,157}

Polarity sensing in membranes is an attempt to transfer this concept from the emission in organic solvents to the highly anisotropic structure of lipid bilayers. Thus, a fluorescent probe will exhibit a shift in its emission spectrum or intensity of emission when it moves from the aqueous polar environment of the cytoplasm of the cell to the non-polar environment of a lipid membrane. This is because the low polarity of the lipid molecules will not effectively stabilize the excited state of the fluorophore. This will lead to a larger energy gap between the ground and excited states of the fluorophore, resulting in emission at shorter wavelengths (blue shift).¹⁰³ It is because of this process that a more widely used class of environment-sensitive fluorophores consists of solvatochromic dyes that exhibit shifts in their emission spectra as a function of properties such as the polarity and hydration of their environment. These fluorescent probes exhibit strong changes in dipole moments upon electronic excitation. Dipole-dipole and specific H-bonding interactions of the dyes with their surroundings change the energy of the probe electronic transitions and thus shift the maxima of their excitation and emission spectra.¹⁰³ Typical examples of such dyes are NBD, Prodan, 7-(dialkylamino)- coumarin, and Nile Red as shown in Scheme 3.1.



Scheme 3.1: Structures of Solvatochromic Probes

In these fluorophores, the dipole moment increases dramatically upon electronic excitation due to an intramolecular charge transfer (ICT) from the electron donating dialkylamino group to the electron accepting carbonyl group as represented in Scheme 3.2.



Scheme 3.2: ICT in Prodan

As a result, these dyes exhibit a red shift of their emission spectrum in response to an increase in solvent polarity and the relaxation rates of their surroundings.¹⁵⁸ Moreover, an additional strong red shift of the Prodan emission is connected with H-bonding to H-bond donor molecules in the environment.¹⁵⁹ Such effects are typical for environment-sensitive

dyes that contain H-bond acceptor groups (such as carbonyl), which are of particular interest for studying membrane hydration. Electrochromic dyes operate by the same photophysical principle as solvatochromic dyes, namely, a strong ICT upon electronic excitation. They are commonly rod-shaped molecules that bear electron donor and acceptor groups on two opposite sides such as the styryl pyridinium dyes (Scheme 3.1).¹⁶⁰ In these probes, the excitation spectra are also affected by the solvation of the highly polar ground states, which results in a blue-shift of the excitation spectra depending on the composition of the lipid that they are inserted in to.^{161,162}

3.6 Conclusion

Environment-sensitive fluorescent probes are important tools for gleaning information about the structure and dynamics in biomembranes. The main advantage of such a probe is the response to change in polarity via a blue shift or increase in intensity. We hypothesized that by taking assistance of this property, we could design a library of environmentally sensitive, thiol reactive fluorescent probes that could be used for the *in situ* determination and quantification of PS in the cell. This would allow us to monitor and understand the complex PS mediated processes and develop a solution for the ailments caused by a dysfunction in these processes.

Chapter 4 – Development of New Environment Sensitive Fluorescent Probes for Lipid-Protein Interactions

4.1 Abstract

Lipids, which are found in cell membranes, control a number of cellular processes through their interactions with proteins. Fluorescent probes have been used to monitor these lipid protein interactions, to gain a better understanding of the complex membrane mediated processes. Commercially available fluorophores utilized for this purpose have several limitations such as photobleaching, damage to cells and difficulty in derivatization. In order to overcome these limitations, a new family of environmentally sensitive fluorescent probes has been synthesized which could be used for the detection and quantification of phosphatidylserine in the cell. These new compounds have low emission in water and very intense emission in hydrophobic solvents making them perfect “turn-on” thiol reactive probes for protein-lipid interactions. Assay results have shown that the new fluorophore can bind irreversibly with a cysteine on the C1B domain of the protein PKC γ . This labeled protein then binds to the phosphatidylserine lipid, wherein the fluorescent probe senses a change in its environment from aqueous polar to lipid non-polar, and hence exhibits an increase in the intensity of emission. These new fluorophores have also been used for the imaging of the cell.

4.2 Introduction

The cell membrane is a biological membrane that separates the interior of a cell from the outside environment. In addition to regulating the movement of substances in and out of a cell, the biological function of a cell membrane affects the fundamental physicochemical properties of the cell. The membrane electrostatics, phase state, hydration, and dynamics determine the structure of the cell and control the binding and transport of molecular and ionic species.¹⁶³ Cellular membranes are responsible for the correct insertion,¹⁶⁴ proper folding,¹⁶⁵ and functioning of membrane proteins.¹⁶⁶

Cellular membranes are made up of phospholipids. Among the phospholipids found in the cell membrane, choline containing lipids such as phosphatidylcholine (PC) and sphingomyelin are found in the exoplasmic region of the cell membrane and the aminophospholipids including phosphatidylserine (PS) and phosphatidylethanolamine occur in the cytosolic part of the cell membrane.¹⁶⁷⁻¹⁶⁹ Although PS is a relatively minor component of most biological membranes,¹⁷⁰ it plays several important roles. A dysfunction in these PS associated processes can lead to cancer, chronic autoimmunity and infections.¹⁷¹⁻¹⁷⁴ It is therefore imperative to develop a method that allows for the quantification of PS and other lipids to understand the complex membrane mediated biological processes.

Florescent techniques have become popular in the recent years for monitoring lipid processes.¹⁷⁵ The unique features of fluorescence techniques in comparison with other tools that are capable of monitoring these properties (NMR, FTIR, EPR) are their ultimate sensitivity and their ability to operate in biological systems without involving isolation of the lipid membranes.¹⁷⁶ Fluorescent probe approaches, especially

environmentally sensitive fluorophores, provide information on the properties of their environment directly by changing their fluorescence characteristics such as wavelength maximum, fluorescence intensity, and fluorescence lifetime.¹⁷⁷

The *in situ* quantitative imaging of cellular lipids with a fluorescent probe has been reported by the Cho group in 2011.¹⁷⁸ They engineered the epsin *N*-terminal homology (ENTH) domain of membrane protein epsin 1,¹⁷⁹⁻¹⁸¹ and labeled it with the commercially available, environmentally sensitive fluorescent probe, 2-dimethylamino-6-acyl-naphthalene (DAN).¹⁸² When the protein labeled with the polarity sensitive fluorophore was bound to the lipid, [phosphatidylinositol-4,5-biphosphate (PtdIns(4,5)P₂)] the change in the environment of the fluorophore, from the polar environment of the protein to the non-polar lipid, resulted in a large blueshift in the emission of DAN which was accompanied by an increase in intensity of emission. This blue shift and increase in the intensity of emission could be used for the quantification of phosphatidylinositol in the cell.¹⁷⁸

A similar approach has been used for the *in situ* determination of PS by designing and constructing a new red fluorescent, environmentally sensitive probe with tunable emission properties and desirable water solubility which after being used to label the membrane protein PKC γ ,¹⁸³ changes its fluorescence intensity upon binding of PKC γ to the lipid PS.

4.3 Thiol Reactive Environment Sensitive Probes

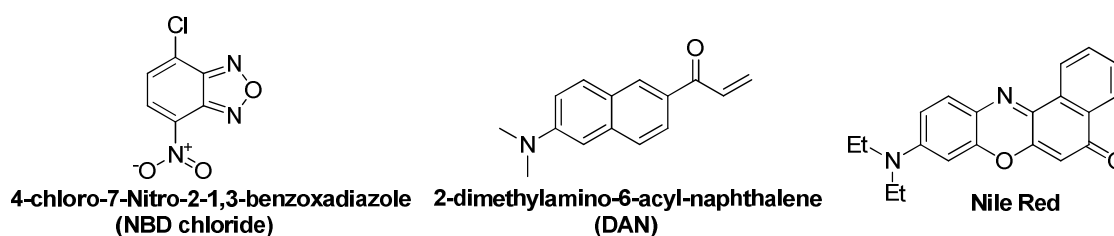
Thiol reactive environment sensitive probes are among the most useful probes in biochemistry.¹⁸⁴ This is because most proteins contain a cysteine which has a free thiol

group. The thiol group of the cysteine could form a disulfide bridge with a thiol on the fluorescent probe.¹⁸⁵ Another more popular approach involves using the thiol of the cysteine as a nucleophile in a Michael addition reaction with a Michael acceptor on the probe.¹⁸⁶ The resulting adduct has a strong C–S bond which does not cleave easily. This ensures that the protein remains labeled with the fluorescent probe during the duration of the study. Proteins can also be engineered to introduce a cysteine near the lipid binding site. This helps place the probe in close proximity to the lipid and hence the change in environment around the fluorophore is reflected in its emission.¹⁸⁷

4.3.1 Limitations of Currently Used Fluorophores

Currently used thiol reactive fluorescent probes for the *in situ* determination of lipids in cells are 4-chloro-7-Nitro-2-1,3-benzoxadiazole, (NBD chloride),¹⁸⁸ 2-dimethylamino-6-acyl-naphthalene (DAN), and Nile Red,¹⁸⁹ (Scheme 4.1). The 7-Nitro-2-1,3-benzoxadiazole (NBD), probe has been developed specifically for the *in situ* determination of PS.¹⁹⁰ NBD-tagged PS has been used extensively but is not efficient because of the distortion in the structure of the lipid upon insertion of NBD.¹⁹¹ The second fluorescent probe, DAN, has favorable spectral properties and can effectively partition into the membrane.^{178,192} It however, has a number of limitations. UV excitation of DAN causes fast photobleaching and could damage the cell. The emission spectrum of DAN overlaps with that of the Enhanced Green Fluorescence Protein¹⁹³ and with the intrinsic fluorescence of other proteins and peptides¹⁹⁴ but since DAN derivatives with fluorescence emission at longer wavelengths are difficult to synthesize, this represents a major challenge in dual imaging using DAN. The third commonly used fluorophore, Nile

Red,¹⁸⁹ is a red fluorescent probe that has been used for the determination and quantification of lipids in cells. Since it has an emission at $> 600\text{nm}$,¹⁹⁵ its emission spectrum does not overlap with the intrinsic fluorescence of the cell. But the synthesis of Nile Red is an arduous process and hence its derivatives are rare. This difficulty in synthesis combined with the poor water-solubility of Nile Red¹⁹⁶ is responsible for the investigation into new red fluorescent probes.



Scheme 4.1: Currently Used Environmentally Sensitive Fluorescent Probes

4.3.2 Desired Properties for New Probe

In order to overcome the limitations of the currently used fluorescent probes, a new probe was designed with the following desirable properties. It was important that the new fluorophore be environmentally sensitive. There should be a change in the emission, preferably a blue shift and an increase in the intensity of emission, when the environment of the fluorophore changed from polar to non-polar. Thus, when the protein labeled with the fluorophore moved from the polar aqueous environment of the cytoplasm of the cell, to the non-polar environment of the lipid, there should be a change in the emission properties of the fluorophore (Figure 4.1). This would signify the binding of the labeled

protein to the lipid and could be used to monitor the lipid-protein interactions.

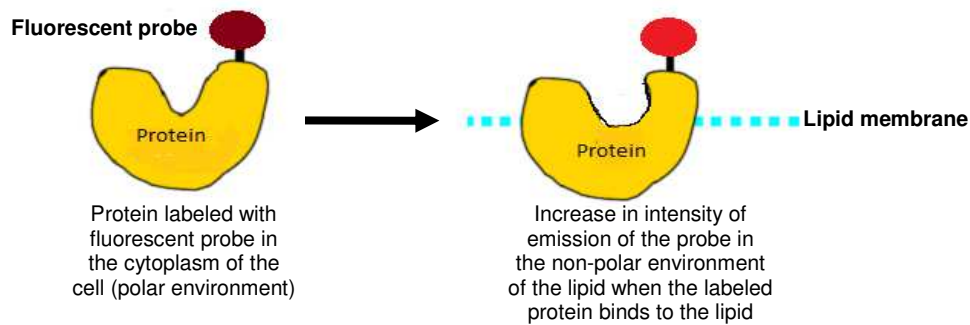


Figure 4.1: Change in the Environment of the Probe results in an Increase in the Intensity of Emission

The fluorophore also had to be soluble in water so that it could be injected into the cell without using organic solvents which would damage the cell. It had to be resistant to photobleaching and hence would not decompose upon exposure to UV light. It should also be easy to synthesize derivatives of the fluorescent probe which would have emissions at longer wavelengths. This would serve a dual purpose; first, the derivatives with emissions at longer wavelengths would not interfere with the intrinsic fluorescence of the cell. Secondly, two fluorophores, one with an emission at a shorter wavelength, and one with an emission at a longer wavelength could be used simultaneously for the *in-situ* determination of two different lipids in the cell. This would help in the better understanding of the complex cellular processes.

4.4 Modification of the Protein

The C1B domain of the PKC γ ¹⁹⁷ protein was modified such that it could bind irreversibly to the fluorophore without affecting the binding affinity of the protein

towards the lipid membrane. In order to achieve binding to the thiol reactive fluorescent probe, a Cysteine (Cys) residue was required to be present near the lipid binding portion of the protein. The PKC γ protein has several Cys, but none near the lipid binding domain. Most of the Cys on the protein were involved in Zn co-ordination and hence unavailable for binding to the probe. One free Cys residue, not involved in Zn co-ordination and which was present far away from the lipid binding site, was mutated to a Serine (Ser) to prevent it from reacting with the thiol reactive fluorescent probe. An Arginine (Arg) residue present near the lipid binding domain was then mutated to a Cys which, through its free thiol, would serve as a Michael donor and bind to the Michael acceptor on the fluorophore. These modifications reduced the binding affinity of the protein toward the lipid (PS) and necessitated the mutating of two Ser on the membrane binding surface to Trp. After all these modifications, (Figure 4.2) the resulting protein could effectively bind to both the fluorophore and the lipid. This work was done by the Cho lab at UIC.

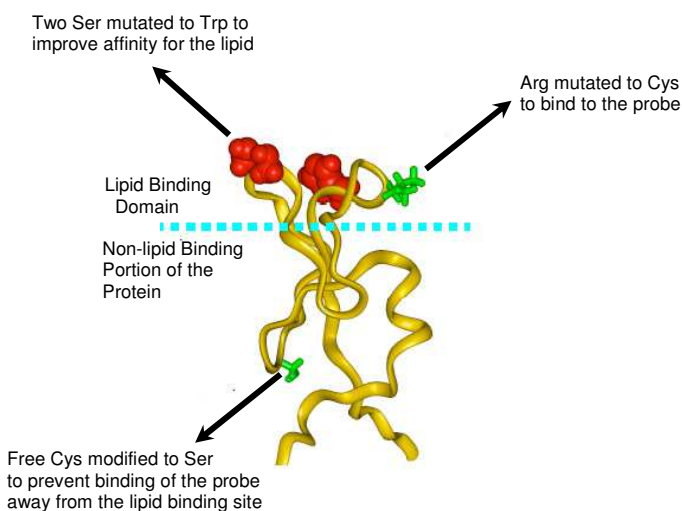


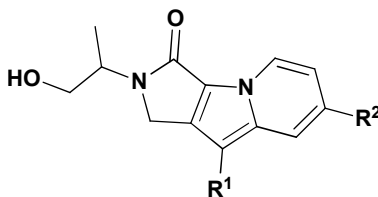
Figure 4.2: Modifications to the PKC γ Protein to Ensure Binding to both the Probe and the Lipid

4.5 Design of New Environmentally Sensitive Probes

Several core structures were examined to find the fluorophore which would meet all the requirements discussed above in terms of water solubility, efficient binding to the protein, environment sensitivity and ease of synthesis. The structure of the fluorophore was modified several times depending on the assays conducted by the Cho lab.

4.5.1 Fluorophore Containing Indolizine Core

Fluorophores with an Indolizine core as shown in Scheme 4.2 were reported by Kim *et. al.* in 2008.¹⁹⁸



Scheme 4.2: Fluorophores Containing an Indolizine Core

The authors then investigated the emission properties for these compounds by varying the R¹ and R² groups. They discovered that by changing the electronics of R¹ and R², the emission could be easily tuned as shown in Figure 4.3.¹⁹⁸

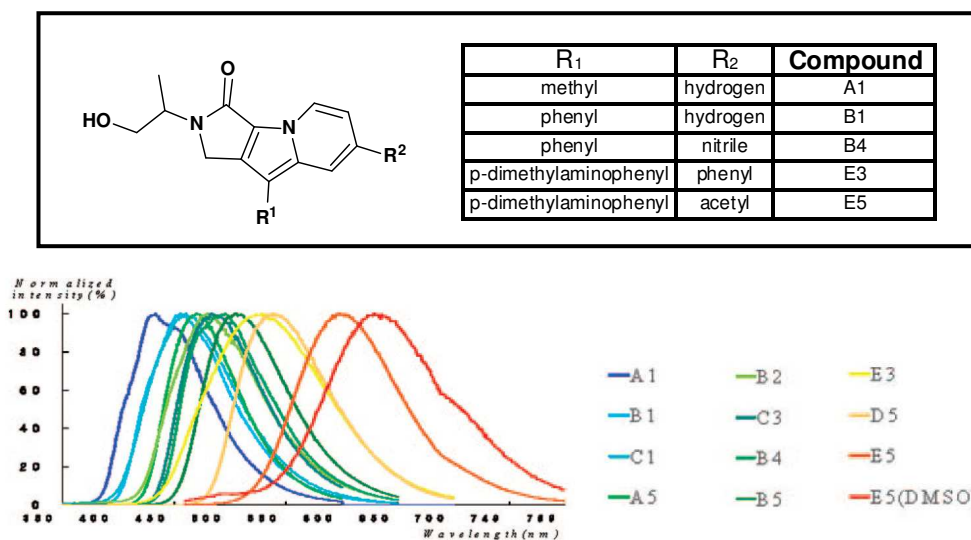
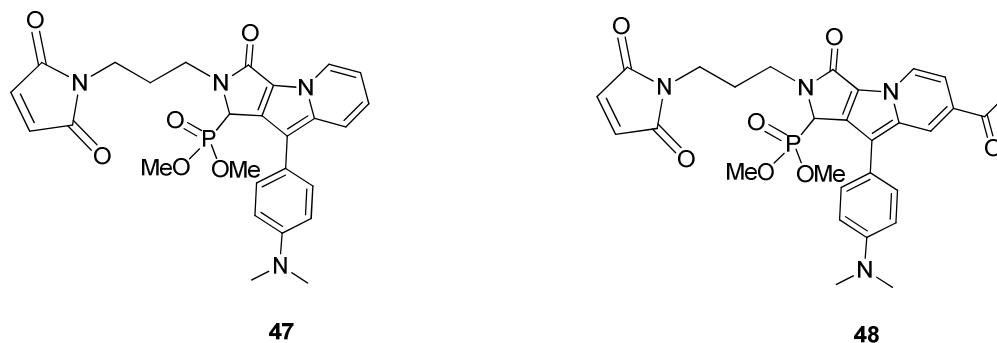


Figure 4.3: Varying the Emission Properties of the Fluorescent Probe

When R^1 was an electron donating group and $R^2 = H$, the compound exhibited blue fluorescence. As R^2 was made more electron withdrawing, there was a shift in the emission towards longer wavelengths as exhibited by the compound B4 which has $R^1 = \text{phenyl}$ and $R^2 = \text{nitrile}$. After using DFT calculations, the authors discovered that R^1 was the HOMO for the system and R^2 was the LUMO. Hence, by placing an electron donating group at R^1 and an electron withdrawing group at R^2 , more electron delocalization would be possible resulting in either orange or red fluorescence. When the HOMO, LUMO gap was decreased by making R^1 strongly electron donating (when $R^1 = p\text{-dimethylaminophenyl}$) and R^2 electron withdrawing ($R^2 = \text{phenyl}$), the compound E3 had yellow fluorescence. By making R^2 a strongly electron withdrawing acetyl group and keeping R^1 as *p*-dimethylaminophenyl, maximum electron delocalization was achieved and the resulting compound exhibited red fluorescence.¹⁹⁸

We sought to model our fluorophores on similar lines by using an indolizine core, changing the substituents at R^1 and R^2 , and increasing water solubility.

4.5.2 Target Fluorophores



Scheme 4.3: Target Fluorophores

Our target fluorophores are shown in Scheme 4.3. These fluorescent probes had the indolizine core and the strongly electron donating *p*-dimethylaminophenyl group at R¹ similar to the fluorophore reported by Kim and coworkers.¹⁹⁸ Compound **1** had R² = H and compound **2**, had R² = acetyl. To increase the water solubility of these otherwise hydrophobic substrates, a phosphonate moiety was introduced into the indolizine core. The phosphonate could be further hydrolyzed to the phosphonic acid which would further improve the water solubility. The effect of the phosphonate on the emission properties, however, was not known. The purpose of introducing the maleimide side chain shall be discussed in the next section.

4.5.3 Introducing the Maleimide Side Chain

As mentioned above in Section 4.3, the protein PKC γ was modified to have a free Cys near its lipid binding domain. The thiol of the Cys could serve as a Michael donor and react with a Michael acceptor on the fluorophore (Figure 4.4). It was therefore necessary to introduce a Michael acceptor onto the target fluorophore. The most widely

available and easy to install Michael acceptor, maleimide was therefore chosen to be installed onto the indolizine core.

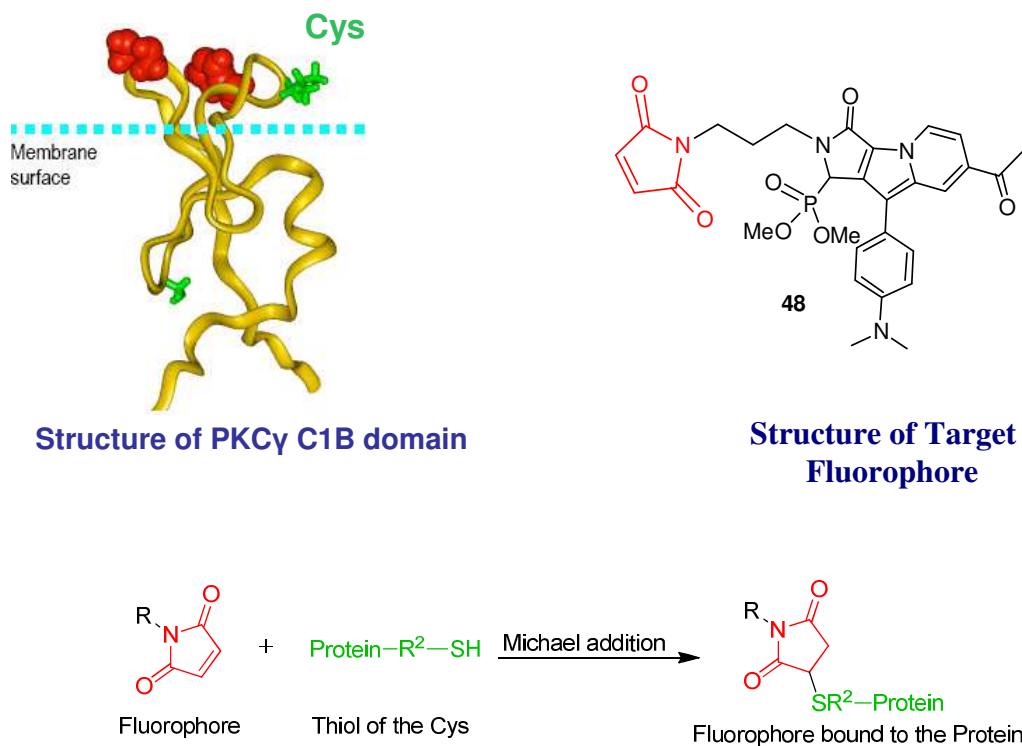
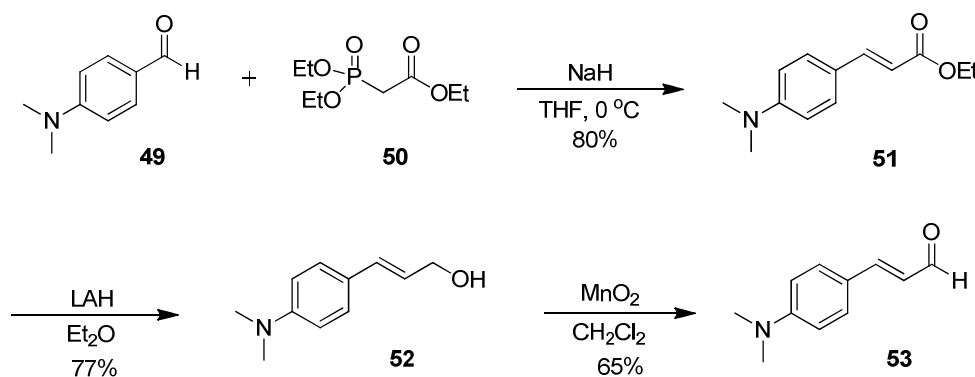


Figure 4.4: Installing a Michael Acceptor on the Target Fluorophore

After the Michael addition reaction, the resulting adduct containing the fluorophore bound to the protein would constitute the labeled protein and this could be used to monitor the lipid-protein interactions. The Michael reaction, forming the new C-S bond, would be an irreversible process, thus ensuring that the fluorophore would not fall off during the course of the experiment.

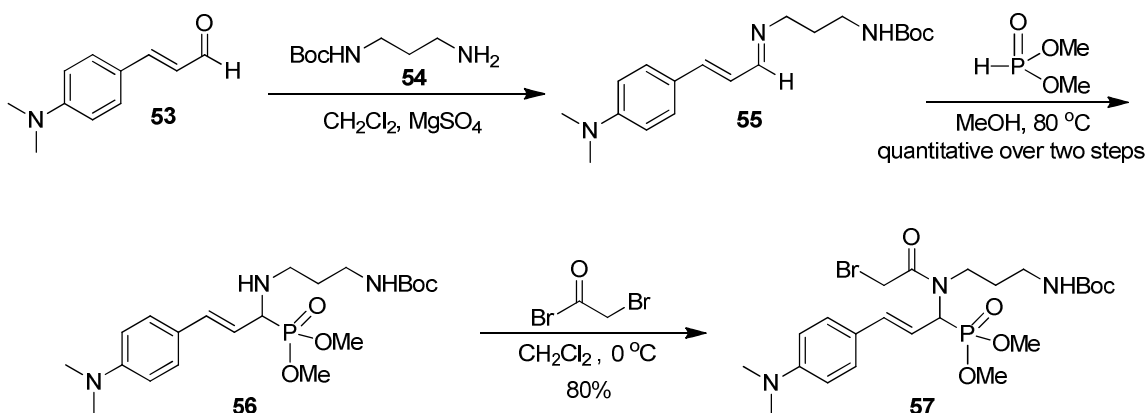
4.6 Green Fluorescent Compound

Our synthesis for target fluorophore **47** which had $R^1 = p$ -dimethylaminophenyl and $R^2 = H$, was based on the synthesis reported by Kim *et. al.*¹⁹⁸ This resulting compound exhibited green fluorescence. The synthesis for **47** begins in Scheme 4.4. *p*-dimethylaminocinnamaldehyde was synthesized from commercially available *p*-dimethylaminobenzaldehyde **49**. A Horner-Wadsworth-Emmons reaction between triethylphosphonoacetate **50** and *p*-dimethylaminobenzaldehyde **49** resulted in the formation of the α,β -unsaturated ester **51**. Reduction with LAH gave the allylic alcohol **52** which was oxidized to the *p*-dimethylaminocinnamaldehyde **53** with MnO_2 .



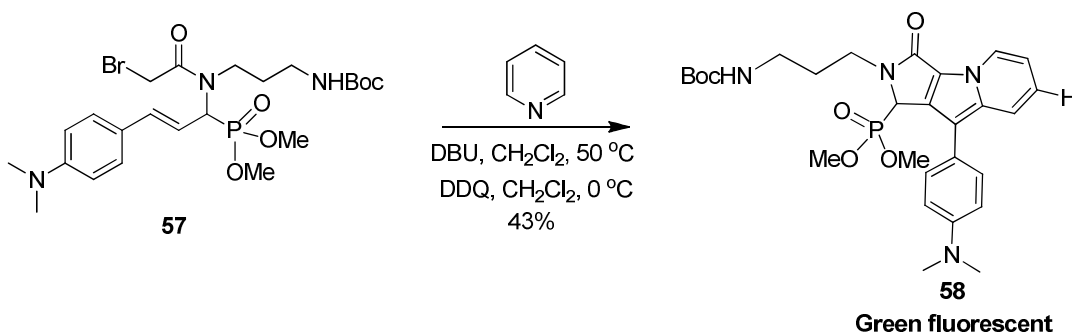
Scheme 4.4: Synthesis of *p*-Dimethylaminocinnamaldehyde

The *p*-dimethylaminocinnamaldehyde **53** was condensed with mono-Boc protected ethylenediamine **54** to form the imine **55** which was then treated with dimethylphosphite to form the phosphonate **56** in a quantitative yield over two steps. The phosphonate was then converted to the α -bromo amide **57** using bromoacetyl bromide and triethylamine (Scheme 4.5). The α -bromo amide **57** is the precursor for the cyclization reaction that forms the indolizine core.



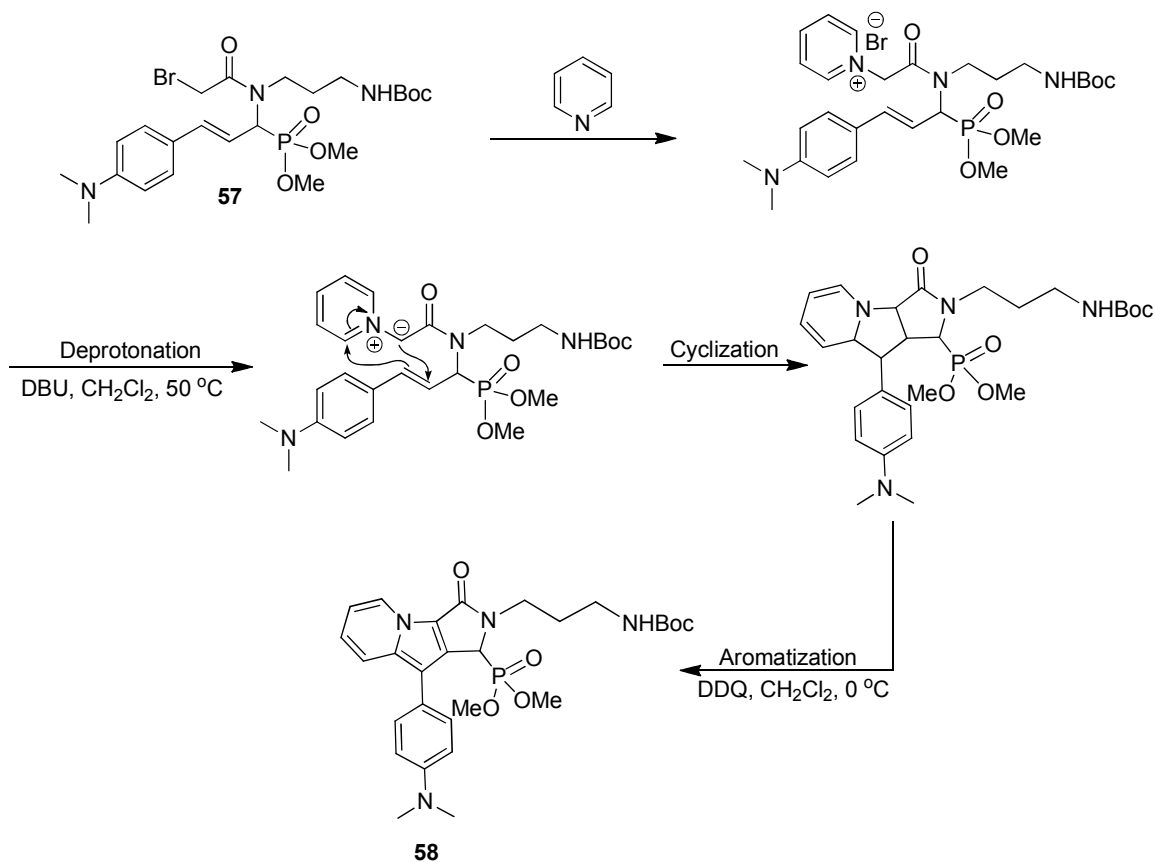
Scheme 4.5: Formation of the α -Bromo Amide

As shown in Scheme 4.6, the α -bromo amide **57** was treated with pyridine. This resulted in an $\text{S}_{\text{N}}2$ reaction to form the pyridinium salt. Deprotonation with DBU was followed by cyclization to form the polycyclic system. Aromatization by DDQ resulted in the formation of the green fluorescent compound **58** (Scheme 4.6).



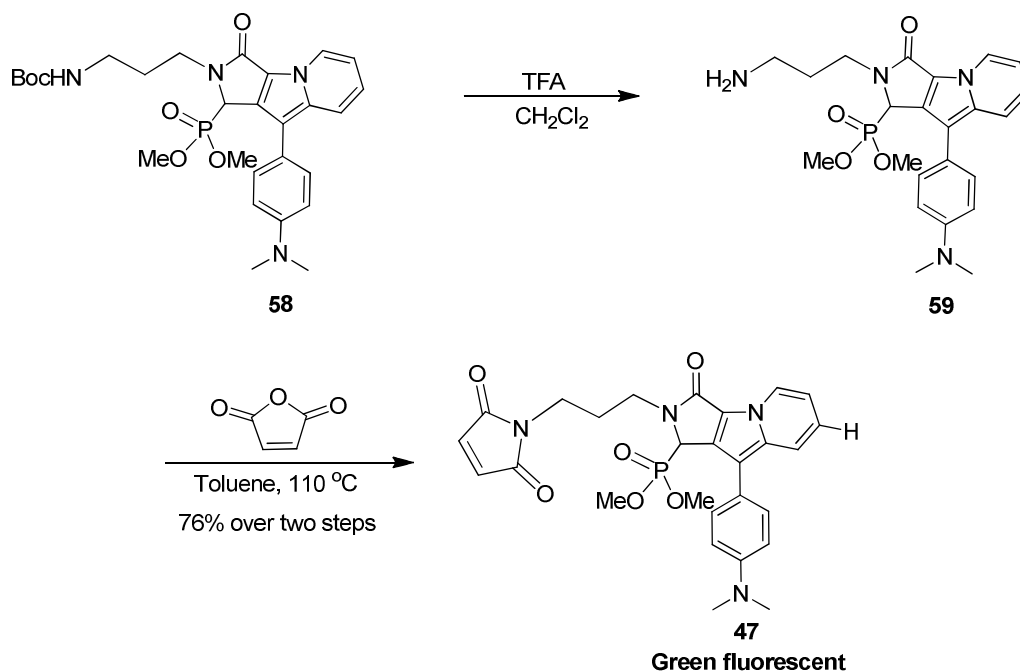
Scheme 4.6: Formation of the Green Fluorescent Compound

The mechanism for the above reaction is shown in Scheme 4.7.



Scheme 4.7: Mechanism of the Reaction to form the Indolizine Core

To convert the green fluorescent compound **58** into the target fluorophore **47**, the sulfide acceptor had to be installed. To this end, the Boc group was deprotected with TFA and the resulting free amine **59** was treated with maleic anhydride to form the maleimide in **47**, which would function as the Michael acceptor for the thiol of the Cysteine (Scheme 4.8).



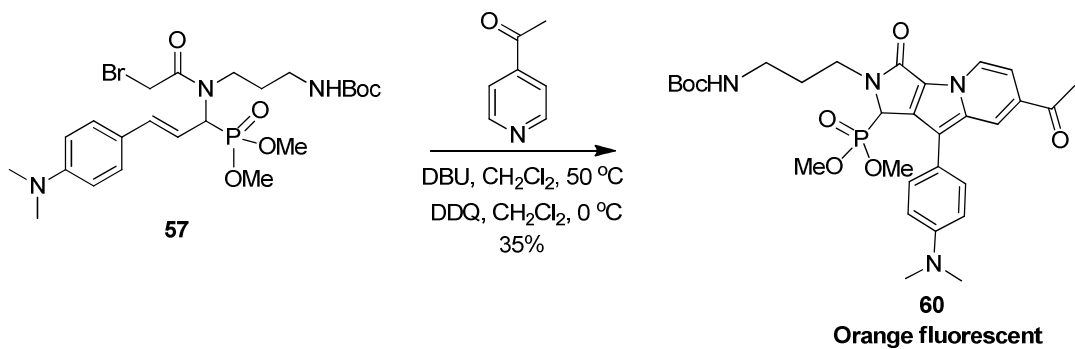
Scheme 4.8: Final steps in the synthesis of the Green Fluorescent Probe

For the indolizine cores reported by Kim *et. al.*,¹⁹⁸ placing the *p*-dimethylaminophenyl at R² and hydrogen at R¹, the compound had yellow fluorescence. Our compound having the same groups at R¹ and R² exhibited green fluorescence. This decrease in the emission could be attributed to the phosphonate group.

4.7 Orange Fluorescent Compound

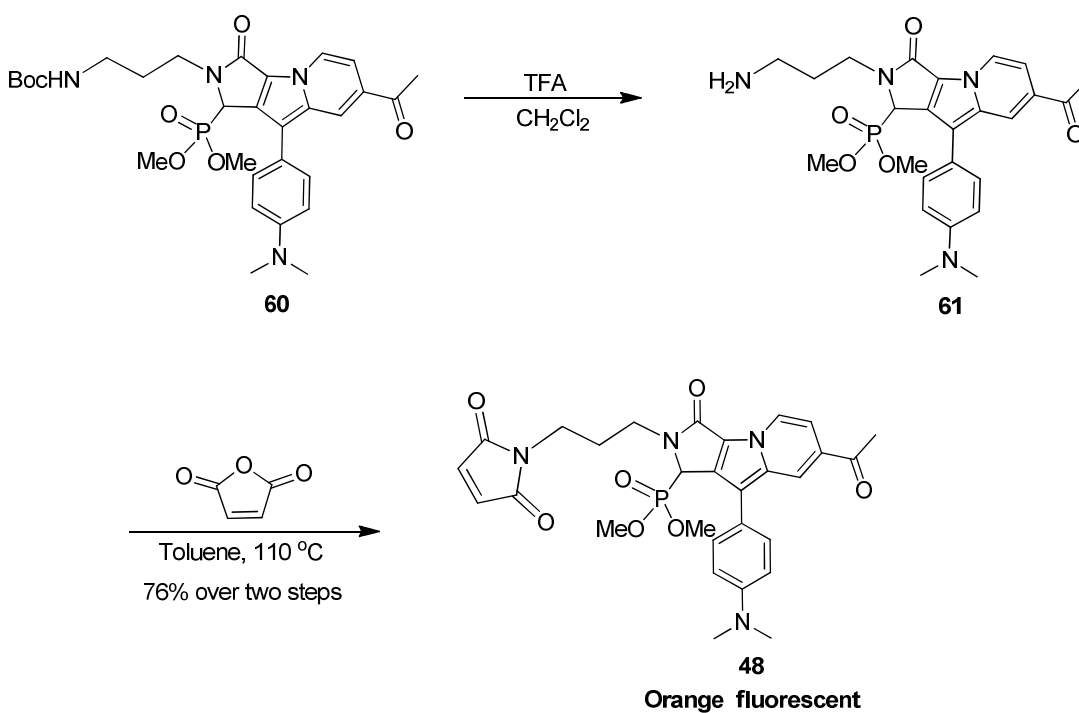
As per the calculations done by the Kim *et. al.*,¹⁹⁸ by making R² more electron withdrawing, the HOMO, LUMO gap could be decreased thereby increasing the wavelength of emission. We therefore decided to place an acetyl group at R² which would result in the compound having orange fluorescence. The synthesis for the orange fluorescent compound was similar to compound **47**. The *p*-dimethylamino cinnamaldehyde **53** was synthesized as shown in Scheme 4.4. It was then converted to the

α -bromo amide **57** following the same sequence as in Scheme 4.5. Cyclization with 4-acetyl pyridine and then rearomatization with DDQ resulted in the desired product **60** (Scheme 4.9).



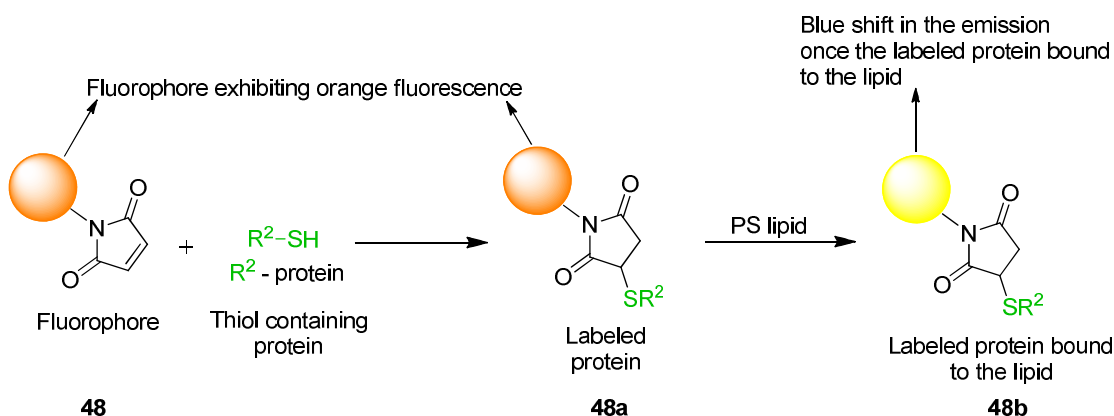
Scheme 4.9: Synthesis of the Orange Fluorescent Compound

This was followed by deprotection of the Boc group and installation of the maleimide to form the desired thiol reactive probe **48** (Scheme 4.10).



Scheme 4.10: Installing the Maleimide Group**4.7.1 Testing the Compound with Phosphatidylserine**

The compound **48** which had an emission in the orange region of the spectrum was first bound to the protein via a Michael reaction between the thiol of the Cys in the protein and the maleimide of the fluorophore. Once this reaction was complete, the labeled protein **48a** was purified by passing it through a column. To a solution of this labeled protein **48a**, was added the PS lipid and the emission of the fluorophore in the presence of the lipid was measured. It was expected that there would be a blue shift (to yellow fluorescent) in the emission of the fluorophore in the presence of the lipid. This would be because there would be a change in the environment of the fluorophore from aqueous to non-polar of the lipid when the labeled protein was bound to the PS lipid **48b** (Figure 4.5).

**Figure 4.5:** Expected Change in the Emission of the Fluorophore

However, once the PS lipid was added to a solution of the labeled protein **48a**, there was no change in the emission of the fluorophore (Figure 4.6).

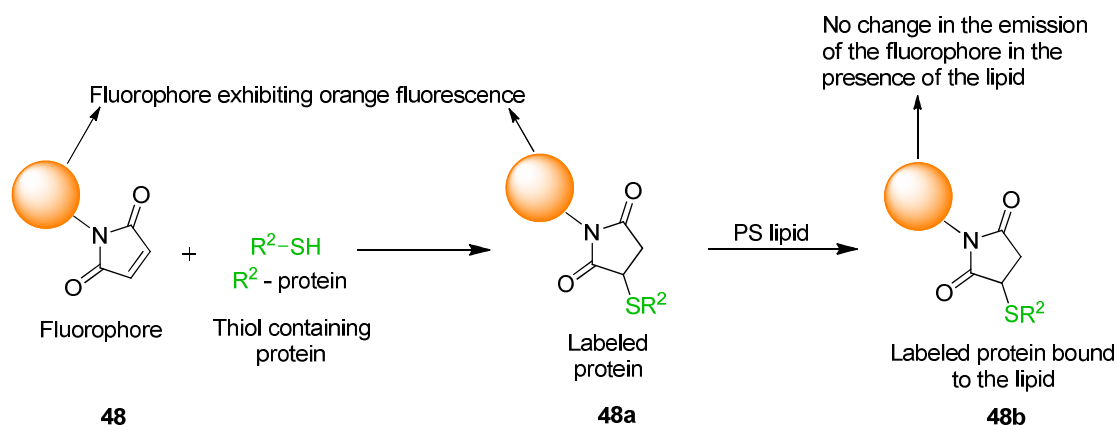


Figure 4.6: No Change in the Observed Emission of the Fluorophore

This lack of blue shift in the emission could be attributed to a rotation of the fluorophore away from the lipid membrane in **48b** as shown in Figure 4.7.

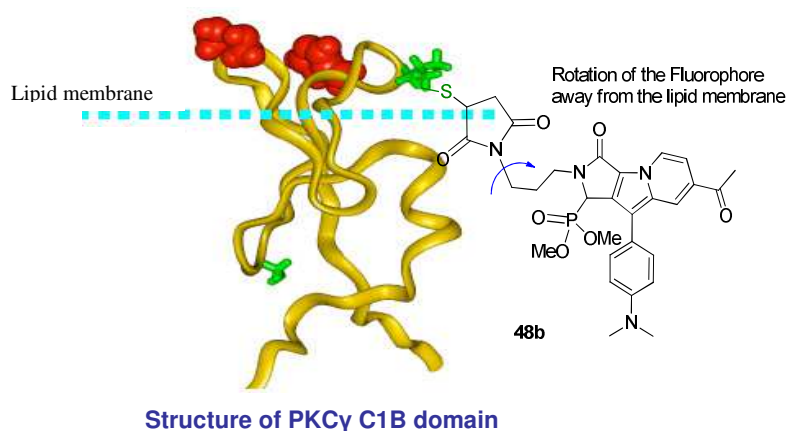


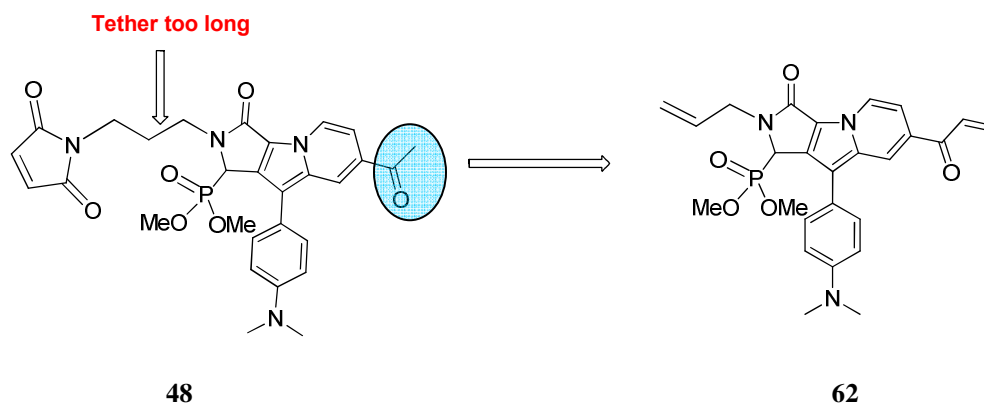
Figure 4.7: Hypothesis to Explain Observed Results

Since the tether length between the maleimide unit and the fluorophore in **48** was three carbon atoms long, we hypothesized that it could allow the rotation of the fluorophore away from the lipid in **48b**. Thus, the fluorophore was far away from the non-polar lipid and hence there was no change in the environment of the fluorescent probe. This could

explain the fact that there was no change in the color or the intensity of the emission when the labeled protein was bound to the lipid.

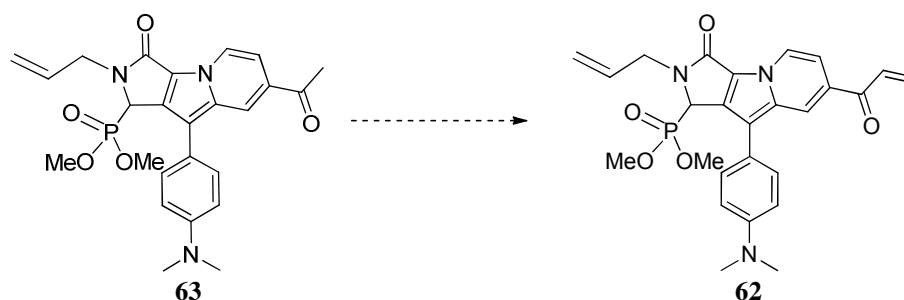
4.7.2 Modification in the Structure of the Fluorophore

Since the fluorophore that we had previously designed did not work well in the presence of the lipid, we decided to introduce some modifications in the structure. From the previous experiment, we had concluded that the tether length between the maleimide and the fluorophore was the problem. Our first approach was to reduce the tether length so that the fluorophore would not be able to rotate away from the lipid membrane. However all attempts to reduce the tether from a three carbon chain to a two or one carbon long tether were unsuccessful. We therefore decided to change the Michael acceptor from a maleimide to an α,β -unsaturated ketone. The easiest method to install this new sulfide acceptor would be to convert the acetyl group at R² in **48** to the α,β -unsaturated ketone **62** (Scheme 4.11). This would serve two purposes, first the α,β -unsaturated ketone would serve as a Michael acceptor to bind to the protein and second, the unsaturated ketone would be more electron withdrawing than the acetyl group, thus further lowering the LUMO. This could result in an increase in the wavelength of the emission, potentially making the compound red fluorescent.



Scheme 4.11: Modifications in the Structure of the Fluorophore

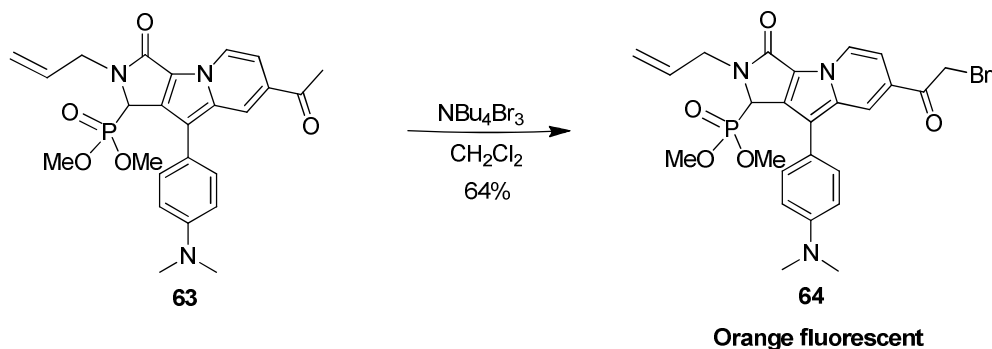
A number of methods were tried to convert the acetyl group at R^2 in compound **63** to the α,β -unsaturated ketone **62**. The compound **63** (Scheme 4.12) was made in a manner similar to Schemes 4.6 and 4.7, but using allyl amine to condense with *p*-dimethylcinnamaldehyde **53** instead of the Boc protected ethylene diamine. However, the vinyl ketone was extremely reactive and would decompose before it could be isolated (Scheme 4.12).



Scheme 4.12: Converting the Acetyl Group at R^2 to the α,β -Unsaturated Ketone

Since the conversion of the acetyl group at R^2 in **63** to the vinyl ketone **62** was not successful, we decided to convert the acetyl group to an α -bromo ketone instead. The α -

bromo ketone in **64** would also function as a Michael acceptor to react with the thiol on the protein, and would be more stable than the vinyl ketone. This conversion was achieved using tertabutylammonium tribromide as shown in Scheme 4.13.



Scheme 4.13: Conversion of the Acetyl Group to the α -Bromo Ketone

The resulting compound **64** exhibited orange fluorescence. When this compound was bound to the protein and then tested in the presence of the PS lipid, it did not show any blue shift but showed an increase in intensity of emission.

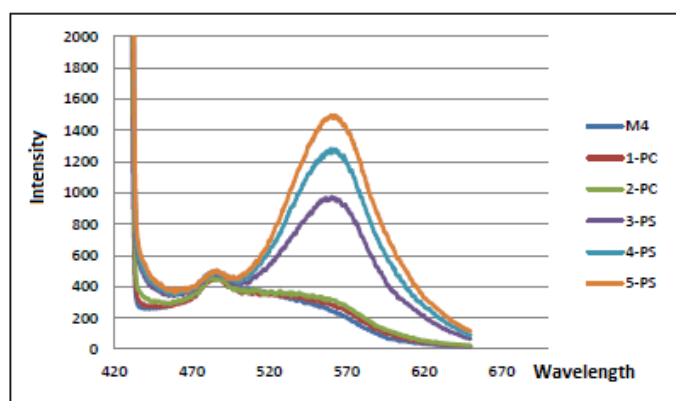


Figure 4.8: Plot of Intensity vs Wavelength that Shows an Increase in Intensity of Emission

As shown above, Figure 4.8 is a plot of intensity of emission vs the wavelength of emission for the orange fluorescent compound **64**. M4 is the intensity for the protein labeled with the fluorophore. When the lipid phosphatidylcholine (PC) is added to the labeled protein, there is no change in the intensity of emission (shown as 1-PC and 2-PC). However, when the lipid PS is added to a solution of the labeled protein, (shown as 3-PS in the graph) there is a 1000 fold increase in intensity. Upon doubling and then tripling the concentration of PS (shown as 4-PS and 5-PS respectively) there is a 1400 fold increase in intensity. This establishes the fact that fluorophore **64** can be used to monitor protein-PS interactions and is specific for PS.

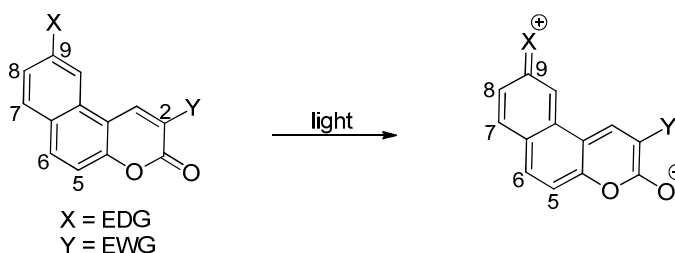
4.8 Designing new Fluorophores

To complete our library of fluorescent probes, we wanted to synthesize a red fluorescent compound. The indolizine fluorescent probe **64** could be successfully used in a physiological system to monitor lipid-protein interactions, but exhibited orange fluorescence. We therefore decided to explore other fluorophore core structures containing either an α -bromo ketone or a vinyl ketone as the sulfide acceptor, in an attempt to ultimately design and synthesize the desired red fluorescent, thiol reactive, environmentally sensitive probe which could be successfully used to monitor protein-PS interactions.

4.8.1 Naphthopyranone Cores

Naphthopyranones belong to the coumarin family, and are considered as coumarins with an additional fused benzene ring. While coumarins have been known to

have interesting photophysical properties and have been extensively investigated for their electronic and photonic applications,¹⁹⁹ there has been limited study on the naphthopyranones. The fluorescence of naphthopyranones varies drastically depending upon the position of substituents on the core (Scheme 4.14). Placing an electron donating group (EDG) at C9 dramatically improves the emission properties. This is because of an intramolecular charge transfer (ICT) from the EDG group to the carbonyl group of the lactone. A synergistic effect to enhance the intensity of emission was observed when an electron withdrawing group (EWG) was placed at C2.²⁰⁰

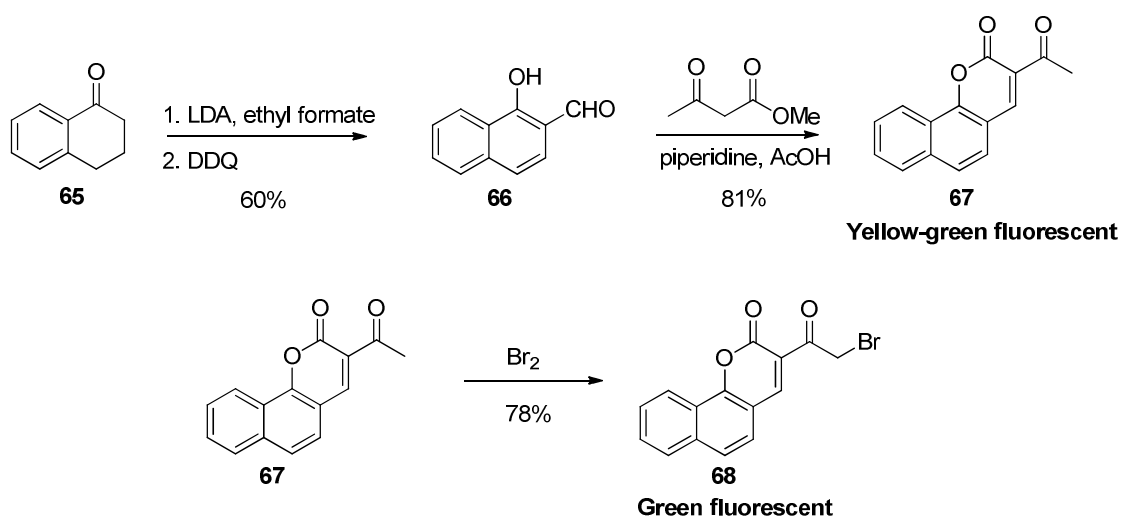


Scheme 4.14: ICT in Naphthopyranones

The Naphthopyranones usually have an emission around 510 nm. We wanted to modify the structures to attempt to make these compounds orange or red fluorescent while also installing a sulfide acceptor. To synthesize this new fluorophore, we started with α -tetralone **65** which was converted to 1-hydroxy-2-naphthaldehyde **66** by using LDA and ethyl formate followed by aromatization with DDQ. The naphthaldehyde was converted to the naphthopyranone **67** via a Knoevenagel Condensation. This compound **67** exhibited green-yellow fluorescence. With the desired core in hand, the ketone was then converted to the α -bromo ketone **68** (Scheme 4.15). The final compound had green fluorescence. However, the main problem with these compounds was their limited water

solubility. They were extremely hydrophobic and hence could not be used to even bind to the protein, which is available as an aqueous solution.

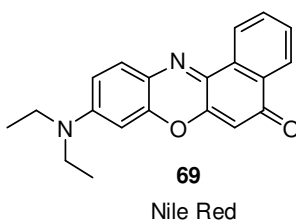
We then attempted to synthesize derivatives of the naphthopyranones which would have electron donating groups like methoxy, hydroxyl or substituted amines at C9. We hypothesized that this would not only increase water solubility, but also result in emission at longer wavelengths. However, all endeavors to further derivatize the naphthopyranone core were unsuccessful.



Scheme 4.15: Synthesis of a Probe Containing the Naphthopyranone Core

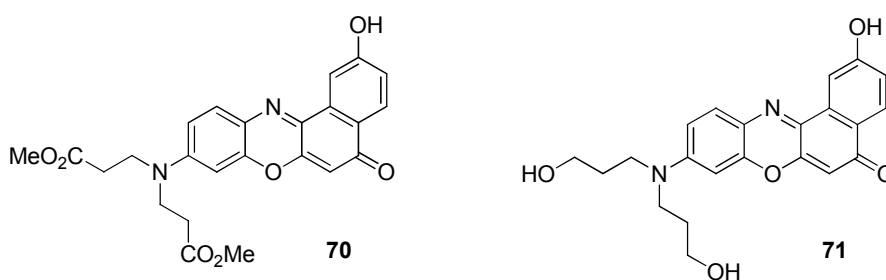
4.8.2 Nile Red Derivatives

Nile Red **69** is a solvatochromic oxazine²⁰¹ dye whose general structure is shown in Scheme 4.16.



Scheme 4.16: General Structure of Nile Red

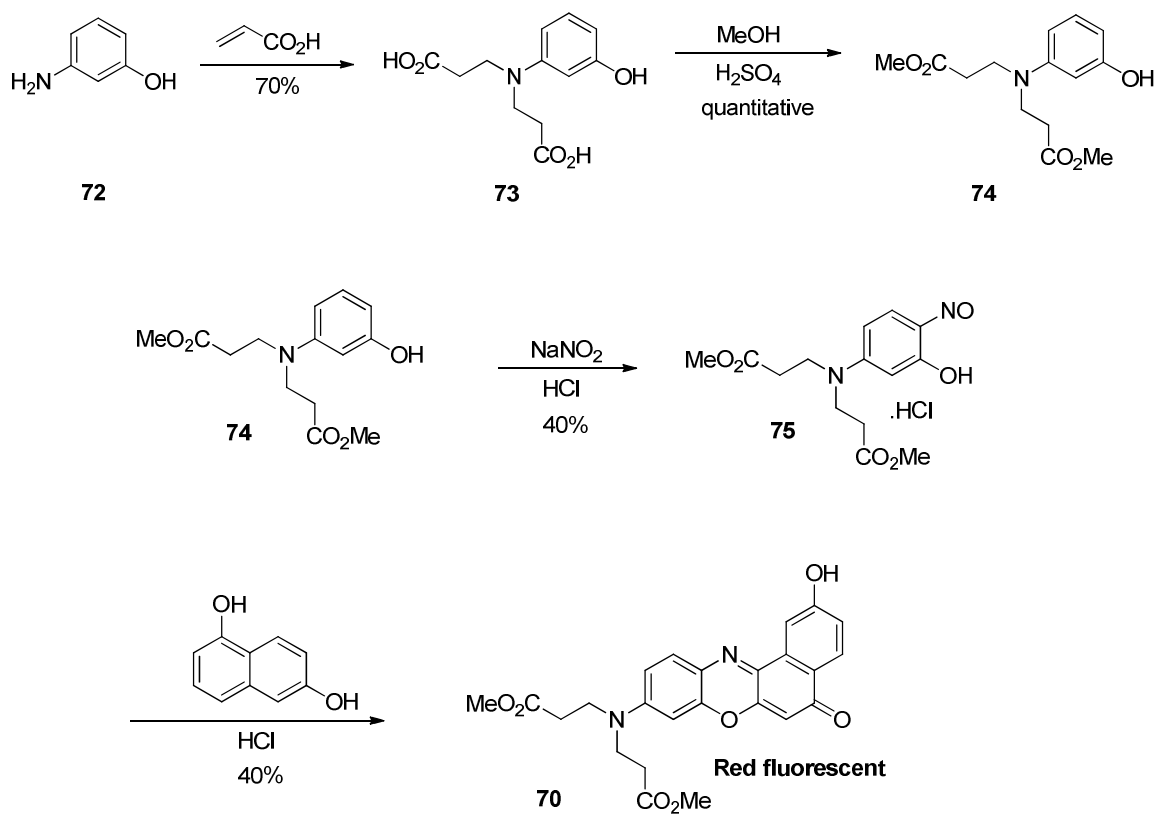
This compound is red fluorescent in organic solvents but is insoluble and non-fluorescent in aqueous media. The Burgess group reported in 2006 that by introducing a hydroxyl group on the core, and modifying the diethyl group on the amine, Nile Red could be made water soluble and fluorescent in an aqueous medium¹⁹⁶ (Scheme 4.17).



Nile Red Derivatives Soluble in Water

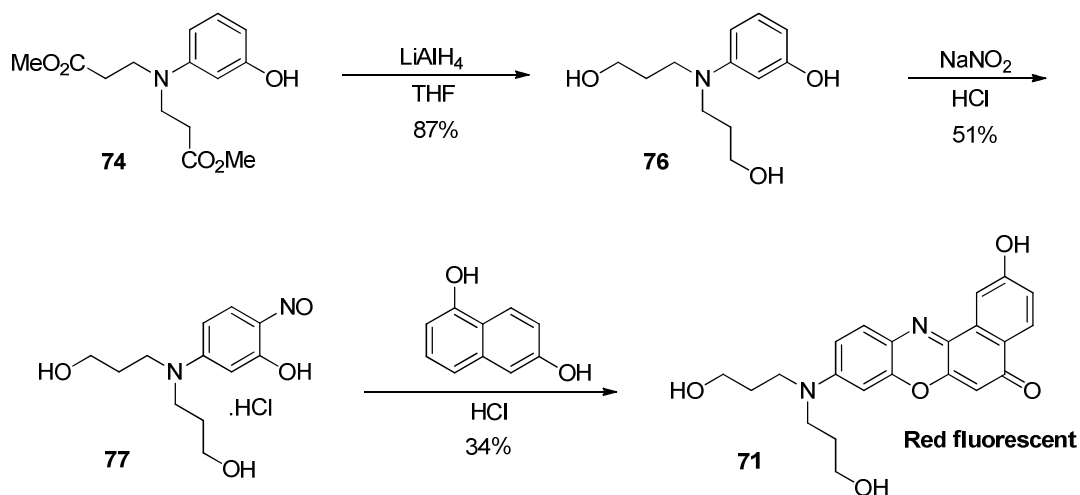
Scheme 4.17: Nile Red Derivatives that are Water Soluble and Red Fluorescent

We decided to model our next fluorescent probe on this Nile Red Derivative. Since it was already water soluble, we needed to introduce a thiol reactive group on the core so that it could bind with the protein. Our synthesis is shown in Scheme 4.18. 3-aminophenol **72**, upon reaction with acrylic acid gave the dicarboxylic acid **73** which was then converted to the dimethylester **74** with methanol. Sodium nitrite and hydrochloric acid were then used to convert the phenol to the nitroso compound **75** which was extremely unstable and was immediately converted to Nile Red **70** upon treatment with naphthol. Nile Red was thus obtained as shiny red crystals, albeit in a low yield.



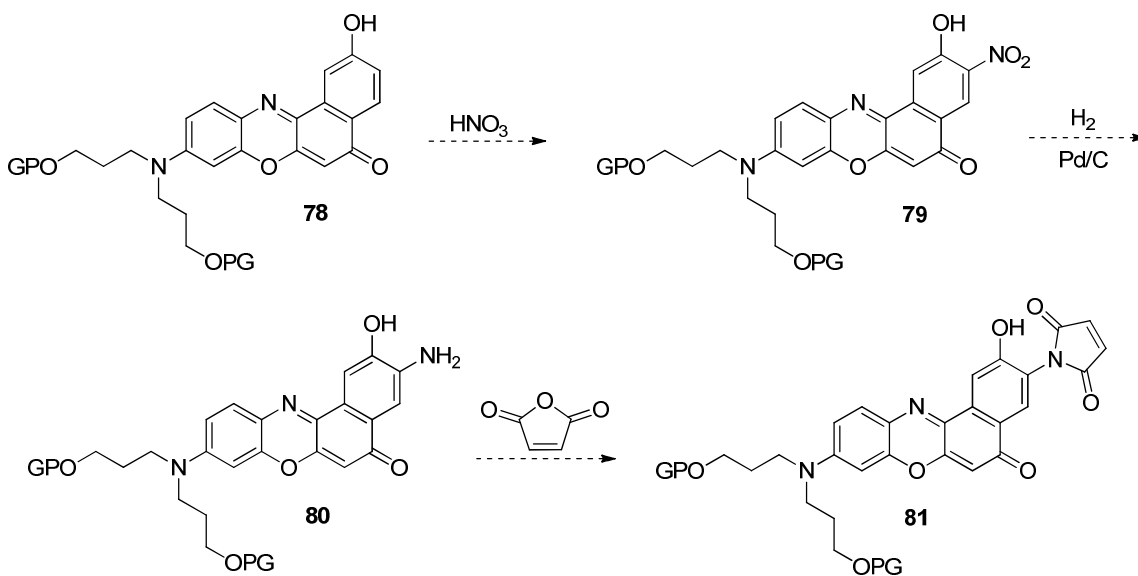
Scheme 4.18: Synthesis of Nile Red Derivative

The other Nile Red derivative reported by the Burgess group¹⁹⁶ was synthesized in a manner similar to the one above. Reduction of diester **74** with lithium aluminium hydride gave diol **76** which was converted to the nitroso compound **77**. Treatment of **77** with 1,6-dihydroxynaphthol gave the Nile Red derivative **71** (Scheme 4.19).



Scheme 4.19: Synthesis of Water Soluble Nile Red Derivative

Our next strategy was to introduce a nitro group onto the core of either **70** or **71** (either the diester or after protection of the diol in **71**) to give **79** which could then be reduced to an amine **80**. The amine **80** could condense with maleic anhydride to form maleimide **81** which could serve as a thiol acceptor (Scheme 4.20).

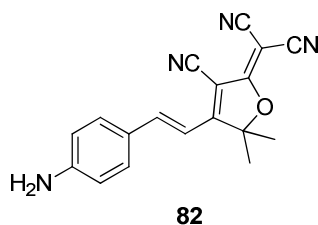


Scheme 4.20: Proposed Modification of Nile Red

However, all attempts to nitrate, brominate or acylate the core of Nile Red failed. Conversion of the phenol to triflate and then cross coupling to introduce an alkene moiety onto the ring, which could be further derivatized, was also unsuccessful. We therefore, decided to try another core structure for the fluorophore.

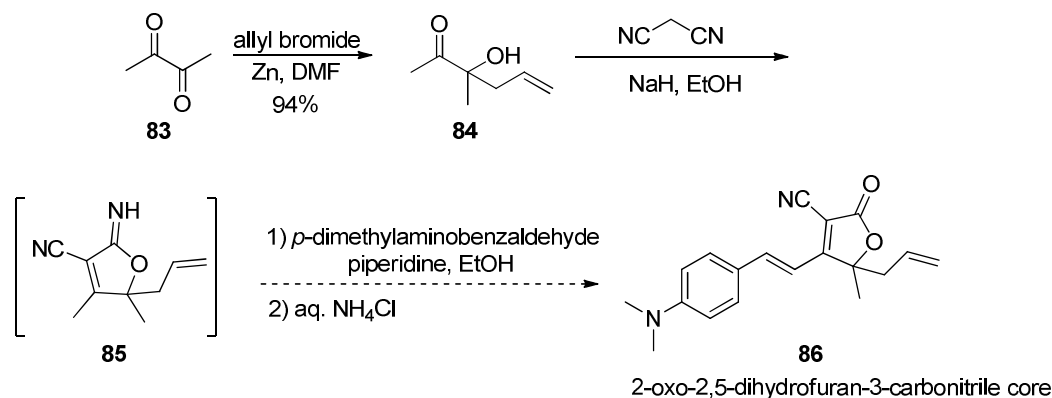
4.9 2-Imino-2,5-Dihydrofuran-3-Carbonitrile Containing Probe

Fluorescent compounds based on a 2-dicyanomethylene-3-cyano-2,5-dihydrofuran core **82** were reported by Tsou *et. al.* in 2009. These fluorescent dyes enabled visualization of nucleic acids, proteins and metabolites in biological systems (Scheme 4.21). The authors also reported that these probes had red fluorescence (if there was an electron donating group such as aniline in conjugation with the core) and high photo stability.²⁰²



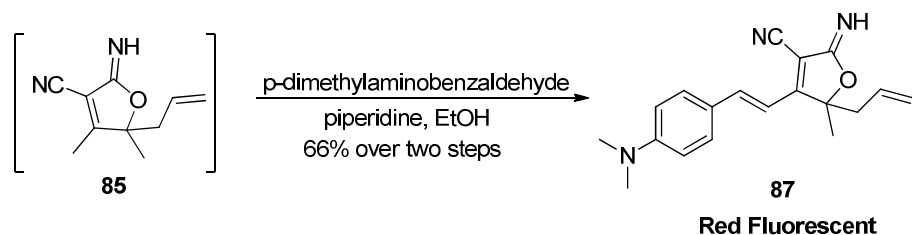
Scheme 4.21: 2-Dicyanomethylene-3-cyano-2,5-dihydrofuran Core

Based on our work with the indolizine cores, we wanted to use *p*-dimethylamino phenyl as the strongly electron donating group, and then reduce the cyano group to install the sulfide acceptor.



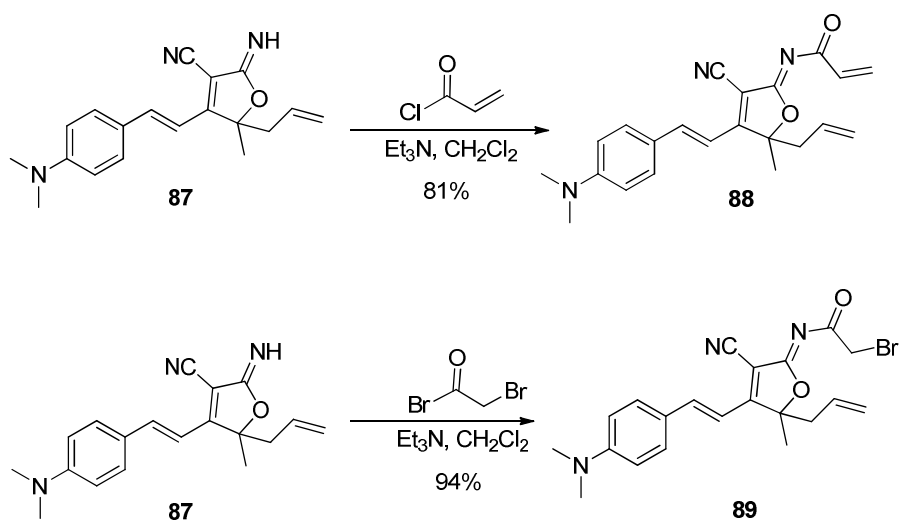
Scheme 4.22: Synthesis of Red Fluorescent Compound

Our synthesis started with a Barbier reaction between 2,3-butanedione **83** and allyl bromide in the presence of Zn (Scheme 4.22). The tertiary alcohol **84** obtained underwent a cyclization with malononitrile followed by Knoevenagel condensation of the intermediate **85** with 4-dimethylaminobenzaldehyde. We expected the imine functionality to hydrolyze to the ketone after work up and isolation, and hence the product to contain a 2-oxo-2,5-dihydrofuran-3-carbonitrile core **86** which could be further manipulated to introduce the dicyanomethylene unit. However, upon further analysis with MS, IR and NMR, we concluded that the product of the Knoevenagel condensation was not the expected ketone, but instead was the imino-intermediate of the cyclization reaction **87** (Scheme 4.23). Such imino intermediates have been observed before in the reaction between salicylic aldehyde and malononitrile.²⁰³ Since the compound **87** exhibited bright red fluorescence, and could easily react with electrophiles, we decided to further explore this new fluorophore with the 2-imino-2,5-dihydrofuran-3-carbonitrile core.



Scheme 4.23: Formation of Fluorophore with 2-Imino-2,5-dihydrofuran-3-carbonitrile Core

The addition of the sulfide acceptor was achieved onto the imine functionality with acryloyl chloride or bromoacetyl bromide to furnish compounds **88** and **89** respectively (Scheme 4.24) which were first tested for their spectroscopic properties and then in the protein assays.



Scheme 4.24: Installing the Sulfide Acceptors

4.9.1 Spectroscopic Properties of the Red Fluorescent Compound in Different Solvents

It is known that the emission spectra of fluorescent compounds containing polar substituents on the aromatic rings are sensitive to the chemical and physical properties of solvents.²⁰⁴ As shown in Figure 4.9, compound **89** also exhibits solvatochromism wherein the emission bands vary in spectral position, shape and intensity depending upon the nature of the solvent.²⁰⁵

Excitation at 500nm using a concentration of 1mg/ml showed an increase in fluorescence intensity when the solvent used was non-polar. Thus, there was a 1000 fold increase in intensity upon changing the solvent from water to methanol and 4000 fold intensity when the solvent was dichloromethane. When chloroform was used as the solvent, the intensity was increased 12000 times, which after dilution was reduced to 6000. The blue shift of the maxima also corresponds to a decrease in the dielectric constant of the solvent. This confirms that the fluorescence of compound **89** is affected by its environment and that there is an increase in the intensity of emission when the environment of the fluorophore is hydrophobic.

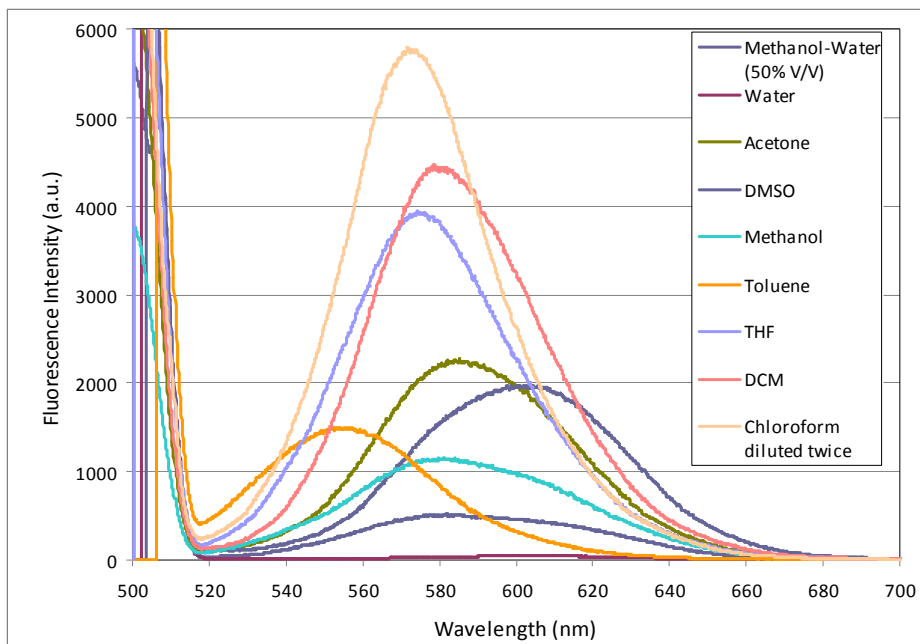


Figure 4.9: Fluorescence Emission Affected by Polarity of Solvents

4.9.2 Protein Labeling and In-Vitro Lipid Binding Assay

The fluorophore **89** was efficiently bound to the protein PKC γ , which then constituted the labeled protein. Varying concentrations of the lipid were then added to a solution of the labeled protein. The results are shown in Figure 4.10.

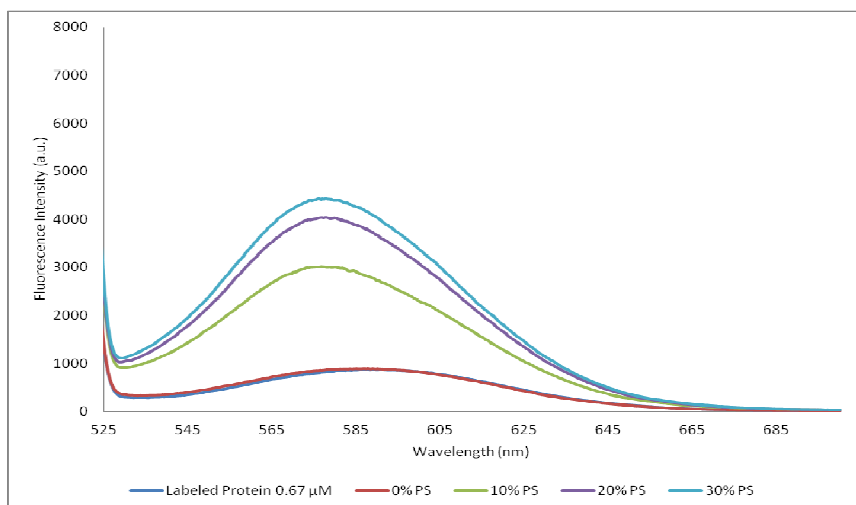


Figure 4.10: Addition of PS to the Labeled Protein

A 0.67 μM concentration of the labeled protein had an emission of 590 nm and an intensity of emission of about 1000 a.u. When a 10% PS solution was added to the labeled protein, there was a three fold increase in intensity to 3000 a.u. When a 20% PS solution was added, there was a four fold increase in intensity. There was only a slight increase in the intensity of emission when a 30% PS solution was used.

A plot of fluorescence intensity vs percentage of PS (Figure 4.11) showed that there was an initial sharp increase in the intensity, which then reached a maximum at 30% PS.

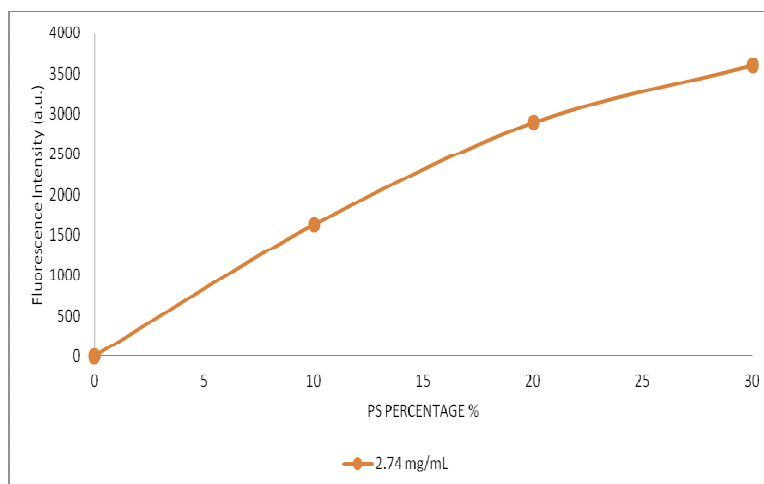


Figure 4.11: Plot of Fluorescence Intensity vs PS percentage

These protein labeling studies and assays were performed by Hamid Afsari in Prof. Wonwha Cho's lab at UIC.

4.10 Conclusion

In conclusion, we have been successful in designing and synthesizing a library of environmentally sensitive, thiol reactive fluorescent probes for the *in situ* determination of the lipid-protein interactions. Our fluorescent probes are tunable, easy to synthesize and cover a broad range of the spectrum from blue, green, yellow, orange and red. The most noteworthy of these probes are compounds **64** and **89**, which are orange and red fluorescent respectively. These compounds are water soluble, thiol reactive and have been used in the physiological system for the determination of PS in the cell. These new fluorescent probes exhibit an increase in intensity when the labeled protein is bound to the lipid because of a change in environment from aqueous polar of the cell to lipid non-polar. Therefore, they can be used for monitoring the PS-protein interactions in the cells

and can help in the understanding of these complex lipid mediated processes, which could in turn assist in finding a cure for diseases resulting from a dysfunction in the PS associated processes.

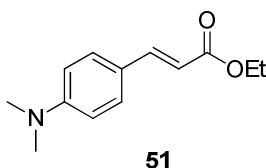
4.11 Supporting Information

4.11.1 Materials and Methods

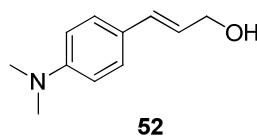
Reactions were carried out in oven or flame-dried glassware under a nitrogen atmosphere unless otherwise noted. Compounds were purchased from Aldrich unless otherwise noted. Tetrahydrofuran (THF) and diethyl ether (Et₂O) were freshly distilled from sodium/benzophenone, and dichloromethane (DCM) was distilled from calcium hydride (CaH₂) under nitrogen atmosphere. Flash chromatography was performed using silica gel 60 Å (32–63 mesh) purchased from Silicycle Inc. Analytical thin layer chromatography (TLC) was performed on 0.25 mm E. Merck precoated silica gel 60 (particle size 0.040–0.063 mm). Yields refer to chromatographically and spectroscopically pure compounds unless otherwise stated. ¹H NMR and ¹³C NMR spectra were recorded on a Bruker DRX-500 spectrometer. Chemical shifts are reported relative to chloroform (δ 7.26) for ¹H NMR and chloroform (δ 77.0) for ¹³C NMR; multiplicities are indicated by s (singlet), d (doublet), t (triplet), q (quartet), qn (quintet), m (multiplet), b (broad), and app (apparent). ¹H NMR signals that fall within a ca. 0.3 ppm range are generally reported as a multiplet, with a single chemical shift value corresponding to the center of the peak. Coupling constants, *J*, are reported in Hz (Hertz). Electrospray ionization (ESI) mass spectra were recorded on a Waters Micromass Q-ToF Ultima in the University of Illinois at Urbana-Champaign. Electron impact (EI) mass

spectra were obtained using a Micromass AutoSpec™. IR spectra were recorded using ATI Mattson, Genesis series FTIR.

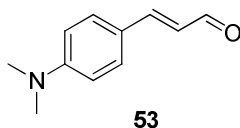
4.11.2 Experimental Procedures and Characterization Data



α,β -unsaturated ester 51: To the triethyl phosphonoacetate (2 g, 8.92 mmol) in THF (15 ml) at 0 °C was added NaH (356 mg, 8.92 mmol) and the reaction stirred at 0 °C for 10 mins and then at room temperature for 30 mins. The reaction was again cooled to 0 °C and 4-dimethylaminobenzaldehyde (950 mg, 6.37 mmol), dissolved in THF (4 ml), was added dropwise to the reaction mixture. It was then stirred at room temperature for 2 h and was quenched with saturated NH₄Cl and extracted with EtOAc (3 x 20 ml). The organic layer was washed with brine, dried with MgSO₄ and concentrated *in vacuo*. Flash chromatography with hexane:EtOAc 4:1 gave the desired product **51** (1.11 g, 80 %). ¹H NMR (500 MHz; CDCl₃): δ 7.62 (d, J = 16.1 Hz, 1H), 7.43 (d, J = 8.5 Hz, 2H), 6.60 (d, J = 8.5 Hz, 2H), 6.18 (d, J = 16.1 Hz, 1H), 4.09 (q, J = 7.4 Hz, 2H), 3.01 (s, 6H), 1.24 (t, J = 7.4 Hz, 3H); ¹³C NMR (125 MHz, CDCl₃): δ 167.9, 151.7, 145.1, 129.7, 122.2, 112.6, 111.8, 60.0, 40.1, 14.4; see Ref 206 for MS data.

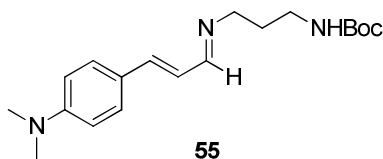


Allylic alcohol 52: A solution of lithium aluminium hydride (242 mg, 6.38 mmol) in Et₂O was cooled to 0 °C and the α,β -unsaturated ester **51** (1 g, 4.56 mmol) was added dropwise to it. The reaction was gradually allowed to warm up to room temperature and stirred at that temperature for 2 h. The reaction was cooled to 0 °C and sodium sulfate decahydrate was added until the white precipitate that formed, persisted. MgSO₄ (2 g) was added and the reaction mixture was filtered. The filtrate was concentrated to give the allylic alcohol **52** (770 mg, 77 %). ¹H NMR (500 MHz; CDCl₃): δ 7.30 (d, J = 8.7 Hz, 2H), 6.70 (d, J = 8.7 Hz, 2H), 6.52 (d, J = 15.8 Hz, 1H), 6.23-6.17 (m, 1H), 4.28 (d, J = 5.9 Hz, 2H), 3.49 (bs, 1H), 2.96 (s, 6H); ¹³C NMR (125 MHz, CDCl₃): δ 150.1, 131.3, 127.6, 125.5, 124.5, 112.7, 63.8, 40.6; see Ref 207 for HRMS.

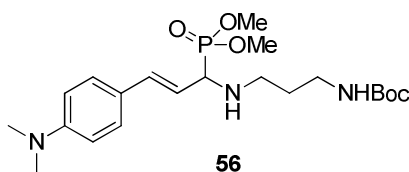


***p*-dimethylaminocinnamaldehyde 53:** To a solution of the allylic alcohol **52** (1 g, 5.64 mmol) in CH₂Cl₂ (40 ml) was added slowly MnO₂ (2.94 g, 33.85 mmol) and the reaction stirred for 1 h. The MnO₂ was filtered and the filtrate concentrated under reduced pressure. Flash chromatography with hexane:EtOAc 3:1 gave the desired aldehyde **53**. ¹H NMR (500 MHz; CDCl₃): δ 9.53 (d, J = 7.9 Hz, 1H), 7.39 (d, J = 8.6 Hz, 2H), 7.31 (d, J = 15.6 Hz, 1H), 6.62 (d, J = 8.6 Hz, 2H), 6.48 (dd, J = 15.6, 7.90 Hz, 1H), 2.98 (s, 6H);

^{13}C NMR (125 MHz, CDCl_3): δ 193.6, 154.1, 152.4, 130.5, 123.5, 121.6, 111.7, 40.0; see Ref 208 for HRMS.

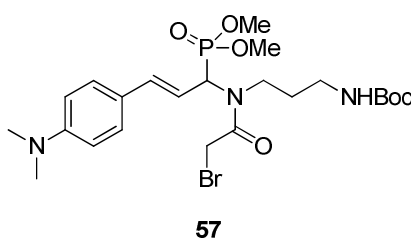


Imine 55: To the 4-dimethylaminocinnamaldehyde **53** (2 g, 11.41 mmol), in CH_2Cl_2 (10 ml) was added the Boc-protected propane-1,3-diamine **54** (2 g, 11.41 mmol) and MgSO_4 (1 g) and the reaction stirred at room temperature under an N_2 atmosphere for 12 h. The reaction was filtered to remove the MgSO_4 and the filtrate concentrated to obtain the imine **55** (3.8 g, 100 %) which was used without further purification. ^1H NMR (500 MHz; CDCl_3): δ 7.96 (d, $J = 8.8$ Hz, 1H), 7.36 (d, $J = 8.7$ Hz, 2H), 6.86 (d, $J = 15.8$ Hz, 1H), 6.72-6.57 (m, 3H), 3.51 (t, $J = 6.5$ Hz, 2H), 3.20 (t, $J = 6.5$ Hz, 2H), 2.89 (s, 6H), 1.84-1.82 (m, 2H), 1.44 (s, 9H); ^{13}C NMR (125 MHz, CDCl_3): δ 162.8, 155.9, 150.3, 133.3, 129.6, 124.7, 120.1, 111.8, 79.5, 59.4, 49.6, 41.3, 31.5, 28.4.

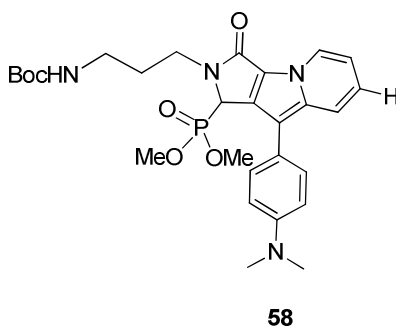


Phosphonate 56: To a solution of the imine **55** (1 g, 3.01 mmol) in MeOH was added dimethylphosphite (0.36 ml, 3.92 mmol) and the reaction refluxed for 10 h. The MeOH was removed under reduced pressure and saturated NH_4Cl added to it. This was followed by extraction with EtOAc (3 x 20 ml). The organic layer was washed with brine, dried with MgSO_4 and concentrated *in vacuo* to give the desired product **56** (1.32 g, 100%) as a

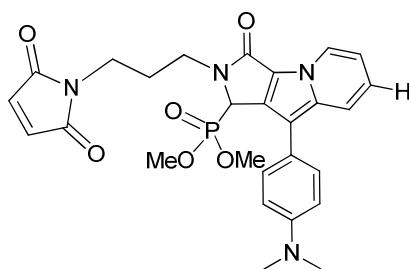
yellow liquid which was used without further purification. ^1H NMR (500 MHz; CDCl_3): δ 7.41-7.27 (m, 3H), 6.60 (d, $J = 8.6$ Hz, 2H) 6.48 (d, $J = 15.6$ Hz, 1H), 5.65 (dd, $J = 9.1$, 20.4 Hz, 1H), 3.52 (dd, $J = 10.7$, 8.5 Hz, 6H), 3.51 (t, $J = 6.5$, 2H), 3.20 (t, $J = 6.5$, 2H), 2.89 (s, 6H), 1.84-1.82 (m, 2H), 1.44 (s, 9H); ^{13}C NMR (125 MHz, CDCl_3): δ 155.3, 151.0, 133.3, 129.6, 129.5, 124.7, 111.8, 79.5, 54.3 (d, $J_{\text{C-P}} = 156.2$ Hz), 53.8 (d, $J_{\text{C-P}} = 7.5$ Hz), 53.2 (d, $J_{\text{C-P}} = 6.2$ Hz), 49.6, 41.3, 31.5, 29.6, 28.4.



α -Bromo amide 57: To the bromoacetyl bromide (0.44 ml, 5.09 mmoles) in anhydrous CH_2Cl_2 (15 ml) at 0°C was added dropwise a mixture of **56** (1.5 g, 3.39 mmoles) and Et_3N (0.70 ml, 5.09 mmoles) in anhydrous CH_2Cl_2 (4 ml). The reaction was stirred for 10 mins when TLC indicated complete consumption of **56**. The reaction mixture was diluted with water (10 ml) and extracted with CH_2Cl_2 (3 x 10 ml). The organic layer was washed with brine, dried with MgSO_4 and concentrated *in vacuo*. Flash chromatography with hexane:EtOAc 3:1 gave the desired product **57** (1.52 g, 80 %). ^1H NMR (500 MHz, CDCl_3): δ 7.24 (d, $J = 8.7$ Hz, 2H), 6.69-6.61 (m, 3H), 6.03-5.96 (m, 1H), 5.63 (dd, $J = 9.1$, 20.3 Hz, 1H), 3.89 (d, $J = 10.7$ Hz, 1H), 3.81 (d, $J = 10.7$ Hz, 1H), 3.74 (dd, $J = 10.7$, 8.5 Hz, 6H), 3.51 (t, $J = 6.5$, 2H), 3.20 (t, $J = 6.5$, 2H), 2.93 (s, 6H), 1.84-1.82 (m, 2H), 1.44 (s, 9H); ^{13}C NMR (125 MHz, CDCl_3): δ 167.2, 150.6, 137.7, 134.4, 127.8, 124.0, 117.0, 113.7, 79.5, 54.6 (d, $J_{\text{C-P}} = 156.4$ Hz), 53.8 ($J_{\text{C-P}} = 7.1$ Hz), 53.2 ($J_{\text{C-P}} = 6.3$ Hz), 49.6, 41.3, 40.3, 31.5, 29.6, 28.4.

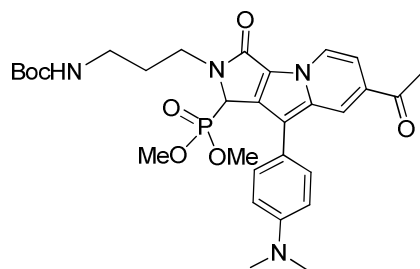


Compound 58: The compound **57** (1 g, 1.77 mmol) and pyridine (6 ml) were stirred at room temperature under N₂ for 6 h. After the complete consumption of **57** the reaction mixture was diluted with toluene (6 ml) and DBU (0.4 ml, 2.65 mmol) was added to it. The reaction was then stirred at 50 °C for 8 h. To the resulting mixture of non-aromatized and fully aromatized products at 0 °C, was added 2,3-dichloro-5,6-dicyanohydroquinone (DDQ) for oxidative aromatization. The reaction mixture was stirred at 0 °C for an additional 30 min. It was filtered through a short bed of silica gel and the filtrate concentrated *in vacuo*. The residue was purified by silica gel flash column chromatography, eluted with hexane:EtOAc 2:1 to afford the desired product **58**. ¹H NMR (500 MHz; CDCl₃): δ 8.61 (d, *J* = 9.2 Hz, 1H), 7.77 (d, *J* = 8.1, 1H), 7.49(d, *J* = 8.1 Hz, 2H), 7.14-7.01 (m, 1H), 6.98 (d, *J* = 8.1 Hz, 2H), 6.94-6.76 (m, 1H), 5.23 (d, *J* = 12.4 Hz, 1H), 3.65-3.60 (m, 2H), 3.56-3.51 (m, 2H), 3.41 (d, *J* = 10.6 Hz, 3H), 3.32 (d, *J* = 10.6 Hz, 3H), 3.01 (s, 6H), 2.05-2.01 (m, 2H), 1.57 (s, 9H); ¹³C NMR (125 MHz, CDCl₃): δ 166.4, 155.9, 151.3, 146.8, 135.9, 128.4, 126.9, 125.9, 124.5, 124.4, 123.5, 122.7, 117.2, 112.1, 79.5, 54.9 (d, *J*_{C-P} = 155.8 Hz), 53.4 (d, *J*_{C-P} = 7.5 Hz), 53.2 (d, *J*_{C-P} = 6.2 Hz), 45.6, 41.3, 39.9, 28.4, 26.5.

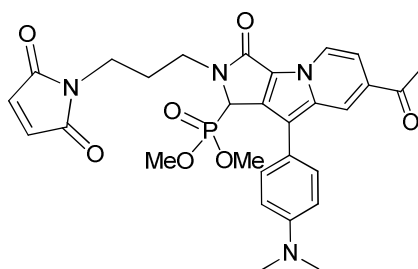


47

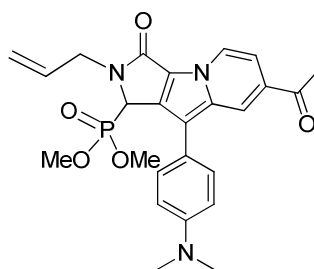
Green Fluorescent compound 47: To a solution of **58** (100 mg, 0.18 mmol) in CH_2Cl_2 (2 ml) was added three drops of TFA and the reaction stirred at room temperature for 10 h. It was quenched with saturated NaHCO_3 and extracted with CH_2Cl_2 (3 x 10 ml). The organic layer was dried with MgSO_4 and concentrated under reduced pressure to give **59**, which was immediately used in the next step. Toluene (4 ml) was added to the crude reaction mixture of **59**, followed by maleic anhydride (88.2 mg, 0.9 mmol) and the reaction heated at reflux for 10 h. Toluene was removed *in vacuo* and the residue purified on column to yield **47** (73 mg, 76 % over two steps) as an orange liquid. ^1H NMR (500 MHz; CDCl_3): δ 8.61 (d, $J = 9.2$ Hz, 1H), 7.77 (d, $J = 8.1$, 1H), 7.49(d, $J = 8.1$ Hz, 2H), 7.14-7.01 (m, 1H), 6.98 (d, $J = 8.1$ Hz, 2H), 6.94-6.76 (m, 1H), 6.38 (d, $J = 5.2$ Hz, 2H) 5.23 (d, $J = 12.4$ Hz, 1H), 3.65-3.60 (m, 2H), 3.56-3.51 (m, 2H), 3.41 (d, $J = 10.6$ Hz, 3H), 3.32 (d, $J = 10.6$ Hz, 3H), 3.01 (s, 6H), 2.05-2.01 (m, 2H); ^{13}C NMR (125 MHz, CDCl_3): δ 172.3, 167.7, 150.8, 148.6, 139.4, 134.7, 129.1, 127.5, 125.9, 123.8, 123.1, 122.7, 122.3, 118.6, 111.1, 55.1 (d, $J_{\text{C-P}} = 156.2$ Hz), 53.6 (d, $J_{\text{C-P}} = 7.5$ Hz), 53.4 (d, $J_{\text{C-P}} = 6.3$ Hz), 44.8, 42.7, 39.9, 25.9.

**60**

Orange Fluorescent Compound 60: The compound **57** (1 g, 1.77 mmol) and 4-acetylpyridine (1 ml, 8.85 mmol) were stirred in CH_2Cl_2 at room temperature under N_2 for 6 h. After the complete consumption of **57** the reaction mixture was diluted with toluene (6 ml) and DBU (0.4 ml, 2.65 mmol) was added to it. The reaction was then stirred at 50 °C for 8 h. To the resulting mixture of non-aromatized and fully aromatized products at 0 °C, was added 2,3-dichloro-5,6-dicyanohydroquinone (DDQ) for oxidative aromatization. The reaction mixture was stirred at 0 °C for an additional 30 min. It was filtered through a short bed of silica gel and the filtrate concentrated *in vacuo*. The residue was purified by silica gel flash column chromatography, eluted with hexane:EtOAc 2:1 to afford the desired product **60** (370 mg, 35%). ^1H NMR (500 MHz; CDCl_3): δ 8.52 (d, $J = 7.2$ Hz, 1H), 8.26 (s, 1H), 7.37-7.33 (m, 3H), 6.86 (d, $J = 8.7$ Hz, 2H), 5.07 (d, $J = 12.9$ Hz, 1H), 3.94-3.80 (m, 2H), 3.64-3.57 (m, 2H), 3.39 (dd, $J = 10.8, 6.9$ Hz, 6H), 3.08 (s, 6H), 2.56 (s, 3H), 2.04-2.01 (m, 2H), 1.57 (s, 9H); ^{13}C NMR (125 MHz, CDCl_3): δ 201.1, 168.1, 157.3, 155.4, 148.8, 137.1, 129.6, 128.2, 128.1, 127.4, 125.3, 125.1, 122.7, 119.4, 116.3, 67.6, 55.1 (d, $J_{\text{C-P}} = 155.7$ Hz), 54.1 (d, $J_{\text{C-P}} = 7.5$ Hz), 53.8 (d, $J_{\text{C-P}} = 6.2$ Hz), 44.8, 42.4, 41.3, 30.2, 28.1, 25.8.

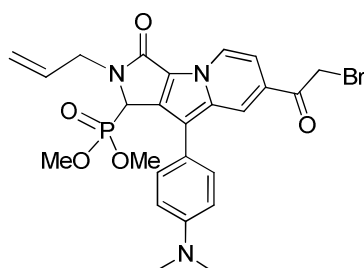
**48**

Orange Fluorescent Compound 48: To a solution of **60** (100 mg, 0.17 mmol) in CH_2Cl_2 (2 ml) was added three drops of TFA and the reaction stirred at room temperature for 10 h. It was quenched with saturated NaHCO_3 and extracted with CH_2Cl_2 (3 x 10 ml). The organic layer was dried with MgSO_4 and concentrated under reduced pressure to give **13**, which was immediately used in the next step. Toluene (4 ml) was added to the crude reaction mixture of **61**, followed by maleic anhydride (87.6 mg, 0.85 mmol) and the reaction heated at reflux for 10 h. Toluene was removed *in vacuo* and the residue purified on column to yield **48** (75 mg, 76 % over two steps) as an orange liquid. ^1H NMR (500 MHz; CDCl_3): δ 8.52 (d, $J = 7.2$ Hz, 1H), 8.26 (s, 1H), 7.37-7.33 (m, 3H), 6.86 (d, $J = 8.7$ Hz, 2H), 6.36 (d, $J = 5.0$ Hz, 2H), 5.07 (d, $J = 12.9$ Hz, 1H), 3.94-3.80 (m, 2H), 3.64-3.57 (m, 2H), 3.39 (dd, $J = 10.8, 6.9$ Hz, 6H), 3.04 (s, 6H), 2.56 (s, 3H), 2.04-2.01 (m, 2H); ^{13}C NMR (125 MHz, CDCl_3): δ 202.4, 168.6, 166.4, 156.1, 147.4, 137.5, 135.8, 130.1, 129.8, 128.6, 125.7, 124.3, 122.7, 121.6, 120.2, 114.9, 54.8 (d, $J_{\text{C-P}} = 156.3$ Hz), 53.8 (d, $J_{\text{C-P}} = 7.5$ Hz), 53.5 (d, $J_{\text{C-P}} = 6.2$ Hz), 43.9, 42.7, 41.3, 30.1, 26.9.



63

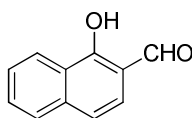
N-allylated Orange Fluorescent compound 63: This compound was prepared in a manner similar to **48**, following the sequence in Schemes 4.4, 4.5 and 4.9; but using allyl amine instead of the Boc-protected propane-1,3-diamine. ^1H NMR (500 MHz; CDCl_3): δ 8.43 (d, $J = 7.2$ Hz, 1H), 8.31 (s, 1H), 7.39 (d, $J = 8.4$ Hz, 2H), 7.16 (dd, $J = 7.2, 0.9$ Hz, 1H), 6.83 (d, $J = 8.4$ Hz, 2H), 5.91-5.33 (m, 1H), 5.23 (t, $J = 13.6$ Hz, 2H), 5.11 (d, $J = 12.9$ Hz, 1H), 4.19 (d, $J = 5.9$ Hz, 2H), 3.34 (dd, $J = 10.8, 6.9$ Hz, 6H), 3.00 (s, 6H), 2.56 (s, 3H); ^{13}C NMR (125 MHz, CDCl_3): δ 195.4, 161.2, 150.9, 149.4, 134.2, 134.0, 133.5, 128.3, 124.3, 122.6, 121.7, 121.3, 121.2, 117.7, 114.7, 113.0, 54.6 (d, $J_{\text{C-P}} = 156.0$ Hz), 53.3 (d, $J_{\text{C-P}} = 7.5$ Hz), 53.1 (d, $J_{\text{C-P}} = 6.2$ Hz), 46.1, 40.5, 26.0.



64

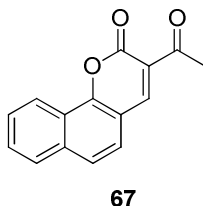
α -Bromo Keone 64: To a solution of **63** (50 mg, 0.103 mmol) in CH_2Cl_2 (2 ml) was added tetrabutylammonium tribromide (74 mg, 0.154 mmol) and the reaction stirred at room temperature for 5 h. The solvent was removed under reduced pressure and the

compound purified by flash chromatography on silica gel, eluted with hexane:EtOAc 3:1 to give **64** (37 mg, 64 %) as an orange solid. ^1H NMR (500 MHz; CDCl_3): δ 8.43 (d, $J = 7.2$ Hz, 1H), 8.31 (s, 1H), 7.39 (d, $J = 8.4$ Hz, 2H), 7.16 (dd, $J = 7.2, 0.9$ Hz, 1H), 6.83 (d, $J = 8.4$ Hz, 2H), 5.91-5.33 (m, 1H), 5.23 (t, $J = 13.6$ Hz, 2H), 5.11 (d, $J = 12.9$ Hz, 1H), 4.34 (s, 2H), 4.19 (d, $J = 5.9$ Hz, 2H), 3.34 (dd, $J = 10.8, 6.9$ Hz, 6H), 3.00 (s, 6H); ^{13}C NMR (125 MHz, CDCl_3): δ 194.4, 161.2, 150.9, 149.4, 134.2, 134.0, 133.5, 128.3, 124.3, 122.6, 121.7, 121.3, 120.2, 117.7, 114.7, 113.0, 54.5 (d, $J_{\text{C-P}} = 156.0$ Hz), 53.3 (d, $J_{\text{C-P}} = 7.5$ Hz), 53.0 (d, $J_{\text{C-P}} = 6.2$ Hz), 46.1, 43.1, 40.5.

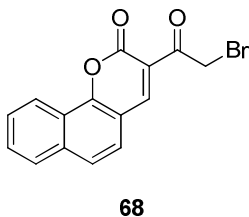
**66**

1-hydroxy-2-naphthaldehyde 66: To a solution of α -tetralone **65** (1 g, 6.84 mmol) in THF (15 ml) at -78 °C was added dropwise a solution of LDA (6.84 mmol) and the reaction was stirred at -78 °C for 40 mins. Ethyl formate, (1.1 ml, 13.68 mmol) was then added slowly and the reaction allowed to warm up gradually to room temperature. It was then stirred at room temperature overnight. To the reaction mixture was added EtOH (8 ml) and then a solution of DDQ (1.5 g, 6.84 mmol) in 1, 4-dioxane (1.5 M). The reaction was the stirred for one hour, after which the solvent was removed *in vacuo*. EtOAc was added to the resulting solid, followed by filtration through a plug of silica. The solvent was removed under vacuum and the crude reaction mixture purified on column by eluting with EtOAc:hexanes 1:40. The product was obtained as a yellow solid (760 mg, 60 %). ^1H NMR (500 MHz; CDCl_3): δ 9.95 (d, $J = 4.6$ Hz, 1H), 8.44-8.42 (m, 1H), 7.78-7.76 (m, 1H), 7.66-7.65 (m, 1H), 7.55-7.54 (m, 1H), 7.47-7.45 (m, 1H), 7.37-7.34 (m, 1H); ; ^{13}C

NMR (125 MHz, CDCl₃): δ 196.3, 161.9, 137.55, 133.41, 130.62, 127.65, 126.49, 126.17, 124.34, 119.48, 114.29.

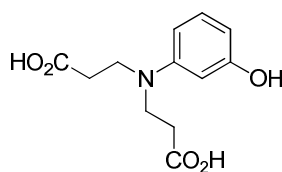


Naphthopyranone 67: To the 1-hydroxy-2-naphthaldehyde **66** (64 mg, 0.4 mmol) and methyl acetoacetate (43 μ l, 0.4 mmol) in dry toluene (2 ml) was added one drop of piperidine and one drop of acetic acid. The reaction flask was then connected to a Dean-Stark apparatus and heated at 110 °C for 14 h. Solvent was removed under vacuum and the reaction mixture was purified on column. The product was eluted with EtOAc:hexanes 1:5 and is a yellow solid (77 mg, 81 %). ¹H NMR (500 MHz; CDCl₃): δ 8.53 (s, 1H), 8.52 (d, *J* = 8.1 Hz, 1H), 7.85 (d, *J* = 8.1 Hz, 1H), 7.69-7.65 (m, 3H), 7.51-7.50 (m, 1H), 2.69 (s, 3H); ¹³C NMR (125 MHz, CDCl₃): δ 195.4, 159.3, 153.7, 148.2, 136.0, 130.1, 129.6, 128.0, 127.6, 125.0, 124.5, 123.2, 122.5, 113.8, 30.6; HRMS (CI⁺) *m/z* calcd. for C₁₅H₁₁O₃ (M+H)⁺ 239.0708, found 239.0705.

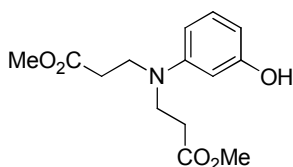


α -Bromo Ketone 68: To the naphthopyranone (25 mg, 0.104 mmol) **67** in 1,4-dioxane:Et₂O (1:1, 6ml) was added dropwise liquid Br₂ (5.3 μ l, 0.104mmol) at room temperature. The reaction was stirred for 90 mins and then poured onto ice. A yellow

solid formed which was filtered and washed with MeOH. The product was then recrystallized from EtOH to give yellow crystals (26 mg, 78 %). ^1H NMR (500 MHz; CDCl_3): δ 8.77 (s, 1H), 8.59-8.57 (d, $J = 8.2$ Hz, 1H), 7.92-7.90 (d, $J = 8.2$ Hz, 1H), 7.76-7.70 (m, 3H), 7.58-7.50 (m, 1H), 4.80 (s, 2H); ^{13}C NMR (125 MHz, CDCl_3): δ 188.8, 159.0, 154.1, 150.2, 136.4, 130.5, 128.1, 127.8, 125.4, 124.5, 123.3, 122.5, 120.8, 113.9, 35.8.

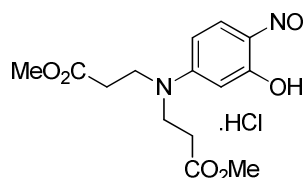
**73**

Dicarboxylic Acid 73: To the 3-aminophenol **72** (500 mg, 4.58mmol) in water (1 ml) was added acrylic acid (0.94 ml, 13.74 mmol) and the reaction heated at 70 °C for 3 h. After cooling to room temperature, EtOH (2 ml) was added and the reaction kept at 5 °C overnight. The white crystals that formed were filtered and washed with cold EtOH and dried to obtain the desired product (811 mg, 70 %). ^1H NMR (500 MHz; acetone- d_6): δ 7.02-6.98 (m, 1H), 6.28-6.24 (m, 2H), 6.19-6.17 (m, 1H), 3.64 (t, $J = 4.5$ Hz, 4H), 2.59 (t, $J = 4.5$ Hz, 4H); ^{13}C NMR (125 MHz, acetone- d_6): δ 172.6, 158.6, 148.6, 130.0, 104.0, 104.2, 99.6, 46.8, 31.7; See Ref 196 for HRMS.



74

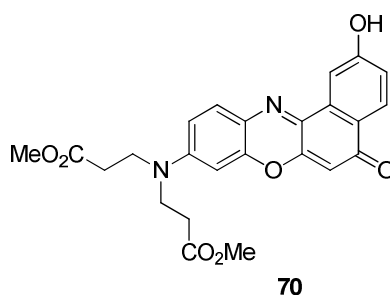
Dimethylester 74: A solution of the dicarboxylic acid **73** (926 mg, 3.66 mmol) in MeOH (10 ml) along with HCl (10 M, 0.1 ml) was refluxed for 12 h. The reaction mixture was cooled and the MeOH removed under vacuum. The residue was dissolved in EtOAc and the organic layer washed with water (3 x 15 ml). The organic layer was dried with Na₂SO₄ and the EtOAc removed under reduced pressure to give the diester as a yellow viscous liquid (1.03 g, 100 %). ¹H NMR (500 MHz; CD₃OD): δ 7.05-6.95 (m, 1H), 6.21-6.15 (m, 3H), 3.65 (s, 6H), 3.58 (t, *J* = 7.2 Hz, 4H), 2.55 (t, *J* = 7.2 Hz, 4H); ¹³C NMR (125 MHz, CD₃OD): δ 173.3, 158.1, 148.2, 130.0, 104.4, 104.0, 99.7, 50.8, 46.7, 32.1; See Ref 196 for HRMS.



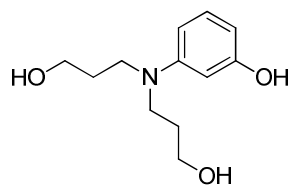
75

Nitroso phenol 75: To a solution of phenol **74** (500 mg, 1.77 mmol) in water (1 ml) at 0 °C was added HCl (10 N, 0.6 ml) followed by slow addition of a solution of sodium nitrite (134 mg, 1.95 mmol) in water (0.8 ml) at 0.05 ml per minute. After the addition of the sodium nitrite, the reaction was stirred at 0 °C for 2.5 h. Water was then removed under vacuum and the residue dissolved in MeOH. It was then dried with MgSO₄, and

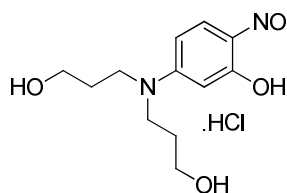
MeOH removed under reduced pressure. The nitroso compound obtained (220 mg, 40 %) was unstable and used in the next step without further purification. ^1H NMR (500 MHz; CD_3OD): δ 7.90 (d, $J = 10.0$ Hz, 1H), 6.42 (d, $J = 10.0$ Hz, 1H), 6.20 (s, 1H), 3.78 (t, $J = 7.0$ Hz, 4H), 3.68 (s, 6H), 2.67 (t, $J = 7.4$ Hz, 4H); ^{13}C NMR (125 MHz, CD_3OD) δ 172.1, 157.5, 154.5, 129.9, 123.4, 120.0, 98.0, 50.9, 46.4, 31.5; see Ref 196 for HRMS.



Nile Red Derivative 70: The nitroso compound **75** (403 mg, 1.30 mmol) and 1,6-dihydroxynaphthol (208 mg, 1.30 mmol) were dissolved in MeOH and HCl (10 N, 0.2 ml) was added/ The reaction was heated at reflux for 5 h. MeOH was removed under reduced pressure and the residue purified immediately on silica gel, eluted with MeOH:EtOAc 1:10 to give the Nile Red derivative (234 mg, 40%) as a dark brown solid. ^1H NMR (500 MHz; CDCl_3): δ 8.03 (d, $J = 8.6$ Hz, 1H), 7.86 (s, 1H), 7.52 (d, $J = 8.6$ Hz, 1H), 7.04 (d, $J = 8.6$ Hz, 1H), 6.98 (d, $J = 8.6$ Hz, 1H), 6.78 (s, 1H), 6.61 (d, $J = 8.6$ Hz, 1H), 3.69 (t, $J = 7.1$ Hz, 4H), 3.64 (s, 6H), 2.60 (t, $J = 7.1$ Hz, 4H); ^{13}C NMR (125 MHz, CDCl_3): δ 183.1, 173.1, 161.8, 153.4, 150.9, 147.3, 141.1, 132.8, 131.9, 129.6, 125.7, 124.9, 124.5, 119.9, 111.0, 109.2, 105.9, 51.9, 45.4, 31.1; see Ref 196 for HRMS.

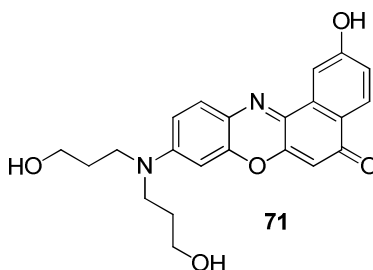
**76**

Diol 76: A solution of diester **74** (1 g, 3.6 mmol) in THF (15 ml) was added dropwise to at 0 °C to a solution of LiAlH₄ (820 mg, 21.6 mmol) in THF (15 ml). A thick white precipitate formed and the reaction was stirred at room temperature for 2 h. It was quenched with water and filtered to remove the white precipitate. The filtrate was concentrated to yield the diol as a white solid (705 mg, 87 %). ¹H NMR (500 MHz; CD₃OD): δ 6.31 (t, *J* = 8.1 Hz, 1H), 5.62 (s, 1H), 5.56 (d, *J* = 7.2 Hz, 1H), 5.52 (d, *J* = 8.1 Hz, 1H) 3.12 (t, *J* = 6.0 Hz, 4H), 2.81-2.73 (m, 4 H), 1.33 (t, *J* = 6.3 Hz, 4H); ¹³C NMR (125 MHz, CD₃OD) δ 167.5, 149.9, 128.9, 108.9, 105.1, 101.5, 60.0, 48.7, 30.3; see Ref 196 for HRMS.

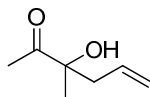
**77**

Nitroso compound 77: To the phenol **76** (115 mg, 0.50 mmol) in water (0.5 ml) at 0 °C was added HCl (10 N, 0.5 ml) via a syringe pump at 0.03 ml/min. The reaction was stirred at 0 °C for 2.5 h and the filtered to remove the solids that formed. Water was then removed under reduced pressure and the residue dissolved in MeOH. It was the dried with MgSO₄ and concentrated. The nitroso compound obtained (74 mg, 51 %) was

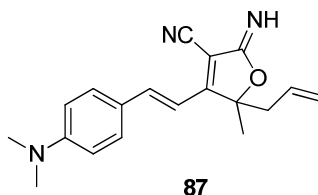
unstable and used in the next step without further purification. ^1H NMR (500 MHz; CD_3OD): δ 7.70 (d, $J = 10.2$ Hz, 1H), 7.26 (d, $J = 10.2$ Hz, 1H), 6.49 (s, 1H), 4.02 (t, $J = 7.4$ Hz, 4H), 3.98 (t, $J = 7.4$ Hz, 4H), 3.81-3.66 (bs, 2H), 2.02-1.86 (m, 4H); ^{13}C NMR (125 MHz, CD_3OD) δ 166.1, 163.6, 144.8, 123.4, 120.0, 98.0, 58.3, 51.1, 31.8; see Ref 196 for HRMS.



Nile Red Derivative 71: To the nitroso compound **77** (94 mg, 0.37 mmol) in DMF (3 ml) was added 1,6-dihydroxynaphthol (59 mg, 0.37 mmol) and the reaction heated to $130\text{ }^\circ\text{C}$ for 5 h. The DMF was removed using vacuum distillation and the residue purified on column, eluted with MeOH:EtOAc 1:10 to give the Nile Red derivative **71** (50 mg, 34 %). ^1H NMR (500 MHz; $\text{DMSO-}d_6$): δ 10.41 (s, 1H), 7.94 (d, $J = 8.4$ Hz, 1H), 7.86 (d, $J = 2.7$ Hz, 1H), 7.56 (d, $J = 9.0$ Hz, 1H), 7.06 (dd, $J = 6.0, 2.4$ Hz, 1H), 6.82 (d, $J = 8.4$ Hz, 1H), 6.66 (s, 1H), 6.14 (s, 1H), 4.63 (d, $J = 4.8$ Hz, 4H), 3.47 (d, $J = 1.5$ Hz, 4H), 1.66-1.78 (m, 4H); ^{13}C NMR (125 MHz, $\text{DMSO-}d_6$): δ 182.3, 161.3, 152.3, 151.9, 147, 139.4, 134.4, 131.4, 128.2, 124.5, 119.1, 110.7, 108.7, 104.8, 97.2, 96.9, 58.9, 48.3, 30.6; see Ref 196 for HRMS.

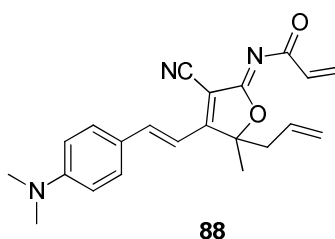
**84**

Tertiary alcohol 84: To the 3,4-butanedione **83** (3 g, 34.8 mmoles) and allyl bromide (5.1 ml, 59.2 mmoles) in DMF (12 ml) was added Zn dust (200 mg) immediately followed by 6 ml of a saturated solution of NH_4Cl in water. After 15 mins, another 100 mg of Zn dust was added followed by 3 ml of saturated NH_4Cl . The reaction was stirred at room temperature for 20 mins when TLC indicated that the 3,4-butanedione was completely consumed. The reaction was quenched by the addition of 10 ml water and 1 ml of 1M HCl. The reaction mixture was extracted with diethyl ether (3×15 ml), the organic layer was separated, dried using MgSO_4 and concentrated. Purification by flash chromatography hexane:EtOAc 3:1 offered the desired keto-alcohol **84** (271 mg, 94% yield) as a colorless liquid. ^1H NMR (500 MHz; CDCl_3): δ 5.86 (m, 1H), 5.07-5.05 (m, 2H), 2.51 (m, 1H), 2.33 (m, 1H), 2.31 (s, 3H), 1.24 (s, 3H); ^{13}C NMR (125 MHz, CDCl_3): δ 211.2, 130.4, 118.2, 93.0, 48.5, 26.2, 22.3; HRMS (ESI) m/z calcd. for $\text{C}_7\text{H}_{13}\text{O}_2$ ($\text{M}+\text{H}$) $^+$ 129.09156, found 129.08963.

**87**

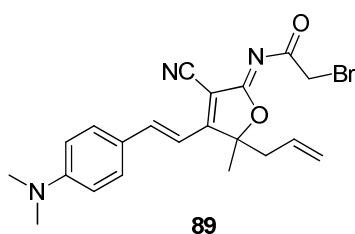
2-imino-2,5-dihydrofuran-3-carbonitrile 87: To a 50 ml round bottom flask containing malononitrile (284 mg, 4.3 mmoles) and flushed with N_2 , was added anhydrous EtOH (10 ml). The reaction was cooled to 0°C and NaH (60% dispersion in mineral oil, 103 mg,

4.3 mmoles) was added. After the evolution of H₂ was complete, the keto-alcohol **84** (500 mg, 3.9 mmoles) was added and the ice bath removed. The reaction turned a brown color and was stirred at room temperature for 25 min. 4-dimethylaminobenzaldehyde (581 mg, 3.9 mmoles) was added to the reaction mixture followed by three drops of piperidine. The reaction immediately turned red. It was stirred at ambient temperature for two minutes. The solvent was removed under reduced pressure and the product immediately purified by flash chromatography on silica gel using hexane:EtOAc 1:9 to afford the product **87** (740 mg, 60%) as a brown-red solid. ¹H NMR (500 MHz, CDCl₃): δ 7.48-7.44 (m, 3H), 6.66-6.58 (m, 3H), 5.65-5.56 (m, 1H), 5.10-5.08 (m, 2H), 3.08 (s, 6H), 2.69-2.55 (m, 2H), 1.62 (s, 3H); ¹³C NMR (125 MHz, CDCl₃): δ 169.4, 166.3, 152.4, 143.8, 130.3, 129.7, 122.1, 120.3, 113.5, 111.9, 109.9, 97.6, 91.0, 43.4, 40.1, 25.1; HRMS (ESI) *m/z* calcd. for C₁₉H₂₂N₃O (M+H)⁺ 308.1763, found 308.1761.



Acrylamide 88: To the acryloyl chloride (19 μl, 0.234 mmoles) in anhydrous CH₂Cl₂ (6 ml) at 0 °C was added dropwise a mixture of **87** (50 mg, 0.156 mmoles) and Et₃N (40 μl, 0.312 mmoles) in anhydrous CH₂Cl₂ (2 ml). The reaction was stirred for 10 mins when TLC indicated complete consumption of **87**. The reaction mixture was diluted with water (10 ml) and extracted with CH₂Cl₂ (3 x 10 ml). The organic layer was washed with brine, dried with MgSO₄ and concentrated *in vacuo*. Flash chromatography with hexane:EtOAc 1:7 gave the desired product **88** (47.3 mg, 81%) as a red solid. ¹H NMR (500 MHz,

CDCl₃): δ 7.56 (d, J = 16.1 Hz, 1H), 7.50 (d, J = 8.9 Hz, 2H), 6.67-6.64 (m, 3H), 6.36-6.27 (m, 2H), 5.86 (dd, J = 9.42, 2.35 Hz, 1H), 5.61-5.53 (m, 1H), 5.16-5.10 (m, 2H), 3.09 (s, 6H), 2.73-2.63 (m, 2H) 1.65 (s, 3H); ¹³C NMR (125 MHz, CDCl₃): δ 174.9, 172.5, 171.1, 166.8, 165.2, 152.7, 145.1, 133.3, 130.8, 130.2, 129.6, 121.9, 121.0, 111.9, 109.5, 93.0, 43.4, 40.1, 25.1; HRMS (ESI) m/z calcd. for C₂₂H₂₄N₃O₂ (M+H)⁺ 362.1869, found 362.1871.



α -Bromoamide 89: To the bromoacetyl bromide (20 μ l, 0.234 mmol) in anhydrous CH₂Cl₂ (6 ml) at 0 °C was added dropwise a mixture of **87** (50 mg, 0.156 mmol) and Et₃N (40 μ l, 0.312 mmol) in anhydrous CH₂Cl₂ (2 ml). The reaction was stirred for 10 mins when TLC indicated complete consumption of **87**. The reaction mixture was diluted with water (10 ml) and extracted with CH₂Cl₂ (3 x 10 ml). The organic layer was washed with brine, dried with MgSO₄ and concentrated *in vacuo*. Flash chromatography with hexane:EtOAc 1:7 gave the desired product **89** (63 mg, 94%) as a red solid. ¹H NMR (500 MHz, CDCl₃): δ 7.60 (d, J = 16.1 Hz, 1H), 7.50 (d, J = 8.9 Hz, 2H), 6.67-6.64 (m, 3H), 5.63-5.56 (m, 1H), 5.18-5.14 (m, 2H), 4.07 (s, 2H), 3.11 (s, 6H), 2.80-2.74 (m, 1H), 2.66-2.62 (m, 1H), 1.68 (s, 3H); ¹³C NMR (125 MHz, CDCl₃): δ 172.0, 160.1, 159.0, 152.9, 145.9, 131.1, 129.5, 121.8, 121.2, 111.9, 111.8, 111.5, 109.2, 93.8, 43.4, 40.1, 32.0, 24.9; HRMS (ESI) m/z calcd. for C₂₁H₂₃N₃O₂Br (M+H)⁺ 428.0974, found 428.0977.

CITED LITERATURE

1. Hall, D. G. *Boronic Acids*, Vol. 2; John Wiley & Sons: Weinheim; **2012**, 1-726
2. Hall, D. G. *Boronic Acids*, Wiley-VCH Verlag GmbH & Co: Weinheim; **2005**, 1-100
3. a) Miyaura, N.; Yamada, K.; Suzuki, A. *Tetrahedron Lett.* **1979**, *20*, 3437; b) Miyaura, N.; Suzuki, A. *Chem. Comm.* **1979**, *19*, 866; c) Suzuki, A. *J. Organometallic Chem.* **1999**, *576*, 147-168
4. a) Hall, D. G. *Boronic Acids*, Vol. 2; Wiley-VCH, Weinheim, **2011**, 1 – 677; b) Miyaura, N.; Suzuki, A. *Chem. Rev.* **1995**, *95*, 2457; c) Suzuki, A. *Angew. Chem.* **2011**, *123*, 6854; *Angew. Chem. Int. Ed.* **2011**, *50*, 6722; d) Kotha, S.; Lahiri, K.; Kashinath, D. *Tetrahedron* **2002**, *58*, 9633; e) Qiao, J. X.; Lam, P. Y. S. *Synthesis* **2011**, 829; f) Hall, D. G. *Synlett* **2007**, 1644; g) Prokopcova, H.; Kappe, C. O. *Angew. Chem.* **2009**, *121*, 2312; *Angew. Chem. Int. Ed.* **2009**, *48*, 2276; h) Severin, K. *Dalton Trans.* **2009**, 5254
5. a) Matteson, D. S. Chapter 1. In *Stereodirected Synthesis with Organoboranes*, Springer: Berlin, **1995**, 1-20; b) Bullen, N. P.; Hodge, P.; Thorpe, F. G.; *J. Chem. Soc., Perkin Trans. 1* **1981**, 1863; c) Salzbrunn, S. J.; Surya Prakash, G. K.; Petasis, N. A.; Olah, G. A. *J. Org. Chem.* **2001**, *66*, 633
6. a) Thiebes, C.; Surya Prakash, G. K.; Petasis, N. A.; Olah, G. A. *Synlett* **1998**, 141; b) Qiu, D.; Mo, F.; Zheng, Z.; Zhang, Y.; Wang, J. *Org. Lett.* **2010**, *12*, 5474.
7. Kirchberg, S.; Tani, S.; Ueda, K.; Yamaguchi, J.; Studer, A.; Itami, K. *Angew. Chem. Int. Ed.* **2011**, *50*, 2387
8. Fleckenstein, C. A.; Plenio, H. *J. Org. Chem.* **2008**, *73*, 3236

9. a) Chu, J.-H.; Chen, C.-C.; Wu, M.-J.; *Organometallics*, **2008**, *27*, 5173; b) Grob, J. E.; Nunez, J.; Dechantsreiter, M. A.; Hamann, L. G. *J. Org. Chem.* **2011**, *6*, 76.
10. a) Billingsley, K. L.; Anderson, K. W.; Buchwald, S. L. *Angew. Chem. Int. Ed.* **2006**, *45*, 3484 b) Lipshutz, B. H.; Abela, A. R. *Org. Lett.* **2008**, *10*, 5329
11. Cooke, G.; Augier de Cremiers, H.; Rotello, V. M.; Tarbit, B.; Vanderstraeten, P. *E. Tetrahedron* **2001**, *57*, 2787
12. Nikishkin, N. I.; Huskens, J.; Verboom, W. *Org. Biomol. Chem.* **2013**, *11*, 3583
13. a) Littke, A. F.; Dai, C.; Fu, G. C. *J. Am. Chem. Soc.* **2000**, *122*, 4020; b) Occhiato, E. G.; Trabocchi, A. Guarna, A. *J. Org. Chem.* **2001**, *6*, 2459; c) Marion, N.; Navarro, O.; Mei, J.; Stevens, E. D.; Scott, N. M.; Nolan, S. P. *J. Am. Chem. Soc.* **2006**, *128*, 4101
14. a) Baxter, J.; Steinhuebel, D.; Palucki, M.; Davies, I. W. *Org. Lett.* **2005**, *7*, 215; b) So, C. M.; Lau, C. P.; Chan, A. S. C.; Kwong, F. Y. *J. Org. Chem.*, **2008**, *73*, 7731
15. a) Chow, W. K.; So, C. M.; Lau, C. P.; Kwong, F. Y. *J. Org. Chem.* **2010**, *75*, 5109; b) Leowanawat, P.; Zhang, N.; Remerita, A.-M.; Rosen, B. M.; Percec, V. *J. Org. Chem.* **2011**, *76*, 9946
16. Zhang, S.; Marshall, D.; Liebeskind, L. S. *J. Org. Chem.* **1999**, *64*, 2796
17. Chen, G. J.; Huang, J.; Gao, L. X.; Han, F. S. *Chemistry* **2011**, *17*, 4038
18. a) Quach, T. D.; Batey, R. A. *Org. Lett.* **2003**, *5*, 4397; b) Fischer, C.; Koenig, B. *Beilstein J. Org. Chem.* **2011**, *7*, 59
19. Krishnamoorthy, R.; Lam, S. Q.; Manley, C. M.; Herr, R. J. *J. Org. Chem.* **2010**, *75*, 1251

20. Gavade, S.; Balaskar, R.; Mane, M.; Pabrekar, P. N.; Mane, D. *Synth. Commun.* **2012**, *42*, 1704
21. MacNeil, S. L.; Familoni, O. B.; Snieckus, V. *J. Org. Chem.* **2001**, *66*, 3662
22. Quasdorf, K. W.; Antoft-Finch, A.; Liu, P.; Silberstein, A. L.; Komaromi, A.; Blackburn, T.; Ramgren, S. D.; Houk, K. N.; Snieckus, V.; Garg, N. K. *J. Am. Chem. Soc.* **2011**, *133*, 6352
23. Djakovitch, L.; Batail, N.; Genelot, M. *Molecules* **2011**, *16*, 5241
24. Rao, D. N.; Rasheed, S. K.; Aravinda, S.; Vishwakarma, R. A.; Das, P. *RSC Advances* **2013**, *3*, 11472
25. Hassan, J.; Sevignon, M.; Gozzi, C.; Schulz, E.; Lemaire M. *Chem. Rev.* **2002**, *102*, 1359
26. Mizuta, S.; Onomura, O. *RSC Advances* **2012**, *2*, 2266
27. Takagi, J.; Takahashi, K.; Ishiyama, T.; Miyaura, N. *J. Am. Chem. Soc.* **2002**, *124*, 8001
28. Li, J. J. *Name Reactions: A collection of Detailed Reaction Mechanisms and Synthetic Applications*, 4th Ed.; Springer: New York, **2009**, 102
29. Chan, D. M. T.; Monaco, K. L.; Wang, R.-P.; Winters, M. P. *Tetrahedron Lett.* **1998**, *39*, 2933
30. Evans, D. A.; Katz, J. L.; West, T. R. *Tetrahedron Lett.* **1998**, *39*, 2937
31. Lam, P. Y. S.; Clark, C. G.; Saubern, S.; Adams, J.; Winters, M. P.; Chan, D. M. T.; Combs, A. *Tetrahedron Lett.* **1998**, *39*, 2941

32. Jiang, L.; Buchwald, S. L. *Palladium-Catalyzed Aromatic Carbon-Nitrogen Bond Formation In Metal-Catalyzed Cross-Coupling Reactions: 2nd Ed.*; Wiley-VCH: Weinheim, **2004**, 699
33. a) Hartwig, J. F. *Angew. Chem. Int. Ed.* **1998**, *37*, 2046; b) Burgos, C. H.; Barder, T. E.; Huang, X.; Buchwald, S. L. *Angew. Chem. Int. Ed.* **2006**, *45*, 4321
34. a) Qiao, J. X.; Lam, P. S. Y. *Synthesis* **2011**, *6*, 829 b) King, A. E.; Brunold, T. C.; Stahl, S. S. *J. Am. Chem. Soc.* **2010**, *132*, 12068
35. Ribas, X.; Jackson, D. A.; Donnadieu, B.; Mahia, J.; Parella, T.; Xifra, R.; Hedman, B.; Hodgson, K. O.; Llobet, A.; Stack, T. D. P. *Angew. Chem. Int. Ed.* **2002**, *41*, 2991
36. Guy, C. S.; Jones, T. C. *Synlett* **2009**, 2253
37. Chan, D. M. T.; Monaco, K. L.; Li, R.; Bonne, D.; Clark, C. G.; Lam, P. Y. S. *Tetrahedron Lett.* **2003**, *44*, 3863
38. Bekolo, H. *Can. J. Chem.* **2007**, *85*, 42
39. Liu, S.; Yu, Y.; Liebeskind, L. S. *Org. Lett.* **2007**, *9*, 1947
40. Zhang, Z.; Yu, Y.; Liebeskind, L. S. *Org. Lett.* **2008**, *10*, 3005
41. Lam, P. S. Y.; Clark, C. G.; Saubern, S.; Adams, J.; Averill, K. M.; Chan, D. M. T.; Combs, A. *Synlett* **2000**, 674
42. Tzschucke, C. C.; Murphy, J. M.; Hartwig, J. F. *Org. Lett.* **2007**, *9*, 761
43. Mckinley, N. F.; O'Shea D. F. *J. Org. Chem.* **2004**, *69*, 5087
44. Huang, F.; Quach, T. D.; Batey, R. A. *Org. Lett.* **2013**, *15*, 3150

45. a) Shade, R. E.; Alan, M.; Hyde, A. M.; Olsen, J.-C.; Merlic, C. A. *J. Am. Chem. Soc.* **2010**, *132*, 1202; b) Winternheimer, D. J.; Merlic, C. A. *Org. Lett.* **2010**, *12*, 2508
46. Rühlmann, K. *Synthesis* **1971**, *5*, 236
47. a) Lapworth, A. *J. Chem. Soc. Trans.* **1904**, *85*, 1206; b) Enders, D.; Niemeier, O.; Balensiefer, T. *Angew. Chem. Int. Ed.* **2006**, *45*, 1463
48. Enders, D.; Niemeier, O.; Henseler, A. *Chem. Rev.* **2007**, *107*, 5606
49. Takikawa, H.; Hachisu, Y.; Bode, K. W.; Suzuki, K. *Angew. Chem. Int. Ed.* **2006**, *45*, 3492
50. Hayakawa, R.; Sahara, T.; Shimizu, M. *Tetrahedron Lett.* **2000**, *41*, 7939
51. Rubottom, G. M.; Vazquez, M. A.; Pelegrina, D. R. *Tetrahedron Lett.* **1974**, *15*, 4319
52. a) Hashiyama, T.; Morikawa, K.; Sharpless, K. B. *J. Org. Chem.* **1992**, *57*, 5067; b) Reddy, D. R.; Thornton, E. R. *J. Chem. Soc. Chem. Commun.* **1992**, 172; c) Adam, W.; Fell, R. T.; Mock-Knoblauch, C.; Saha-McIler, C. R. *Tetrahedron Lett.* **1996**, *37*, 6531; d) Moriarty, R. M., Hou, K.-C. *Tetrahedron Lett.* **1984**, *25*, 691; e) Evans, D. A.; Morrissey, M. M.; Dorow, R. L. *J. Am. Chem. Soc.* **1985**, *107*, 4346
53. a) Kano, T.; Maruoka, K. *J. Am. Chem. Soc.* **2009**, *131*, 3450; b) Jing, G. C.; Wang, W.; Lee, E.; Ritter, T. *J. Am. Chem. Soc.* **2011**, *133*, 1760
54. a) Smith, A. M. R.; Hii, K. K. *Chem. Rev.* **2011**, *111*, 1637; b) Janey, J. M. *Angew. Chem.* **2005**, *117*, 4364; *Angew. Chem. Int. Ed.* **2005**, *44*, 4292
55. Petrassi, H. M.; Sharpless, K. B.; Kelly, J. W. *Org. Lett.* **2001**, *3*, 139

56. Jiang, H.; Lykke, L.; Pedersen, S. U.; Xiao, W.-J.; Jorgensen, K. A. *Chem. Commun.* **2012**, 48, 7203
57. a) Rubottom, G. M.; Gruber, J. M.; Mong, G. M. *J. Org. Chem.* **1976**, 41, 1673;
b) Rubottom, G. M.; Mott, R. C.; Juve, Jr., H. D. *J. Org. Chem.* **1981**, 46, 2717
58. Claisen, L. *Ber. Dtsch. Chem. Ges.* **1912**, 45, 3157
59. Ilardi, E. A.; Stivala, C. E.; Zakarian, A. *Chem. Soc. Rev.* **2009**, 38, 3133
60. a) Li, X.; Ovasaka, T. V. *Org. Lett.* **2007**, 9, 3837; b) Li, X., Kyne, R. E.; Ovasaka, T.V. *Tetrahedron* **2007**, 63, 1899
61. Momose, T.; Hama, N.; Higashino, C.; Sato, H.; Chida, N. *Tetrahedron Lett.* **2008**, 49, 1376
62. Hiersemann, M.; Nubbemeyer, U. *The Claisen Rearrangement: 2nd Ed.*; John Wiley & Sons: Weinheim, **2007**, 1-591
63. ApSimon, J. *The Total Synthesis of Natural Products, Volume 7: 1st Ed.*; John Wiley & Sons: Weinheim, **2009**, 1-480
64. Srikrishna, A.; Lakshmi, B. V. *Tetrahedron Lett.* **2005**, 46, 4879
65. Martin Castro, A. M. *Chem. Rev.* **2004**, 104, 2939
66. Welch, J. T.; Eswarakrishnan, S. *J. Am. Chem. Soc.* **1987**, 109, 6716
67. a) Corey, E. J.; Enders, D. *Tetrahedron Lett.* **1976**, 17, 3; b) Job, A.; Janeck, C. F.; Bettray, W.; Peters, R.; Enders, D. *Tetrahedron* **2002**, 58, 2253
68. Enders, D.; Knopp, M. *Tetrahedron* **1996**, 52, 5805
69. Davies, S. G.; Garner, A. C.; Nicholson, R. L.; Osborne, J.; Savory, E. D.; Smith, A. D. *Chem. Commun.* **2003**, 2134

70. a) Roush, W. R. *J. Org. Chem.* **1991**, *56*, 4151; b) Schreiber, S. L.; Wang, Z. *J. Am. Chem. Soc.* **1985**, *107*, 5303; c) Mihelich, E. D.; Daniela, K.; Eickhoff, D. J. *J. Am. Chem. Soc.* **1981**, *103*, 7690
71. Kurth, M. J.; Decker, O. H. W. *J. Org. Chem.* **1986**, *51*, 1377
72. Gluchowski, C.; Tiner-Harding, T.; Smith, J. K.; Bergbreiter, D. E.; Newcomb, M. *J. Org. Chem.* **1984**, *49*, 2650
73. Tamaru, Y.; Furukawa, Y.; Mizutani, M.; Kitao, O.; Yoshida, Z. *J. Org. Chem.* **1983**, *48*, 3631
74. Welch, J. T.; Eswarakrishnan, S. *J. Org. Chem.* **1985**, *50*, 5909
75. Burke, S. D.; Pacofsky, G. J.; Piscopio, A. D. *J. Org. Chem.* **1992**, *57*, 2228
76. Santos, D.; Ariza, X.; Garcia, J.; Lloyd-Williams, P.; Martínez-Laporta, A.; Sánchez, C. *J. Org. Chem.* **2013**, *78*, 1519
77. Pratt, L. M.; Bowles, S. A.; Courtney, S. F.; Hidden, C.; Lewis, C. N.; Martin, F. M.; Todd, R. S. *Synlett* **1998**, 531
78. a) Hoffman, R. W. *Chem. Rev.* **1989**, *89*, 1841; b) Hoveyda, A. H.; Evans, D. A.; Fu, G. C. *Chem. Rev.* **1993**, *93*, 1307
79. Evans, D. A.; Bartoli, J.; Shih, T. L. *J. Am. Chem. Soc.* **1981**, *103*, 2127
80. Yamazaki, T.; Shinohara, N.; Kitazume, T.; Sato, S. *J. Org. Chem.* **1995**, *60*, 8140
81. Cieplak, A. S. *Chem. Rev.* **1999**, *99*, 1265
82. Dong, V. M.; MacMillan, D. W. C. *J. Am. Chem. Soc.* **2001**, *123*, 2448
83. a) Liu, P.; Seo, J. H.; Weinreb, S. M. *Angew. Chem. Int. Ed.* **2010**, *49*, 2000; b) Seo, J. H.; Liu, P.; Weinreb, S. M. *J. Org. Chem.* **2010**, *75*, 2667

84. Matsuta, Y.; Kobari, T.; Kurashima, S.; Kumakura, Y.; Shinada, M.; Higuchi, K.; Kawasaki, T. *Tetrahedron Lett.* **2011**, *52*, 6199
85. Takiguchi, S.; Iizuka, M.; Kumakura, Y.; Murasaki, K.; Ban, N.; Higuchi, K.; Kawasaki, T. *J. Org. Chem.* **2010**, *75*, 1126
86. a) Maruoka, K.; Banno, H.; Yamamoto, H. *J. Am. Chem. Soc.* **1990**, *112*, 7791; *Tetrahedron: Asymmetry* **1991**, *2*, 647; b) Maruoka, K.; Yamamoto, H. *Synlett* **1991**, 793
87. Uyeda, C.; Rötheli, A. R.; Jacobsen, E. N. *Angew. Chem. Int. Ed.* **2010**, *49*, 9753
88. Kaeobamrung, J.; Mahatthananchai, J.; Zheng, P.; Bode, J. W. *J. Am. Chem. Soc.* **2010**, *132*, 8810
89. Miller, S. P.; Morcken, J. P. *Org. Lett.* **2002**, *4*, 2743
90. Patil, A. S.; Mo, D.-L.; Wang, H.-Y.; Mueller, D. S.; Anderson, L. L. *Angew. Chem. Int. Ed.* **2012**, *51*, 7799
91. Bartovic, A. *J. Heterocyclic Chem.* **2000**, *37*, 827
92. Trend, R. M.; Ramtohul, Y. K.; Ferreira, E. M.; Stoltz, B. M. *Angew. Chem. Int. Ed.* **2003**, *42*, 2892
93. Othman, R. B.; Bousquet, T.; Fousse, A.; Othman, M.; Dalla, V. *Org. Lett.* **2005**, *7*, 2825
94. Taldone, T.; Zatorska, D.; Patel, H. J.; Sun, W.; Patel, M. R.; Chiosis, G. *Heterocycles* **2013**, *87*, 91
95. a) Liebeskind, L.; Srogl, J. *J. Am. Chem. Soc.* **2000**, *122*, 11260; b) Yu, Y.; Liebeskind, L. S. *J. Org. Chem.* **2004**, *69*, 3554

96. Haugland, R. P. *The Handbook. A Guide to Fluorescent Probes and Labeling Technology*, 10th Ed.; Molecular Probes: Eugene, Oregon, USA **2005**
97. Arroyo, I. J.; Hub, R.; Tang, B. Z.; Lopez, F. I.; Pena-Cabrera, E. *Tetrahedron* **2011**, *67*, 7244
98. a) Tebbe, F. N.; Parshall, G. W.; Reddy, G. S. *J. Am. Chem. Soc.* **1978**, *100*, 3611;
b) Beadham, I.; Micklefield, J. *Curr. Org. Syn.* **2005**, *2*, 231
99. a) Corey, E. J.; Bakshi, R. K.; Shibata S. *J. Am. Chem. Soc.* **1987**, *109*, 5551; b)
Corey, E. J. et al. *J. Am. Chem. Soc.* **1987**, *109*, 7925. b) Corey, E. J.; Shibata, S.;
Bakshi, R. K. *J. Org. Chem.* **1988**, *53*, 2861
100. Ryu, D. H.; Corey, E. J. *J. Am. Chem. Soc.* **2003**, *125*, 6388
101. Fujii, A.; Hashiguchi, S.; Uematsu, N.; Ikariya, T.; Noyori, R. *J. Am. Chem. Soc.*
1996, *118*, 2521
102. Hoye, T. R.; Jeffrey, C. S.; Shao, F. *Nat. Protoc.* **2007**, *2*, 2451
103. Leventis, P.A.; Grinstein S. *Annu. Rev. Biophys.* **2010**, *39*, 407
104. Eyster, K. M. *Adv. Physiol. Educ.* **2007**, *31*, 5
105. Lippincott-Schwartz, J.; Phair, R. D. *Annu Rev Biophys.* **2010**, *39*, 559
106. Clària, J. *Recent Pat. Anticancer Drug Discov.* **2006**, *1*, 369
107. Fernández-Checa, J. C. *Biochem. Biophys. Res. Commun.* **2003**, *304*, 471
108. Ehnholm, C. *Cellular Lipid Metabolism*; 1st Ed.; Springer: Helinski, Finland,
2009
109. Alberts, B.; Johnson, A.; Lewis, J. et al. *Molecular Biology of the Cell*, 4th Ed.;
Garland Science: New York, 2002; 1-376
110. Zimmermann, U.; Pilwat, G.; Pequex, A.; Gilles, R. *J. Membr. Biol.* **1980**, *54*, 103

111. University of Guelph, Frances Sharom Lab www.uoguelph.ca/~fsharom/research/research.html (accessed May 10th 2013)
112. Cooper, G. M. *The Cell: A Molecular Approach*, 2nd Ed.; Sinauer Associates: Sunderland, MA, USA, 2002; 1-400
113. Berg, J. M.; Tymoczko, J. L.; Stryer, L. Lipids and Cell Membranes. In *Biochemistry*, 5th Ed.; W H Freeman: New York, USA, 2002
114. Halifax Regional School Board <http://hrsbstaff.ednet.ns.ca/> (accessed May 10th 2013)
115. Alder-Baerens, N.; Lisman, Q.; Luong, L.; Pomorski, T.; Holthuis, J. C. M. *Mol. Biol. Cell* **2006**, *17*, 1632
116. Celebrating Science <http://asweexplore.blogspot.com> (accessed on May 11th 2013)
117. Vance, J. E. *J. Lipid Res.* **2008**, *49*, 1377
118. Murphy, E. J.; Anderson, D. K.; Horrocks, L. A. *J. Neurosci. Res.* **1993**, *34*, 472
119. Folch, J. et. al. *J. Biol. Chem.* **1942**, *174*, 439
120. Xenabioherbals <http://www.xenabioherbals.net/phosphatidylserine-555188.html> (accessed on May 12th 2013)
121. Swairjo, M. A.; Concha, N. O.; Kaetzel, M. A.; Dedman, J. R.; Seaton, B. A. *Nat. Struct. Biol.* **1995**, *2*, 968
122. Vance, J. E.; Steenbergen, R. *Prog. Lipid. Res.* **2005**, *44*, 207
123. McLaughlin, S.; Murray, D. *Nature* **2005**, *438*, 605
124. Palfrey, H. C.; Wasrm, A. *J. Biol. Chem.* **1985**, *260*, 16021
125. Meers, P.; Mealy, T. *Biochemistry* **1993**, *32*, 11711

126. O'Toole, P.J. .; Wolfe, C.; Ladha, S.; Cherry, R. J. *Biochim. Biophys. Acta* **1999**, *1419*, 64
127. Fadok, V. A.; Voelker, D. R.; Campbell, P. A.; Cohen, J. J.; Bratton, D. L.; Henson, P. M. J. *Immunol.* **1992**, *148*, 2207
128. Miyanishi, M.; Tada, K.; Koike, M.; Uchiyama, Y.; Kitamura, T.; Nagata, S. *Nature* **2007**, *450*, 435
129. Park, D.; Hochreiter-Hufford, A.; Ravichandran, K. S. *Curr. Biol.* **2009**, *19*, 346
130. Shirastsuchi, A.; Umeda, M.; Ohba, Y.; Nakanishi, Y. *J. Biol. Chem.* **1997**, *272*, 2354
131. BioCat <http://www.biocat.com> (accessed on May 15th 2013)
132. Gregory, C. D.; Devitt, A. *Immunol.* **2004**, *113*, 1
133. Bevers, E. M.; Comfurius, P.; van Rijn, L. N.; Hemker, H. C.; Zwaal, R. F. *Eur. J. Biochem.* **1982**, *122*, 429
134. Williamson, P.; Bevers, E. M.; Smeets, E. F.; Comfurius, P.; Schlegel, R. A.; Zwaal, R. F. *Biochemistry* **1995**, *34*, 10448
135. AOCS Lipid Library <http://lipidlibrary.aocs.org/> (accessed on May 15th 2013)
136. Folch, J.; Lees, M.; Sloane Stanley, G. H. *J. Biol. Chem.* **1957**, *226*, 497
137. Analysis of Lipids <http://people.umass.edu/~mcclemen/581Lipids.html> (accessed on May 16th 2013)
138. Peterson, B. L.; Cummings, B. S. *Biomed. Chromatogr.* **2006**, *20*, 227
139. Stein, J. M.; Smith, G. A.; Luzio, J. P. *Biochem. J.* **1991**, *274*, 375
140. Amenta, J. S. *J. Lipid Res.* **1964**, *5*, 270
141. Schneiter, R. et. al. *J Cell Biol.* **1999**, *146*, 741

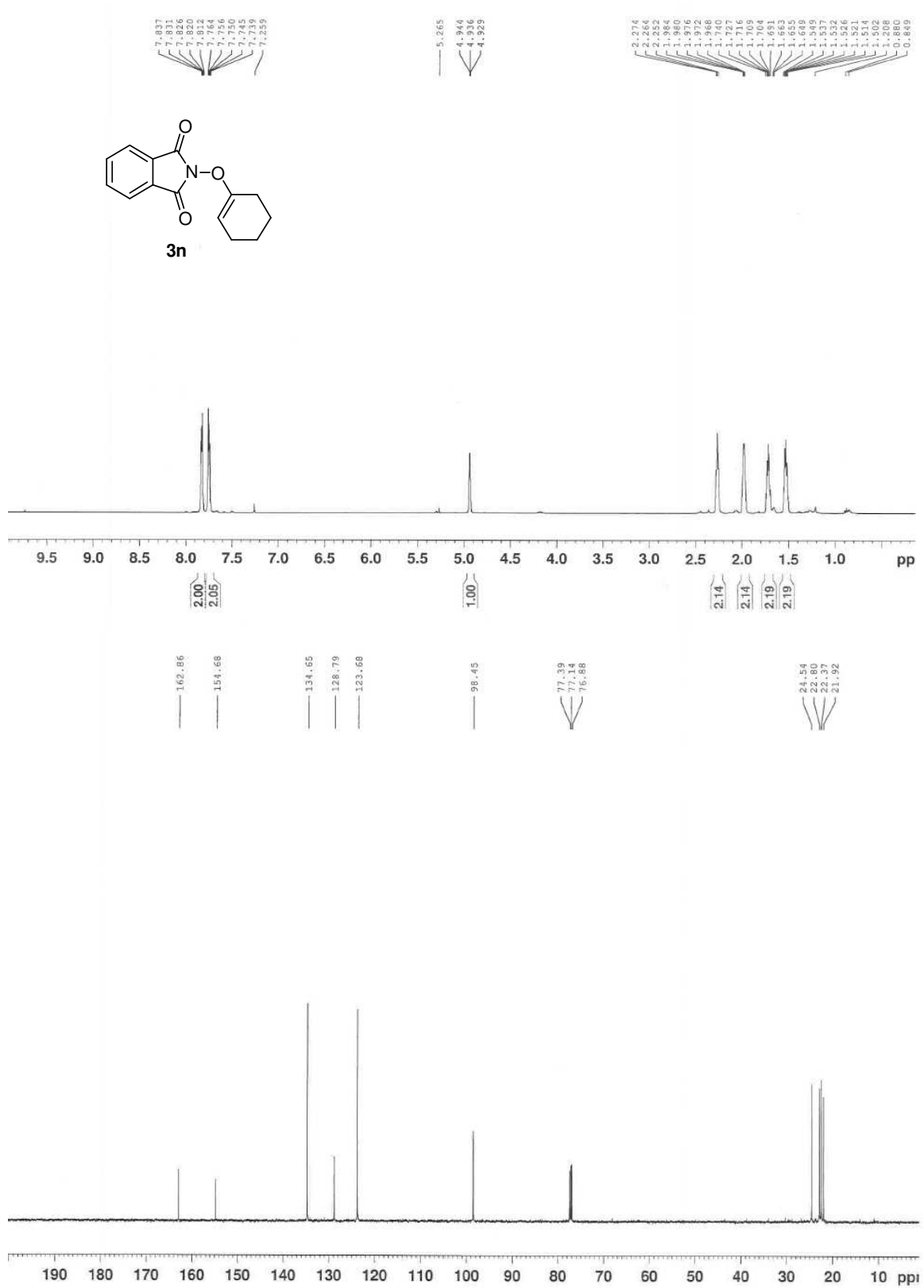
142. Bouchart, A.; Bouchart, F.; Richet, C.; Kol, O.; Leroy, Y.; Timmerman, P.; Huet, G.; Bohin, J. P.; Zanetta, J. P. *Anal. Biochem.* **2005**, 340, 231
143. Sommer, U.; Herscovitz, H.; Welty, F. K.; Costello, C. E. *J. Lipid Res.* **2006**, 47, 804
144. Maziarz E. P.; Baker, G. A.; Mure, J. V.; Woodab, T. D. *Int. J. Mass Spectrom.* **2000**, 202, 241
145. Flannagan, R. S.; Grinstein, S. *Methods Mol. Biol.* **2010**, 591, 121
146. Demchanko, A. P. *Advanced Fluorescence Reporters in Chemistry and Biology I: Fundamentals and Molecular Design*, 1st Ed.; Springer-Verlag: Berlin, Germany, **2010**, 1-21
147. Chudakov, D. M.; Matz, M. V.; Lukyanov, S.; Lukyanov, K. A. *Physiol. Rev.* **2010**, 90, 1103
148. Chen, N.-T. Et. al. *Int. J. Mol. Sci.* **2012**, 13, 16598
149. Introduction to Fluorescence Sensing by Alexander Demchanko <http://books.google.com/books> (accessed on May 20th 2013)
150. Hebbbar, S.; Lee, E.; Manna, M.; Steinert, S.; Kumar, G. S.; Wenk, M.; Wohland, T.; Kraut, R. *J. Lipid Res.* **2008**, 49, 1077
151. Blooma, M.; Evansa, E.; Mouritsena, O. G. *Q. Rev. Biophys.* **1991**, 24, 293
152. Lentz, B. R. *Chem. Phys. Lipids* **1980**, 50, 171
153. Haidekker, M. A.; Theodorakis, E.A. *Org. Biomol. Chem.* **2007**, 5, 1669
154. Reichardt, C. *Chem. Rev.* **1994**, 94, 2319
155. Parisio, G.; Marini, A.; Biancardi, A.; Ferrarini, A.; Mennucci, B. *J. Phys. Chem B.* **2011**, 115, 9980

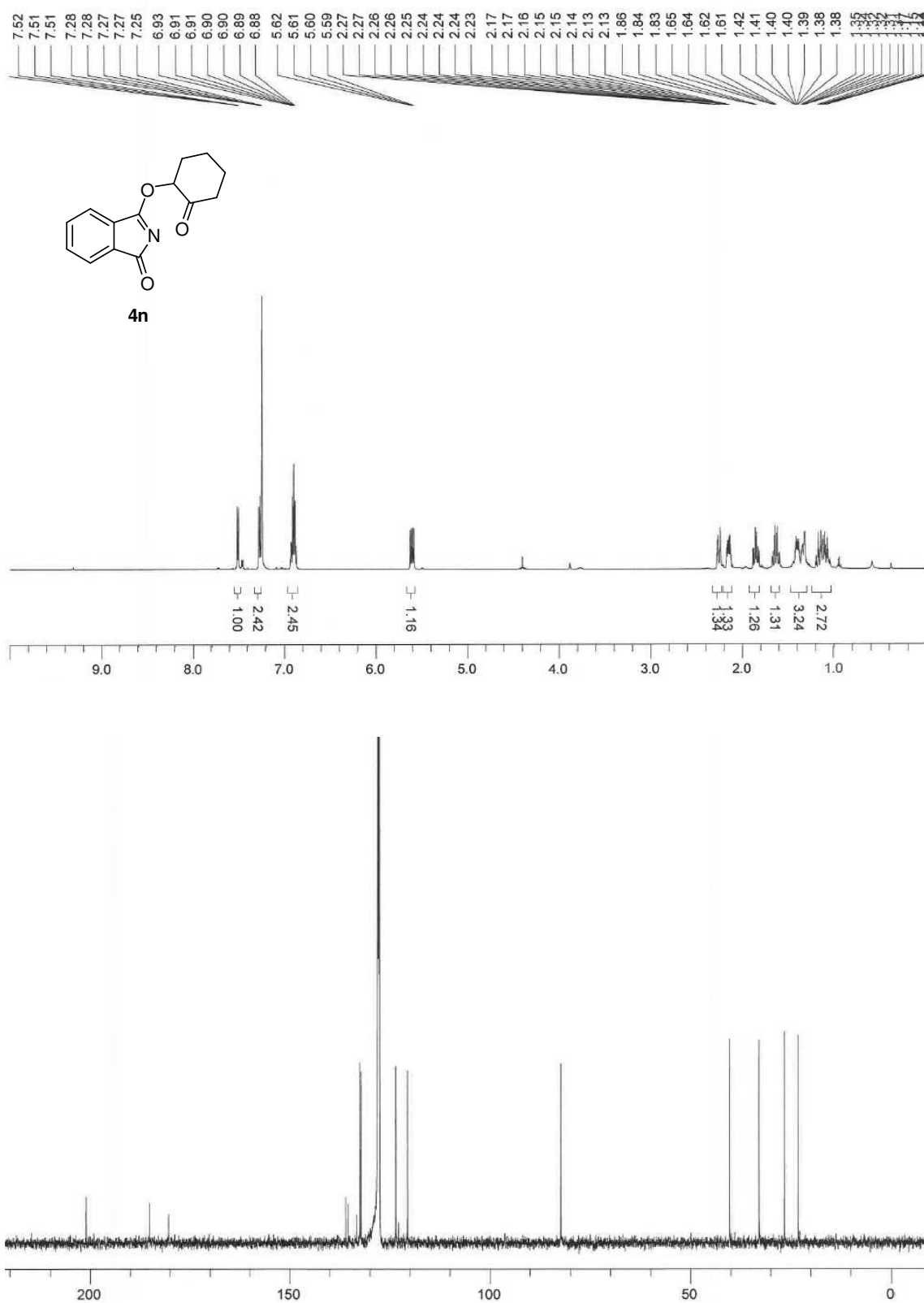
156. Molecular Expressions Optical Microscope Primer
<http://micro.magnet.fsu.edu/primer/java/jablonski/solventeffects/> (accessed on July 22nd 2013)
157. Sykora, J.; Kapusta, P.; Fidler, V.; Hof, M. *Langmuir* **2002**, *18*, 571
158. Parasassi, T.; Di Stefano, M.; Loiero, M.; Ravagnan, G.; Gratton, E. *Biophys. J.* **2004**, *66*, 763
159. Catalan, J.; Perez, P.; Laynez, J.; Blanco, F. G. *J. Fluoresc.* **1990**, *1*, 215
160. Bublitz, G. U.; Boxer, S. G. *Annu. Rev. Phys. Chem.* **1997**, *48*, 213
161. Clarke, R. J.; Kane, D. J. *Biochim. Biophys. Acta.* **1997**, *1323*, 223
162. Jin, L.; Millard, A. C.; Wuskell, J. P.; Dong, X.; Wu, D. et al. *Biophys. J.* **2006**, *90*, 2563
163. Peter, C.; Hummer, G. *Biophys. J.* **2005**, *89*, 2222
164. Cooper, G. M. *The Cell: A Molecular Approach*, 2nd Ed.; Sinauer Associates: Sunderland, MA, USA, **2000**, 1-25
165. Dowhan, W.; Bogdanov, M. *Biochim. Biophys. Acta.* **2012**, *1818*, 1097
166. Dowhan, W.; Bogdanov, M. *Biochem. Soc. Trans.* **2011**, *39*, 767
167. Fadeel, B.; Xue, D. *Crit. Rev. Biochem. Mol. Biol.* **2009**, *44*, 264
168. Karmakar, S.; Cummings, R. D.; McEver, R. P. *J. Biol. Chem.* **2005**, *280*, 28623
169. McLaughlin, S.; Murray, D. *Nature* **2005**, *438*, 605
170. Chaurio, R. A.; Janko, C.; Munoz, L. E.; Frey, B.; Herrmann, M.; Gaipl, U. S. *Molecules* **2009**, *14*, 4892
171. Li, M. O. *Science* **2003**, *302*, 1560

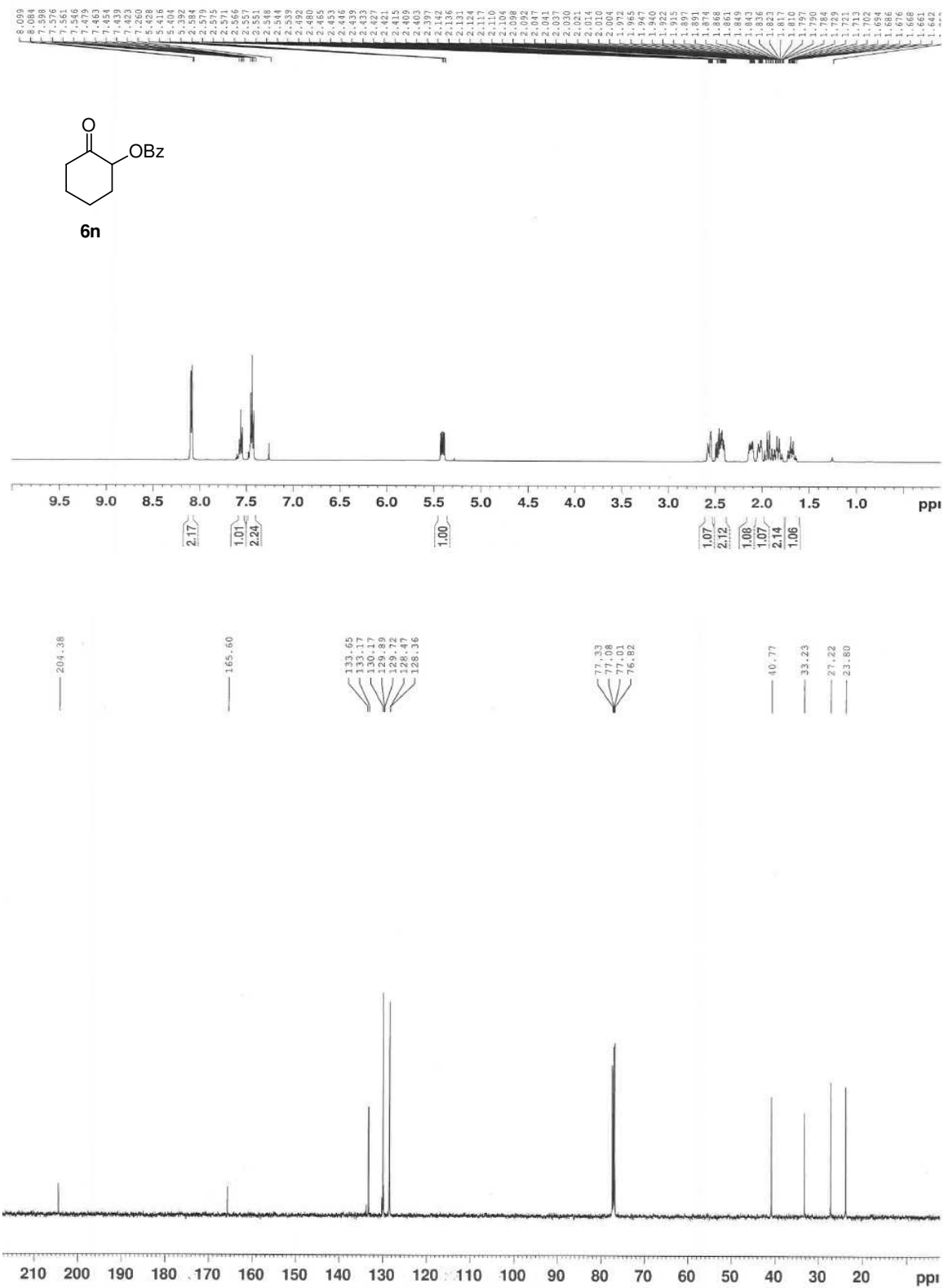
172. AOCS Lipid Library (<http://lipidlibrary.aocs.org/index.html>) (Accessed on June 20, 2013)
173. Schutters, K.; Reutelingsperger, C. *Apoptosis* **2010**, *15*, 1072
174. Zwaal, R. F. A.; Comfurius, P.; Bevers, E. M. *Cell. Mol. Life Sci.* **2005**, *62*, 971
175. Kwok, V.; Vachon, E.; Downey, G. P. *Methods Mol. Biol.* **2009**, *531*, 301
176. Demchenko, A. P.; Mély, Y.; Duportail, G.; Klymchenko, A. S. *Biophys J.* **2009**, *96*, 3461
177. a) Berezin, M. Y.; Achilefu, S. *Chem Rev.* **2010**, *110*, 2641; b) Sameiro, M.; Gonçalves, T. *Chem Rev.* **2009**, *109*, 190
178. Yoon, Y.; Lee, P. J.; Kurilova, S.; Cho, W. *Nat. Chem.* **2011**, *3*, 868
179. Itoh, T.; Koshiba, S.; Kigawa, T.; Kikuchi, A.; Yokoyama, S.; Takenawa, T. *Science* **2001**, *291*, 1047
180. Ford, M. G. J.; Mills, I. G.; Peter, B. J.; Vallis, Y.; Praefcke, G. J. K.; Evans, P. R.; McMahon, H. T. *Nature* **2002**, *419*, 361
181. Stahelin, R. V.; Long, F.; Peter, B. J.; Murray, D.; De Camilli, P.; McMahon, H. T.; Cho, W. *J. Biol. Chem.* **2003**, *278*, 28993
182. Brown, H. *Methods in Enzymology, Volume 434: Lipidomics and Bioactive Lipids: Lipids and Cell Signaling*, 1st Ed.; Academic Press, **2007**, 1-392
183. Saito, N.; Shirai, Y. *J. Biochem.* **2002**, *132*, 683
184. Loving, G.; Imperiali, B. *Bioconjug. Chem.* **2009**, *20*, 2133
185. Selwert, B.; Hayen, H.; Karst, U. *J. Am. Soc. Mass Spectrom.* **2008**, *19*, 1
186. Peng, H.; Chen, W.; Cheng, Y.; Hakuna, L.; Strongin, R.; Wang, B. *Sensors* **2012**, *12*, 15907

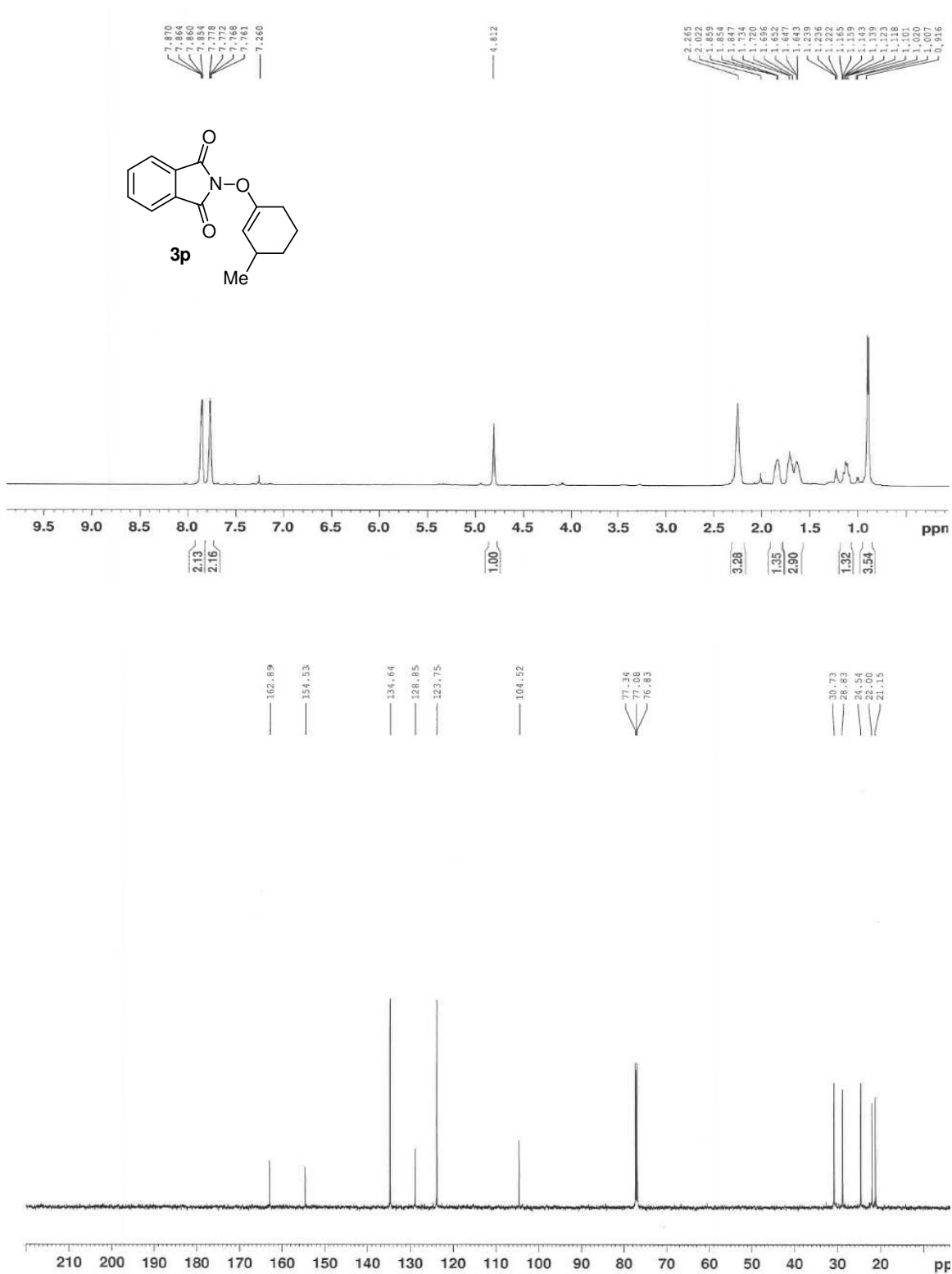
187. a) AOCS Lipid Library (<http://lipidlibrary.aocs.org/index.html>) (Accessed on June 28, 2013) b) Loura, L. M. S.; Prieto, M.; Fernandes, F. *Eur. Biophys. J.* **2010**, *39*, 565
188. a) Miki, M. *J. Biochem.* **1985**, *97*, 1067; b) Bragg, P. D.; Hou, C. *Biochim. Biophys. Acta.* **1999**, *1413*, 159; c) Devaux, P. F.; Seigneuret, M. *BBA – Rev. Biomembranes* **1985**, *822*, 63
189. a) Hawe, A.; Sutter, M.; Jiskoot, W. *Pharm. Res.* **2008**, *25*, 1487; b) Sun, C.; Yang, J.; Li, L.; Wu, X.; Liu, Y.; Liu, S. *J. Chromatogr. B* **2004**, *803*, 173
190. a) Park, S.-Y.; Kim, S.-Y.; Jung, M.-Y.; Bae, D.-J.; Kim, I.-S. *Mol. Cell. Biol.* **2008**, *28*, 5288; b) Mazères, S.; Schram, V.; Tocanne, J. F.; Lopez, A. *Biophys. J.* **1996**, *71*, 327
191. Schneggenburger, P. E.; Beerlink, A.; Weinhausen, B.; Salditt, T.; Diederichsen, U. *Eur. Biophys. J.* **2011**, *40*, 417
192. Bowe, C. L. et. al. *Proc. Natl. Acad. Sci. USA* **1997**, *94*, 12218.
193. Cinelli, R. A.; Ferrari, A.; Pellegrini, V.; Tyagi, M.; Giacca, M.; Beltram, F. *Photochem. Photobiol.* **2000**, *71*, 771
194. a) Russell, J. D.; Hilger, R. T.; Ladrör, D. T.; Tervo, M. A.; Scalf, M.; Shortreed, M. R.; Coon, J. J.; Smith, L. M. *Anal. Chem.* **2011**, *83*, 2187; b) Royer, C. A.; Mann, C. J.; Matthews, C. R. *Biophys. J.* **1992**, *63*, 741
195. Greenspan, P.; Fowler, S. D.. *J. Lipid Res.* **1985**, *26*, 781
196. Jose, J.; Burgess, K. *J. Org. Chem.* **2006**, *71*, 7835
197. Ananthanarayanan, B.; Stahelin, R. V.; Digman, M. A.; Cho, W. *J. Biol. Chem.* **2003**, *278*, 46886

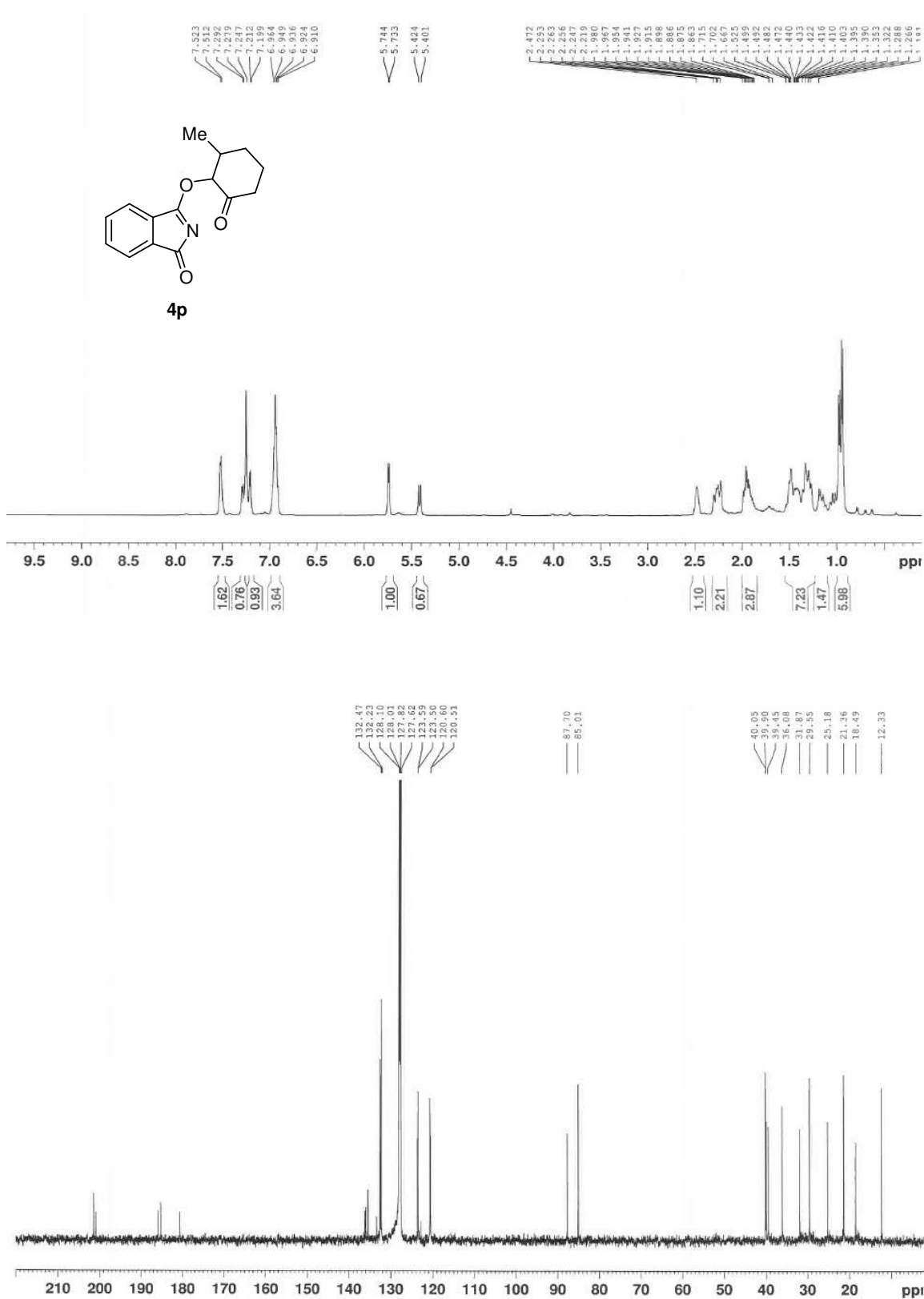
198. Kim, E.; Koh, M.; Ryu, J.; Park, S. B. *J. Am. Chem. Soc.* **2008**, *130*, 12206
199. a) Zhao, W.; Bian, W. *Comp. Theor. Chem.* **2007**, *818*, 43; b) Wagner, B. D. *Molecules* **2009**, *14*, 210; c) Kuzetsova, N. A.; Kaliya, O. L. *Russ. Chem. Rev.* **1992**, *61*, 683
200. Langmuir, M. E.; Yang, J.-R.; Moussa, A. M.; Laura, R.; LeCompte, K. A. *Tetrahedron Lett.* **1995**, *36*, 3989
201. Briggs, M. S.; Bruce, I.; Miller, J. N.; Moody, C. J.; Simmonds, A. C.; Swann, E. *J. Chem. Soc. Perkin Trans. I* **1997**, 1051
202. Tsou, L. K.; Zhang, M. M.; Hang, H. C. *Org. Biomol. Chem.* **2009**, *7*, 5055
203. Boutome, H.; Hartmann, H. *Monatsh. Chem.* **1997**, *128*, 71
204. Lakowicz, J. R. *Principles of Fluorescence Spectroscopy*, 1st Ed.; Plenum Press: New York and London, **1983**, 1-200
205. Hantzsch, A. *Chem. Ber.* **1922**, *55*, 953
206. El-Batta, A.; Jiang, C.; Zhao, W.; Anness, R.; Cooksy, A. L.; Bergdahl, M. *J. Org. Chem.* **2007**, *72*, 5244
207. Turnbull, M. D. *J. Chem. Soc., Perkin Trans. I* **1997**, *8*, 1241
208. Keller, M.; Erdmann, D.; Pop, N.; Pluym, N.; Teng, S.; Bernhardt, G.; Buschauer, A. *Bioorg. Med. Chem.* **2011**, *19*, 2859

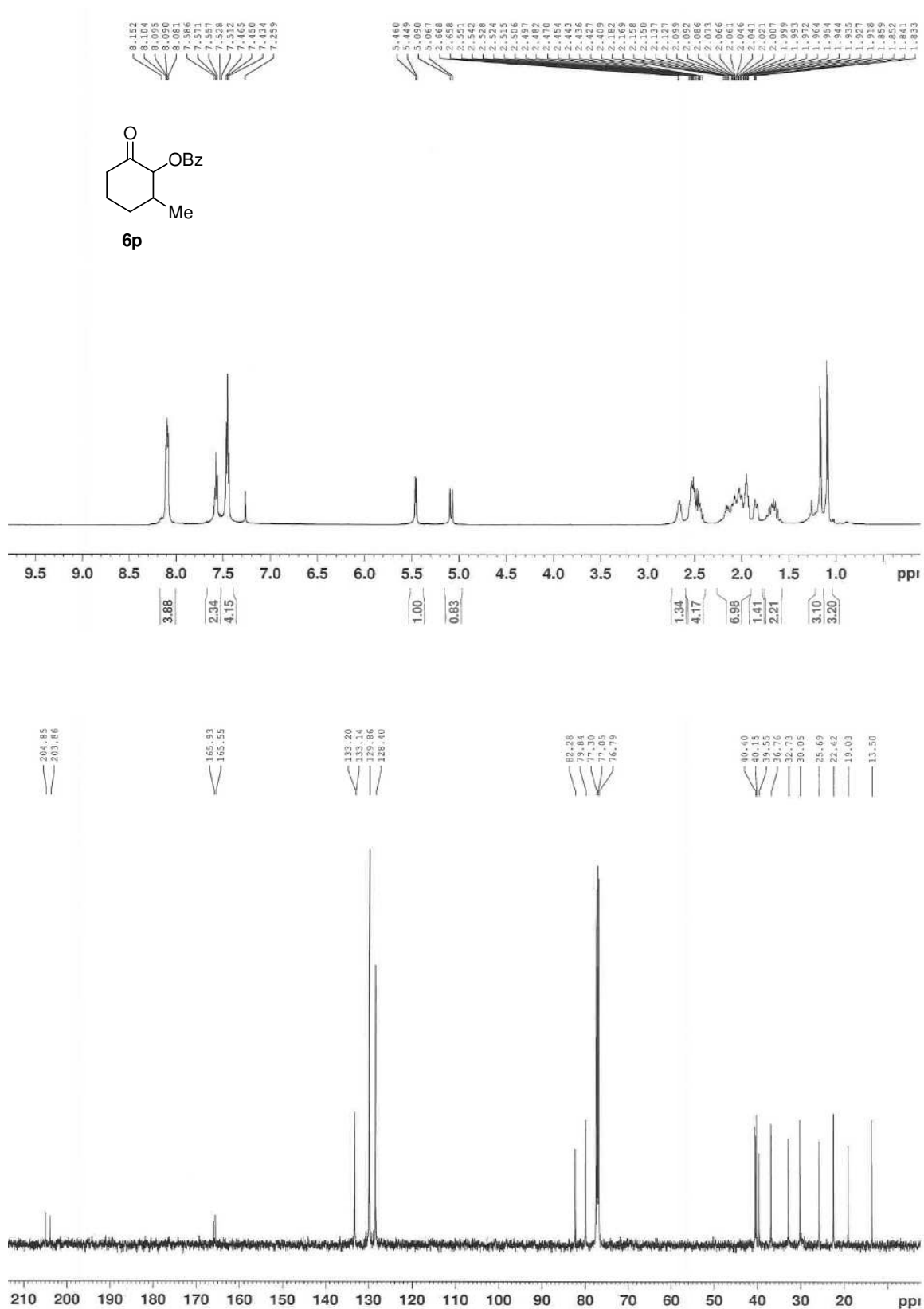
APPENDIX A: ^1H NMR and ^{13}C NMR spectra of **3n**

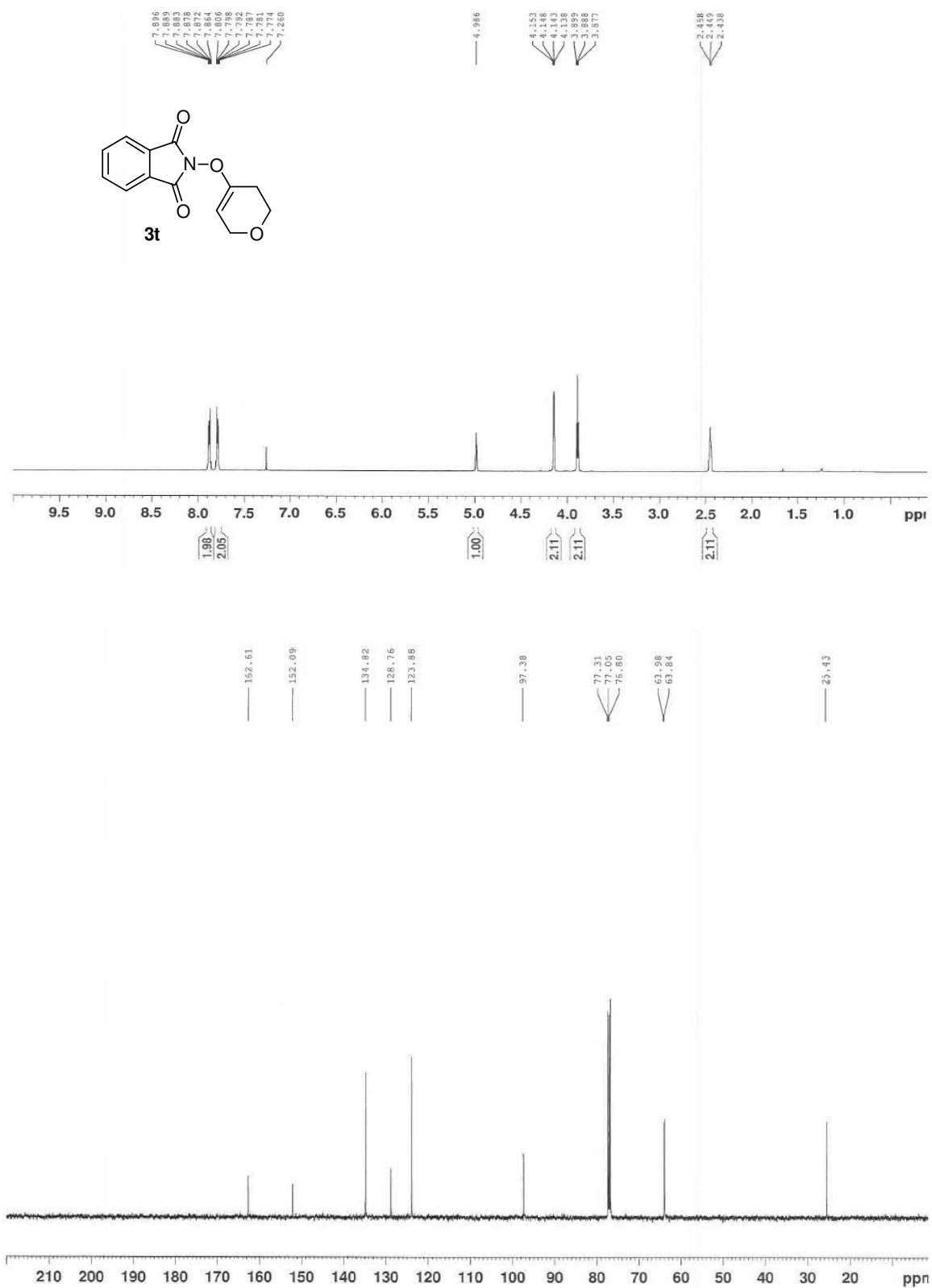
APPENDIX B: ^1H NMR and ^{13}C NMR spectra of **4n**

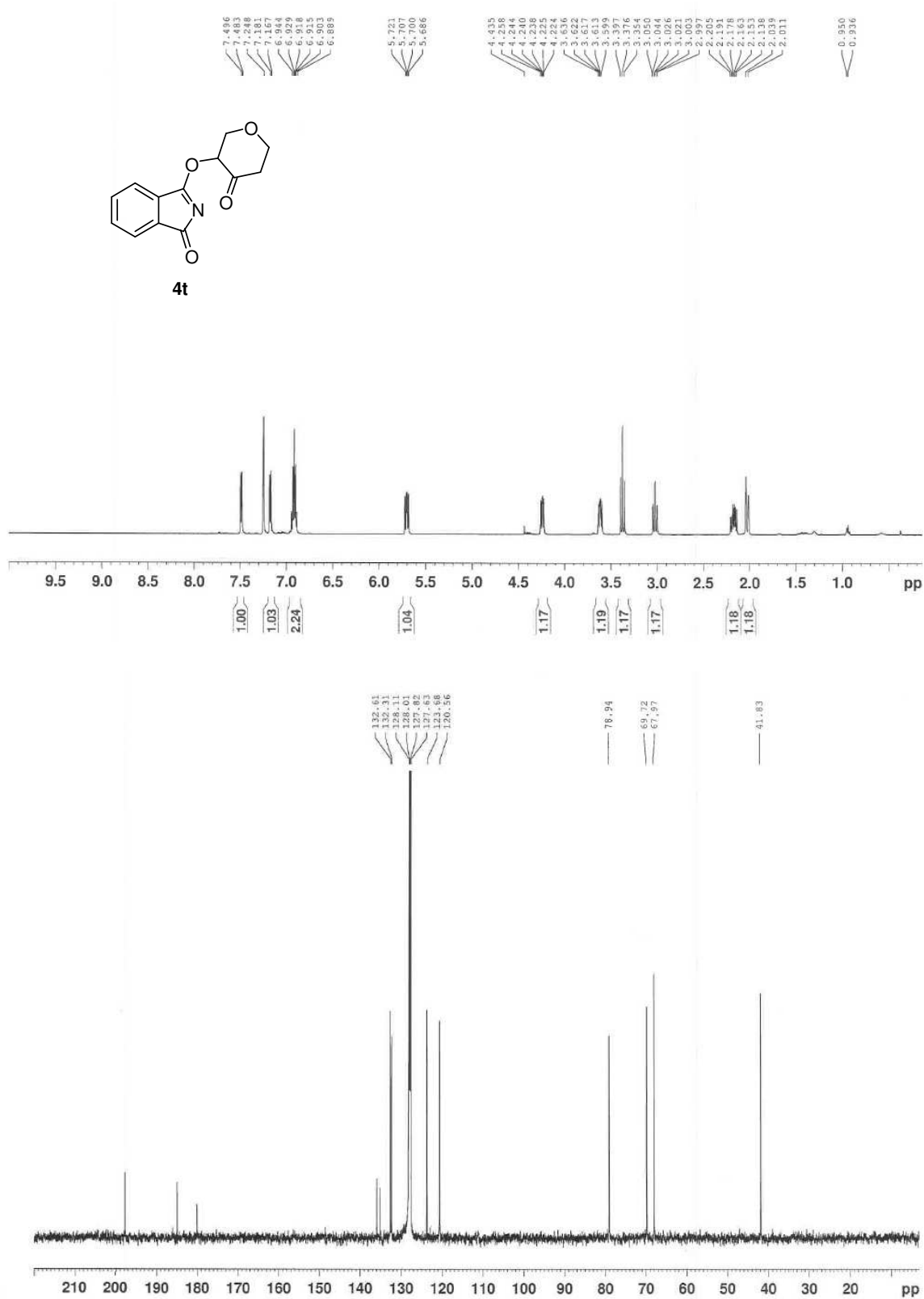
APPENDIX C: ^1H NMR and ^{13}C NMR spectra of **6n**

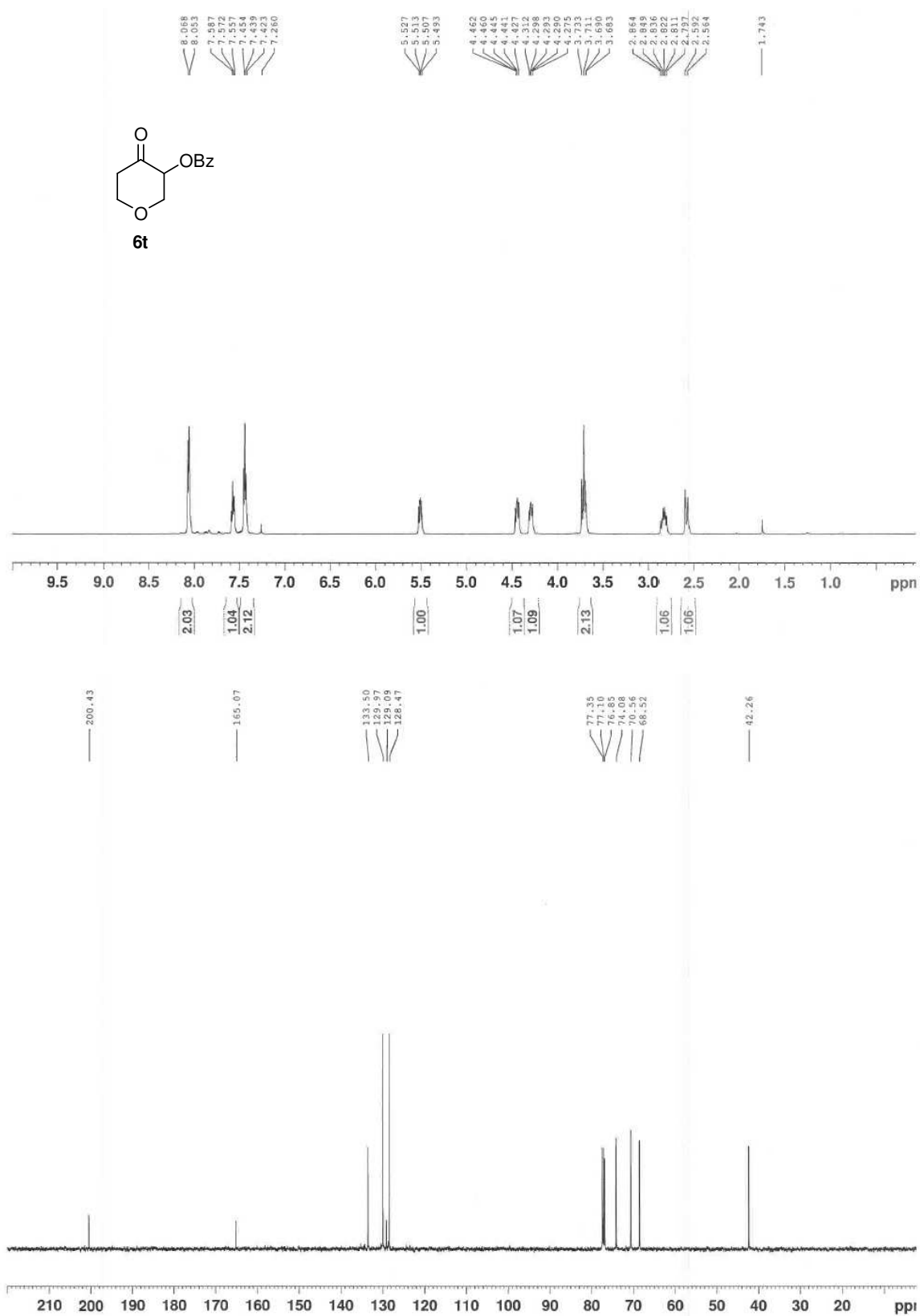
APPENDIX D: ^1H NMR and ^{13}C NMR spectra of **3p**

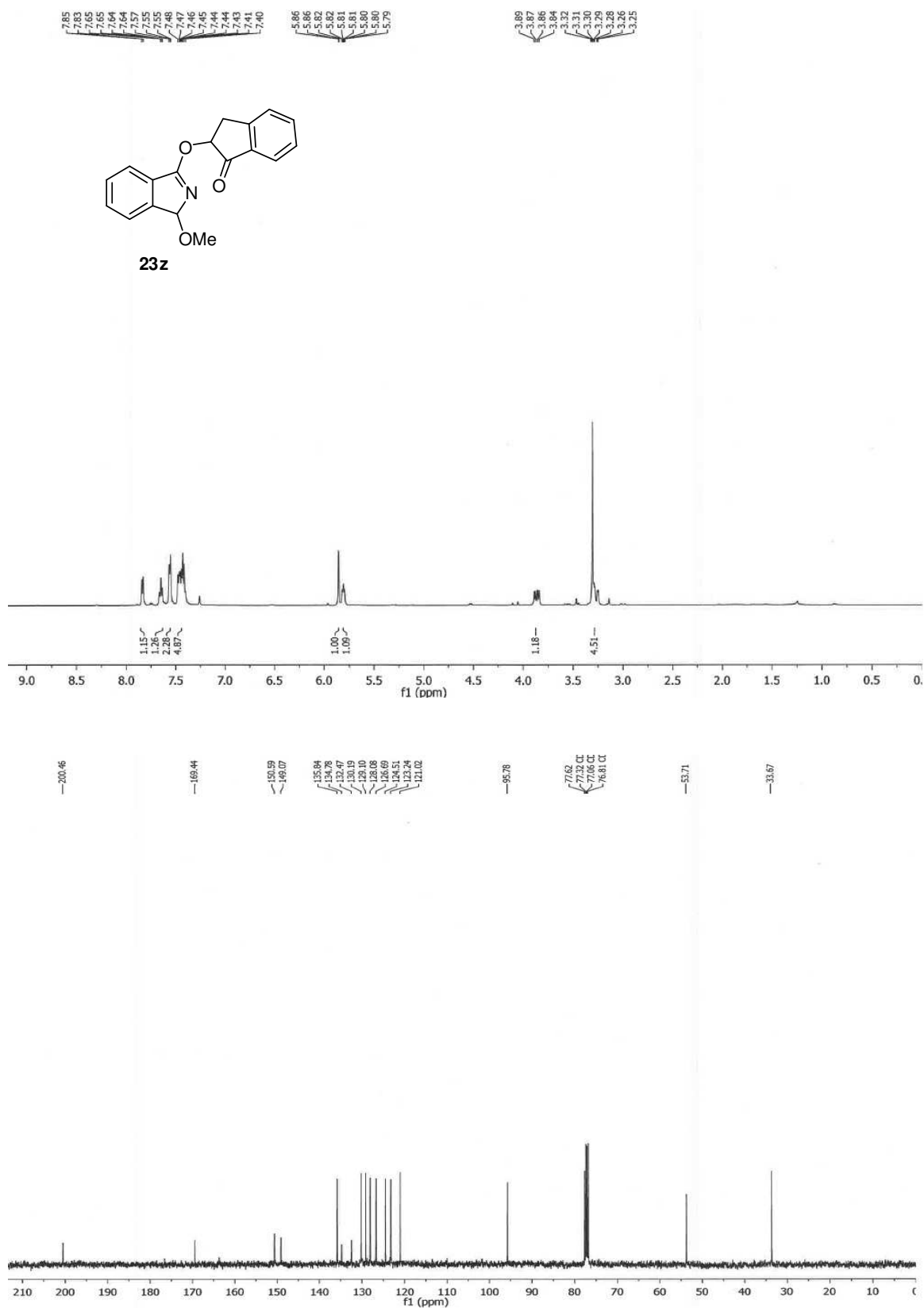
APPENDIX E: ^1H NMR and ^{13}C NMR spectra of **4p**

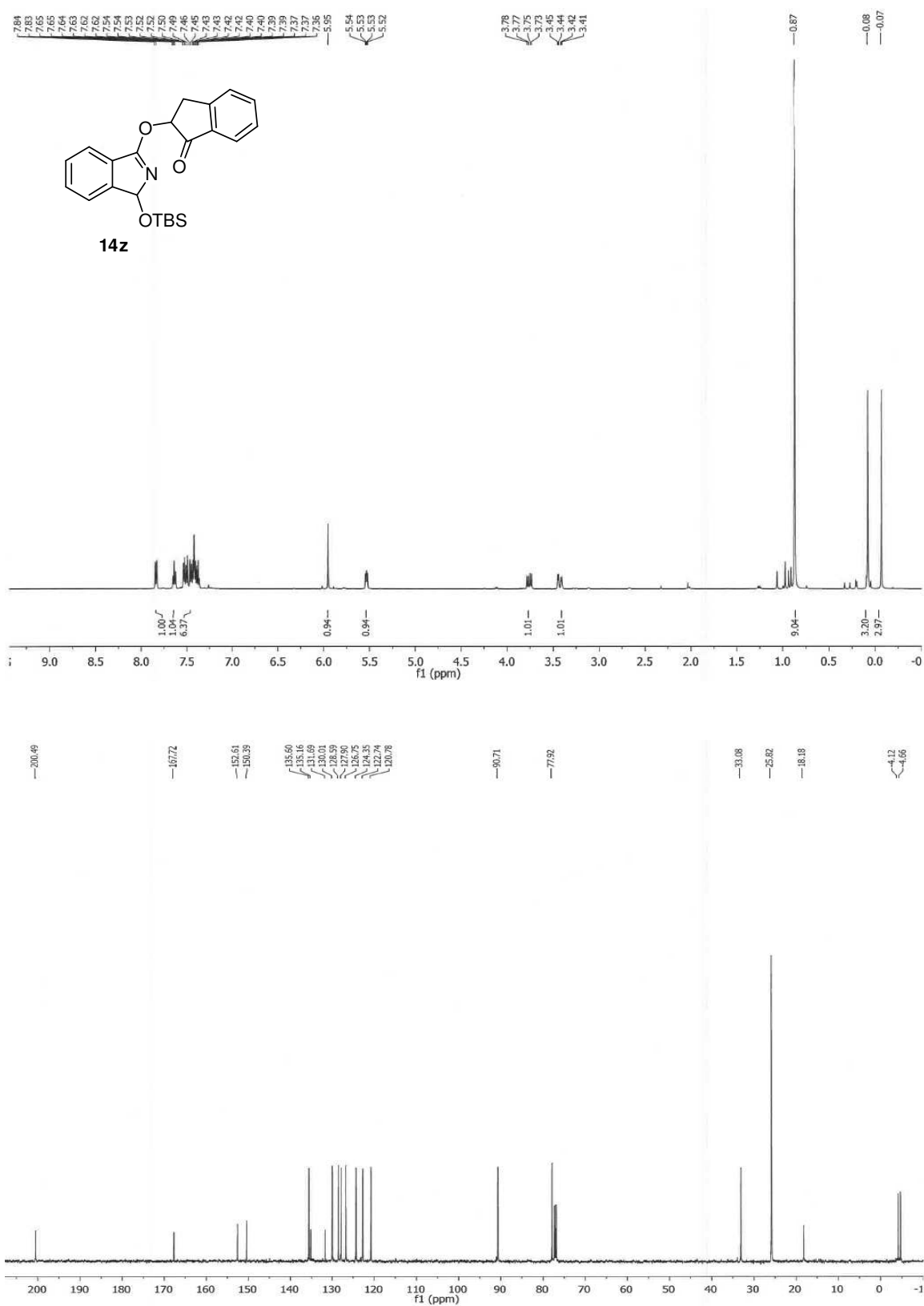
APPENDIX F: ^1H NMR and ^{13}C NMR spectra of **6p**

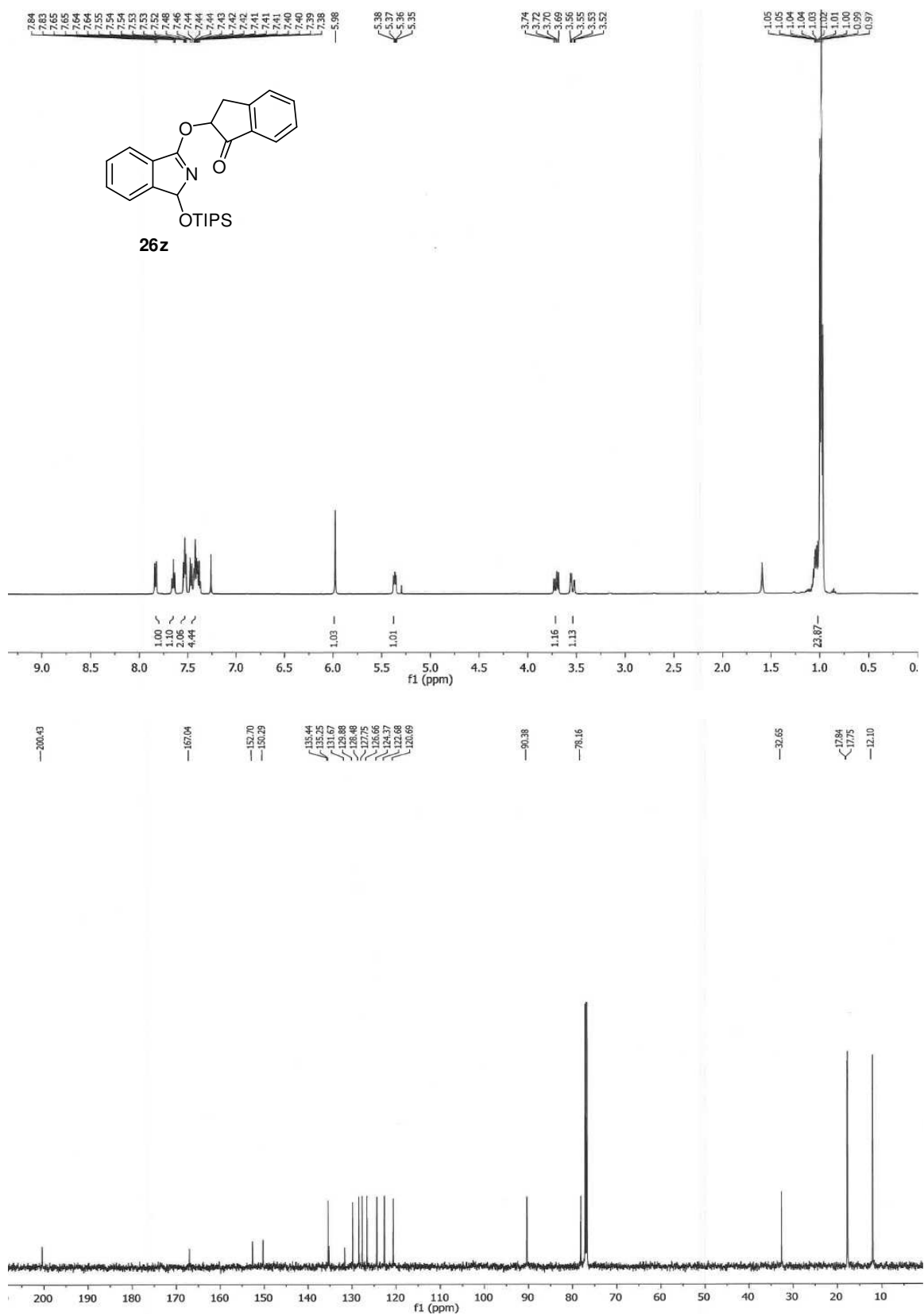
APPENDIX G: ^1H NMR and ^{13}C NMR spectra of **3t**

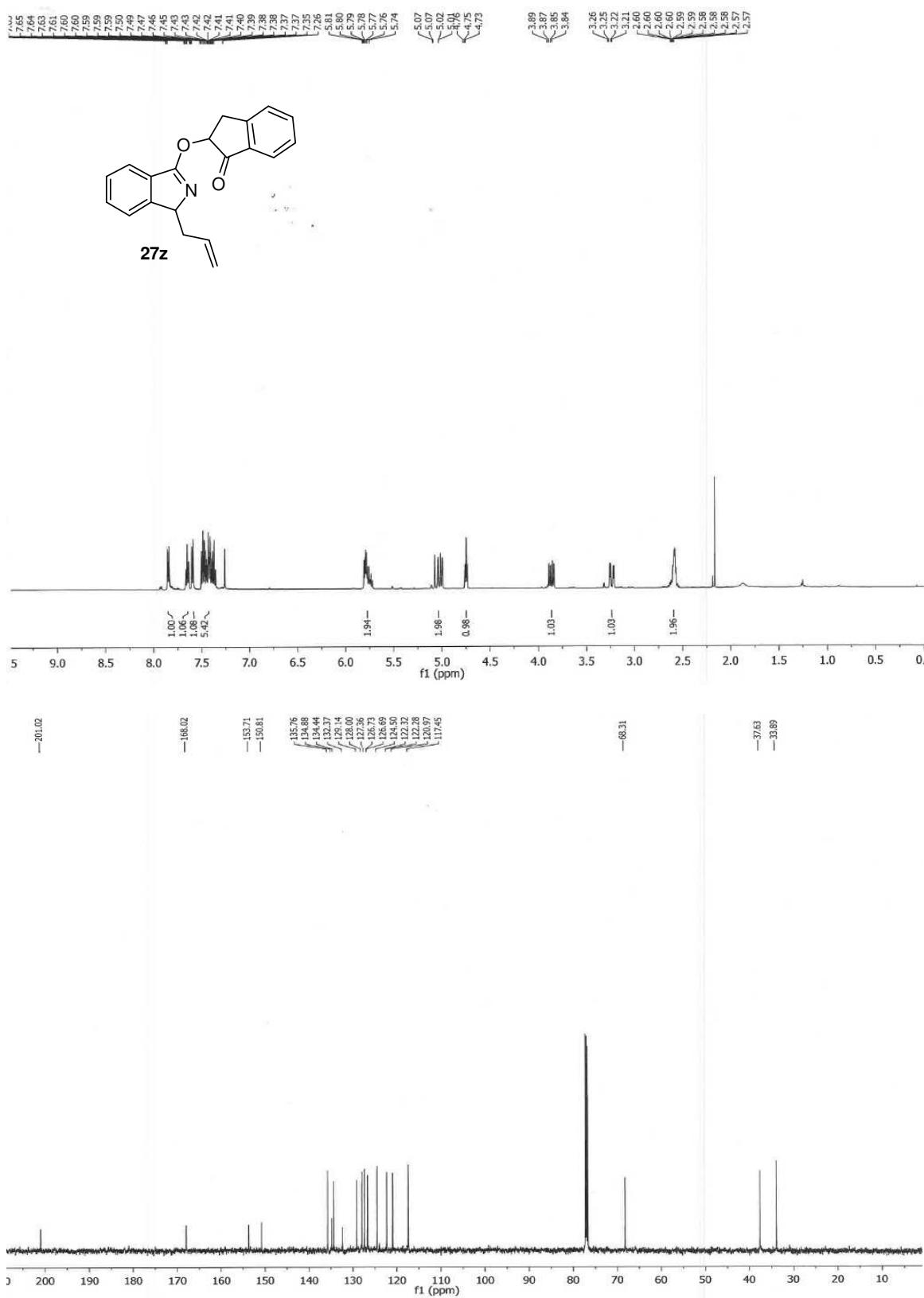
APPENDIX H: ^1H NMR and ^{13}C NMR spectra of **4t**

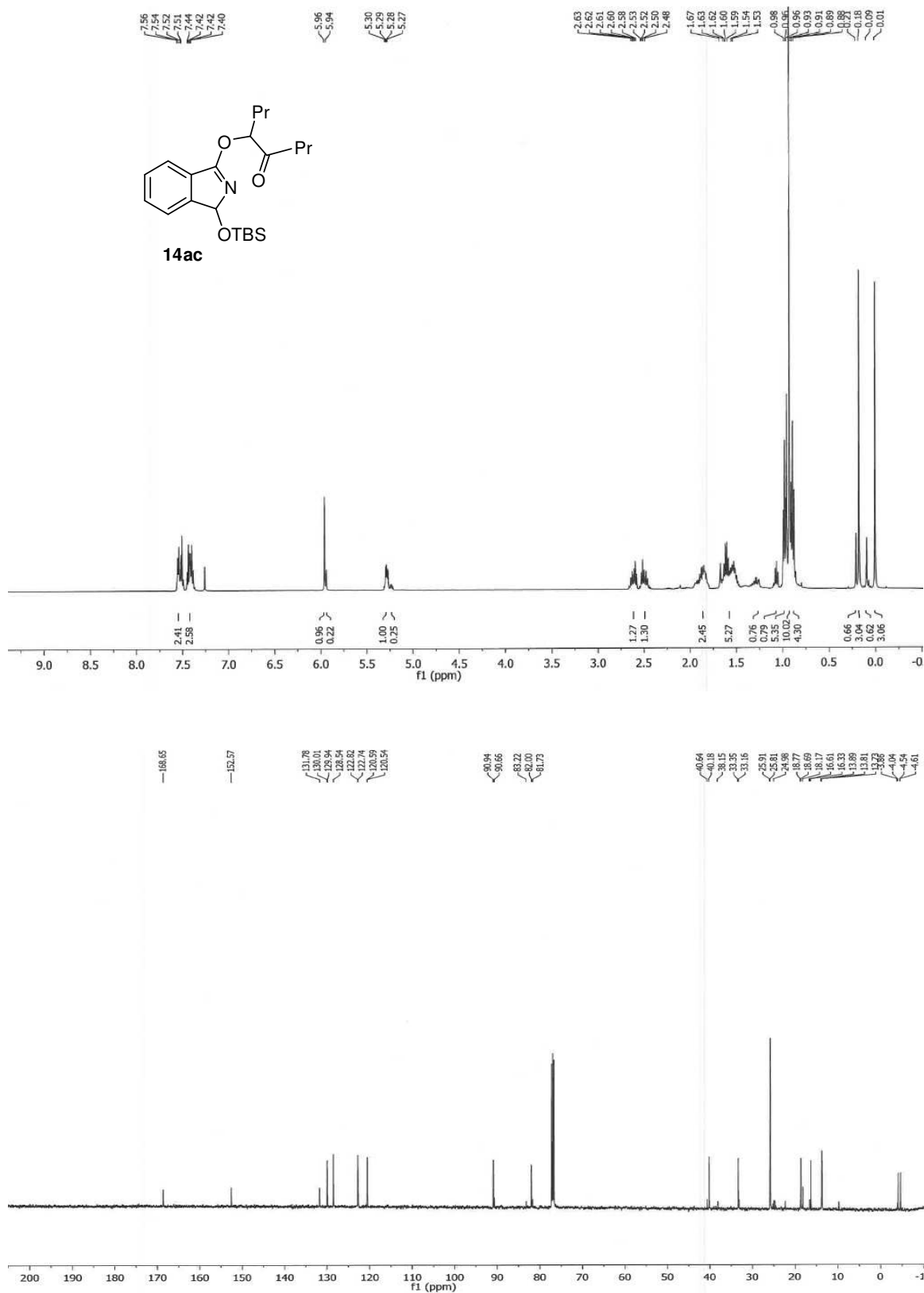
APPENDIX I: ^1H NMR and ^{13}C NMR spectra of **6t**

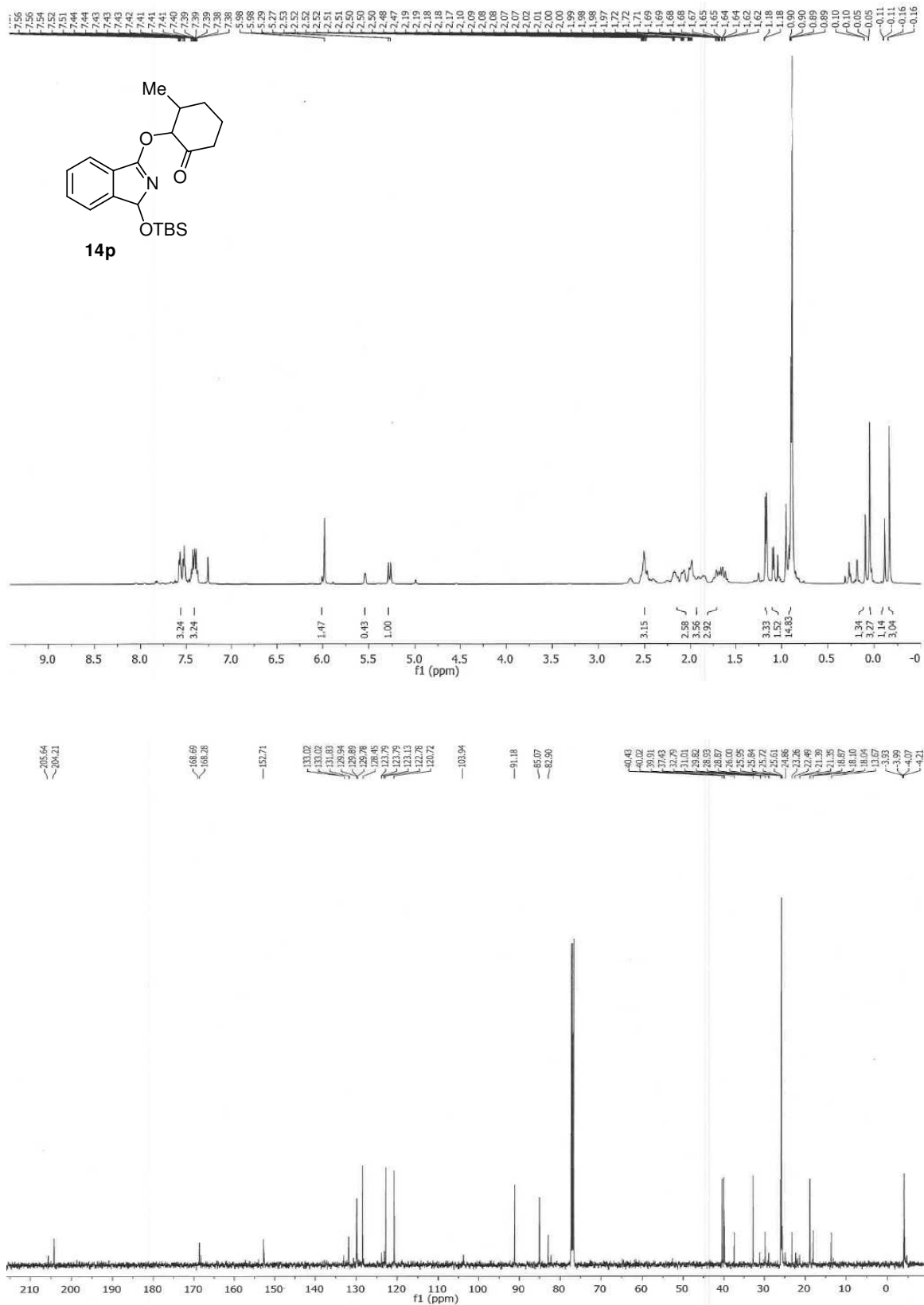
APPENDIX J: ^1H NMR and ^{13}C NMR spectra of **23z**

APPENDIX K: ^1H NMR and ^{13}C NMR spectra of **14z**

APPENDIX L: ^1H NMR and ^{13}C NMR spectra of **26z**

APPENDIX M: ^1H NMR and ^{13}C NMR spectra of **27z**

APPENDIX N: ^1H NMR and ^{13}C NMR spectra of **14ac**

APPENDIX O: ^1H NMR and ^{13}C NMR spectra of **14p**

APPENDIX P: Full X-ray Determination Data for 14z

TITL cdwla9_0ma in P2(1)/c
 CELL 0.71073 19.1961 7.6951 15.2163 90.000 97.590 90.000
 ZERR 4.00 0.0026 0.0010 0.0020 0.000 0.002 0.000
 LATT 1
 SYMM -x, y+1/2, -z+1/2
 SFAC C H N O Si
 UNIT 92 108 8 8 4
 L.S. 10
 ACTA
 BOND \$H
 FMAP 2
 PLAN -5
 HTAB
 CONF
 WGHT 0.100000 0.000000
 FVAR 0.180730
 TEMP 0.000
 Si1 5 0.676871 0.693399 0.131594 11.000000 0.063990 =
 0.066890 0.068030 -0.003360 0.006800 -0.012130
 O1 4 0.701322 0.839588 0.207479 11.000000 0.093680 =
 0.065110 0.077370 -0.009510 0.009670 -0.034650
 O2 4 1.047181 1.051443 0.293515 11.000000 0.074000 =
 0.139730 0.060610 0.021890 -0.000790 0.009680
 N1 3 0.800545 1.009481 0.181250 11.000000 0.062850 =
 0.056050 0.058990 -0.004390 0.010010 -0.010380
 O3 4 0.903749 1.135206 0.250109 11.000000 0.055900 =
 0.074100 0.058390 -0.012990 0.013180 -0.009480
 C1 1 0.534177 0.749774 0.133531 11.000000 0.069390 =
 0.185550 0.228160 -0.031950 0.031740 0.009640

 AFIX 137
 H22 2 0.522824 0.751562 0.070174 11.000000 -1.500000
 H1 2 0.551059 0.862101 0.153890 11.000000 -1.500000
 H21 2 0.492911 0.721178 0.159947 11.000000 -1.500000

 AFIX 0
 C2 1 0.592162 0.611016 0.160438 11.000000 0.079430 =
 0.089950 0.103770 -0.014550 0.018140 -0.027990
 C3 1 0.727132 1.008723 0.199388 11.000000 0.058860 =
 0.060180 0.067190 -0.001600 0.006100 -0.012100

 AFIX 13
 H20 2 0.697440 1.071037 0.152295 11.000000 -1.200000

APPENDIX P (continued)

AFIX 0

C4 1 0.834953 1.098347 0.242584 11.000000 0.048590 =
0.047730 0.060220 0.001300 0.007560 -0.003450

C5 1 0.942823 1.063123 0.184458 11.000000 0.058790 =
0.063890 0.054220 -0.001090 0.016150 0.002200

AFIX 13

H15 2 0.932280 0.939016 0.176785 11.000000 -1.200000

AFIX 0

C6 1 1.020321 1.087946 0.219182 11.000000 0.059030 =
0.069840 0.059950 -0.003320 0.005100 0.009390

C7 1 1.053989 1.163851 0.147722 11.000000 0.051090 =
0.057310 0.056190 -0.010510 0.011900 0.000770

C8 1 1.124194 1.202663 0.146378 11.000000 0.060990 =
0.069060 0.074720 -0.016930 0.008680 0.006600

AFIX 43

H14 2 1.157638 1.178382 0.194795 11.000000 -1.200000

AFIX 0

C9 1 1.142969 1.278791 0.070607 11.000000 0.065590 =
0.083620 0.092180 -0.017930 0.026820 -0.014870

AFIX 43

H2 2 1.189795 1.306454 0.067877 11.000000 -1.200000

AFIX 0

C10 1 0.597228 0.582121 0.260469 11.000000 0.217500 =
0.169960 0.125730 -0.002190 0.080290 -0.096070

AFIX 137

H26 2 0.556275 0.520938 0.273657 11.000000 -1.500000

H3 2 0.600154 0.692388 0.290238 11.000000 -1.500000

H27 2 0.638436 0.514889 0.280335 11.000000 -1.500000

AFIX 0

C11 1 0.744634 0.520845 0.142807 11.000000 0.101390 =
0.101660 0.134440 -0.013700 -0.005200 0.010350

AFIX 137

H4 2 0.790134 0.572147 0.142026 11.000000 -1.500000

H5 2 0.735291 0.440529 0.094409 11.000000 -1.500000

H6 2 0.743624 0.460358 0.197803 11.000000 -1.500000

AFIX 0

C12 1 0.668435 0.787774 0.019385 11.000000 0.142640 =

APPENDIX P (continued)

0.100330 0.080380 0.003540 0.013980 -0.015500

AFIX 137

H8 2 0.631247 0.872082 0.012995 11.000000 -1.500000
 H7 2 0.657868 0.697369 -0.023795 11.000000 -1.500000
 H9 2 0.711794 0.843034 0.010500 11.000000 -1.500000

AFIX 0

C13 1 1.093490 1.313878 -0.000358 11.000000 0.084260 =
 0.080890 0.072200 -0.002630 0.029560 -0.011060

AFIX 43

H10 2 1.107431 1.364830 -0.050644 11.000000 -1.200000

AFIX 0

C14 1 1.024024 1.275902 0.000785 11.000000 0.069070 =
 0.079370 0.055790 -0.003960 0.015580 -0.000320

AFIX 43

H13 2 0.991089 1.299936 -0.048194 11.000000 -1.200000

AFIX 0

C15 1 1.003525 1.201095 0.076042 11.000000 0.054100 =
 0.057210 0.051430 -0.008840 0.010250 0.002670
 C16 1 0.931285 1.154596 0.094913 11.000000 0.055770 =
 0.072800 0.055780 -0.001680 0.004300 0.003360

AFIX 23

H12 2 0.908249 1.077947 0.049465 11.000000 -1.200000
 H11 2 0.902758 1.257982 0.097748 11.000000 -1.200000

AFIX 0

C17 1 0.795070 1.165789 0.310915 11.000000 0.055150 =
 0.048490 0.050300 0.001640 0.009160 -0.002690
 C18 1 0.812684 1.260901 0.386627 11.000000 0.057550 =
 0.066760 0.061560 -0.002700 0.009380 -0.000020

AFIX 43

H19 2 0.858336 1.301005 0.402310 11.000000 -1.200000

AFIX 0

C19 1 0.760987 1.295696 0.439027 11.000000 0.077300 =
 0.080090 0.065180 -0.007720 0.017460 0.008480

APPENDIX P (continued)

AFIX 43

H18 2 0.771337 1.360984 0.490530 11.000000 -1.200000

AFIX 0

C20 1 0.694141 1.233510 0.414825 11.000000 0.067020 =
0.098880 0.080010 -0.009020 0.024470 0.005420

AFIX 43

H17 2 0.659900 1.257428 0.451021 11.000000 -1.200000

AFIX 0

C21 1 0.675998 1.137873 0.339633 11.000000 0.059300 =
0.081650 0.086440 -0.005660 0.019640 -0.004930

AFIX 43

H16 2 0.630440 1.096695 0.324539 11.000000 -1.200000

AFIX 0

C22 1 0.727852 1.104425 0.286692 11.000000 0.058560 =
0.052420 0.066540 0.000270 0.011750 0.000300C23 1 0.572144 0.441585 0.111161 11.000000 0.127220 =
0.132750 0.192760 -0.046430 0.027200 -0.074790

AFIX 137

H23 2 0.606411 0.353925 0.130247 11.000000 -1.500000

H25 2 0.570677 0.460047 0.048548 11.000000 -1.500000

H24 2 0.526765 0.404309 0.123721 11.000000 -1.500000

AFIX

HKLF 4 1 1 0 0 0 1 0 0 0 1

END

HKLF 4 1 1 0 0 0 1 0 0 0 1

REM cdwla9_0ma in P2(1)/c

REM R1= 0.0478 for 1790 Fo > 4sig(Fo) and 0.0600 for all 2159 data

REM 258 parameters refined using 0 restraints

VITA**ADITI PATIL****EDUCATION:**

Doctor of Philosophy, Ph.D. in Organic Chemistry
August 2007 - present

Master of Science, M.Sc. in Organic Chemistry
June 2004 - May 2006
University of Pune, Pune, India

Bachelor of Science, B.Sc. in Chemistry
June 2001 - May 2004
University of Pune, Pune, India

WORK EXPERIENCE:

Research Assistant
Department of Chemistry, University of Illinois at Chicago, Chicago, IL
August 2007 - present

Teaching Assistant
Department of Chemistry, University of Illinois at Chicago, Chicago, IL
August 2007 - May 2012

Research Mentor
Illinois Mathematics and Science Academy, Chicago, IL
August 2010 - April 2011

Project Assistant
National Chemical Laboratory, Pune, India
October 2006 - April 2007

Intern
National Chemical Laboratory, Pune, India
December 2005 - April 2006

Research Scholar
Indian Academy of Sciences
Hyderabad central University, Hyderabad, India
May 2005 - August 2005

HONORS & AWARDS:

- 1) Moriarty Graduate Fellowship, Department of Chemistry, UIC, Chicago, IL
August 2012 - August 2013
- 2) ACS Travel Award for the Fall 2012 National Meeting, Philadelphia, PA
August 2012
- 3) Abbott Scholar at Abbott Scholar's Symposium, Abbott Park, IL
August 2012
- 4) Silver medal, Master of Science, University of Pune, Pune, India
May 2006
- 5) Research Scholar at Indian Academy of Sciences, Hyderabad, India
May 2005

PROFESSIONAL AFFILIATIONS:

Member, American Chemical Society, Organic Chemistry Division
April 2012 - present

PUBLICATIONS:

- 1) "Preparation of Enantioenriched α -Oxygenated Ketones by the Diastereoselective Dioxygenation of Alkenyl Boronic Acids," Patil, A.; Ballantine, J.; Kroc, M.; Anderson, L.L. Manuscript in preparation
- 2) "Preparation of α -Oxygenated Ketones by the Dioxygenation of Alkenyl Boronic Acids," Patil, A.; Mo, D-L.; Wang, H-Y.; Mueller, D.S.; Anderson, L.L. *Angew. Chem. Int. Ed.* 2012, 51, 7799
- 3) "Improved Method for the Synthesis of β -Carbonyl Silyl-1,3-Dithianes by the Double Conjugate Addition of 1,3-Dithiol to Propargylic Carbonyl Compounds," Mukherjee, S.; Kontokosta, D.; Patil, A.; Rallapalli, S.; Lee, D. *J. Org. Chem.* 2009, 74, 9206
- 4) "pH-Regulated "Off-On" fluorescence signaling of d-block metal ions in aqueous media and realization of molecular IMP logic function," Sarkar, M.; Bhandia, S.; Patil, A.; Ansari, M.B.; Samanta, A. *New J. Chem.* 2006, 30, 1557